Adsorption Technology & Design

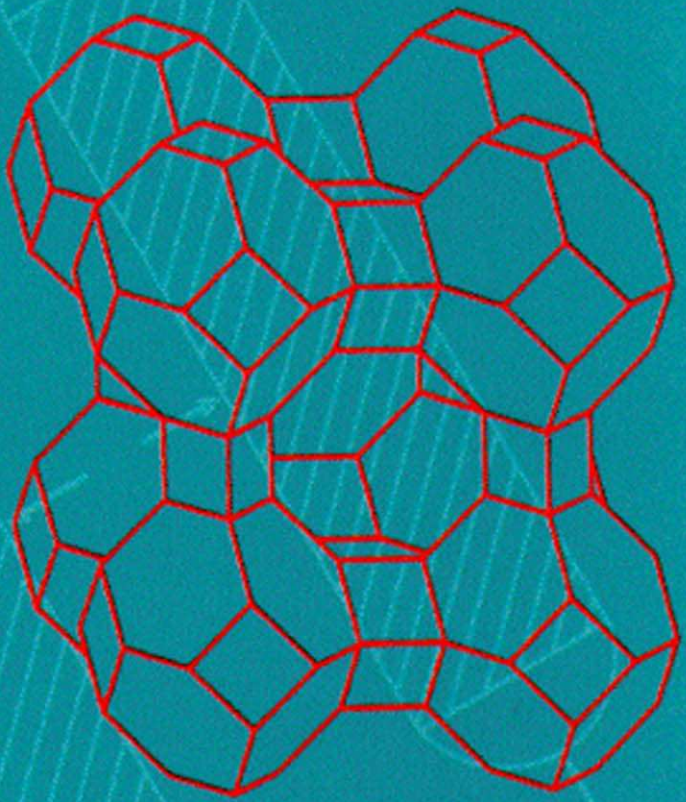

Barry Crittenden &
W John Thomas

Adsorption Technology and Design

This Page Intentionally Left Blank

Adsorption Technology and Design

W. John Thomas and Barry Crittenden

BUTTERWORTH HEINEMANN

Butterworth-Heinemann
Linacre House, Jordan Hill, Oxford OX2 8DP
225 Wildwood Avenue, Woburn, MA 01801-2041
A division of Reed Educational and Professional Publishing Ltd

A member of the Reed Elsevier plc group

OXFORD BOSTON JOHANNESBURG
MELBOURNE NEW DELHI SINGAPORE

First published 1998

British Library Cataloguing in Publication Data
Thomas, W. J.
Adsorption technology and design
1 Adsorption
I Title II Crittenden, B. D.
660.2'84235

ISBN 0 7506 1959 7

Library of Congress Cataloguing in Publication Data
Thomas, W. J.
Adsorption technology and design/W. John Thomas and Barry Crittenden.
p. cm.
Includes bibliographical references and index.
ISBN 0 7506 1959 7
1 Adsorption. I Crittenden, B. D. (Barry D.) II Title.
TP156.A35T47 97–24159
660'.284235–dc21 CIP

Typeset at The Spartan Press Ltd,
Lymington, Hants
Printed in Great Britain

Contents

This Page Intentionally Left Blank

Foreword

When asked about the most important technology for the Process Industries, most people might offer 'reaction'. If one considers where value is really added, it is more probably in the separation and purification of the products. It is therefore a great pleasure to find that Professors Crittenden and Thomas have made a major contribution to this with their new book. My career has been spent in the Industrial Gases industry where cost-effectiveness of separation processes is the main way of creating competitive advantage. In the last few years, adsorption technology has become increasingly important in market development and market share. It has allowed on-site gas generation, with considerable price reduction, where previously we would have supplied liquefied gases. This increased commercialization of the technology stimulates further research into both the adsorbates and their applications, the virtuous circle.

In *Adsorption Technology and Design*, we find a carefully crafted blend of theory, practice and example. The reader who seeks only an overview is as well served as the experienced practitioners seeking to broaden their knowledge. Chapters 1 and 2 are an introduction that allows the non-practitioner to gain some understanding of the history and technology. Chapters 3 and 4 deal with the theory of adsorption equilibria and adsorption kinetics respectively. These well-structured chapters define the basic science of the subject and provide the essential grounding necessary to allow applications development. Chapters 5 and 6 are a comprehensive description of processes and cycles and their design procedures. Here the practitioner may gain experience or inspiration to innovate. These chapters are suitable reading for both the novice and the expert. Chapter 7 is the consolidation of the book. Here we see how theory is put into commercial practice. It also clearly illustrates the variety of possible approaches to particular processes and the rate of development of the technology. Finally

in Chapter 8 we have a review of available literature that is free from criticism or comment.

I have no doubt that this book is a significant milestone for the subject and that it will enjoy the success it deserves.

Professor Keith Guy, FEng, FIChemE

1

The development of adsorption technology

1.1 INTRODUCTION

The ability of some solids to remove colour from solutions containing dyes has been known for over a century. Similarly, air contaminated with unpleasant odours could be rendered odourless by passage of the air though a vessel containing charcoal. Although such phenomena were not well understood prior to the early twentieth century, they represent the dawning of adsorption technology which has survived as a means of purifying and separating both gases and liquids to the present day. Indeed, the subject is continually advancing as new and improved applications occur in competition with other well-established process technologies, such as distillation and absorption.

Attempts at understanding how solutions containing dyes could be bleached, or how obnoxious smells could be removed from air streams, led to quantitative measurements of the concentration of adsorbable components in gases and liquids before and after treatment with the solid used for such purposes. The classical experiments of several scientists including Brunauer, Emmett and Teller, McBain and Bakr, Langmuir, and later by Barrer, all in the early part of the twentieth century, shed light on the manner in which solids removed contaminants from gases and liquids. As a result of these important original studies, quantitative theories emerged

which have withstood the test of time. It became clear, for example, that the observed effects were best achieved with porous solids and that adsorption is the result of interactive forces of physical attraction between the surface of porous solids and component molecules being removed from the bulk phase. Thus adsorption is the accumulation of concentration at a surface (as opposed to absorption which is the accumulation of concentration within the bulk of a solid or liquid).

The kinetic theory of gases, developed quantitatively and independently by both Maxwell and Boltzmann in the nineteenth century, with further developments in the early part of the twentieth century by Knudsen, reveals that the mass of a gas striking unit area of available surface per unit time is $p(M/2\Pi R_g T)^{1/2}$, where p is the gas pressure and M is its molecular mass. As discussed later (Chapter 4), according to the kinetic theory of gases the rate of adsorption of nitrogen at ambient temperature and 6 bar pressure is 2×10^4 kg m^{-2}s^{-1}. At atmospheric pressure this would translate to 0.33×10^4 kg m^{-2}s^{-1}. Ostensibly then, rates of adsorption are extremely rapid. Even accounting for the fact that adsorbate molecules require an energy somewhat greater than their heat of liquefaction (q.v. Chapter 3) the above quoted rates would only be reduced by a factor $\exp(-E_a/R_gT)$: if E_a, the energy required for adsorption, were 10 kJ mol^{-1} at ambient temperature and pressure, the rate of adsorption would be 4.5×10^2 kg m^{-2}s^{-1}. However, observed rates are less than this by a factor of at least 10^{-10} for several reasons, principally the resistance offered by mass transfer from the bulk fluid to the surface of the porous solid and intraparticle diffusion through the porous structure of the adsorbent. Such transport resistances are discussed more fully in Chapter 4.

Industrial applications of adsorbents became common practice following the widespread use of charcoal for decolourizing liquids and, in particular, its use in gas masks during the 1914–18 World War for the protection of military personnel from poisonous gases. Adsorbents for the drying of gases and vapours included alumina, bauxite and silica gel; bone char and other carbons were used for sugar refining and the refining of some oils, fats and waxes; activated charcoal was employed for the recovery of solvents, the elimination of odours and the purification of air and industrial gases; fuller's earth and magnesia were found to be active in adsorbing contaminants of petroleum fractions and oils, fats and waxes; base exchanging silicates were used for water treatment while some chars were capable of recovering precious metals. Finally, some activated carbons were used in medical applications to eliminate bacteria and other toxins. Equipment for such tasks included both batch and continuous flow configurations, the important consideration for the design of which was to ensure adequate contact between adsorbent and fluid containing the component to be removed (the adsorbate).

1.2 EARLY COMMERCIAL PRACTICE

Full details of early commercial practice can be found in the writings of Mantell (1951). The oil industry used naturally occurring clays to refine oils and fats as long ago as the birth of that industry in the early part of the twentieth century. Clay minerals for removing grease from woollen materials (known as the practice of fulling) were used extensively. The mineral came to be known as fuller's earth. Its composition consists chiefly of silica with lower amounts of alumina, ferric oxide and potassium (analysed as the oxide). Other naturally occurring clays (kaolin and bentonite) also contain large proportions of silica with smaller proportions of alumina and were also used for bleaching oils and petroleum spirits. Two methods were in common use for decolouring oil and petroleum products: the oil could be percolated through a bed of granular clay or it could be directly contacted and agitated with the clay mineral. The oil or lubricant to be bleached was first treated with sulphuric acid and a little clay, filtered and subsequently run into mixing agitators containing the adsorbent clay and which decolourized the lubricant after a sufficiently long contact time (of the order of one to three minutes) and at a suitable temperature (usually about 60–65°C).

Another mineral, which was widely used as a drying agent, was refined bauxite which consists of hydrated aluminium oxide. It was also used for decolourizing residual oil stocks. Another form of aluminium oxide mineral is florite which adsorbs water rapidly and does not swell or disintegrate in water. Consequently, it was, and still is, used for the drying of gases and organic liquids. The early practice was to utilize beds of florite at room temperature through which was pumped the organic liquid containing moisture. Reactivation of the bed was accomplished by applying a vacuum and heating by means of steam coils located within the bed. Alternatively, the beds were reactivated by circulating an inert gas through the adsorbent, the desorbed water being condensed on emergence from the bed in cooled receptacles.

Some types of carbon were in common use for decolourizing and removing odours from a wide variety of materials. Carbons were also used for treating water supplies. The decolourization of liquids, including the refining of sugar melts, was accomplished by mixing the carbon adsorbent with the liquid to be bleached and subsequently filtering. In some cases the residual adsorbent was regenerated for further use by passing steam through a bed of the spent adsorbent. In the case of water treatment, non-potable waters were either percolated through beds of carbonaceous adsorbent, or activated carbon was added to water in mixing tanks. The resulting effluent was then treated with chlorine to remove toxins. Alternatively, the contaminated water was first treated with excess chlorine and then allowed

to percolate through a carbon bed. The method of water treatment depended on both the extent and form of contamination. The spent carbonaceous adsorbents were usually regenerated by steaming in a secondary plant. Activated carbons were in general use during the first three decades of the twentieth century for the purification of air and for recovering solvents from vapour streams. The carbon adsorbents were activated prior to use as an adsorbent by treatment with hot air, carbon dioxide or steam. The plants for solvent recovery and air purification were among the first to employ multibed arrangements which enabled regeneration of the carbon adsorbent (usually by means of hot air or steam) while other beds were operating as adsorbers. Thus the concept of cyclic operation began to be adopted and applied to other operations on a broader basis.

The dehumidification of moisture-laden air and the dehydration of gases were, and still are, achieved by means of silica gel as an adsorbent. In 1927, for example, an adsorption unit containing silica gel was installed to dehumidify iron blast furnace gases at a factory near Glasgow. It has been pointed out (Wolochow 1942) that this plant was the first known plant using a solid adsorbent for dehumidifying blast furnace gases. Six silica gel units treated one million cubic metres of air per second. Five of the units acted as adsorbers while the sixth unit was being regenerated. An arrangement of piping and valves enabled each adsorber to be switched sequentially into use as an adsorber, thus providing for a continuous flow of dehumidified gas. This unit is an example of one of the earlier thermal swing processes in operation.

1.3 MODERN PRACTICE

Thermal swing adsorption (TSA) processes gradually became dominant for a variety of purposes by the end of the first quarter of the twentieth century. But it was not until the advent of adsorbents possessing molecular sieving properties when processes for the separation of gaseous mixtures developed. Naturally occurring and synthesized alumina–silica minerals (discussed in Chapter 2) have unique crystalline structures, the microporosity of which is precisely determined by the configuration of silica –alumina cages linked by four- or six-membered oxygen rings. Such structures admit and retain molecules of certain dimensions to the exclusion of others, and are therefore excellent separating agents. Barrer (1978) extensively researched and reviewed the adsorptive properties of these materials which are referred to as zeolites. Walker *et al.* (1966a, 1966b), on the other hand, thoroughly investigated the adsorptive properties of microporous carbons and laid many of the foundations for the development

of molecular sieve carbons, which are less hydrophilic than zeolites, and can therefore separate wet gaseous streams effectively.

Although the development of a whole range of laboratory synthetic zeolites, stimulated by the researches of Barrer, precipitated a rapid growth in commercial pressure swing adsorption (PSA) processes (a selection of which are described in Chapter 7), as a historical note it should be stated that the first patents filed for such processes were due to Finlayson and Sharp (1932) and Hasche and Dargan (1931). More than two decades elapsed before two commercial processes for the separation of air, patented by Guerin de Montgareuil and Domine (1964) and Skarstrom (1958), became the foundation for pressure swing adsorption separation techniques on a commercial scale. The essential difference between the earlier thermal swing processes (TSA), and the pressure swing process (PSA) is in the method by which the adsorbent is regenerated following adsorption of the most strongly adsorbed component of a gaseous or liquid mixture. Increase in temperature of the adsorbent bed is the driving force for desorption in TSA processes whereas reduction in total pressure enables desorption in PSA processes. The rapid growth in the number of patents for PSA processes shown in Figure 1.1 is testimony to the successful commercialization of these processes. Their prominence is due principally to the much shorter cycle times required for the PSA technique than TSA methods. Thermal swing processes require cycle times of the order of hours on account of the large thermal capacities of beds of adsorbent. Reduction in pressure to achieve desorption may, on the other hand, be accomplished in minutes rather than hours. Not all TSA processes can, however, be simply transposed into PSA processes solely because of the difference in adsorbent bed regeneration times. TSA processes are often a good choice when components of a mixture are strongly adsorbed, and when a relatively small change in temperature produces a large extent of desorption of the strongly adsorbed species. PSA processes are more often adopted when a weakly adsorbed component is required at high purity: furthermore, cycle times are much shorter than in TSA processes and therefore greater throughputs are possible utilizing PSA techniques.

TSA and PSA processes are, by virtue of the distinct adsorption and regeneration components of the cycle, not continuous processes, although a continuous flow of product may be achieved by careful design and bed utilization. Moving bed and simulated moving bed processes are, however, by their very nature truly continuous. Examples of these are given in Chapter 7, but here it suffices to say that a number of continuous commercial processes for the separation of aromatic mixtures, the separation of n-paraffins from branched and cycloalkanes, the production of olefins from olefin and paraffin mixtures and the isolation of fructose from corn syrup, have been in operation since the early 1980s.

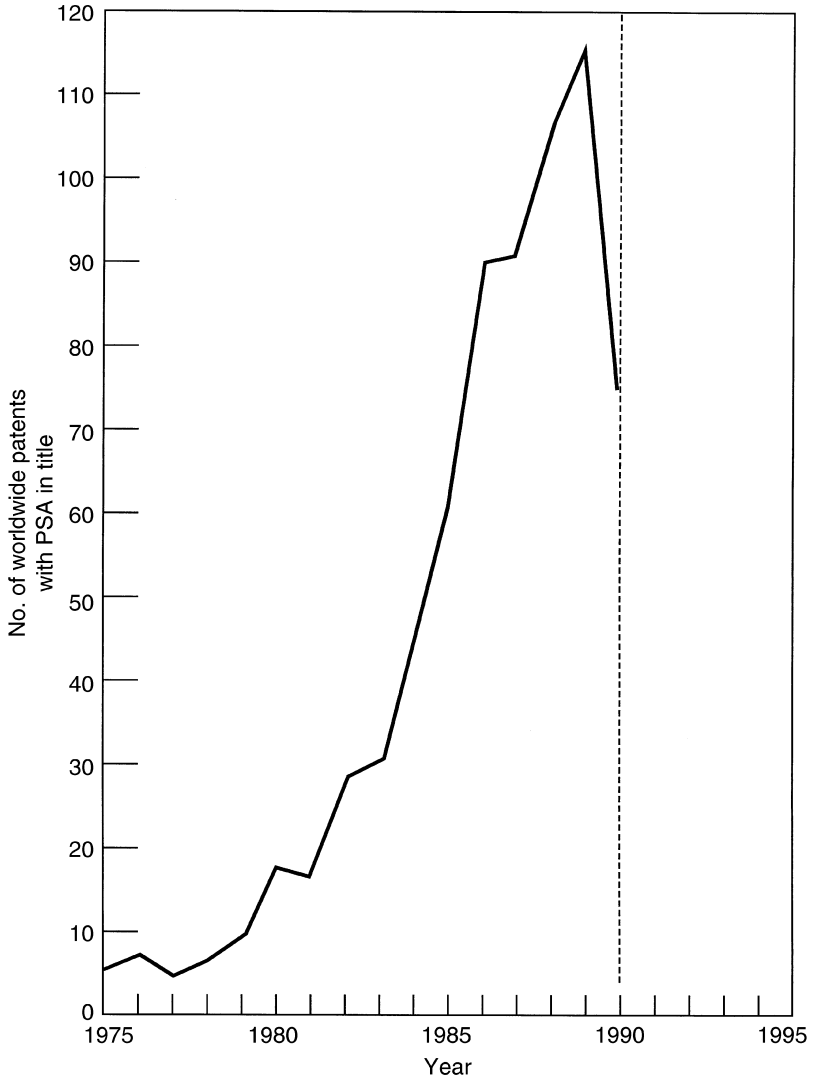

***Figure** 1.1 Growth of patents relating to PSA processes (adopted from Sircar, 1991).*

Until relatively recently, chromatographic processes have been confined to the laboratory for purposes of the analysis of gaseous and liquid mixtures. The pharmaceutical industry has also utilized the principles of chromatography for preparing batches of pharmaceutical products. Elf-

Aquitaine, however, operate a large-scale commercial chromatographic process for the separation of n- and i-paraffins from light naphtha feeds and this is briefly described in Section 7.8.

REFERENCES

Barrer, R. M. (1978) *Zeolites and Clay Minerals as Sorbents and Molecular Sieves*, Academic Press

Finlayson, D. and Sharp A. J. (1932) British Patent 365092

Guerin de Montgareuil, P. and Domine, D. (1964) US Patent 3,155,468

Hasche, R. L. and Dargan, W. N. (1931) US Patent 1,794,377

Mantell, C. L. (1951) *Adsorption*, McGraw-Hill

Sircar, S. (1991) *Recents Progres en Genie des Procedes*, Eds Meunier, F. and Levan, D. 5, No. 17, p. 9

Skarstrom, C. W. (1960) US Patent 2944627

Walker, P. L. Jr, Lamond, T. G. and Metcalf, J. E. (1966a) *2nd Conf. Ind. Carbon and Graphite*, p. 7. Soc. Chem. Ind., London

Walker, P. L. Jr, Austin, L. G. and Nandi, S. P. (1966b) *Chemistry and Physics of Carbon*, edited by P. L. Walker Jr, Marcel Dekker

Wolochow (1942) *Metal Progress*, October, p. 546 (abstract of Bulletin 1078 Can. Nat. Res. Labs, Ottawa, Canada)

2

Adsorbents

To be technically effective in a commercial separation process, whether this be a bulk separation or a purification, an adsorbent material must have a high internal volume which is accessible to the components being removed from the fluid. Such a highly porous solid may be carbonaceous or inorganic in nature, synthetic or naturally occurring, and in certain circumstances may have true molecular sieving properties. The adsorbent must also have good mechanical properties such as strength and resistance to attrition and it must have good kinetic properties, that is, it must be capable of transferring adsorbing molecules rapidly to the adsorption sites. In most applications the adsorbent must be regenerated after use and therefore it is desirable that regeneration can be carried out efficiently and without damage to mechanical and adsorptive properties. The raw materials and methods for producing adsorbents must ultimately be inexpensive for adsorption to compete successfully on economic grounds with alternative separation processes.

The high internal surface area of an adsorbent creates the high capacity needed for a successful separation or purification process. Adsorbents can be made with internal surface areas which range from about 100 m^2/g to over 3000 m^2/g. For practical applications, however, the range is normally restricted to about 300–1200 m^2/g. For most adsorbents the internal surface area is created from pores of various size. The structure of an adsorbent is shown in idealized form in Figure 2.1. Many adsorbent materials, such as carbons, silica gels and aluminas, are amorphous and contain complex networks of interconnected micropores, mesopores and macropores. In contrast, in zeolitic adsorbents the pores or channels have precise

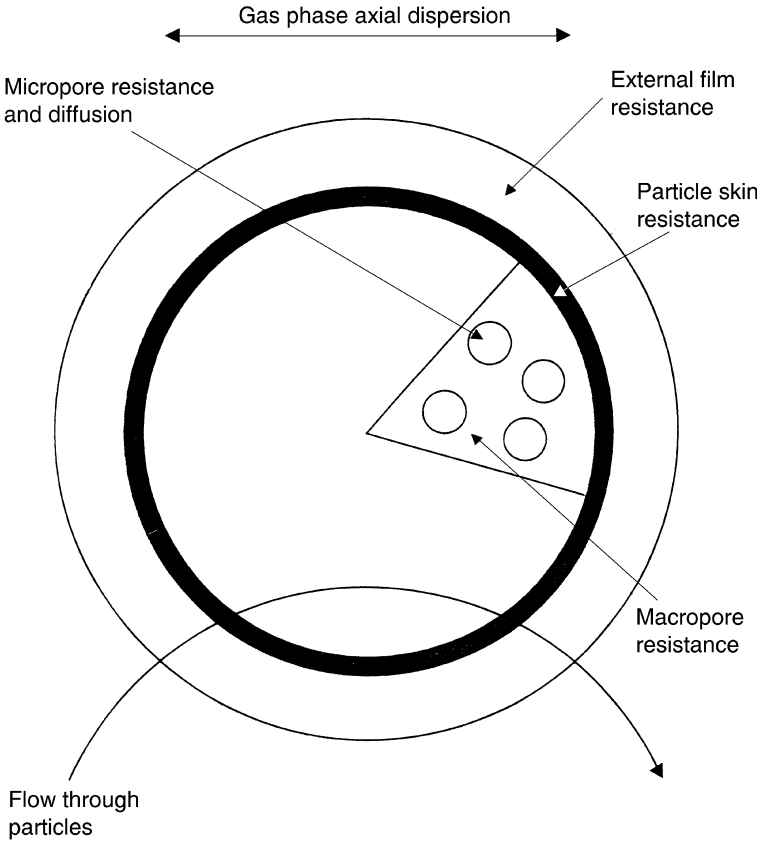

Figure 2.1 *Sketch showing the general structure of an adsorbent particle and associated resistances to the uptake of fluid molecules.*

dimensions although a macroporous structure is created when pellets are manufactured from the zeolite crystals by the addition of a binder. Fluid molecules which are to be adsorbed on the internal surface must first pass through the fluid film which is external to the adsorbent particle, thence through the macroporous structure into the micropores where the bulk of the molecules are adsorbed.

As shown in Figure 2.2, pore sizes may be distributed throughout the solid, as in the case of an activated carbon, or take very precise values as in the case of zeolite crystals. Pore sizes are classified generally into three ranges: macropores have 'diameters' in excess of 50 nm, mesopores (known also as transitional pores) have 'diameters' in the range 2–50 nm, and

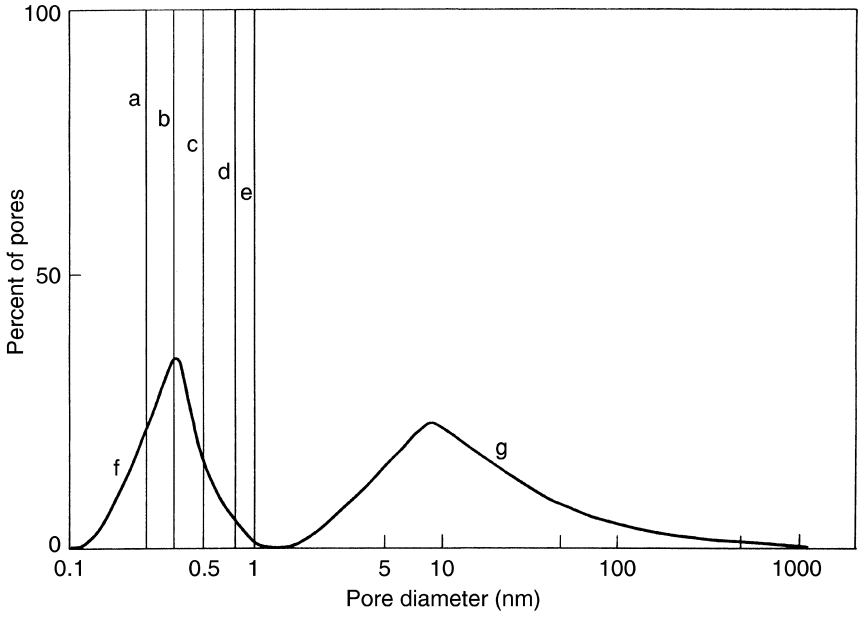

Figure 2.2 *Micropore size distributions of (a) zeolite type 3A, (b) 4A, (c) 5A, (d) 10X, (e) 13X, (f) molecular sieve carbon and (g) activated carbon (adapted from Yang 1987).*

micropores have 'diameters' which are smaller than 2 nm. The largest pores within an adsorbent are generally in the submicron size range and they account for only a small fraction of the total pore volume.

The surface area of an adsorbent material is generally obtained from nitrogen adsorption measurements made at liquid nitrogen temperatures (77 K). The results are then interpreted using the BET isotherm (see Section 3.3.4). Pore volumes can be obtained by measuring the amount of an adsorbate, such as nitrogen, which is adsorbed at a given pressure over a range of pressure up to the saturated vapour pressure. It is assumed then that condensation occurs in small pores and Kelvin's equation (see Section 3.2) can be used to determine the largest pore size into which the gas can condense. Different pressures can be used to obtain the pore size distribution. Mercury porosimetry is a technique which can be used to determine the pore size distribution. Initially, all gas is evacuated from the adsorbent and then pressure is used to force mercury into the pores. The pore size distribution can then be obtained from the pressure–volume curves.

A broad range of adsorbent materials is available for fluid purification and

separation applications. Most are manufactured but a few, such as some zeolites, occur naturally. Each material has its own characteristics such as porosity, pore structure and nature of its adsorbing surfaces. Each or all of these properties can play a role in the separation process. The extent of the ability of an adsorbent to separate molecule A from molecule B is known as its selectivity. The separation factor provides a numerical value for selectivity and is defined as follows:

$$\alpha_\alpha = \frac{X_i/Y_i}{X_j/Y_j} \tag{2.1}$$

Here, X_i and Y_i are strictly the equilibrium mole fractions of component i in the adsorbed and fluid phases, respectively. In practice, the units of X and Y can be altered to suit the system under study, bearing in mind that it is important in comparative studies for α_α to remain non-dimensional. For example, X_j could represent the loading of component j on the adsorbent in units of mg/g, rather than mole fraction. Selectivity may manifest itself in one or a number of ways in any particular separation process.

(1) Differences may exist in the thermodynamic equilibria for each adsorbate–adsorbent interaction; this is often known as the equilibrium effect.
(2) Differences may exist in the rates at which different adsorbates travel into the internal structure of the adsorbent; this is often known as the kinetic effect.
(3) Pore openings may be too small to allow penetration by one or more of the adsorbates; this is known as the molecular sieving effect and can be considered to be an extreme case of the kinetic effect.
(4) Differences may exist in the rate at which different adsorbates can be desorbed from the adsorbent; this is generally known as the desorption effect.

Equilibrium separation factors depend upon the nature of the adsorbate – adsorbent interactions, that is, on whether the surface is polar, non-polar, hydrophilic, hydrophobic, etc. and on the process conditions such as temperature, pressure and concentration. Kinetic separations are generally, but not exclusively, possible only with molecular sieve adsorbents such as zeolites and carbon sieves. The kinetic selectivity in this case is largely determined by the ratio of micropore diffusivities of the components being separated. For a useful separation to be based on kinetics the size of the adsorbent micropores must be comparable with the dimensions of the diffusing adsorbate molecules.

More than one mechanism of separation can be exploited in some applications but in others certain mechanisms can be counterproductive. Consider, for example, the separation of oxygen and nitrogen. The equilibrium isotherms for oxygen, nitrogen and argon on a 5A zeolite are shown schematically in Figure 2.3 (some actual data for this system are given in Chapter 7). The equilibrium loading of nitrogen is much greater than that of oxygen and argon and therefore it is possible to use the equilibrium effect with a 5A zeolite to adsorb nitrogen preferentially and hence to obtain relatively high purity oxygen from air. In practice, the purity of oxygen by this commercially successful process is limited to a maximum of 96% because argon (present in air at a concentration around 1%) is also not adsorbed preferentially and therefore leaves in the oxygen product. The equilibrium isotherms for oxygen and nitrogen on a carbon molecular sieve are shown in Figure 2.4. For this adsorbent it is clear that the differences in the isotherms might not be large enough to create a commercially attractive separation of oxygen and nitrogen if the equilibrium effect were to be used. Figure 2.5 however shows that the rate of uptake of oxygen by the carbon molecular sieve is 40–50 times that of nitrogen, particularly in the first few minutes. The reason for this, while not completely understood, is associated with the greater effective diffusivity of oxygen than nitrogen in the carbon

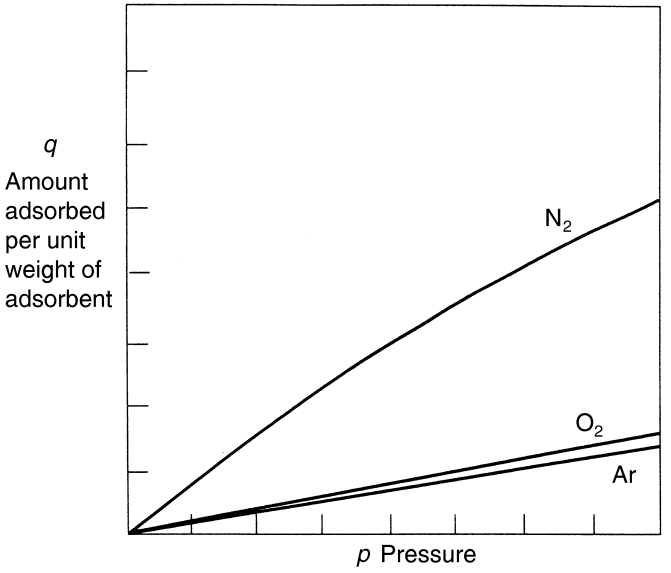

Figure 2.3 *Sketch of equilibrium isotherms of oxygen, nitrogen and argon on zeolite 5A at 20°C (redrawn from Crittenden 1992, p. 4.17).*

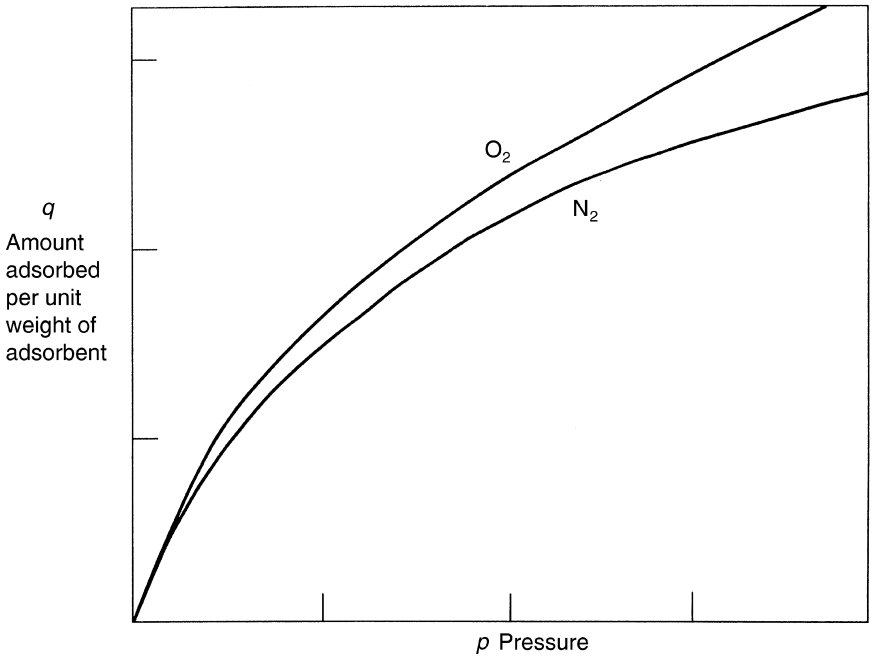

Figure 2.4 *Sketch of equilibrium isotherms of oxygen and nitrogen on molecular sieve carbon at 20°C (redrawn from Crittenden 1992, p. 4.17).*

molecular sieve. It is clear therefore that to produce high purity nitrogen from air using a carbon molecular sieve the adsorption time needs to be relatively short to exploit the kinetic effect and not allow the equilibrium effect to become significant. The production of high purity nitrogen by means of pressure swing adsorption using a carbon molecular sieve is indeed a commercially successful process. Both the production of high purity O_2 and high purity N_2 are described in Section 7.3.4.

The drying of ethanol using 3A zeolite is a good example of the true molecular sieving effect. Zeolite 3A has a window size of about 0.29 nm which is large enough for water molecules with a molecular diameter of 0.26 nm to pass into the crystal cavities. Ethanol has a molecular diameter of about 0.45 nm and hence is excluded from the crystal cavities because it cannot pass through the channels. Other zeolites can be used for the true molecular sieving effect. Figure 2.6 shows schematically the ability of 5A zeolite to separate linear and iso-paraffins by allowing the former to pass through the channels into the cavities while excluding the latter.

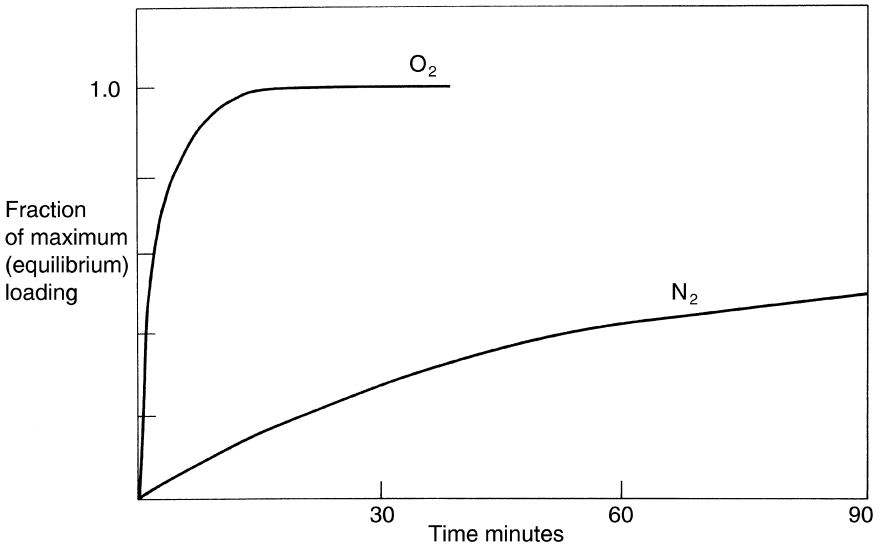

Figure 2.5 *Sketch of the fractional uptake rates of oxygen and nitrogen in molecular sieve carbon (redrawn from Crittenden 1992, p. 4.18).*

In order to withstand the process environment, adsorbents are usually manufactured in granular, spherical or extruded forms with sizes most often in the range 0.5–8 mm. Special shapes such as tri-lobe extrudates are available so that pressure drops can be kept low when the adsorbent is packed in a vessel. Other forms are available for special purposes, such as powders and monoliths. Some adsorbent materials, particularly zeolites, require a binder material in order not only to provide mechanical strength but also to provide a suitable macropore structure such that adsorbate molecules can gain ready access to the internal microporous structure. Example adsorbents are shown in Figure 2.7.

2.1 ACTIVATED CARBONS

Carbonaceous materials have long been known to provide adsorptive properties. The earliest applications may date back centuries with the discovery that charred materials could be used to remove tastes, colours and odours from water. Now activated carbons are used widely in industrial applications which include decolourizing sugar solutions,

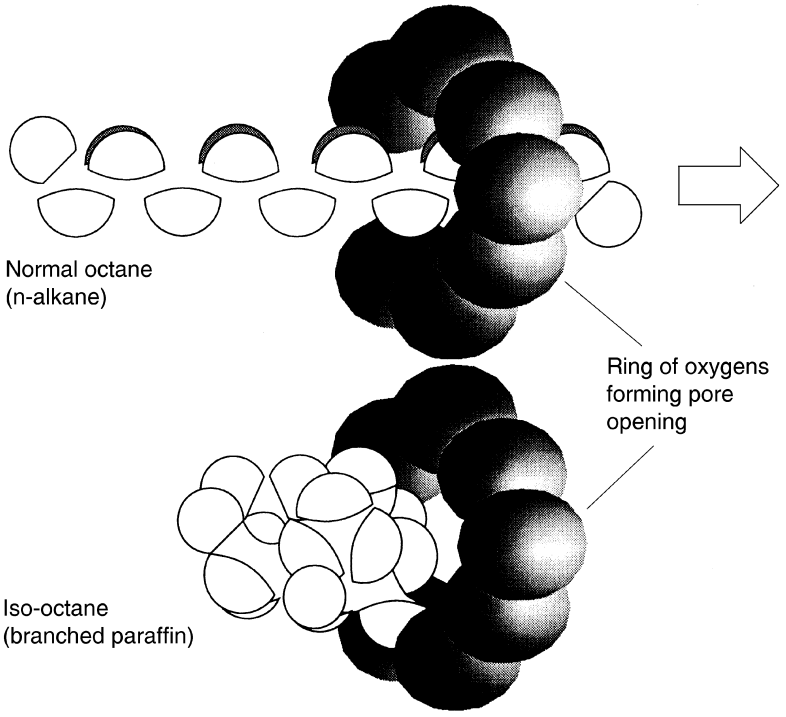

Figure 2.6 *Sketch showing the molecular sieving effect for normal and iso-paraffins in a 5A zeolite (redrawn from Gioffre 1989).*

personnel protection, solvent recovery, volatile organic compound control, hydrogen purification, and water treatment.

Activated carbons comprise elementary microcrystallites stacked in random orientation and are made by the thermal decomposition of various carbonaceous materials followed by an activation process. Raw materials include hard and soft woods, rice hulls, refinery residuals, peat, lignin, coals, coal tars, pitches, carbon black and nutshells, such as coconut. There are two types of manufacturing process, involving gas activation or chemical activation. The gas activation process first involves heating in the absence of air at 400–500°C to drive off volatile materials and to form small pores. Activation is then carried out with, for example, steam at between 800 and 1000°C. Other gases such as carbon dioxide or flue gases can be used instead. Chemical activation (Keller *et al.* 1987) can be carried out using, for example, zinc chloride or phosphoric acid to produce an activated carbon

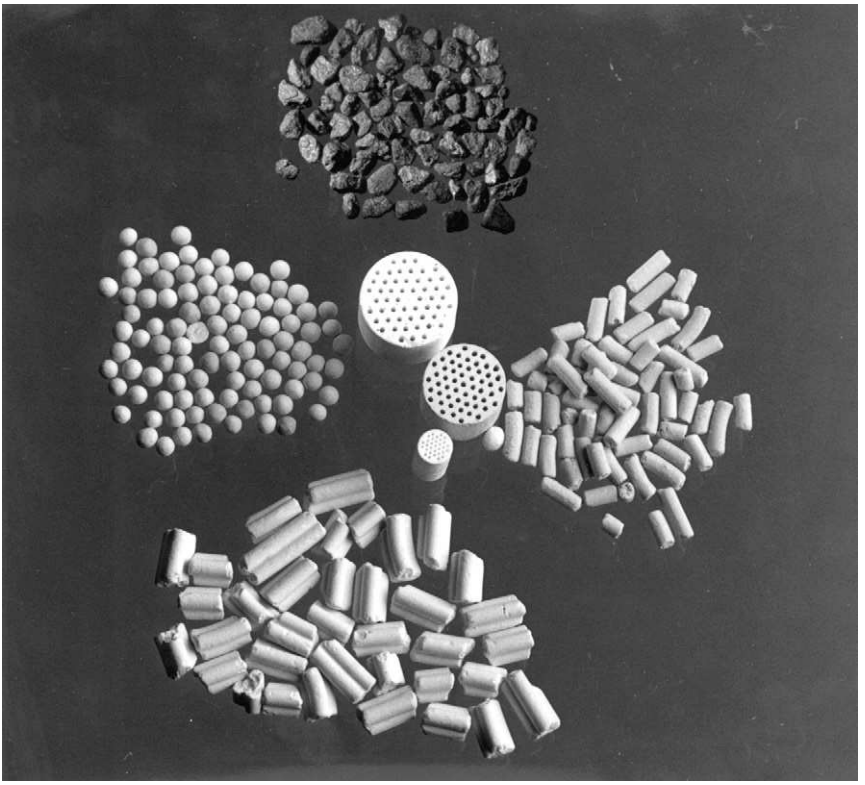

Figure 2.7 *Example adsorbents*

directly from the raw material, although the pores tend to be larger than with materials produced via steam activation. Granular materials for use in packed beds have particle sizes typically in the range 0.4–2.4 mm. Activated carbon cloths are made from cellulose-based woven cloth and can have a higher capacity and better kinetic properties than the granular, but cheaper, forms. Cloths can have both high external surface areas and high internal surface areas. Activated carbons can now be manufactured in monolithic forms for low pressure drop applications or for the bulk storage of natural gas.

Activated carbons contain a full range of pore sizes as shown in Table 2.1. Micropore diameters are generally less than 2 nm while macropore diameters are generally greater than 50 nm. Some pores may be inaccessible

because they are closed at both ends. Control of the pore sizes and of their distribution in the manufacturing process allows a broad range of adsorbents to be available offering widely differing selectivities. Carbons for gas phase applications require smaller pores while carbons for liquid phase applications tend to have larger pore diameters, of the order of 3 nm or larger. Carbons for liquid phase applications also need to be made with surfaces of the appropriate wettability.

Table 2.1 *Pore sizes in typical activated carbons**

	Micropores	*Mesopores or transitional pores*	*Macropores*
Diameter (nm)	<2	2–50	>50
Pore volume (cm^3/g)	0.15–0.5	0.02–0.1	0.2–0.5
Surface area (m^2/g)	100–1000	10–100	0.5–2
(Particle density 0.6–0.9 g/cm^3; porosity 0.4–0.6)			

* Adapted from Ruthven 1984, p. 8.

Pore volumes of carbons are typically of the order of 0.3 cm^3/g. Porosities are commonly quoted on the basis of adsorption with species such as iodine, methylene blue, benzene, carbon tetrachloride, phenol or molasses. The quantities of these substances adsorbed under different conditions give rise to parameters such as the Iodine Number, etc. Iodine, methylene blue and molasses numbers are correlated with pores in excess of 1.0, 1.5 and 2.8 nm, respectively. Other relevant properties of activated carbons include the kindling point (which should be over 370°C to prevent excessive oxidation in the gas phase during regeneration), the ash content, the ash composition, and the pH when the carbon is in contact with water. Some typical properties of activated carbons are shown in Table 2.2.

The surface of an activated carbon adsorbent is essentially non-polar but surface oxidation may cause some slight polarity to occur. Surface oxidation can be created, if required, by heating in air at around 300°C or by chemical treatment with nitric acid or hydrogen peroxide. This can create some hydrophilic character which can be used to advantage in the adsorption of polar molecules but can cause difficulties in other applications such as the

Table 2.2 *Typical properties of activated-carbon adsorbents**

	Liquid-phase carbons		*Vapour-phase carbons*	
Physical properties	*Wood base*	*Coal base*	*Granular coal*	*Granular coal*
Mesh size (Tyler)	−100	−8 + 30	−4 + 10	−6 + 14
$CC1_4$ activity (%)	40	50	60	60
Iodine number	700	950	1000	1000
Bulk density (kg/m^3)	250	500	500	530
Ash (%)	7	8	8	4

Adsorptive properties	Vapour-phase carbons (wt %)
H_2O capacity at 4.6 mm Hg, 25°C	1
H_2O capacity at 250 mm Hg, 25°C	5–7
n-C_4 capacity at 250 mm Hg, 25°C	25

* From Keller *et al.* 1987, p. 654

adsorption of organic compounds from humid gas streams. In general, however, activated carbons are hydrophobic and organophilic and therefore they are used extensively for adsorbing compounds of low polarity in water treatment, decolourization, solvent recovery and air purification applications. One advantage of activated carbon is that the adsorption of organic molecules tends to be non-specific. One problem with activated carbons however occurs in solvent recovery when ketones are present. Self-heating with these compounds has been known to cause fires in adsorption beds.

Granular activated carbon (GAC) is widely used in water treatment, for example to remove pesticides from potable water. Once exhausted, GAC needs to be removed from the process equipment to be regenerated and reactivated in a special furnace. As an example, the Herreshof furnace is shown in Figure 2.8. It comprises several refractory hearths down through which the carbon passes. The GAC is rabbled across each hearth by rotating arms and is contacted with hot gases flowing upwards through the furnace. The top hearths remove water from the incoming GAC. The hearths progressively further down the furnace pyrolyse organics and at the bottom cause gasification and reactivation to occur. The furnace is usually fed with steam, natural gas and air. The gas atmosphere is a reducing one in order to

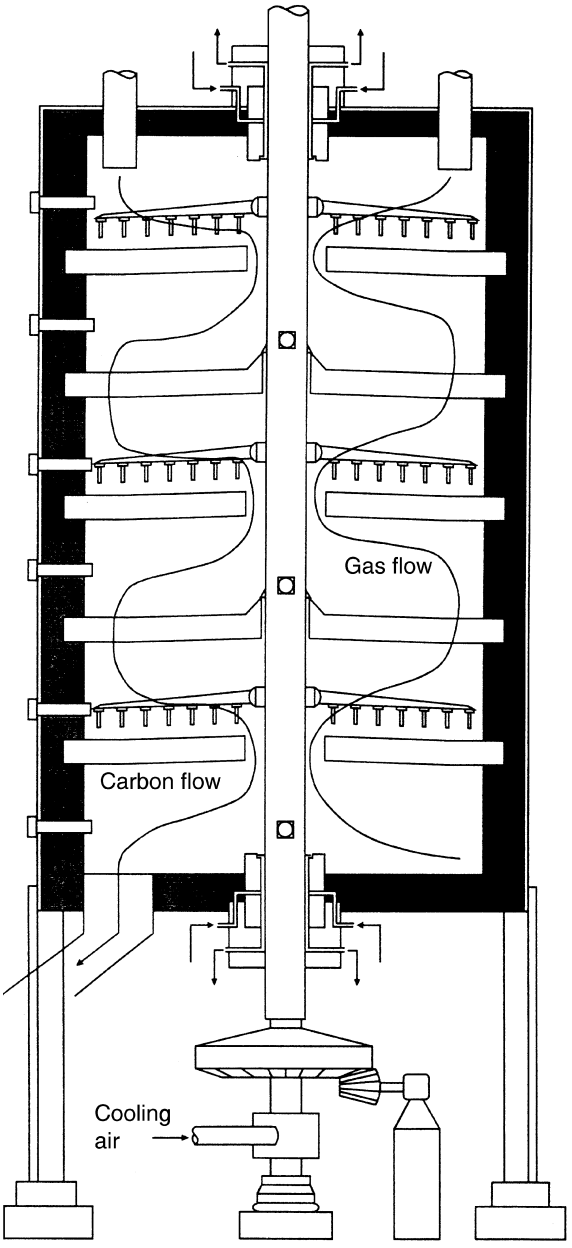

Figure 2.8 *Multiple hearth furnace for the thermal regeneration of granular activated carbon.*

prevent oxidation of the carbon. Being a combustion process, tight controls on environmental discharges are in place and the regeneration process is prescribed for Integrated Pollution Control by the UK's Environment Agency.

In powdered form activated carbon can be used directly, usually in batch applications, but it cannot then be recovered easily for regeneration. Two possibilities exist. First powdered activated carbon can be filtered off in batch processing for subsequent regeneration. Alternatively, it can remain in the sludge in water treament applications for subsequent disposal.

2.2 CARBON MOLECULAR SIEVES (CMS)

Special manufacturing procedures can be used to make amorphous carbons which have a very narrow distribution of pore sizes with effective diameters ranging from 0.4–0.9 nm. Raw materials can be chemicals such as polyvinylidene dichloride and phenolic resin, or naturally occurring materials such as anthracite or hard coals. As shown in Figure 2.9 the pore structure of activated carbons can be modified to produce a molecular sieve carbon by coating the pore mouths with a carbonized or coked thermosetting polymer. In this way, good kinetic properties may be obtained which create the desired selectivity, although the adsorptive capacity is somewhat lower than for activated carbons. The surface is essentially non-polar and the main

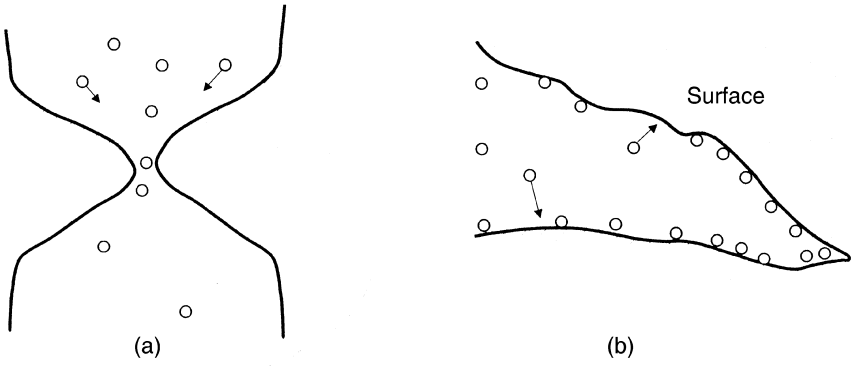

Figure 2.9 *Molecular sieve carbons made by Bergbau-Forschung: (a) Type CMSN2 with bottlenecks near 0.5 nm formed by coke deposition at the pore mouth; (b) Type CMSH2 formed by steam activation (redrawn from Jüntgen et al.* 1981).

process application is the production of high purity nitrogen from air by pressure swing adsorption.

Despite the fact that much of the early work was based on polymeric precursors, the first industrial manifestation of pressure swing adsorption technology with carbon molecular sieves in the 1970s was based on Bergbau Forschung's coal-derived material which was manufactured by modifying the underlying carbon pore structure by depositing carbon in the pore mouths through the cracking of an organic material (Jüntgen *et al.* 1981). This development was followed by a competitive CMS from Japan, which was again based on pore structure modification by carbon deposition but this time using a coconut shell char precursor (Ohsaki and Abe 1984). More recently there has been a resurgence of interest in the production of new CMS materials with the emphasis being placed on higher pore volume precursors combined with the use of chemical vapour deposition using organics such as iso-butylene for improving the oxygen to nitrogen selectivity (Cabrera *et al*. 1993).

2.3 CARBONIZED POLYMERS AND RESINS

Resins such as phenol formaldehyde and highly sulphonated styrene/divinyl benzene macroporous ion exchange resins can be pyrolysed to produce carbonaceous adsorbents which have macro-, meso- and microporosity. Surface areas may range up to 1100 m^2/g. These adsorbents tend to be more hydrophobic than granular activated carbon and therefore one important application is the removal of organic compounds from water.

2.4 BONE CHARCOALS

Animal bones can be carbonized to produce adsorbent materials which have only meso- and macropores and surface areas around 100 m^2/g. The pore development activation step used with activated carbons is dispensed with. The surface is carbon and hydroxyl apatite in roughly equal proportions and this dual nature means that bone charcoals can be used to adsorb metals as well as organic chemicals from aqueous systems. Decolourizing sugar syrup is another application.

2.5 POLYMERIC ADSORBENTS

A broad range of synthetic, non-ionic polymers is available particularly for analytical chromatography applications. For preparative and industrial uses, commercially available resins in bead form (typically 0.5 mm diameter) are based usually on co-polymers of styrene/divinyl benzene and acrylic acid esters/divinyl benzene and have a range of surface polarities. The relevant monomers are emulsion polymerized in the presence of a solvent which dissolves the monomers but which is a poor swelling agent for the polymer. This creates the polymer matrix. Surface areas may range up to 750 m^2/g.

Selective adsorption properties are obtained from the structure, controlled distribution of pore sizes, high surface areas and chemical nature of the matrix. Applications include the recovery of a wide range of solutes from the aqueous phase, including phenol, benzene, toluene, chlorinated organics, PCBs, pesticides, antibiotics, acetone, ethanol, detergents, emulsifiers, dyes, steroids, amino acids, etc. Regeneration may be effected by a variety of methods which include steam desorption, solvent elution, pH change and chemical extraction.

2.6 SILICA GEL

Silica gel is a partially dehydrated polymeric form of colloidal silicic acid with the formula $SiO_2.nH_2O$. This amorphous material comprises spherical particles 2–20 nm in size which aggregate to form the adsorbent with pore sizes in the range 6–25 nm. Surface areas are in the range 100–850 m^2/g, depending on whether the gel is low density or regular density. The surface comprises mainly SiOH and SiOSi groups and, being polar, it can be used to adsorb water, alcohols, phenols, amines, etc. by hydrogen bonding mechanisms. Other commercial applications include the separation of aromatics from paraffins and the chromatographic separation of organic molecules.

At low temperatures the ultimate capacity of silica gel for water is higher than the capacity on alumina or zeolites. At low humidity, however, the capacity of silica gel for moisture is less than that of a zeolitic desiccant. On the other hand, silica gel is more easily regenerated by heating to 150°C than zeolitic materials which need to be heated to about 350°C. Silica gel therefore tends to be used for drying applications in which high capacity is required at low temperature and moderate water vapour pressures. The heat of adsorption of water vapour is about 45 kJ/mol. Silica gel may lose activity through polymerization which involves the surface hydroxyl groups. Typical properties of adsorbent grade silica gel are summarized in Table 2.3.

Table 2.3 *Typical properties of adsorbent-grade silica gel**

	Physical properties
Surface area (m^2/g)	830
Density (kg/m^3)	720
Reactivation temperature (°C)	130–280
Pore volume (% of total)	50–55
Pore size (nm)	1–40
Pore volume (cm^3/g)	0.42
Adsorption properties	Percent by weight
H_2O capacity at 4.6 mm Hg, 25°C	11
H_2O capacity at 17.5 mm Hg, 25°C	35
O_2 capacity at 100 mm Hg, −183°C	22
CO_2 capacity at 250 mm Hg, 25°C	3
n-C_4 capacity at 250 mm Hg, 25°C	17

* From Keller *et al.* 1987, p. 652

2.7 ACTIVATED ALUMINA

Activated alumina is a porous high area form of aluminium oxide with the formula $Al_2O_3.nH_2O$. Its surface is more polar than that of silica gel and, reflecting the amphoteric nature of aluminium, has both acidic and basic characteristics. Surface areas are in the range 250–350 m^2/g. Because activated alumina has a higher capacity for water than silica gel at elevated temperatures it is used mainly as a desiccant for warm gases including air but in many commercial applications it has now been replaced by zeolitic materials. Gases for which activated alumina is suitable include argon, helium, hydrogen, low molecular weight alkanes (C_1–C_3), chlorine, hydrogen chloride, sulphur dioxide, ammonia and fluoroalkanes. Other uses for activated alumina include chromatography and drying of liquids such as kerosene, aromatics, gasoline fractions and chlorinated hydrocarbons.

2.8 CLAY MATERIALS

Like zeolites, clays can be synthesized or taken from natural deposits. Unlike zeolites however, they comprise layer silicates which imbibe guest molecules between their siliceous layers causing their crystals to swell. Fuller's earth is an activated natural montmorillonite. Its pore size is altered and its surface area increased by acid treatment to 150–250 m^2/g. It is

relatively inexpensive and can be used for re-refining edible and mineral oils, adsorbing toxic chemicals, removing pigments, etc. The cationic forms are capable of adsorbing a range of polar molecules and non-polar molecules if some water is present.

The spaces between the natural layers can be enlarged to form pillared interlayered clays. This is carried out by ion exchanging the charge compensation cations with polynuclear metal ion hydro-complexes which are formed in hydrolysed solutions of polyvalent metal ions such as Al(III) or Zr(IV). The polynuclear cations dehydrate on calcination to create metal oxide clusters which act as pillars between the clay layers and create spaces of molecular dimensions. Example separations with pillared clays include the separation of oxygen and nitrogen, and the separation of isomers.

2.9 ZEOLITES

Zeolites are porous crystalline aluminosilicates which comprise assemblies of SiO_4 and AlO_4 tetrahedra joined together through the sharing of oxygen atoms. More than 150 synthetic zeolite types are known, the most important commercially being the synthetic types A and X, synthetic mordenite and their ion-exchanged varieties. Of the 40 or so mineral zeolites the most important commercially are chabazite, faujasite and mordenite. Cavities (or cages) are contained within the framework of a zeolite and are connected by regular channels (pores) which are of molecular dimensions and into which adsorbate molecules can penetrate. In crystal form, zeolites are distinct from other adsorbents in that, for each type, there is no distribution of pore size because the crystal lattice into which the adsorbate molecules can or cannot enter is precisely uniform. The internal porosity is high and thus the majority of adsorption takes place internally. For this reason zeolites are capable of separating effectively on the basis of size and they have been assigned the popular description of molecular sieves. The processes of adsorption and desorption of molecules in zeolites are based on differences in molecular size, shape and other properties such as polarity. For physical adsorption the cavities fill and empty reversibly and the mechanism is generally considered to be one of pore filling. Hence the surface area concepts presented for other types of adsorbent strictly do not apply.

The channel size is determined by the number of atoms which form the apertures (or windows) leading to the cages. For example, apertures may be constructed from rings of 6, 8, 10 or 12 oxygen atoms together with the same number of aluminium and/or silicon atoms. Cages formed with 6 oxygen atom apertures can admit only the smallest molecules such as water and ammonia. Zeolites containing 8, 10 and 12 oxygen atom rings have limiting

aperture sizes of 0.42, 0.57 and 0.74 nm, respectively, and are penetrable by molecules of increasing size. It is possible for molecules slightly larger than the aperture size to gain access to the cavities because of the vibration of molecules and of the crystal lattice. Figure 2.10 shows a schematic representation of the framework structure of zeolite A and the faujasite analogues X and Y. A fuller introduction to the structures of different zeolite types is provided by Ruthven (1984).

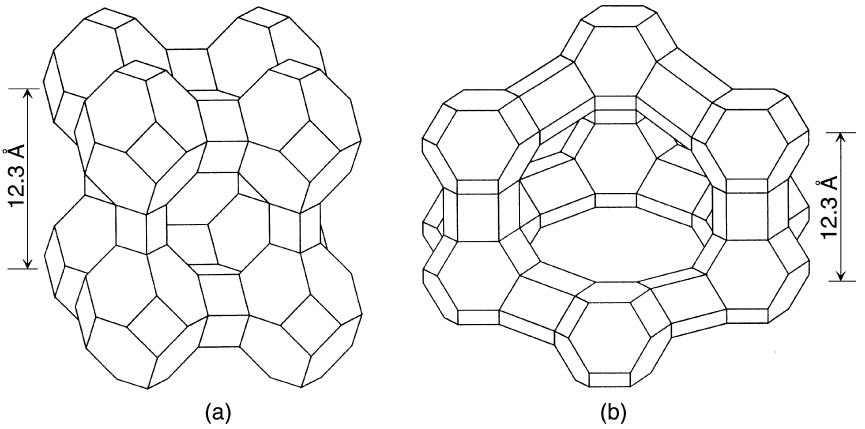

Figure 2.10 *Schematic representation showing the framework structure of (a) zeolite A and (b) zeolites X and Y (redrawn from Ruthven 1984, p. 13).*

The empirical formula of a zeolite framework is $M_{2/n}.Al_2O_3.xSiO_2.yH_2O$ where x is greater than or equal to 2, n is the cation valency and y represents the water contained in the cavities. The water can be reversibly removed by heating leaving a microporous structure which may account for up to 50% of the crystals by volume. The ratio of oxygen atoms to combined silicon and aluminium atoms is always equal to two and therefore each aluminium atom introduces a negative charge on the zeolite framework which is balanced by that of an exchangeable cation. Changing the position and type of the cation changes the channel size and properties of the zeolite, including its selectivity in a given chemical system. The positions occupied by cations in a framework depend on the number of cations per unit cell. Considering type A zeolite as an example, all cations can be accommodated at sites within the cages if Ca^{2+} is the cation. Replacing Ca^{2+} by Na^{+} increases the number of cations per unit cell. In this case the additional cations are accommodated in sites within the eight rings of the apertures so that the windows become partially obstructed

and the channel size is reduced to 0.38 nm. If the Ca^{2+} is replaced by K^+ then the larger cation reduces the channel size even further to 0.3 nm.

In addition to changes to the cationic structure, the Si/Al ratio can be varied during manufacture from unity to well over 1000. Thus zeolites with widely different adsorptive properties may be tailored by the appropriate choice of framework structure, cationic form and silica to alumina ratio in order to achieve the selectivity required for a given separation. Many zeolites are extremely polar and therefore separations may be effected using both molecular sieving and internal surface property effects. The kinetic selectivity is determined from the free diameters of the windows in the intra-crystalline channel structure. Examples of such diameters, together with the principal properties and main uses of zeolites, are given in Table 2.4.

Table 2.4 *Some important applications of zeolite adsorbents**

Framework	*Cationic form*	*Formula of typical unit cell*	*Window*	*Effective channel diameter (nm)*	*Application*
	Na	$Na_{12}[(A10_2)_{12}(SiO_2)_{12}]$	8-ring (obstructed)	0.38	Desiccant. CO_2 removal from natural gas
A	Ca	$Ca_5Na_2[(A10_2)_{12}(SiO_2)_{12}]$	8-ring (free)	0.44	Linear paraffin separation. Air separation
	K	$K_{12}[(A10_2)_{12}(SiO_2)_{12}]$	8-ring (obstructed)	0.29	Drying of cracked gas containing C_2H_4, etc.
	Na	$Na_{86}[(A10_2)_{86}(SiO_2)_{106}]$	12-ring	0.84	Pressure swing H_2 purification
X	Ca	$Ca_{40}Na_6[(A10_2)_{86}(SiO_2)_{106}]$	12-ring	0.80	Removal of mercaptans from natural gas
	Sr, Ba[a]	$Sr_{21}Ba_{22}[(A10_2)_{86}(SiO_2)_{106}]$	12-ring	0.80	Xylene separation
	Na	$Na_{56}[(A10_2)_{56}(SiO_2)_{136}]$	12-ring	0.80	Xylene separation
Y	K	$K_{56}[(A10_2)_{56}(SiO_2)_{136}]$	12-ring	0.80	Xylene separation
Mordenite	Ag	$Ag_8[(A10_2)_8(SiO_2)_{40}]$	12-ring	0.70	I and Kr removal from nuclear off-gases
	H	$H_8[(A10_2)_8(SiO_2)_{40}]$			
Silicalite	—	$(Si0_2)_{96}$	10-ring	0.60	Removal of organics from water
ZSM-5	Na	$Na_3[(A10_2)_3(SiO_2)_{93}]$	10-ring	0.60	Xylene separation

[a] Also K-BaX

* Adapted from Ruthven 1984, p. 25

The ionic nature of most zeolites means that they have a high affinity for water and other polar molecules such as carbon dioxide and hydrogen sulphide. However, as the silica-to-alumina ratio is increased the material can become hydrophobic. Silicalite, a pentasilzeolite, effectively contains no aluminium and, as with de-aluminized Y-type zeolite, can be used to remove hydrocarbons from aqueous systems and from humid gases. They therefore find applications in the removal of volatile organic compounds from air. As an alternative to activated carbons high silica zeolites have several advantages. First, they can be used at relatively high humidities. Carbons take up appreciable quantities of moisture at high humidity thereby limiting their effectiveness for VOC control. Secondly, zeolites are inorganic and hence they can be regenerated in air, subject to flammability considerations. Thirdly, high silica zeolites do not show catalytic activity and problems of heating with ketones do not arise as with carbons.

Commercially available synthetic zeolites are generally produced via the following sequence of steps: synthesis, pelletization and calcination. Synthesis is carried out under hydrothermal conditions, i.e. crystallization from aqueous systems containing various types of reactant. Gels are crystallized in closed systems at temperatures which vary between room temperature and 200°C. The time required may vary from a few hours to several days. The crystals are filtered, washed, ion exchanged (if required) and then mixed with a suitable clay binder. The pellets are then formed, usually as spheres or extrudates before being dried and fired to provide the final product. The binder must provide the maximum resistance to attrition while facilitating the diffusion of adsorbates into the microporous interior.

2.10 SELECTION OF AN ADSORBENT

The property which is most commonly studied initially is the equilibrium isotherm(s) for the chemical system to be separated or purified. Equilibrium data is required for the temperature and pressure ranges of interest and must be obtained experimentally if it is not available from the adsorbent vendor. Isotherms for the pure species provide an indication of the suitability of an adsorbent for a particular separation but care needs to be taken when interpreting information when more than one species is to be adsorbed. If the equilibrium data indicates that an adsorbent might be suitable for the desired separation then it is necessary to determine whether the kinetic properties are appropriate. Even though most separations are effected because of the equilibrium effect it is still necessary to ensure that the rate of

uptake of the adsorbates is suitable and that the appropriate purities can be achieved. Again recourse may need to be given to experimentation if the adsorbent vendor cannot supply the kinetic information. Further information on equilibria and kinetics is provided in Chapters 3 and 4, respectively.

Given that the equilibria and kinetics of adsorption are appropriate, consideration must next be given to the means by which the adsorbent is going to be regenerated, if it is not to be discarded after use. Depending on the process application, regeneration can be effected by changing the pressure and/or the temperature or by some other physical or chemical alteration to the system. Further information is provided in Chapter 5. Consideration must also be given to factors such as the strength of the adsorbent, its chemical resistance, its resistance to coking, etc., as well as to its availability and price.

Finally, Table 2.5 lists typical applications of common types of adsorbent. A few of the applications are described in detail in Chapter 7.

Table 2.5 *Typical applications of commercial adsorbents*

Type	*Typical applications*
Silica Gel	Drying of gases, refrigerants, organic solvents, transformer oils Desiccant in packings and double glazing Dew point control of natural gas
Activated alumina	Drying of gases, organic solvents, transformer oils Removal of HCI from hydrogen Removal of fluorine and boron-fluorine compounds in alkylation processes
Carbons	Nitrogen from air Hydrogen from syn-gas and hydrogenation processes Ethene from methane and hydrogen Vinyl chloride monomer (VCM) from air Removal of odours from gases Recovery of solvent vapours Removal of SO_x and NO_x Purification of helium Clean-up of nuclear off-gases Decolourizing of syrups, sugars and molasses Water purification, including removal of phenol, halogenated compounds, pesticides, caprolactam, chlorine

Table 2.5 *cont.*

Type	*Typical applications*
Zeolites	Oxygen from air Drying of gases Removing water from azeotropes Sweetening sour gases and liquids Purification of hydrogen Separation of ammonia and hydrogen Recovery of carbon dioxide Separation of oxygen and argon Removal of acetylene, propane and butane from air Separation of xylenes and ethyl benzene Separation of normal from branched paraffins Separation of olefins and aromatics from paraffins Recovery of carbon monoxide from methane and hydrogen Purification of nuclear off-gases Separation of cresols Drying of refrigerants and organic liquids Separation of solvent systems Purification of silanes Pollution control, including removal of Hg, NO_x and SO_x from gases Recovery of fructose from corn syrup
Polymers and resins	Water purification, including removal of phenol, chlorophenols, ketones, alcohols, aromatics, aniline, indene, polynuclear aromatics, nitro- and chlor-aromatics, PCBs, pesticides, antibiotics, detergents, emulsifiers, wetting agents, kraftmill effluents, dyestuffs Recovery and purification of steroids, amino acids and polypeptides Separation of fatty acids from water and toluene Separation of aromatics from aliphatics Separation of hydroquinone from monomers Recovery of proteins and enzymes Removal of colours from syrups Removal of organics from hydrogen peroxide
Clays (acid treated and pillared)	Treatment of edible oils Removal of organic pigments Refining of mineral oils Removal of polychlorinated biphenyls (PCBs)

REFERENCES

Cabrera, A. L., Zehner, J. E., Coe, C. G., Gaffney, T. R., Farris, T. S. and Armor, J. N. (1993) *Carbon*, **31**, 969

Crittenden, B. D. (1992) Selective adsorption – a maturing but poorly understood technology, in *Current Best Practice in Separations Technology*, The R&D Clearing House, London, pp. 4.17/18

Gioffre, A. J. (1989) Molecular sieves and abscents, a new approach to odour control, UOP literature reprinted from *Nonwoven's World*, August, 1989

Jüntgen, H., Knoblauch, K. and Harder, K. (1981) *Fuel*, **60**, 817

Keller II, G. E., Anderson, R. A. and Yon, C. M. (1987) Adsorption, Chapter 12 in *Handbook of Separation Process Technology* (edited by R. W. Rousseau), Wiley-Interscience, New York

Ohsaki, T. and Abe, S. (1984) Kuraray Chemical Company, US patent 4,458,022

Ruthven, D. M. (1984) *Principles of Adsorption and Adsorption Processes*, Chapter 1, Wiley-Interscience, New York

Yang, R. T. (1987) *Gas Separation by Adsorption Processes*, Butterworths, Boston

3

Fundamentals of adsorption equilibria

The phenomenon of adsorption – the accumulation of concentration at a surface – is essentially an attraction of adsorbate molecules (a gaseous or liquid component) to an adsorbent surface (a porous solid). Interaction between adsorbate and adsorbent consists of molecular forces embracing permanent dipole, induced dipole and quadrupole electrostatic effects, otherwise known as van der Waal's forces. The preferential concentration of molecules in the proximity of a surface arises because the surface forces of an adsorbent solid are unsaturated. Both short range (repulsive) and longer range (attractive) forces between adsorbate and adsorbent become balanced when adsorption occurs. For reasons which will be revealed later, adsorption is nearly always an exothermic process. Physical adsorption (as distinct from chemisorption involving the sharing or exchange of electrons between adsorbate and adsorbent) of a gas or vapour is normally characterized by the liberation of between 10 and 40 kJ mol^{-1} of heat which is close to values associated with heats of liquefaction of gases. The heat evolved on adsorption of a solute onto a solid from a liquid, however, is strongly dependent on the source and history of the solid adsorbent. Nevertheless the heat evolved when a porous solid is immersed in a liquid solvent containing an adsorbable solute is of the same order of magnitude as the heat of adsorption of a saturated vapour onto a porous solid.

3.1 FORCES AND ENERGETICS OF ADSORPTION

When a molecule having three degrees of freedom of translation approaches an unsaturated surface, at least one degree of freedom of translation is lost as a consequence of its attraction to the surface where it is constrained to movement across the adsorbent surface. In principle, at least, the force fields associated with gas phase molecules as they approach one another can be calculated by means of the Lennard-Jones (1928, 1932) potential energy equation incorporating a term arising from molecular attractive forces (inversely proportional to the sixth power of the separation distance between molecules) and a repulsive force (inversely proportional to the twelfth power of the separation distance). Constants multiplying each of these terms are derived from molecular susceptibilities and polarizabilities deduced from spectroscopic data. Clearly, when an adsorbate molecule approaches a solid adsorbent surface, the molecule interacts with a large assemblage of atoms in the crystal lattice of the adsorbent simultaneously. Despite such difficulties, the potential energies (and hence heats of adsorption) of the vapours of non-polar substances on graphitized carbon black have been calculated (Kiselev 1960) using semi-empirical formulations of the potential energy function. Kiselev (1971) was also successful in computing heats of adsorption of gases in the cages of zeolite structures.

Although it is beyond the scope of this chapter to outline any of the detail of force field calculations, it is instructive to see from Figure 3.1 how the potential energy curves of an adsorbate–adsorbent system relate to experimental heats of adsorption. The potential energy function $U(r)$ (the sum of all interactions between an adsorbate molecule and molecules in the lattice of the adsorbent) passes through a minimum known as the potential well, the depth $U(r_0)$ of which is the energy of adsorption at a temperature of absolute zero. The depth corresponds to several kilojoules per mole. For a given adsorbate–adsorbent system $U(r_0)$ equates closely with measured heats of adsorption. Such heats of adsorption can be measured from calorimetric experiments or adsorption isotherms and isobars. Physical adsorption is an exothermic process and heat is always released when adsorption occurs. That this is always the case may be justified thermodynamically. When any spontaneous process occurs (physical adsorption of a gas at a porous surface is one such instance) there is a decrease in Gibbs free energy ($\Delta G < 0$). Further, there must also be a decrease in entropy because the gaseous molecules lose at least one degree of freedom (of translation) when adsorbed. It follows then from the thermodynamic expression

$$\Delta G = \Delta H - T\Delta S$$

that ΔH also decreases (that is, heat is released).

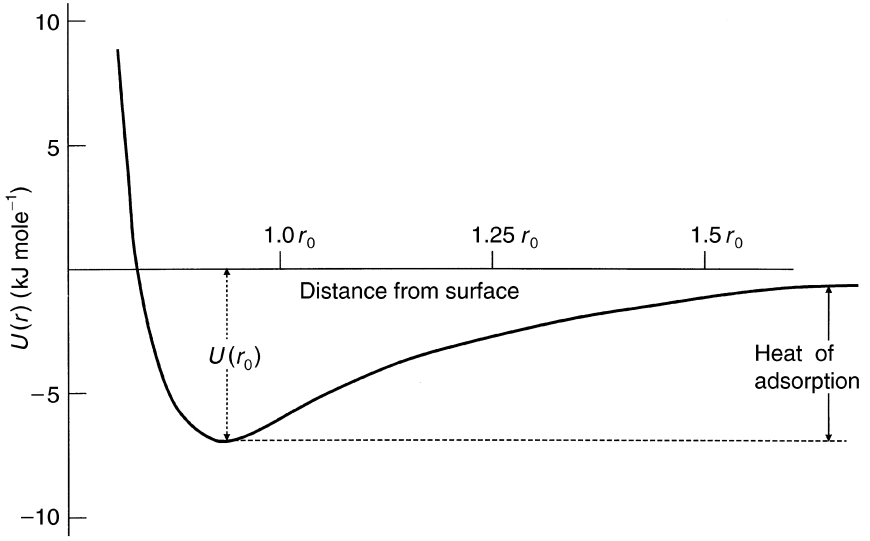

Figure 3.1 *Potential energy diagram for adsorption*

3.2 EXPERIMENTAL ADSORPTION ISOTHERMS

If a quantity q of a gas or vapour is adsorbed by a porous solid at constant temperature and the steady state equilibrium partial pressure is p (or concentration c) then the function $q(p)$ is the adsorption isotherm. Isotherms can take one of several forms (known as types I to V) illustrated by Figure 3.2. Each of these types is observed in practice but by far the most common are types I, II and IV. An inherent property of type I isotherms is that adsorption is limited to the completion of a single monolayer of adsorbate at the adsorbent surface. Type I isotherms are observed for the adsorption of gases on microporous solids whose pore sizes are not much larger than the molecular diameter of the adsorbate; complete filling of these narrow pores then corresponds to the completion of a molecular monolayer. Type II isotherms do not exhibit a saturation limit. Near to the first point of inflexion of such isotherms a monolayer is completed following which adsorption occurs in successive layers. Adsorbents which have a wide distribution of pore sizes form type II isotherms, condensation of the adsorbate vapour occurring within the larger pores. The adsorbent displays a higher capacity for adsorption as the adsorbate saturated vapour pressure is approached. Similarly type III isotherms, which are continuously convex with respect to the partial pressure axis, show a steady increase in adsorption

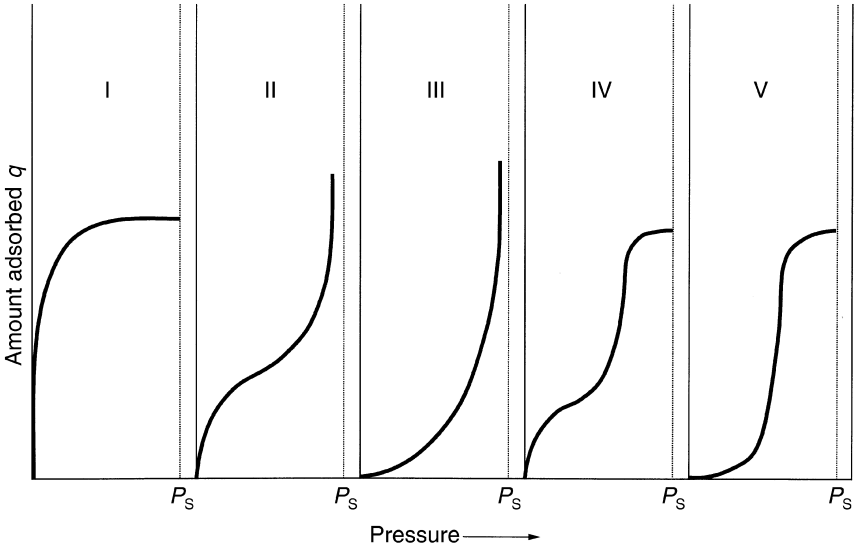

Figure 3.2 *The five types of adsorption isotherm.*

capacity with increasing relative pressure. Type IV isotherms are similar to type II isotherms except that adsorption terminates near to a relative pressure of unity. Type V isotherms are similar to type III isotherms at low relative pressure but then a point of inflexion is reached and a saturation limit is approached as the relative pressure is further increased.

It is not uncommon for isotherms of types II and IV to have a hysteresis loop. Above a relative pressure of about 0.2 many porous adsorbents desorb a larger quantity of vapour at a given relative pressure than the amount corresponding to adsorption. This is illustrated in Figure 3.3a. Everett (1958) showed that such hysteresis loops can provide useful information concerning the geometric shapes of pores in which vapour condensation occurs. Without entering into a discourse on the origin and causes of hysteresis loops, it suffices to say that the underlying reason why such a phenomenon occurs is the way liquid menisci form and disintegrate. When a liquid surface is concave to its own vapour in equilibrium with the liquid, Thompson (1871) showed that the vapour pressure is lower than it would be if the liquid surface were planar. This becomes a significant point when considering condensation of a vapour within narrow pores and capillaries. If μ_0 and μ are the chemical potentials of the vapour above a plane and curved surface, respectively, Thompson deduced, using a thermodynamic argument, that the difference amounted to $R_g T \ln (p_s/p_a)$ where p_s is the saturated vapour

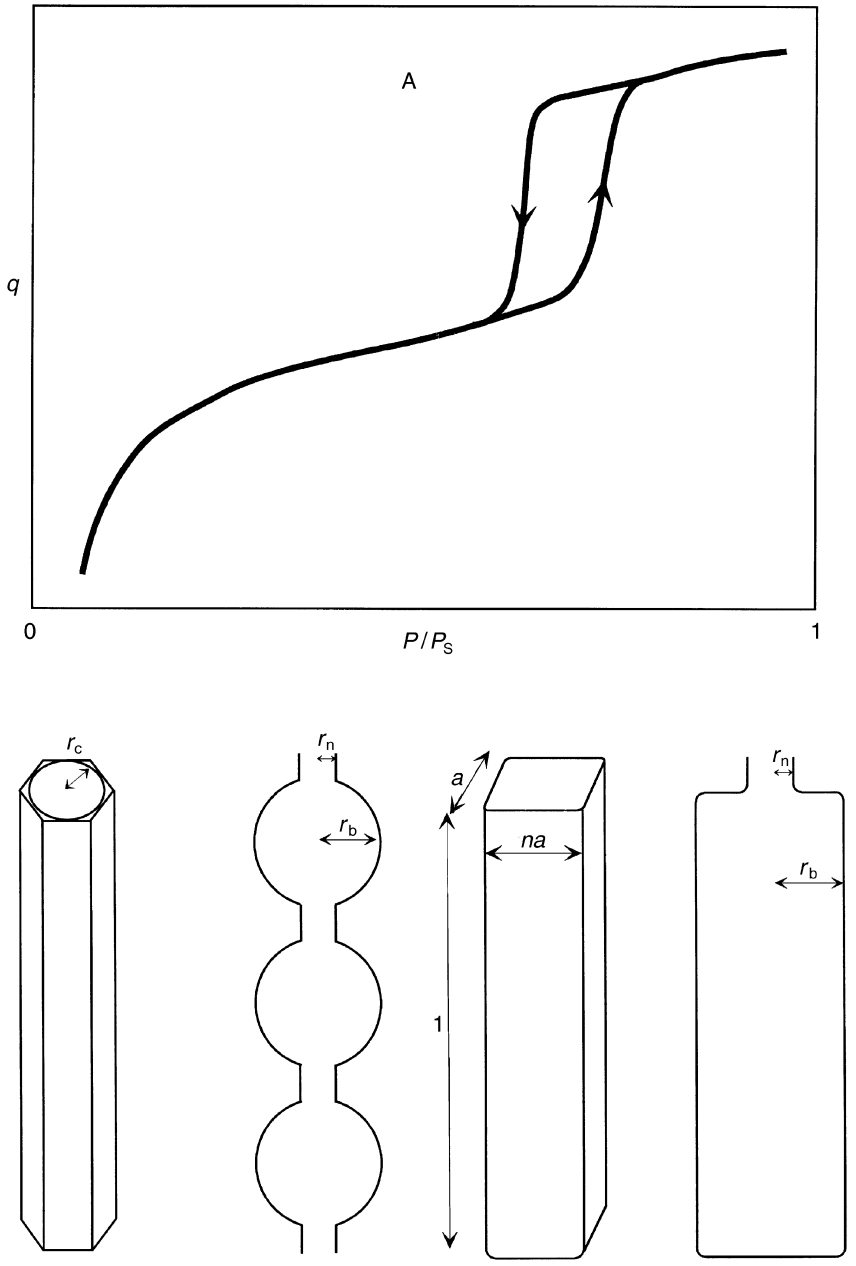

Figure 3.3a *Type A hysteresis loops and possible pore configurations.*

pressure above a plane surface, p_a is that above a curved surface and T is the absolute temperature at which the comparison is made. Now if an annular ring of liquid commences to form in a capillary by the condensation of dn moles of vapour, the work done against the liquid surface is $(\mu_0 - \mu)\mathrm{d}n$ and the force stabilizing the liquid condensate is $-\sigma \mathrm{d}A$, where σ is the surface tension of the pure liquid and dA is the consequential decrease in surface area as the annular ring of liquid increases. Equating the work done to the stabilizing force

$$R_g T \ln (p_s/p_a)\mathrm{d}n = -\sigma \mathrm{d}A \tag{3.1}$$

If the pore in which condensation occurs is an open-ended cylindrical capillary then dA is $2\pi l \mathrm{d}r$ where l is the capillary length and dr is the increase in the radius of the annular liquid film. The number of moles dn transferred from vapour to liquid will be $2\pi l r \mathrm{d}r/V_m$ where V_m is the molar volume of the liquid. Substituting these quantities into equation (3.1) yields the relation

$$p_a = p_s \exp(-\sigma V_m/rR_gT) \tag{3.2}$$

first formulated by Cohan (1938) to describe the gradual filling of a cylindrical capillary. If the pore geometry is other than that of a cylinder, then dn/dA is different and consequently the right-hand side of equation (3.2) differs accordingly. On desorption the free energy decreases and the pore, now full of liquid condensate, will have a hemispherical meniscus at each end. The number of moles transferred will be $4\pi r^2 \mathrm{d}r/V_m$ and the corresponding decrease in area is $8\pi r \mathrm{d}r$. Equating the stabilizing force to the gain in free energy $(\mu_0 - \mu)\mathrm{d}n$ when desorption occurs at a pressure p_d, the equation

$$p_d = p_s \exp(-2\sigma V_m/rR_gT) \tag{3.3}$$

results, similar to that first proposed by Thompson† (1871) and known as the Kelvin equation. The relationship between the pressure on adsorption p_a and that on desorption p_d from an open-ended cylindrical capillary is thus

$$(p_a/p_s)^2 = (p_d/p_s) \tag{3.4}$$

Whenever p_a and p_d are not coincident the relationship between them depends on the pore geometry. For the ink-bottle shaped closed pores described by McBain (1935) with a neck radius $r_n < r_b$ the radius of the wider body, then $(p_a/p_s)^2 > p_d/p_s$ provided also that $r_b < 2r_n$. On the other hand for open-ended pores with a wider body than neck at each end, $(p_a/p_s)^2 < p_d/p_s$. The above arguments are more fully discussed elsewhere (Thomas and Thomas 1967 and 1997, Gregg and Sing 1967, and Everett 1958) although it should be noted that alternative theories such as that proposed by Foster

†W. T. Thompson (1871) was the distinguished physicist who succeeded to a peerage and took the title Lord Kelvin.

(1952) can account for differences between p_a and p_d exhibited by hysteresis loops. Geometric shapes of pores corresponding to the different classes of hysteresis loop are sketched in Figure 3.3b.

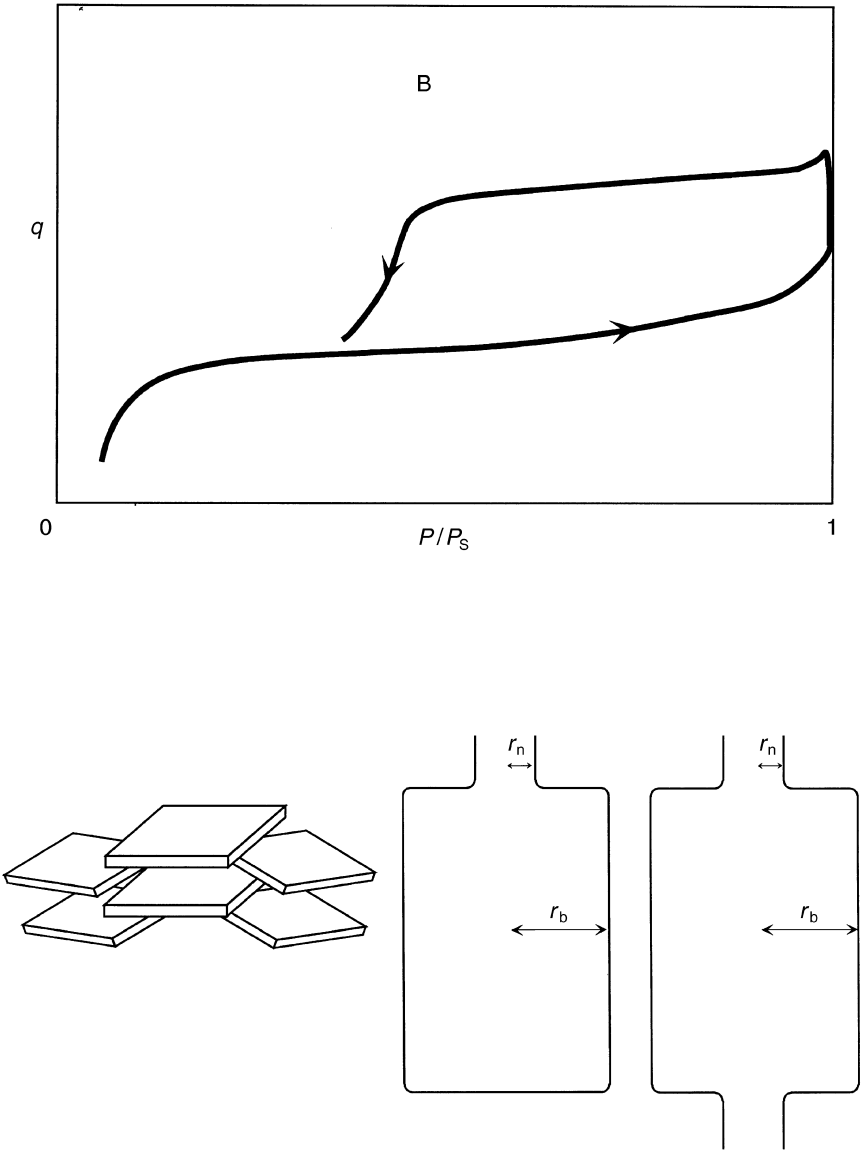

Figure 3.3b *Type B hysteresis loops and possible pore configurations.*

3.3 THEORIES OF ADSORPTION EQUILIBRIA

A variety of different isotherm equations have been proposed, some of which have a theoretical foundation and some being of a more empirical nature. Many of these equations are valid over small relative pressure ranges but do not fit experimental data when tested over the full range of relative pressures. Only those which are commonly used for the description of the physical adsorption of gases or vapours onto the surface of porous adsorbents will be outlined. Some of these theories, as shown later, can be extended to describe the simultaneous adsorption of two or more components.

3.3.1 The Langmuir isotherm

This isotherm describes adsorbate–adsorbent systems in which the extent of adsorbate coverage is limited to one molecular layer at or before a relative pressure of unity is reached. Although the isotherm, proposed originally by Langmuir (1918), is more usually appropriate for the description of chemisorption (when an ionic or covalent chemical bond is formed between adsorbent and adsorbate), the equation is nevertheless obeyed at moderately low coverages by a number of systems and can, moreover, be readily extended to describe the behaviour of binary adsorbate systems. The isotherm was formulated on the basis of a dynamic equilibrium between the adsorbed phase and the gaseous or vapour phase. It was argued that the rate at which adsorbate gas molecules strike a surface of an adsorbent is proportional to the product of the partial pressure p of the gas and the fraction $(1 - \theta)$ of surface remaining uncovered by adsorbate and therefore available as adsorption sites. Langmuir further supposed that the rate of desorption from the surface is directly proportional to the fractional surface coverage θ and that the rates of adsorption and desorption are equal at equilibrium. Thus

$$k_a p\,(1 - \theta) = k_d \theta \tag{3.5}$$

where k_a and k_d are the respective rate constants for adsorption and desorption, respectively. The more usual form of the equation is written

$$\theta = q/q_m = bp/(1 + bp) \tag{3.6}$$

where b is k_a/k_d and q_m is the quantity q of adsorbate adsorbed in a single monolayer. The ratio q/q_m can be measured and expressed in different ways. For the present we will choose to represent the ratio by the number of moles of a component adsorbed compared with the number of moles of that

component which could be adsorbed in a monolayer. Alternative ways to express the ratio are on the basis of volume of gas adsorbed (at NTP) or on a weight basis.

The simple derivation given assumes that a single molecule occupies a single surface site and that there is no lateral interaction between adjacent adsorbed molecules. Application of the kinetic theory of gases reveals that the constant b can be identified as

$$\frac{1}{b} = \frac{\nu}{\sigma}(2\pi mkT)^{1/2} \exp\left(-\frac{Q}{R_g T}\right) \tag{3.7}$$

where ν is the pre-exponential factor of the desorption rate coefficient, σ the condensation coefficient (defined as the fraction of those molecules that are adsorbed with an activation energy greater than the energy of activation for adsorption E_a), m is the mass of the adsorbate molecule, k is the Boltzmann constant and Q the heat of adsorption (the difference between the activation energies E_d and E_a necessary for desorption and adsorption, respectively).

It is important to note the implicit assumptions made in arriving at the Langmuir isotherm. These are (i) the heat of adsorption Q is constant and independent of coverage (a consequence of no lateral interaction between adsorbate molecules), (ii) each adsorbate molecule occupies only one site and (iii) the adsorption is localized (that is molecules remain at the site of adsorption until desorbed).

Examples of gas adsorption onto porous solids which obey the Langmuir equation are CH_4 – sodalite and Ar – sodalite (Barrer and Vaughan 1971). Other systems such as Kr – carbon (Sykes and Thomas 1960) and C_3H_8 – 5A zeolite (Ruthven and Loughlin 1972) show apparent conformity to the Langmuir equation, as indeed do many other gas–solid systems, but on closer examination reveal departures, especially at coverages approaching saturation of the surface and at raised temperatures. Linearization of the Langmuir equation, of which one form is

$$p/q = 1/bq_m + p/q_m \tag{3.8}$$

will yield values of b and q_m. For obedience to the Langmuir isotherm, values derived from the slopes and intercepts of plots of p/q against p should remain constant over a wide range of both partial pressures and temperature, while equation (3.6) should be tested for the full range of coverage from $\theta = 0$ to $\theta = 1$. Figure 3.4 illustrates data for a system which apparently conforms to the Langmuir isotherm.

3.3.2 Henry's law

At low pressures equation (3.6) reduces to the linear form

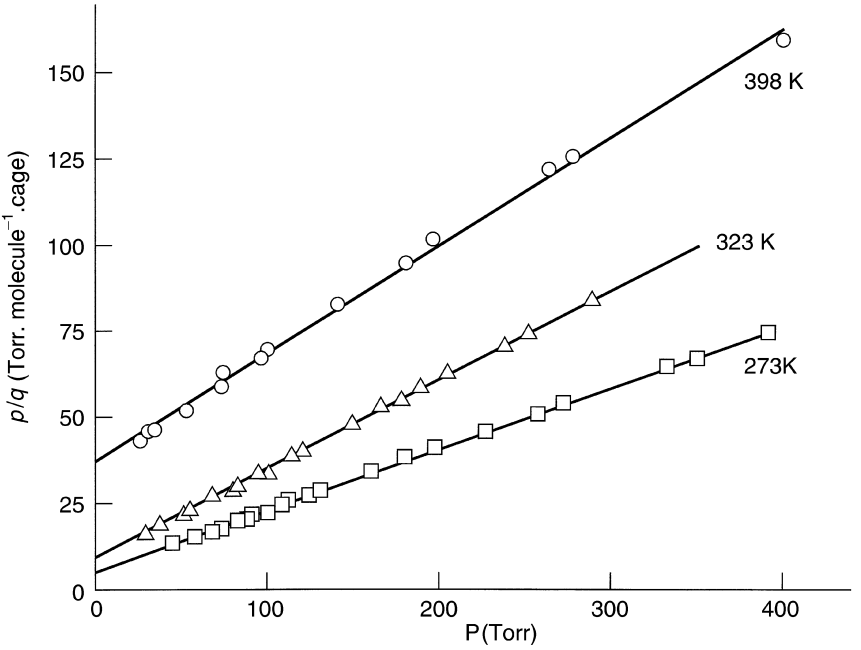

Figure 3.4 *The adsorption of propane on a 5A zeolite apparently obeys a Langmuir isotherm (source: Ruthven and Loughlin 1972).*

$$\theta = q/q_m = bp \tag{3.9}$$

A frequently used form of equation (3.9) is obtained by substituting R_gTc for p assuming the adsorbate obeys the perfect gas laws. Thus

$$q = q_m b R_g T c = K(T)c \tag{3.10}$$

where $K(T)$, which incorporates b and q_m, is known as Henry's constant and is temperature dependent. At constant low coverage the constant b in equation (3.7) is proportional to $T^{-1/2}$ exp (Q/R_gT). It follows then that $K(T)$ is proportional to $T^{1/2}$ exp (Q/R_gT). Neglecting the weak component $T^{1/2}$ of the variable, one obtains

$$\ln K = Q/R_gT \tag{3.11}$$

identical in form to the integrated classic van't Hoff equation. Evaluation of the heat of adsorption Q may thus be obtained from the slope of a plot of ln K against $1/T$ for low coverages. Figure 3.5 shows such a plot for the rare gases adsorbed on a 5A zeolite adsorbent.

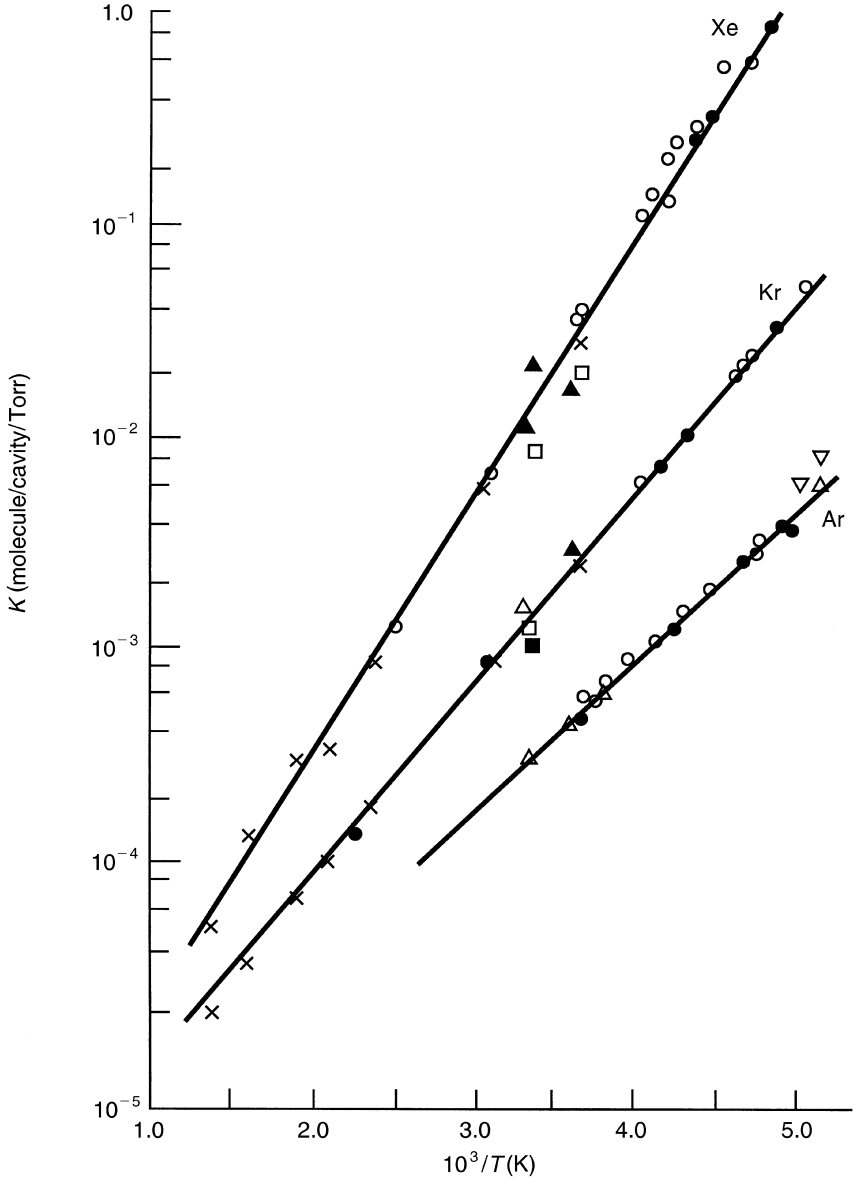

Figure 3.5 *Henry's Law obedience. Data is for Ar, Kr and Xe on a 5A zeolite (source: Derrah and Ruthven 1975).*

3.3.3 The Freundlich isotherm

There is abundant evidence to show that, for many systems, the heat of adsorption decreases in magnitude with increasing extent of adsorption. If the decline in heat of adsorption is logarithmic, it implies that adsorption sites are distributed exponentially with respect to an adsorption energy which differs between groups of adsorption sites. This is precisely the assumption made by Zeldowitch as early as 1935 in his derivation of a now classic isotherm reflecting the variation in heat of adsorption with coverage. The equation obtained by Zeldowitch is synonymous with the well-known Freundlich isotherm, previously considered to be an empirical isotherm. Although the derivation of the isotherm by Laidler (1954) will not be recapitulated here, the theory leads to

$$\ln\theta = \frac{R_g T}{Q_0} \ln p + \text{constant} \tag{3.12}$$

for small values of θ. Q_0 is a constant contained in a term $\exp(Q/Q_0)$ which Zeldowitch introduced to account for the way in which the energy of adsorption sites was distributed. Equation (3.12) may be recast into the familiar Freundlich isotherm

$$\theta = kp^{1/n} \tag{3.13}$$

valid for $n > 1$. Unlike the Langmuir isotherm it does not indicate an adsorption limit when coverage is sufficient to fill a monolayer ($\theta = 1$). The isotherm may be regarded as a convenient representation of the Langmuir equation at intermediate coverages ($0 < \theta < 1$). Application of the Freundlich equation to the adsorption of organic chemicals onto carbons is common and the hybrid Langmuir–Freundlich theory has proved useful in correlating data for the adsorption of gas mixtures.

3.3.4 The Brunauer–Emmett–Teller (BET) equation

Except for type I (Langmuir) isotherms, all the other types referred to in Section 3.2 imply that the extent of adsorption does not reach a limit corresponding to completion of a monolayer. The formation of multilayers, however, is implicit in the theory proposed by Brunauer, Emmett and Teller (1938) who, in agreement with Langmuir, argued that the rate of condensation (adsorption) onto the bare surface equals the rate of evaporation from the first layer of adsorbate. If θ denotes the fraction of surface which is bare and $z_m\,\theta_1$ the number of first layer sites occupied (in which z_m is the number of molecules necessary to complete a monolayer and θ_1 is the corresponding

fraction of sites) then, for dynamic equilibrium between the gas phase at pressure p and the first layer of adsorbate,

$$a_1 p\theta_0 = b_1 z_m \theta_1 e^{-E_1/R_g T} \tag{3.14}$$

In equation (3.14) a_1 is the number of molecules which would successfully condense onto the bare surface per unit time per unit pressure and b_1 is the frequency with which molecules possessing sufficient energy E_1 leave the surface; the term $e^{-E_1/R_g T}$ in the equation is the probability that molecules have an energy greater than E_1 to escape from the first layer. For layers of molecules subsequent to the first layer, the BET theory supposes that the probability of molecules evaporating from those layers is equal and given by $e^{-E_L/R_g T}$, where E_L is identified as the heat of liquefaction. For adsorbed molecules between the layers $(i-1)$ and i, therefore,

$$a_i p\theta_{i-1} = b_i z_m e^{-E_1/R_g T} \qquad i = 2, 3, ..., n \tag{3.15}$$

It is further assumed in the BET theory that a_i/b_i $(= c)$ is constant for a given temperature. The sum $\Sigma_i(i\theta_1)$ from $i = 1$ to $i = n$ is the fractional extent of adsorption (because θ_i is the fraction of occupied sites corresponding to the ith layer which have i molecules stacked one upon the other). The actual number of molecules adsorbed is thus $z_m \Sigma_i(i\theta_i)$. Now the ratio z/z_m is equivalent to the ratio q/q_m of the quantity of adsorbate adsorbed (expressed as either mass or volume at standard temperature and pressure) to the total capacity of the adsorbent. Because the adsorbate vapour totally condenses when the saturated vapour pressure p_s is reached, then $\theta_1 = \theta_2$ when $p = p_s$ and so

$$a_2 p_s = b_2 z_m e^{-E_L/R_g T} \tag{3.16}$$

Following lengthy algebraic manipulation, the BET equation is obtained from equations (3.14), (3.15) and (3.16). In its most useful form the BET equation is written

$$\frac{p}{q(p_s - p)} = \frac{1}{q_m c} + \frac{(c-1)}{q_m c} \cdot \frac{p}{p_s} \tag{3.17}$$

At a fixed temperature a plot of the left-hand side of equation (3.17) against p/p_s would yield a slope $(c-1)/q_m c$ and intercept $1/q_m c$ thus enabling both q_m and c to be determined. The BET equation is extensively applied to the determination of the surface area of porous adsorbents (q.v. Chapter 4).

The inherent assumptions in the BET theory which are important to note are (i) no interaction between neighbouring adsorbed molecules and (ii) the heat evolved during the filling of second and subsequent layers of molecules

equals the heat of liquefaction. Neither of these assumptions is strictly valid, but despite such difficulties, the BET equation has been widely applied as a semi-empirical tool for the investigation of the characteristics of porous adsorbents. By appropriate choice of c and q_m the equation can be made to fit any of the isotherm types II to V inclusive. For small values of p/p_s the BET equation reduces to the Langmuir equation. A typical BET plot (with volume v replacing q as explained in Section 3.3.1) displaying a distinct intercept and slope from which the surface area of the adsorbent may be estimated is shown in Figure 3.6.

3.3.5 Polanyi's Potential Theory

The Potential Theory as originally conceived by Polanyi is well documented in the classic text by Brunauer (1943). Polanyi considered contours of equipotential energy above solid surfaces and ascribed a volume ϕ_i to the space between the ith equipotential surface of energy ε and the adsorbent surface. The potential ε was assumed to be independent of temperature so that $\varepsilon = f(\phi)$ is essentially an isotherm equation. The adsorption potential is defined as the work of compression of the gas from a pressure p to the saturation pressure p_s. For one mole of a perfect gas of volume v in an open thermodynamic system the adsorption potential is therefore

$$\varepsilon = \int_{p}^{p_s} v \, dp = R_g T \ln(p_s/p) \tag{3.18}$$

assuming that the work of creating a liquid surface is small in comparison with the magnitude of ε. The volume in the adsorption space is

$$\phi = nV_m \tag{3.19}$$

where n is the number of moles adsorbed per unit mass of adsorbent and V_m is the molar volume. By plotting ε as a function of ϕ a characteristic curve $\phi(\varepsilon)$ is obtained which represents, for a given adsorbate–adsorbent system, the extent of adsorption at any relative pressure and temperature below the critical temperature of the gas. The validity of the characteristic curve may be extended for application to non-ideal gases and vapours by substituting fugacities, f, for partial pressures.

Two different applications of the potential theory, one for microporous solids and the other for adsorbents with larger pores, have been formulated and will now be briefly considered. Dubinin (1960) related the volume v adsorbed in micropores to the adsorption potential. Earlier, Dubinin and

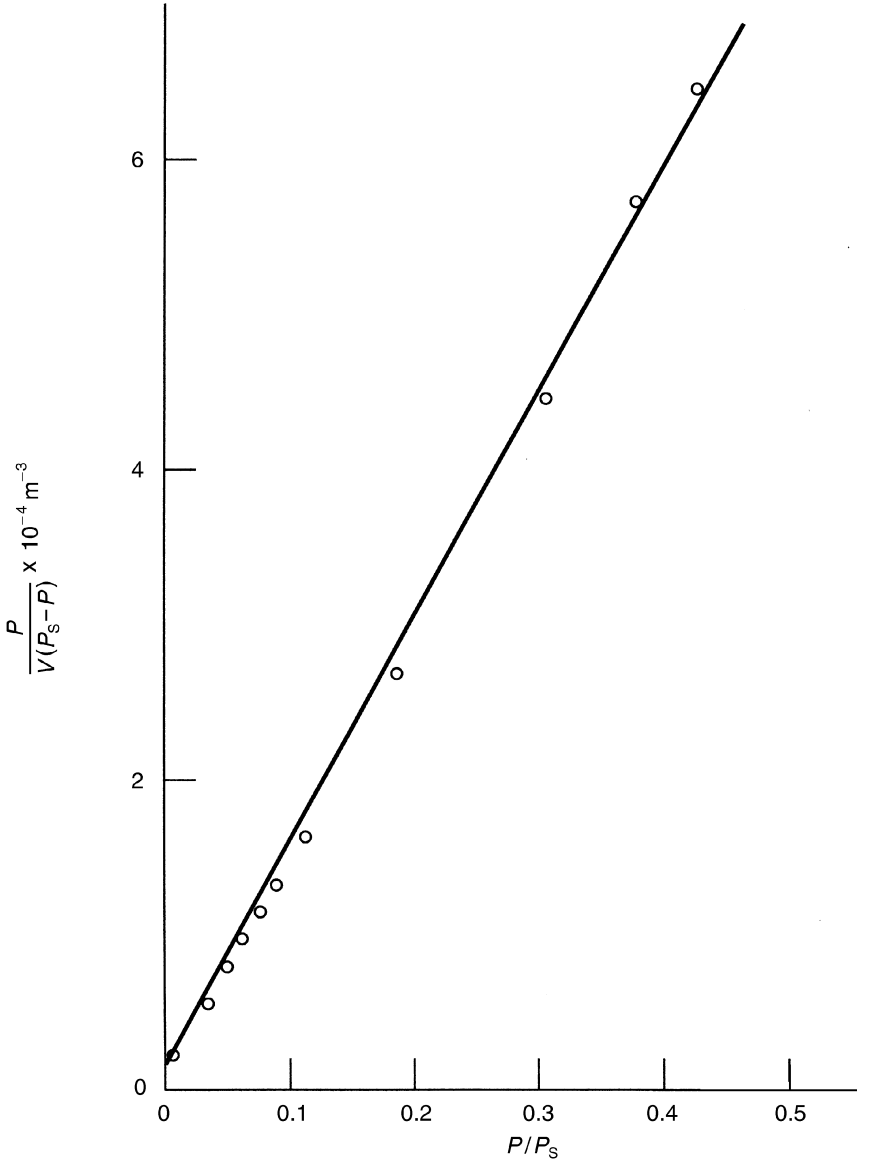

Figure 3.6 *Estimation of monolayer volume from BET plot. Data is for N_2 adsorbed on silica gel at 77 K.*

Radushkevich (1947) found that there is a direct correlation between the molar volume in the liquid state and the affinity coefficient β characterizing the polarizibility of the adsorbate and assumed that $\varepsilon_i/\varepsilon_j = \beta_i/\beta_j = V_{mi}/V_{mj}$. For non-polar and weakly polar adsorbates such a correlation is not always obeyed but, despite this shortcoming, the relationship is utilized in order to force the characteristic curves of all gases on the same adsorbent to be coincident so that now $\varepsilon = \beta f(\theta)$ – a unique method of obtaining a universal isotherm for a given adsorbent.

The semi-empirical equation which Dubinin obtained relating adsorbed volume v to the adsorption potential ε is

$$v/v_0 = \exp(-\kappa\varepsilon^2/\beta^2) \tag{3.20}$$

where v_0 is the total capacity of the adsorbent to adsorb the gas or vapour. Substitution of equation (3.18) into equation (3.20) gives, in logarithmic form,

$$\ln(v/v_0) = -\kappa(R_g T/\beta)^2 \{\ln(p/p_s)\}^2 \tag{3.21}$$

Figure 3.7(a) illustrates a characteristic curve for the adsorption of tetrafluoroethene on charcoal for four different temperatures while Figure 3.7(b) is the corresponding plot of equation (3.21). Dubinin claimed that the volume v_0 represents the micropore volume which can be extracted from equation (3.21) by plotting $\ln(v/v_0)$ against $(\ln p/p_s)^2$.

For pores of larger diameter in which capillary condensation is not important, the term (ε/β) was employed by Dubinin and Radushkevich (1947) in equation (3.18) rather than $(\varepsilon/\beta)^2$ used subsequently by Dubinin (1960). Extensive work by Marsh and Wynne- Jones (1964) and by Lamond and Marsh (1964) on the adsorption of N_2 and CO_2 on porous carbons has enabled the application of equation (3.20), for the determination of monolayer volumes, to be tested. It was shown that a reliable monolayer volume could only be extracted if there is no capillary condensation at low relative pressures. The success which these latter authors achieved in extending the theory of Dubinin and Radushkevich for the determination of monolayer volumes (as opposed to micropore capacities v_o) is attributable to the interpretation by Marsh *et al*. of Foster's (1952) descriptions of the differences between the adsorption potential when micropores and macropores become progressively filled with adsorbate. It emerges that the spontaneous filling of large diameter pores, resulting in capillary condensation, occurs if the adsorption potential is high and the repulsive forces are low. This corresponds to strong adsorbate–adsorbent affinity and weak interaction between successive adsorbate layers.

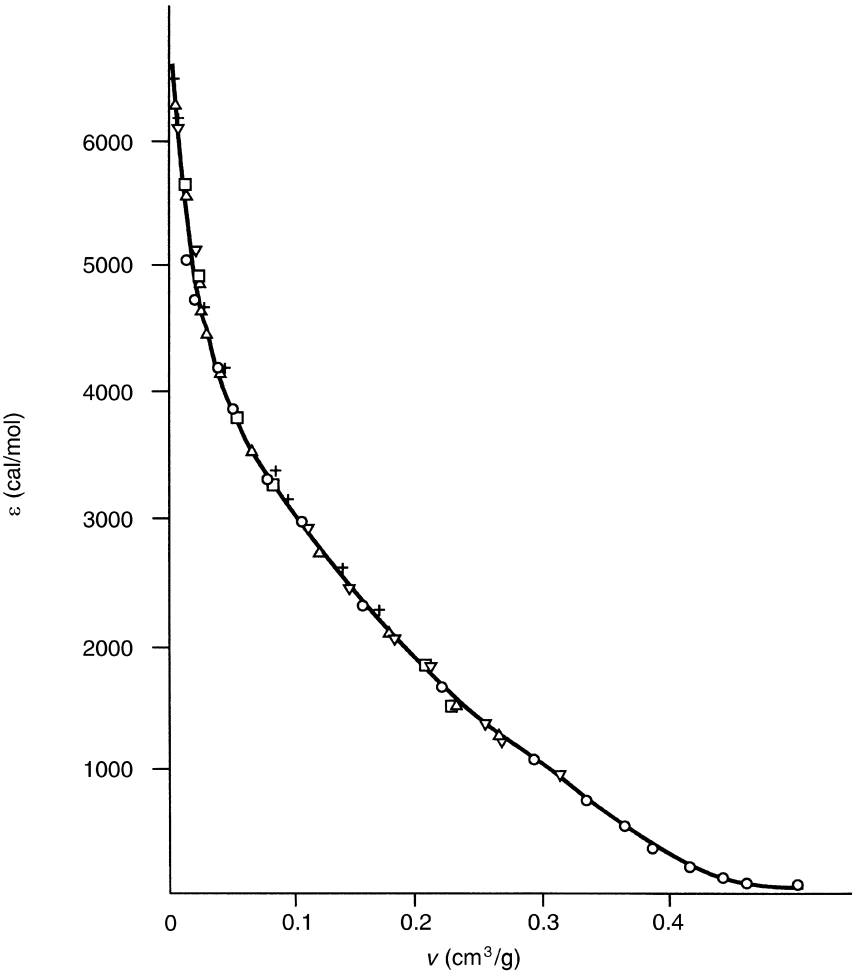

Figure 3.7(a) *(a) Polanyi characteristic curve $\varepsilon(v)$* for C_2F_4 on activated carbon +, 33.3°C (critical temperature); □, 0°C; ▽, −28°C; △, − 40°C; ○, −76.3°C (source: Dubinin 1960, p. 235).

3.3.6 The Gibbs adsorption isotherm

Willard Gibbs (1928), in his comprehensive treatment of the thermodynamics of systems at equilibrium, supposed that the adsorbent is inert in a thermodynamic context. The Gibbs function for a mobile adsorbate (an adsorbate which is not localized at particular adsorption sites)

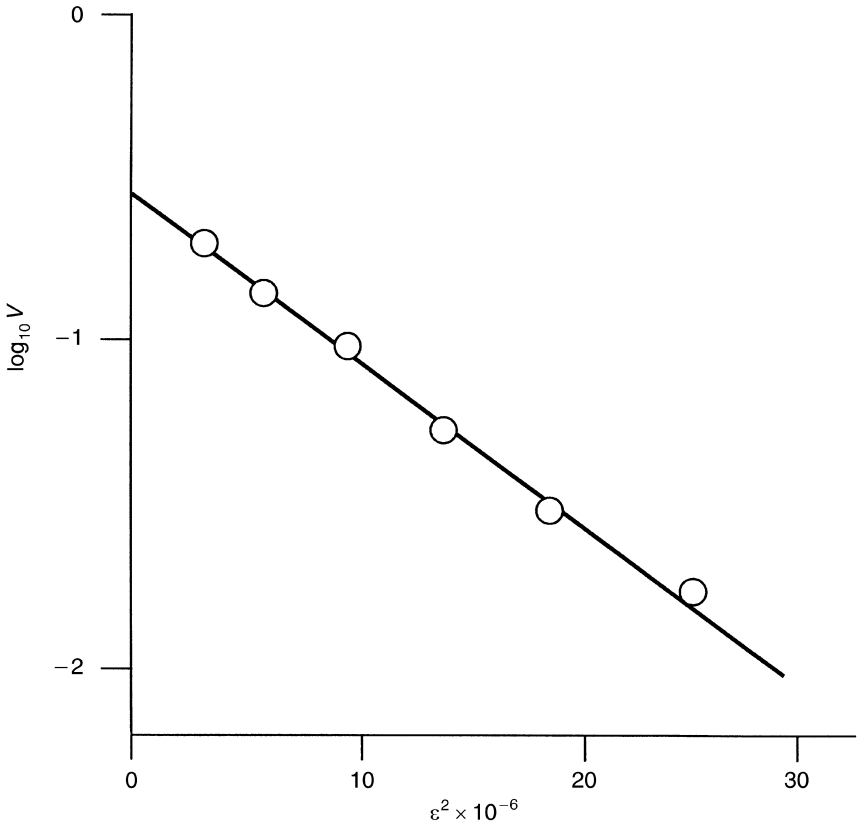

Figure 3.7(b) *log_{10} V* as a function of ε^2 (Dubinin plot) for the same system (as in Fig. 3.7a).

may be represented as $G\ (p,\ T,\ A,\ n)$ where A is the area over which the adsorbate has distributed itself and n is the number of moles of adsorbate on the adsorbent surface. At constant temperature T and pressure p a change in G can be written

$$\mathrm{d}G = \left(\frac{\partial G}{\partial A}\right)_{p,T,n} \mathrm{d}A + \left(\frac{\partial G}{\partial n}\right)_{p,T,A} \mathrm{d}n \tag{3.22}$$

because it is a thermodynamic property which depends on the initial and final states only, and any changes in G can therefore take place along any desired path (in this case an initial change at constant n and subsequently a change at constant A to complete the total change in G). The negative value

of the partial differential $(\partial G/\partial A)_{p,T,n}$ is termed the spreading pressure π while the positive value of $(\partial G/\partial \mathrm{n})_{p,T,A}$ is the chemical potential μ of the adsorbate in the potential field of the adsorbent. The integrated form of equation (3.22) is therefore

$$G = -\pi A + \mu n \tag{3.23}$$

On general differentation we thus obtain

$$\mathrm{d}G = -\pi \mathrm{d}A + A\mathrm{d}\pi + \mu \mathrm{d}n + n\mathrm{d}\mu \tag{3.24}$$

which shows how all the variables A, π, n and μ contribute to a change in G. Subtracting equation (3.24) from (3.20) and writing $(\partial G/\partial A)_{p,T,n} = -\pi$ and $(\partial G/\partial n)_{p,T,A} = \mu$, results in the equation

$$-A\mathrm{d}\pi + n\mathrm{d}\mu = 0 \tag{3.25}$$

Substituting the classic thermodynamic relation $\mu(p)$ for the vapour phase at pressure p,

$$\mathrm{d}\mu = R_\mathrm{g}T\mathrm{d}\ln p \tag{3.26}$$

where p is the partial pressure of the adsorbate, one obtains

$$A\mathrm{d}\pi = nR_\mathrm{g}T\mathrm{d}\ln p \tag{3.27}$$

which is the differential form of the Gibbs adsorption isotherm. In its integral form it becomes

$$\pi = R_\mathrm{g}T \int_0^{p_\mathrm{s}} (n/A)\,\mathrm{d}\ln p = (R_\mathrm{g}T/MS_\mathrm{g}) \int_0^{p_\mathrm{s}} q(p)\,\mathrm{d}\ln p \tag{3.28}$$

in which $q(p)$ is the mass of gas adsorbed per unit mass of adsorbent (a function of partial pressure), M the molecular mass of adsorbate and S_g the surface area per unit mass of adsorbent. Both S_g and $q(p)$ are directly measurable at a given temperature and the integral can be determined by numerical integration. A value for the spreading pressure π may be thus calculated. Alternatively, if the adsorbent surface is a liquid (such as a fatty acid film on water) then the surface area of the liquid film can be found by independent measurements of the isotherm $q(p)$ and spreading pressure π. The latter quantity can be measured using an ingenious device known as the Langmuir trough which enables the liquid film to be confined between barriers on the liquid surface and hence defining its area; the force necessary to keep the liquid film coherent is measured by means of a balance upon which weights are placed.

If an equation of state relating π, A and T is specified then substitution into equation (3.27) followed by integration leads directly to a relation between π and p. The simplest equation of state is $\pi A = nR_gT$, analogous to the perfect gas law, and it is a simple matter to show that this equation of state substituted into the differential form of the Gibbs isotherm leads to Henry's law (q.v. Section 3.3.2). If, on the other hand, $(A - \alpha)$ replaces A in the equation of state (therefore allowing for the total extent, α, of area which the adsorbate molecules occupy), the result of substitution in equation (3.27) is Volmer's isotherm

$$bp = [\theta/(1-\theta)][\exp(\theta/1-\theta)] \tag{3.29}$$

provided the integration constant is defined so that Henry's law ($\theta = bp$) is obeyed as the pressure tends to zero and θ is assumed to equal α/A.

3.3.7 Statistical thermodynamic model

Although it is beyond the scope of this chapter to discuss details of the statistical thermodynamic approach to the formulation of isotherms, it is nevertheless important to point out that there has been some success (Ruthven 1984, Ruthven and Wong 1985) in applying the theory to the adsorption of gases in regular cage-like structures of zeolites. The well-defined cages with well-defined interconnecting channels can be considered as independent subsystems so that interaction between molecules adsorbed in neighbouring cages can be ignored. Each cage will only adsorb a limited number of adsorbate molecules. The so-called grand partition function is then formulated which describes how the potential energy of molecules within the cage is distributed. For this purpose a configurational integral is written which is the integral of the exponential of the negative value of potential energies over the position of each and every molecule within the cage. A Lennard-Jones potential is employed as the potential energy function. Ruthven (1971) and Barrer (1978) assumed that the sorbate behaves as a van der Waals gas and thus accounted for the reduction in free volume caused by the presence of the adsorbate molecules. The configurational integral was thus greatly simplified and results in an expression for the number of sorbate molecules per cage. As the number of cages is known from the structure of the zeolite, the result can be expressed as an isotherm which takes the form

$$\bar{s} = \frac{Kp + A_2(Kp)^2 + \ldots A_n(Kp)^n/(n-1)!}{1 + Kp + A_2(Kp)^2/2! \ldots A_n(Kp)^n/n!} \tag{3.30}$$

where $\bar{s}$ is the average number of molecules per zeolite cage, K is Henry's

constant (Section 3.3.2) and $A_s = (1 - s\alpha/v)^s$ identifies each adsorbate molecule from $s = 2$ to $s = n$, the maximum number of molecules in the cage. α and v are the effective volume of an adsorbate molecule and the cage volume, respectively. When $v \leq 2\alpha$ only one molecule per cage can be accommodated and equation (3.30) reduces to the Langmuir equation. When v/α is sufficiently large there would be free mobility of adsorbate throughout the zeolite structure. A family of curves, with q_s the quantity of adsorbate at full saturation as parameter, is obtained when q/q_s is plotted as a function of Kp. When $q_s = 1$ a form equivalent to the Langmuir equation (3.6) is obtained and when $q_s = \infty$ a form equivalent to the Volmer equation (3.29) is obtained.

3.4 ADSORPTION OF GASEOUS MIXTURES

The techniques used to obtain single-component experimental isotherms (see Chapter 4) may also be employed to gather data for multicomponent isotherms with the additional premise that for every quantity of adsorbate mixture adsorbed by the adsorbent the composition of the gas phase must be determined. Thus, collecting experimental data for multicomponent gaseous mixtures is very time-consuming. It has become customary, however, to employ single-component adsorption data to predict the adsorption properties of a binary or multicomponent gaseous mixture. Success has been achieved for some binary gas mixtures although it is by no means reasonable to assume that the methods of prediction to be described are in any way universal.

Correlations based upon the Langmuir, Polanyi and Gibbs theories for the adsorption of gases have emerged and the statistical thermodynamic approach outlined by Ruthven has also been extended to incorporate the adsorption of gaseous mixtures. Each of these different approaches is described in the following sections and their relative applicability and constraints noted.

3.4.1 The Extended Langmuir equation

The Langmuir isotherm can easily be extended to apply to gaseous mixtures by simply assuming, as an additional constraint to those which are explicit in the Langmuir theory, that for each gaseous component an equilibrium exists between the amount adsorbed at the surface and the partial pressure of that component in the gas phase. Fractional coverage θ_i and partial pressure p_i are ascribed to each of the components, the total surface coverage being the

sum of coverages of the individual components. The resulting isotherm for component i is

$$\theta_i \left(= \frac{q_i}{q_{\mathrm{m}i}} \right) = \frac{b_i p_i}{1 + \sum_1^n b_i p_i} \tag{3.31}$$

where $q_{\mathrm{m}i}$ is the quantity of component i in a monolayer of mixed adsorbates. It has been shown, by invoking thermodynamic principles, that, for consistency, the monolayer quantity or volume for each of the adsorbed components must be identical. This means, for example, that $q_{\mathrm{m}i} = q_{\mathrm{m}j}$ (Kemball *et al*. 1948, Broughton 1948). For a gas mixture containing adsorbate molecules which would occupy substantially different areas on adsorption, such a constraint is unrealistic and so the monolayer capacities of each adsorbate are then regarded as empirical quantities. $q_{\mathrm{m}i}$ in equation (3.31) would thus be replaced by an empirical constant a_i. However, such empirical constants may not be applicable over an extended range of partial pressures and their use should then be restricted to the range of partial pressures for which they are ostensibly constant.

Indeed, the extended Langmuir equation (3.31) provides a satisfactory correlation of single component isotherm data for carbon dioxide–carbon monoxide mixtures adsorbed on a porous activated carbon (Battrum and Thomas 1991). From the single-component isotherm data for CO_2 values of a_{CO_2} and b_{CO_2} may be obtained from the intercept and slope of a linear plot of $1/q_{CO_2}$ against $1/p_{CO_2}$. Similarly values of a_{CO} and b_{CO} are obtained from single component isotherm data for CO. The values so obtained are then substituted into equation (3.31) to obtain the isotherms for each of the components CO_2 and CO in the mixture. On the other hand, for mixtures of benzene and toluene vapours, the extended Langmuir isotherm for binary mixture adsorption on an activated charcoal is only correlated by the constants obtained from the single component toluene isotherm when the constant b_B for benzene was determined empirically by linearizing the extended Langmuir equation for the component toluene (Thomas and Lombardi 1971). Data relating to the adsorption of benzene–toluene vapour mixtures on charcoal do not conform with the condition that a_T and a_B are equal. This is demonstrated by defining a separation factor

$$K_{12} = \frac{q_2/c_2}{q_1/c_1} \tag{3.32}$$

by analogy with the definition for vapour–liquid mixtures in which a comparison is made of the relative volatilities of each component. If Q_T and C_T represent total concentrations of adsorbed and gas (or vapour) phases, respectively, then equation (3.32) may be written in the alternative form

$$\frac{q_1}{Q_T} = \frac{c_1 C_T}{K_{12} + (1 - K_{12})(c_1/C_T)} \tag{3.33}$$

A plot of c_1Q_T/q_1C_T as a function of c_1/C_T should yield a straight line if K_{12} is constant (or $b_1 = b_2$ for equal q_m values). Figure 3.8 is such a plot for a benzene-toluene vapour mixture absorbed on charcoal. There is considerable scatter of the experimental points (the scatter being much greater than the expected experimental error) with K_{BT} varying between 5.5 and 7.2.

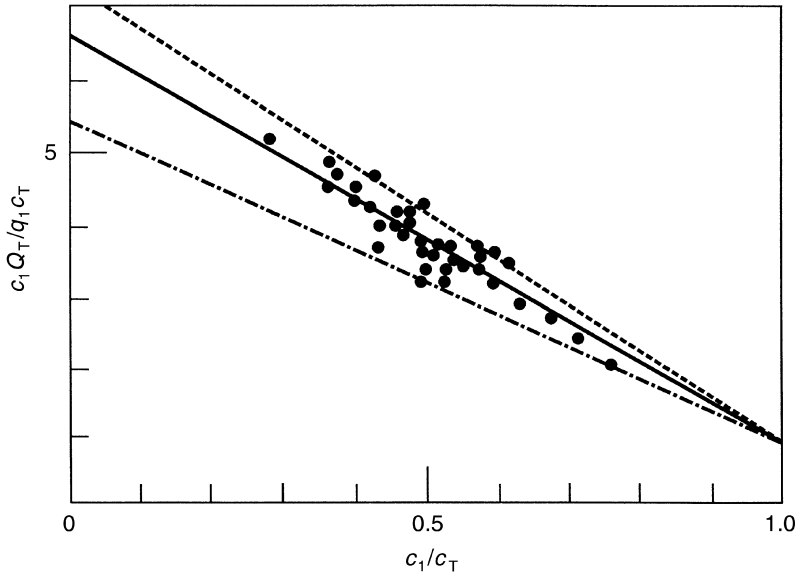

Figure 3.8 *Data for benzene–toluene mixtures absorbed on charcoal at 150°C showing variation of the separation factor —K_{BT} = 6.6, ---K_{BT} = 7.2; -·-·K_{BT} = 5.5 (source: Thomas and Lombardi 1971).*

3.4.2 The Lewis correlation

If, for a binary mixture $a_1 = a_2$ and equation (3.31) is obeyed then, if q_1^0 and q_2^0 are the adsorbed phase concentrations for the pure components at pressures p_1^0 and p_2^0 while q_1 and q_2 are the corresponding quantities for the mixture at partial pressures p_1 and p_2, we can write

$$\frac{q_1}{q_1^0} + \frac{q_2}{q_2^0} = 1 \tag{3.34}$$

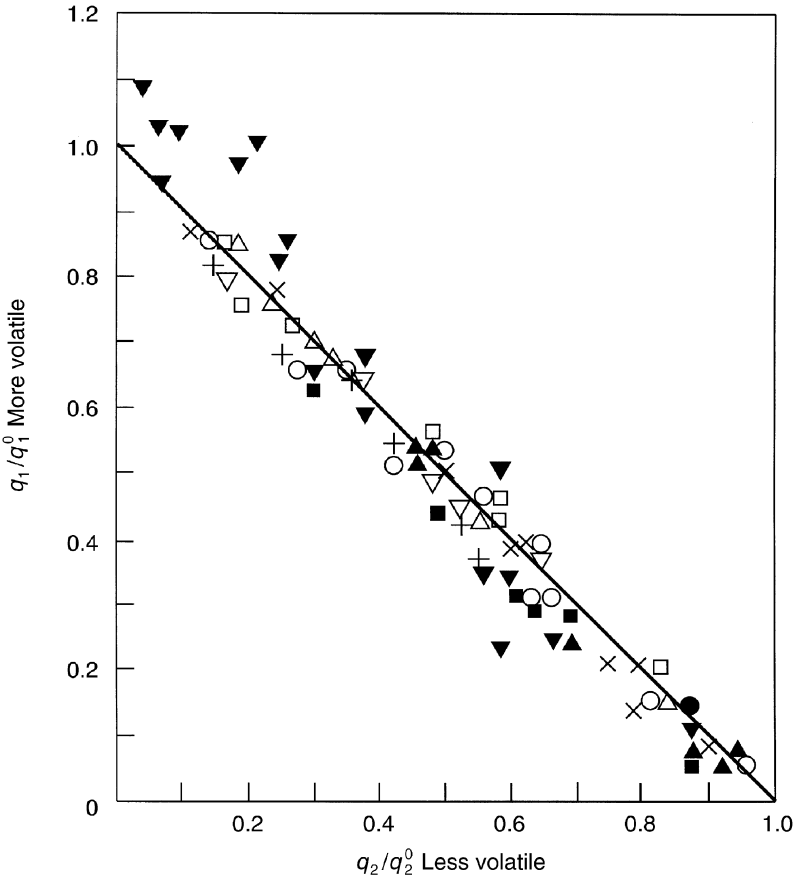

Figure 3.9 *Lewis correlation for sorption of hydrocarbons on silica-gel and activated carbons.*

PCC carbon	Columbia carbon	Silica gel
○, *C_2H_4–C_3H_8*	▽, CH_4–C_2H_4	▼, CH_4–C_2H_4
△, *C_4H_{10}–C_4H_8*	●, C_2H_4–C_2H_6	+, C_2H_6–C_3H_8
□, *i*–C_4H_{10}–C_4H_8	■, C_2H_4–C_3H_6	×, *i*–C_4H_{10}–i–C_4H_8

(source: Lewis *et al.* 1950).

provided $p_1^0 = p_2^0 = (p_1 + p_2)$. This correlation was first proposed by Lewis *et al.* (1950) and is of general applicability as an empirical relation. Figure 3.9 is a demonstration that the relation is well obeyed for the adsorption of hydrocarbon mixtures on silica gel. If the maximum capacity for micropore filling of the adsorbent is m_0 and V_m is the molar volume of the adsorbate

mixture then the total number n_T of moles of mixture adsorbed is m_0/V_m. The number of moles n_i of a component i, however, is $x_i.n_T$ where x_i is the mole fraction of component i. Provided no volume change is assumed for mixing, then the partial molar volumes are additive so that $V_m = \sum x_i V_i^0$ where V_i^0 is the molar volume of component i for adsorption of the pure gas at the same temperature and total pressure as the mixture is adsorbed. Hence it follows that

$$\sum \frac{n_i}{n_i^0} = 1 \tag{3.35}$$

where n_i^0 is written for m_0/V_i^0. The main advantage of a correlation like equation (3.35) is that it contains both pure component and mixture data. Figure 3.9 illustrates that hydrocarbons adsorbed on silical gel and on a carbon obey the Lewis relation.

3.4.3 Grant and Manes model

This model for mixed adsorption (Grant and Manes 1966) is based upon the idea of equipotential energies among the components of the adsorbed mixture and is thus related to the Polanyi potential theory discussed in Section 3.3.5. As previously recorded, Dubinin and Radushkevich (1947) postulated a direct relation between the affinity coefficient β_i of a component i and the molar volume V_{mi} of the saturated pure liquid. The equipotential energy concept for two components is thus $(\varepsilon_i/\beta_i) = (\varepsilon_j/\beta_j)$. Hence, by use of equation (3.18) for each component

$$\frac{R_g T}{V_{mi}} \ln \frac{(p_s)_i}{p_i} = \frac{R_g T}{V_{mj}} \ln \frac{(p_s)_j}{p_j} \tag{3.36}$$

However, there were substantial deviations from the correlation given by equation (3.36) when applied over a wide range of temperatures and pressures. Grant and Manes (1966), by utilizing the molar volume V'_m of the liquid at its normal boiling point and fugacities rather than partial pressures, showed that data could be correlated fairly well. Assuming that Raoult's law applies to the partial pressure p_i of each component and its mole fraction x_i in the adsorbed phase, the correlation becomes

$$\left(\frac{\varepsilon}{V'_m}\right)_i = \frac{R_g T}{V'_m} \ln \left\{\frac{x_i (f_s)_i}{f_i}\right\} \tag{3.37}$$

where $(f_s)_i$ and f_i are, respectively, the fugacity of the pure component i at its saturated vapour pressure at temperature T and the fugacity of i in the gas mixture. Assuming Raoult's Law is obeyed, f_i is found from the relationship $f_i = x_i f_i^*$ where f_i^* is the fugacity exerted by i if it were a pure adsorbate at the

total adsorbed volume of the mixture. From data for pure component adsorption, the mole fraction x_i of component i in the mixture can be computed. This is accomplished by an iterative procedure, first assuming an x_i and calculating $(\varepsilon/V'_m)_i$ from equation (3.37) adopting values of f_i and f_{si} from single component data. The correct values for the set x_i correspond to $(\varepsilon/V'_m)_i$ being the same for all components. Thus the molar volume of the mixture may be found because it is assumed that molar volumes are additive such that (V_{mix}) for the mixture is $\sum x_i V_{\text{m}i}$ and $n_i = x_i\, n_{\text{T}}$. The molar volume, $V_{\text{m}i}$, is that of the saturated liquid at the temperature which corresponds to the saturated vapour pressure p_{si} $(= y_i P/x_i)$ where y_i is the mole fraction of i in the vapour phase and P the total pressure. Figure 3.10 illustrates experimental data for three hydrocarbon

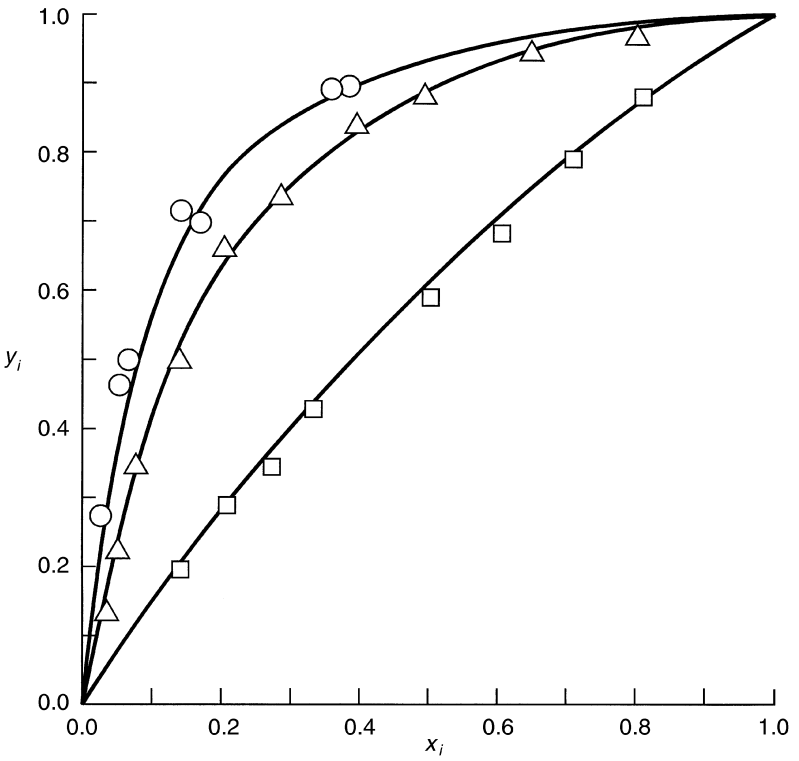

Figure 3.10 *Model of Grant and Manes correlating binary mixture data. ○, CH_4–C_2H_4; △, C_2H_6–C_3H_8; □, C_2H_4–C_2H_6; — calculated from model (source: Szepesy and Illes 1963; experimental data: Grant and Manes 1966).*

mixtures compared with predictions made employing single-component adsorption data and applying the method of Grant and Manes.

3.4.4 Ideal adsorbed solution (IAS) model

Equilibrium between the adsorbed phase and the gas or vapour phase requires the chemical potentials in each phase to be equal. If p_i^0 (a function of spreading pressure), denoted $p_i^0(\pi)$, is the saturated vapour pressure exerted by component i in its pure state at the same temperature and spreading pressure of the adsorbed state and x_i is the mole fraction of i in the adsorbed phase, then the pressure p_i exerted by component i in the mixture is

$$p_i = p_i^0(\pi)\, x_i \tag{3.38}$$

which is equivalent to Raoult's law for ideal liquid–vapour systems. If the mole fraction of i in the vapour phase is y_i and the total pressure is P, then the equilibrium conditions between component i in the adsorbed phase and the same component i in the vapour phase requires

$$y_i P = p_i^0(\pi)\, x_i \tag{3.39}$$

For equal spreading pressures in a mixture the condition $\pi_i = \pi_j = \pi_{\text{mix}}$ must be obeyed. Thus from equation (3.28) (which gives the spreading pressure π in terms of the moles adsorbed), for a mixture composed of components i and j we can write

$$\pi A/RT = \int_0^{p_i^0} n_i^0(p)\mathrm{d}\ln p = \int_0^{p_i^0} n_j^0(p)\mathrm{d}\ln p \tag{3.40}$$

where $n_i^0(p)$ is the isotherm for the pure component i and $n_j^0(p)$ is the isotherm for pure j. The above two equations are subject to the conditions $\sum x_i = \sum y_i = 1$ and define the adsorbed mixture. Assuming the total pressure P and mole fraction y_i of component i in the vapour phase are known, then the calculation procedure for a binary mixture would be to find p_{s1}, p_{s2} and x_1 from the three equations (3.38), (3.39) and (3.40). The integrals in (3.40) may be evaluated numerically provided the form of the pure component isotherms $n^0(p)$, or equivalently $q^0(p)$, are known. Once values of $p^0{}_1$, $p^0{}_2$ and x_1 have been found, n_1 and n_2 may be calculated. A similar procedure would be followed for a multicomponent mixture. Figure 3.11 is a comparison of experimental data, determined by Szepesy and Illes (1963), with mixture isotherms computed from single-component isotherm data.

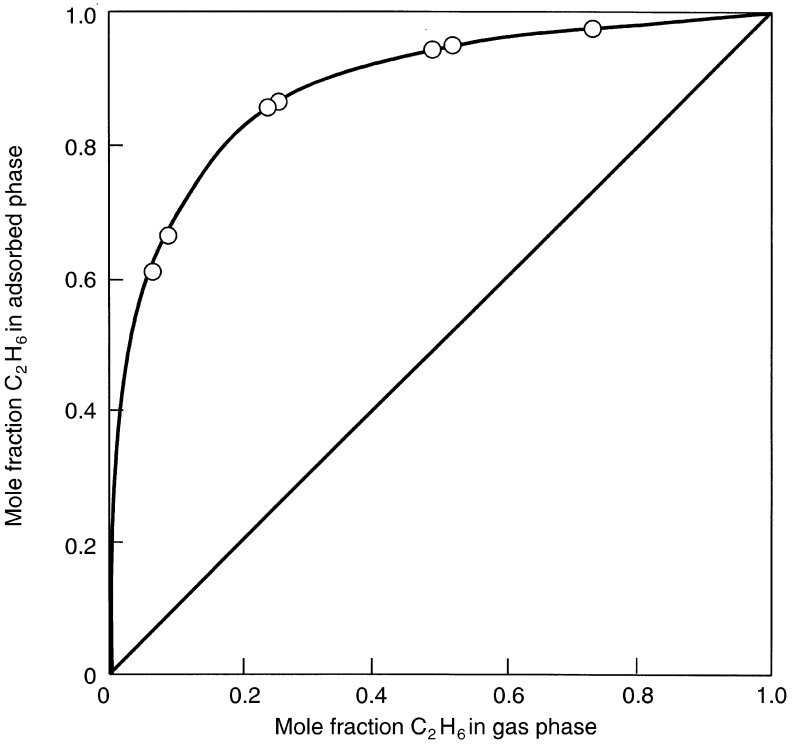

Figure 3.11 *Comparison of IAS model with experimental results for methane –ethane mixtures adsorbed on activated carbon at 1 atm and 20°C (source: Myers and Prausnitz 1965; experimental data: Szepesy and Illes 1963).*

Many binary mixtures, however, do not behave ideally when in the adsorbed state. The IAS model is then modified by incorporating activity coefficients γ for each component as a measure of their departure from ideality. Provided both the temperature T and the spreading pressure π are specified, then, because the chemical potentials in the adsorbed and gas phases are equal at equilibrium one may write

$$\mu_{ia} = [\mu_i^0\ (T) + R_g T \ln \{p_{si}(\pi).\gamma_{ia} x_{ia}\}] = \mu_{ig} = [\mu_i^0\ (T) + R_g T \ln p_i] \qquad (3.41)$$

leading immediately to

$$p_i = y_i\, P = p_i^0\ (\pi)\, \gamma_i\, x_i \qquad (3.42)$$

Comparing equations (3.42) and (3.39), it is clear that the only additional

parameters introduced to account for non-ideality are the activity coefficients γ_i. Hence a similar procedure of calculation as for the IAS model may be adopted to obtain isotherms for non-ideal mixtures from single-component data if the activity coefficients are known. Alternatively, the method may be used to determine activity coefficients for the adsorbed phase having calculated the spreading pressure from an equation such as (3.40) and then employing equation (3.42).

3.4.5 Vacancy solution model

Suwanayuen and Danner (1980) formulated a theory of adsorption for single components which was extended to a binary mixture. They also claimed that the model is applicable to multicomponent mixtures. It was assumed that the gas phase and the adsorbed phase are each composed of a hypothetical solvent (termed the vacancy) and identifiable adsorbates. A vacancy, in this theory, is considered to be a vacuum entity which occupies adsorption space which can be filled by an adsorbate. Thus, adsorption equilibrium for a mixture of n adsorbable components translates to an equilibrium between (n + 1) vacancy solutions (n adsorbate species and the vacancy). The chemical potential of a component i in the gas phase is

$$\mu_{ig} = \mu^0_{ig} + R_g T \ln(\phi_i y_i P) \tag{3.43}$$

where ϕ_i is the fugacity coefficient accounting for any non-ideality, y_i is the mole fraction of component i in the gas phase and P is the total pressure. Application of classical thermodynamics to the adsorbed phase (considered as the adsorbate in the potential field of an inert adsorbent) gives the Gibbs function as

$$G_s = -\pi A + n_s \mu_s (T, \pi) \tag{3.44}$$

at constant temperature and pressure. The chemical potential $\mu_s (T, \pi)$ is a function of temperature T and spreading pressure π rather than temperature and pressure as it would be in the gas phase. Differentiation of this equation with respect to molar quantity n_s at constant spreading pressure yields

$$\mu_s(T, \bar{A}) = -\pi \bar{A}_i + \mu_s(T, \pi) \tag{3.45}$$

where $\mu_s(T, \bar{A})$ is the chemical potential as a function of temperature and partial molal area. Classical solution thermodynamics gives the chemical potential as a function of temperature and partial molal area and for a component i is written

$$\mu_{is}(T, \bar{A}_i) = \mu^0_{is}(T) + R_g T \ln(\gamma_{is} x_{is}) \tag{3.46}$$

where $(\gamma_{is}\, x_{is})$ is the product of mole fraction x_{is} and the activity coefficient γ_{is} of component i in the adsorbed phase solution.

Substitution of $\mu_{is}\ (T, \bar{A}_i)$ into equation (3.45) for a component i in the vacancy solution thus yields

$$\mu_{is}(T, \pi) = \mu^0_{i\,s}(T) + R_g T \ln(\gamma_{is} x_{is}) + \pi \bar{A}_i \tag{3.47}$$

Equilibrium between the two vacancy solutions in the gas and adsorbed phases demands that $\mu_{ig} = \mu_{is}$ and so, from equations (3.43) and (3.47),

$$f_i y_i P/(\gamma_{is} x_{is}) = \exp\{(\mu^0_{is} - \mu^0_{ig})/R_g T\} \exp(\pi \bar{A}_i / R_g T) \tag{3.48}$$

Equation (3.48) relates the mole fraction y_i of component i in the gas phase to the mole fraction x_{is} in the adsorbed phase. The latter is based on the total number of moles of the adsorbed vacancy solution. To interpret experimental data an expression is required relating the experimentally measured mole fraction of component i in the adsorbed phase, x_{ie}, to the corresponding vacancy solution quantity x_i. For components $i = 1, 2$ the equation is $x_{is} = x_{ie}\theta$ where θ is the ratio of the total number of moles n_{Ts} in the vacancy solution to the total number of moles n_{Te} adsorbed as measured experimentally. The mole fraction of vacancies in the vacancy solution is then $x_{vs} = (1 - \theta)$. Substitution of x_{is} in equation (3.48) gives

$$\phi_i y_i P = (\gamma_{is} x_i^e \theta) \exp\{(\mu^0_{is} - \mu^0_{ig})/R_g T\} \exp(\pi \bar{A}_i / R_g T) \tag{3.49}$$

All of the terms on the right-hand side of equation (3.49) may be obtained from pure component adsorption data. As the equation is valid for the whole range of concentrations, it is therefore also applicable at infinite dilution when ϕ_i, γ_i, γ_{is} and x_{ie} are unity and the spreading pressure is zero. For such conditions

$$\exp\{(\mu^0_{is} - \mu^0_{ig})/R_g T\} = P/\theta \tag{3.50}$$

and so may be found from single-component data at low coverages where the isotherm is linear. The partial molal area $\bar{A}$ may also be computed by means of the integrated form of the Gibbs adsorption isotherm given by equation (3.28). Fugacity and activity coefficients, however, are found by somewhat tedious fitting of experimental data to an idealized isotherm such as that of Langmuir. Multiplication of the Langmuir equation by a function containing one or more parameters, only found by regression, then correlates equation (3.49) with single-component data and, after a number of iterations, gives values for ϕ_i and γ_i. The VSM theory, although based on fundamental principles, is thus semi-empirical.

Despite the obviously tedious calculations involved, the VSM has been very successful in predicting binary isotherms from single component data. Figure 3.12 shows how closely the model conforms to experimentally determined data for four pairs of gases adsorbed on an activated carbon. Because interaction between adsorbed species and between adsorbates and adsorbent is taken into account in the VSM, the model is capable of predicting azeotrope formation. Figure 3.13 is an example where azeotrope formation is predicted for the adsorption of a mixture of $i - C_4H_{10}$ and C_2H_4 on zeolite 13X.

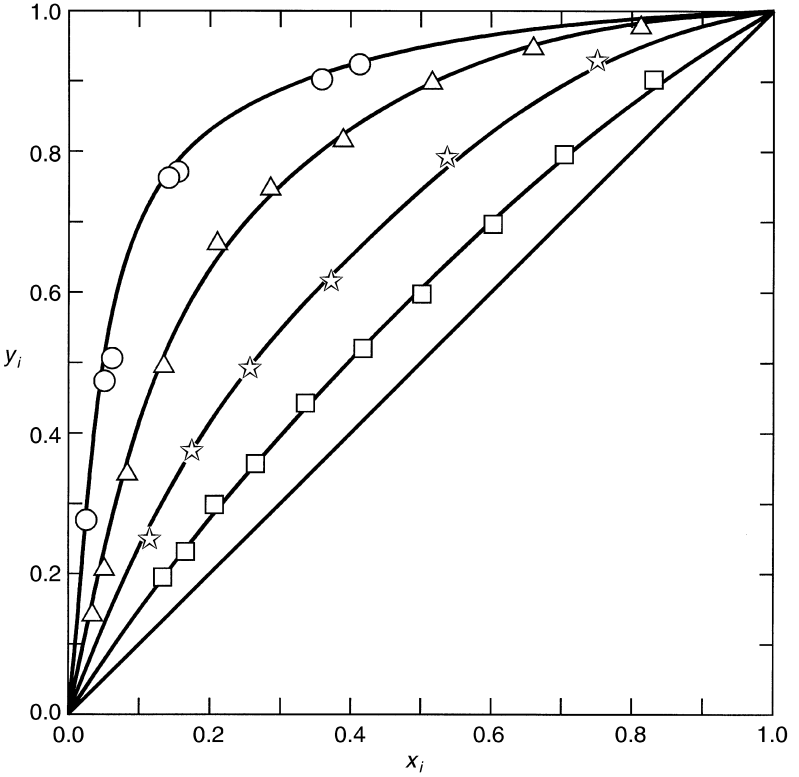

Figure 3.12 *Comparison of VSM model with experimental data for gas mixtures adsorbed on activated carbon at 1 atm and 293.2K. ○, CH_4–C_2H_6; □, C_2H_4–C_2H_6; △, C_2H_6–C_3H_8; ☆, CO_2–C_2H_4 (source: Suwanayuen and Danner, 1980; experimental data: Szepesy and Illes, 1963).*

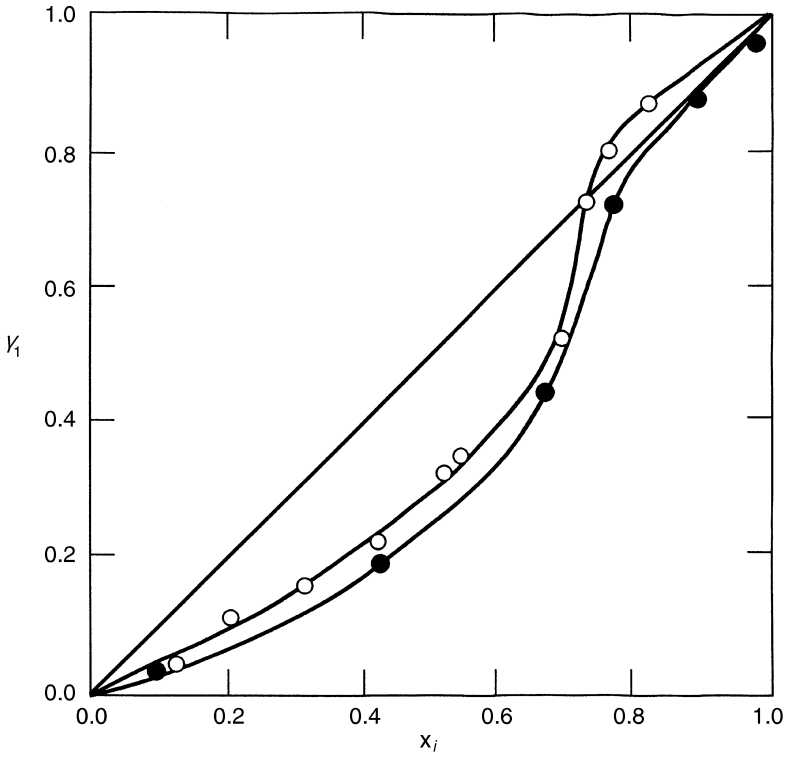

Figure 3.13 *Phase diagram for adsorption on a zeolite 13X at 137.8 kPa and 298 K of i – C_4H_{10}–C_2H_6 mixture forming azeotropes. ○, 298 K; ●, 373 K (source: Hyun and Danner 1982).*

3.5 STATISTICAL THERMODYNAMICS MODEL FOR MIXTURES

An additional assumption has to be introduced in order to extend the statistical thermodynamic approach to mixtures. The configurational integral is modified to account for adsorbate molecular interaction. The form used by Ruthven (1984) is a geometric mean of the coefficients A_{is} and A_{js} for the respective pure components. This is equivalent to assuming ideal behaviour for the mixing of components. The isotherm obtained by Ruthven is, for a binary mixture of components 1 and 2 adsorbed on a zeolite

$$q_i = \frac{K_1 p_1 + \sum_j \sum_i \{(K_1 p_1)^i (K_2 p_2)^j / (i-1)!j!\} A_{ij}}{1 + K_1 p_1 + K_2 p_2 \sum_j \sum_i \{(K_1 p_1)^i (K_2 p_2)^j / i!j!\} A_{ij}} \tag{3.51}$$

where

$$A_{ij} = (A_{1s}^{i}\, A_{2s}^{j}\,)^{1/(i+j)} \tag{3.52}$$

A condition which must be met is $(i\alpha_1 + j\alpha_2) \leq v$, where α_1 and α_2 are the effective volumes of the respective adsorbate molecules, v is the cage volume, and i and j are the number of molecules of species 1 and 2, respectively, in a cage.

The model outlined has been successful for predicting the mixed adsorption of hydrocarbons adsorbed on zeolites from single component data. Figure 3.14 compares experimental and theoretical predictions for a mixture of n-heptane and cyclohexane on a 13X zeolite.

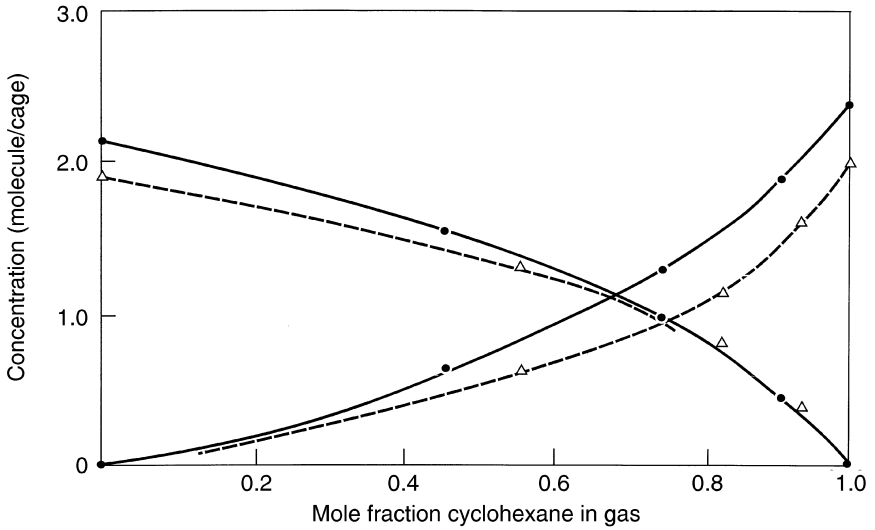

Figure 3.14 *Comparison of generalized thermodynamic statistical model with experimental results for n-heptane–cyclohexane mixtures adsorbed on a 13X zeolite. The points represent experimental data while the continuous and discontinuous lines are predictions based on single component isothermal data (source: Goddard and Ruthven 1984).*

REFERENCES

Barrer, R. M. (1978) *Zeolites and Clay Minerals as Sorbents and Molecular Sieves*, Academic Press

Barrer, R. M. and Vaughan, D. E. (1971) *J. Phys. Chem. Solids*, **32**, 731

Battrum, M. J. and Thomas, W. J. (1991) *Trans. I. Chem. Eng.,* **69A**, 119

Broughton, D. B. (1948) *Ind. Eng. Chem.* **40**, 1506

Brunauer, S. (1943) *The Adsorption of Gases and Vapours*, Princeton University Press

Brunauer, S., Emmett, P. H. and Teller, E. (1938) *J. Am. Chem. Soc.*, **60**, 309

Cohan, L. H. (1938) *J. Am. Chem. Soc.*, **60**, 433

Derrah, R. I. and Ruthven, D. M. (1975) *Can. J. Chem.*, **53**, 996

Dubinin, M. M. (1960) *Chem. Rev.*, **60**, 235

Dubinin, M. M. and Radushkevich, L. V. (1947) *Dokl. Akad. Nauk. SSR*, **55**, 327

Everett, D. H. (1958) *Industrial Carbon and Graphite*, p. 272, Society of Chemical Industry, London

Foster, A. G. (1952) *J. Chem. Soc.*, 1806

Gibbs, J. W. (1928) *Collected Works*, Yale University Press, Newhaven CT

Goddard, M. and Ruthven, D. M. (1984) *Proc. Sixth Int. Conf. on Zeolites, Reno, Nevada, July 1983 (Butterworths)*

Grant, R. J. and Manes, M. (1964) *Ind. Eng. Chem. Fundamentals*, **3**, 221

Grant, R. J. and Manes, M. (1966) *Ind. Eng. Chem. Fundamentals*, **5**, 490

Gregg, S. J. and Sing, K. S. W. (1967) *Adsorption, Surface Area and Porosity*, Chapter 3, Academic Press

Hyun, S. H. and Danner, R. P. (1982) *J. Chem. Eng. Data*, **27**, 196

Kemball, C., Rideal, E. K. and Guggenheim, E. A. (1948) *Trans. Faraday Soc.*, **42**, 952

Kiselev, A. V. (1971) *Adv. Chem.*, **102**, 37

Kiselev, A. V. (1960) *Quart. Rev.*, **XIII**, 257

Laidler, K. J. (1954) in *Catalysis*, ed. P. H. Emmett, Vol 1, p. 75, Reinhold, New York

Lamond, T. G. and Marsh, H. (1964) *Carbon*, **1**, 281, 293

Langmuir, K. (1918) *J. Chem. Soc.*, **40**, 1361

Lennard-Jones, J. E. (1932) *Trans. Faraday Soc.*, **28**, 333

Lennard-Jones, J. E. and Dent, B. M. (1928) *Trans. Faraday Soc.*, **24**, 92

Lewis, W. K., Gilliland, E. R., Chertow, B. and Hoffman, W. H. (1950) *J. Am. Chem. Soc.*, **42**, 1319

Marsh, H. and Wynne-Jones, W. F. K. (1964) *Carbon*, **1**, 269

McBain, J. W. (1935) *J. Am. Chem. Soc.*, **57**, 699

Myers, A. L. and Prausnitz, J. M. (1965) *AIChEJ*, **11**, 121

Ruthven, D. M. (1971) *Nature Phys. Chem.*, **232**(29), 70

Ruthven, D. M. (1984) *Principles of Adsorption and Adsorption Processes*, p. 75 *et seq*, John Wiley, New York

Ruthven, D. M. and Loughlin, K. F. (1972) *J. Chem. Soc. Faraday Trans.*, **68**, 696

Ruthven, D. M. and Wong, F. (1985) *Ind. Eng. Chem. Fundamentals*, **24**, 27

Suwanayuen, S. and Danner, R. P. (1980) *AIChEJ*, **26**, 68

Sykes, K. W. and Thomas, J. M. (1960) *Proc. 4th Carbon Conf.*, p. 29, Pergamon Press

Szepesy, L. and Illes, V. (1963 and 1964) *Acta Chim. Hung.*, **35**, 37 and *ibid*. **36**, 245

Thomas, W. J. and Lombardi, J. L. (1971) *Trans. I. Chem.Eng.*, **49**, 240

Thomas, J. M. and Thomas, W. J. (1967) *Introduction to Principles of Heterogeneous Catalysis*, Chapter 4, Academic Press

Thomas, J. M. and Thomas, W. J. (1997) *Principles and Practice of Heterogeneous Catalysis*, Chapter 4, VCH

Thompson, W. T. (1871) *Phil. Mag.*, **42**, 448

4

Rates of adsorption of gases and vapours by porous media

4.1 INTRINSIC RATES OF ADSORPTION AND TRANSPORT EFFECTS

If a clean non-porous adsorbent surface were exposed to a gas or vapour adsorbate and the fluid boundary layer adjacent to the surface offered no resistance to transport of gas to the surface, then the rate of adsorption would be extremely rapid. The classical kinetic theory of gases may be invoked to assess the order of magnitude of such intrinsic adsorption rates. Physical adsorption entails attractive van der Waal's forces between adsorbate and adsorbent (outlined in Section 3.1) and the energy barrier which molecules have to overcome in order that adsorption may occur is usually very small. The energy released when physical adsorption occurs is close to the heat of liquefaction of the adsorbate gas, while for desorption to take place an approximately similar quantity of heat has to be absorbed. Thus, the processes of adsorption and desorption are reversible and non-activated. This is in contrast to chemisorption when moderately strong chemical bonds are formed and molecules have to have sufficient energy (the activation energy) to surmount the energy barrier and fall into the lower potential well of the chemisorbed state. From the kinetic theory of gases an upper limit may be placed on the mass of a gas striking unit area of surface

per unit time. If M is the molecular mass of the gas in question, p its pressure and T the absolute temperature, the rate (measured in kg m^{-2} s^{-1}) at which molecules strike the surface may be expressed as

$$R_m = p(M/2\pi R_g T)^{1/2} \tag{4.1}$$

We compare the intrinsic rate of adsorption of nitrogen with an experimentally observed rate of adsorption of nitrogen at 6 bar and 25°C (Crittenden *et al.* 1995). Appropriate substitution of numerical values into equation (4.1) gives the maximum intrinsic rate of adsorption as 2×10^4 kg m^{-2} s^{-1}. On the other hand, the experimentally observed rate is approximately 4×10^{-8} kg m^{-2} s^{-1} (*c.* 0.33 mol s^{-1} at 6 bar, 25°C onto a surface of 250 m^2 g^{-1}). Thus the intrinsic rate of adsorption is some 10^{12} times faster than the observed rate of adsorption. It is generally acknowledged throughout the literature on physical adsorption processes that the dominant rate-controlling step is not the actual physical attachment of adsorbate to adsorbent (normally referred to as very rapid) but rather intraparticle transport of gas within the porous structure of the adsorbent to its available surface. Interparticle transport from bulk fluid to the external surface of the porous adsorbent may also have an effect on the overall rate of adsorption under some circumstances.

Transport resistances which influence the overall rate of adsorption are:

(1) mass and heat transfer of adsorbate to and from the exterior surface of the adsorbent (known as interparticle transport);
(2) Maxwellian diffusion (bulk molecular diffusion) in moderately large pores (macropores) or Knudsen diffusion in pores (micropores) which have a diameter smaller than the mean free path of the adsorbate molecules;
(3) intracrystalline diffusion within the channel and cage-like structure of molecular sieve materials such as zeolites and silicalites;
(4) surface diffusion when adsorbate molecules move freely over the internal surface of adsorbents in parallel with intraparticle diffusion;
(5) heat transfer within the interior of particles occasioned by the exothermic nature of adsorption.

The relative importance of these resistances largely depends on the nature of the adsorbent and adsorbate and the conditions of temperature and pressure in which the adsorption occurs. As shown in Chapter 6 any model representing an adsorber must include mass and heat balances for the fluid phase and also transport processes within the porous particles.

4.2 TRANSPORT PROCESSES IN POROUS SOLIDS

We consider each of the possible resistances to rapid adsorption which are listed above and examine their significance and magnitude. Interparticle (external to particles) transport resistance occurs in series with the intraparticle (within particles) transport resistances, enumerated 2, 3 and 4, which, if each were present, would be in parallel.

4.2.1 Interparticle mass and heat transport

Rates at which mass and heat are transported between a flowing bulk fluid phase and the exterior surface of the adsorbent particles are limited by a relatively thin layer of comparatively stagnant fluid immediately adjacent to, and completely enveloping, each of the solid particles. Such layers can be thought of as films of stagnant fluid or, as described by a more elaborate theory, in terms of so-called mass and heat transfer boundary layers. For the purposes of application to adsorption either of these concepts can be accommodated by defining the mass or heat flux from fluid to solid as the product of a lumped coefficient and a linear driving force. These mass and heat transfer coefficients for the respective interparticle processes subsume the thickness of the film or boundary layer and relevant fluid properties while the driving force is simply the difference in concentration (mass transport) or temperature (heat transport) between bulk fluid and exterior surface of the particle. The rate of mass transport of a specific component from bulk fluid to the exterior surface of a particle, expressed as the number of moles of the component transferred per unit adsorbent bed volume per unit time, is

$$R = ka_p\,(c_g - c) \tag{4.2}$$

where k is the mass transfer coefficient and a is the exterior surface area of a solid particle per unit volume. The dimensions of k are thus LT^{-1} or, in SI units, m s^{-1}. An analogous equation describes the rate of heat transfer

$$R_h = ha_p\,(T - T_g) \tag{4.3}$$

where T is the temperature at the exterior surface of the solid, T_g the bulk fluid temperature and h is the heat transfer coefficient which will have units (SI system) W m^{-2} K^{-1} if the rate of heat transfer is based on unit volume of adsorbent bed. Whereas equation (4.2) indicates mass transfer during adsorption from bulk fluid to surface ($c_g > c$), because adsorption is exothermic (see Section 3.1) heat is released from within the pellet and is transferred from the particle exterior surface to the bulk fluid ($T > T_g$).

Boundary layer theory predicts different values of coefficients for the

front (upstream) face and the back (downstream) surface of a particle due to differing flow conditions which prevail at these positions. However, average values, known as average film coefficients, are used in practice. Correlations exist for the estimation of these coefficients as functions of fluid properties and particle size.

Wakao and Funazkri (1978) revealed that when mass transfer coefficients were measured by experiments involving adsorption or evaporation, the mass balance for the bed (see Chapter 6) should include a term accounting for axial dispersion. Previous correlations of experimental data were based upon a mass balance equation for the packed bed ignoring axial dispersion. It was shown that the mass transfer coefficient could be expressed in terms of the dimensionless Sherwood number (*Sh*) by the relation

$$Sh = kd_p/D = 2.0 + 1.1\ Sc^{0.33}\ Re^{0.6} \tag{4.4}$$

if axial dispersion were included in the analysis of experimental results and that the value of k was about twice that for a value of $Re = 10$ if axial dispersion were neglected. The dimensionless Reynolds number, *Re*, in equation (4.4) is defined as $\rho u d_p/\mu$ (where ρ is the fluid density, u the superficial fluid velocity, μ the fluid viscosity and d_p the particle diameter) while the dimensionless Schmidt number, *Sc*, is defined as $\mu/\rho D$ (where D is the diffusion coefficient for bulk Maxwellian transport of the component being transported from fluid to solid). Should one have to rely on experimental data obtained which excludes any consideration of axial dispersion, then it is best to estimate the mass transfer coefficient from the use of the so-called *j* factor, which for mass transfer is

$$j_D = (k\rho/\mu)\ Sc^{0.66} = (0.458/e)\ (Re)^{0.41} \tag{4.5}$$

and where e is the bed voidage.

Alternatively the Ranz and Marshall (1952) correlation,

$$Sh = 2.0 + 0.6\ Sc^{0.33}\ Re^{0.5} \tag{4.6}$$

may be used when axial dispersion is not included in the bed mass balance.

The heat transfer coefficient h from solid to fluid may be estimated from a correlation for the Nusselt number, *Nu*, suggested by Lemcoff *et al.* (1990) and which is similar to the correlation given by equation (4.4) for mass transfer,

$$Nu = hd_p/\lambda_f = 2.0 + 1.1\ Pr^{0.33}\ Re^{0.6} \tag{4.7}$$

The dimensionless Prandtl number *Pr* is defined as $c_f\mu/\lambda_f$, c_f being the heat capacity of the fluid and λ_f the corresponding thermal conductivity. At moderate and higher values of the Reynolds number the correlation appears to be good but at low values of *Re* a significant scatter of data is evident. The

poor correlation at low *Re* may well arise because of the inherent assumption of a uniform interface boundary condition leading to errors in the evaluation of the thermal conductivity λ_f. From the analogy between heat and mass transfer due to Chilton and Colburn (1934) implying that the *j* factors for heat (j_H) and mass (j_D) transfer are numerically equal, another correlation frequently used is

$$j_H = (h/c_f\mu)\,(c_f\mu/\lambda_f)^{0.66} = (0.458/e)\,(Re)^{0.41} \tag{4.8}$$

Heat generated by the adsorption of a component in the gas or liquid phase by the porous solid has to be transported not only between solid and fluid in an operating column, but is subsequently dissipated by transport from fluid to vessel wall and thence to the surrounding environment. A correlation due to Leva (1949) may be used to assess the resistance to heat transfer between fluid and vessel wall. A film heat transfer coefficient estimated from a correlation described by McAdams (1954) enables the evaluation of heat transfer resistance from the vessel wall to the surroundings.

4.2.2 Diffusion in porous materials

Adsorption is a surface phenomenon, so that the more surface that is available for adsorption the greater is the capacity of the adsorbent for the adsorbate. Hence, as discussed in Chapter 2, adsorbents have maximum ability to adsorb when the internal structure of these materials is porous, thus allowing access of adsorbate molecules to the largest amount of internal surface. The total mass flux due to an adsorbate entering a porous structure is the sum of fluxes due to gaseous diffusion (Maxwellian and/or Knudsen diffusion, depending on the pore radii), convective diffusion (occasioned by the displacement of one molecular species by another), surface diffusion (in which molecules are transported across a surface rather than through the gaseous phase contained by the pores of the material) and viscous flow (usually negligible for physical adsorption when there is only a small pressure gradient along pores).

Maxwellian and Knudsen diffusive fluxes

In pores of diameter much greater than the mean free path of a molecule, diffusion occurs by a process of molecular collisions in the gas phase within the pore (Maxwellian or bulk diffusion) but, if the molecular mean free path is much greater than the pore diameter, diffusion occurs by molecules colliding with the pore walls (Knudsen diffusion). Both of these transport processes occur with a decreasing concentration gradient and may be described by means of Fick's law of diffusion with an appropriate diffusion

coefficient. The classical kinetic theory of gases (Present 1958) reveals that the diffusion of a gas is determined by the mean velocity of molecules and the distance they travel before they collide either with another molecule (molecular or Maxwellian diffusion) or with the wall of a narrow capillary (Knudsen diffusion). When the mean free path λ is smaller than the dimensions of a containing conduit, unconstrained molecular transport occurs; if, on the other hand, the mean free path is greater than the radius of a narrow channel (for example, pores within a porous solid) through which molecules are travelling, then Knudsen diffusion obtains.

Pore size distribution data obtained from gas desorption (Barret *et al.* 1951) and mercury porisimetry experiments together with a knowledge of adsorbate molecular size thus enables the mode of diffusive transport to be ascertained. It should be noted that both molecular and Knudsen diffusion may occur in the same porous medium when the porous medium contains both macropores and micropores (revealed from an analysis of a bimodal pore size distribution curve). Unconstrained molecular diffusion, D_{M}, and Knudsen diffusion, D_{K}, coefficients are subsequently calculated from formulae derived from transport properties of fluids (gaseous and liquid) and the kinetic theory of gases. The molecular diffusivity for a binary gas mixture of A and B is evaluated from the Chapman–Enskog theory (Chapman and Cowling 1951) equation

$$D_{\mathrm{M}} = \frac{(1.858 \times 10^{-7}) T^{3/2} \left((1/M_{\mathrm{A}}) + (1/M_{\mathrm{B}})\right)^{1/2}}{P \sigma_{\mathrm{AB}}^2 I} \tag{4.9}$$

in which D_{M} is expressed in units $\mathrm{m^2\,s^{-1}}$, M_{A} and M_{B} are the molecular masses of the species A and B, σ_{AB} is a constant in the Lennard-Jones potential function and I is the collision integral (see Section 3.1). The Knudsen diffusivity, in contrast to the bulk diffusion coefficient, is calculated from the kinetic theory formula

$$D_{\mathrm{K}} = \frac{2}{3} r\bar{c} = \frac{2}{3} \mathrm{r} \left(\frac{8 R_{\mathrm{g}} T}{\pi M}\right)^{1/2} \tag{4.10}$$

where r is the pore radius, $\bar{c}$ the average molecular velocity and M the molecular mass. When the mean free path and pore radius are of a similar magnitude the resultant diffusivity is calculated in proportion to the individual bulk and Knudsen diffusivities. According to Pollard and Present (1948), for adsorption and desorption, equimolar counterdiffusion occurs and so the resultant resistance to diffusion is the sum of the resistances to bulk diffusion and Knudsen diffusion. Thus the net diffusion coefficient D is given by

$$1/D = (1/D_{\mathrm{M}}) + (1/D_{\mathrm{K}}) \tag{4.11}$$

Equations (4.9), (4.10) and (4.11) give the values of the Maxwellian (or bulk), Knudsen and resultant diffusion coefficients, respectively, for unconstrained transport in a single straight cylindrical pore. However, a gaseous component diffusing to the interior of a porous material travels tortuous pathways and is impeded by the volume fraction of solid unavailable for diffusion so that the resultant flux would be less than would otherwise be calculated by the above equations. Accordingly an effective diffusivity D_e represents the net reduced diffusion coefficient in a porous medium. It may be estimated by one of several methods. Experimental methods (outlined in Section 4.3) are the most reliable way of obtaining the effective diffusivity although an empirical method of estimation is often used. If ε_p is the intrapellet void fraction and τ a factor (termed the tortuosity) accounting for the tortuous nature of the pores (diffusing molecules have to travel longer distances than if the pores were straight) then one may write

$$D_e = \varepsilon_p D/\tau \tag{4.12}$$

Because $\varepsilon_p < 1$ and $\tau > 1$ then $D_e < D$ always. For most porous materials of known particle porosity, the value of τ lies within the range 1.5 to 10. In the field of catalysis, many related practical catalysts have a tortuosity factor between 1.8 and 3. Satterfield (1970) has outlined the method of obtaining τ. The effective diffusion coefficient D_e is found by an appropriate experimental method (see Section 4.3) for particles of known porosity and the resultant diffusivity, D, calculated from a knowledge of pore size distribution data. τ can then be calculated directly from equation (4.12). Figure 4.1 shows a plot of the ratio of the measured effective diffusivity to the calculated resultant diffusivity, D_e/D, as a function of measured porosity ε_p. Most of the points correlate with a line of slope 1.5 when a logarithmic scale is used for ordinate and abscissa. Yang and Liu (1982) conclude that τ is also a function of ε_p and show that for most porous structures D_e/D is approximately equal to ε_p^2/τ.

The random pore model of Wakao and Smith (1962) for a bidisperse pore structure may also be applied in order to estimate D_e. It was supposed that the porous solid is composed of stacked layers of microporous particles with voids between the particles forming a macroporous network. The magnitude of the micropores and macropores becomes evident from an experimental pore size distribution analysis. If D_m and D_μ are the macropore and micropore diffusivities calculated from equations (4.9) and (4.10), respectively, the random pore model gives the effective diffusivity as

$$D_e = \varepsilon_m^2 D_m + \varepsilon_\mu^2 (1 + 3\varepsilon_m) D_\mu/(1 - \varepsilon_m) \tag{4.13}$$

where ε_m and ε_μ are the macro and micro void fractions, respectively.

Many adsorbents have a broad distribution of pore sizes and neither

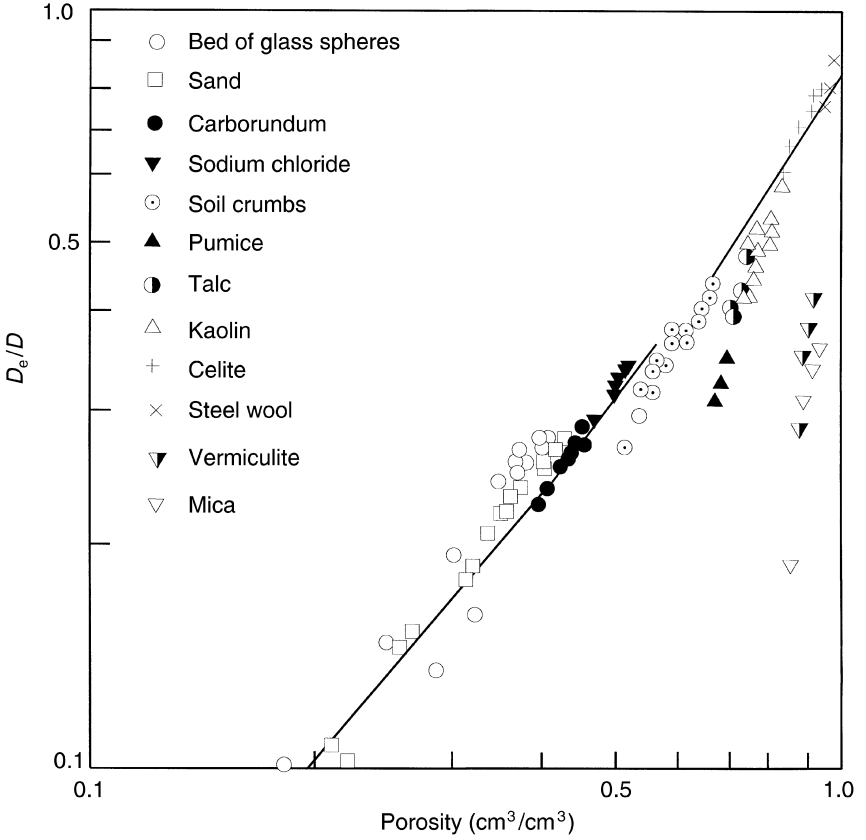

Figure 4.1 *Ratio of measured to calculated diffusivities as a function of porosity (source: Currie 1960).*

conform to a monodisperse nor a bidisperse porous structure. If $f(r)\mathrm{d}r$ is the volume fraction of pores having a size between r and $(r + \mathrm{d}r)$ then the effective diffusivity may be calculated from the integral

$$D_e = \frac{1}{\tau} \int_0^\infty D(r) f(r) \mathrm{d}r \tag{4.14}$$

arising from the parallel pore model of Johnson and Stewart (1965). The integral can be evaluated numerically provided the volume distribution of pores is known from a pore size analysis.

Surface diffusion

Surface diffusion of molecules across the interior surface of the adsorbent is another possible mode of diffusive transport. It occurs in parallel with bulk and Knudsen diffusion both of which describe diffusion through the gaseous space contained within pores. Adsorbed species, however, may possess mobility and move across the surface to other vacant adsorption sites. Surface diffusion only occurs when molecules are adsorbed and provided the surface attractive forces are not so strong as to prevent surface mobility. Surface diffusion is most likely to be significant in porous adsorbents with a high surface area and narrow pores. The total diffusive flux is then the sum of the contributions from Knudsen diffusion, bulk diffusion (if there are some wider pores as well as narrow pores) and surface diffusion. Because surface diffusion cannot be easily measured directly, the surface diffusive flux has to be estimated by subtraction of the sum of calculated effective Knudsen and bulk diffusive fluxes from the total flux measured experimentally in a Wicke and Kallenbach (1941) cell (see Section 4.3.1). The magnitude of the surface diffusion coefficient D_s found in this way has been reported to be within the range 10^{-7} to 10^{-10} m^2 s^{-1}. The temperature coefficient for surface diffusion can be described by an equation analogous to that of the Arrhenius equation widely used in chemical kinetics. Thus one writes

$$D_s = D_o \exp(-E_s/R_g T) \tag{4.15}$$

where D_o is the pre-exponential factor for surface diffusion. The value of E_s is generally less than the heat of adsorption. Furthermore, the overall unidirectional flux J (sum of fluxes for Knudsen and surface diffusion) in the direction z given by

$$J = -\left\{D_K \frac{dc}{dz} + \rho_p D_s \frac{dq}{dz}\right\} = -\left\{D_K + \rho_p D_s K\right\}\frac{dc}{dz} \tag{4.16}$$

implies that the net contribution to the flux from surface diffusion depends on the product $D_s K$ (where K is the Henry's law constant given by dq/dc) and not simply D_s. Because K normally decreases with increase of temperature more rapidly than D_s increases, the extent of surface diffusion generally declines with increase in temperature. The data of Schneider and Smith (1968) confirms such decreasing effect of surface diffusion with increase of temperature. Except at low concentrations (in the concentration region where Henry's law is obeyed) D_s is found to be strongly dependent on surface concentration (Gilliland *et al.* 1974, Sladek *et al.* 1974) which is proportional to the amount adsorbed.

Diffusion in isothermal zeolite crystals

As discussed in Chapter 2, the class of adsorbents known as zeolites form crystalline structures containing apertures (referred to as windows) of molecular dimensions through which molecules of adsorbate smaller than the aperture may enter the well-defined internal channels leading to the larger cavities within the crystal where the sites for adsorption are located. Diffusion into zeolites is therefore relatively slow because of the restricted access. Diffusion coefficients D_c associated with zeolite crystal structures have magnitudes in the range 10^{-13} to 10^{-15} m^2 s^{-1}.

The rate of adsorption of gases by zeolites may be assessed from batch experiments in which finite quantities of adsorbate are admitted to a vessel containing the adsorbent and, either from weight changes of the adsorbent or from information concerning gas concentration, the uptake of adsorbate followed as a function of time (see Sections 4.3.2 and 4.3.4 for experimental methods). Models of adsorption of gases by zeolites can also be formulated and compared with experimental kinetic data. Assuming that a crystal of zeolite may be regarded as an approximately spherical object, a steady state isothermal (heat of adsorption rapidly dissipated) material balance (Fick's second law of diffusion) on the adsorbate yields

$$\frac{1}{r^2}\frac{\partial}{\partial r}\left(r^2 D_c \frac{\partial q}{\partial r}\right) = \frac{\partial q}{\partial t} \tag{4.17}$$

At the centre of the crystal, considerations of symmetry require that

$$r = 0 \qquad \frac{\partial q}{\partial r} = 0 \quad \text{for all } t \geq 0 \tag{4.18}$$

while at the periphery of the crystal

$$r = r_c \qquad q = q_o \tag{4.19}$$

The initial condition, provided the amount adsorbed is small in comparison with the total quantity of adsorbate introduced, may be interpreted as a constant concentration of adsorbate and is represented by

$$t = 0 \qquad q = q_{oi} \quad \text{for all r} \geq 0 \tag{4.20}$$

The average adsorbate concentration through the crystal may be computed from

$$\bar{q} = \frac{3}{r_c^3}\int_0^{r_c} qr^2 \, dr \tag{4.21}$$

The set of equations (4.17) to (4.21) inclusive was solved analytically by Ruckenstein *et al*. (1971) who compared the mass of adsorbate adsorbed at a given time, m_t, with the amount adsorbed after an infinite lapse of time, m_∞, (when the crystals were saturated with adsorbate). They expressed the ratio m_t/m_∞, as a function of time t. It should be noted that, for small quantities of adsorbate introduced to the system the adsorption isotherm is linear and $q = Kp$. The intercrystalline diffusivity can then be regarded as independent of adsorbate concentration. The theoretical fractional approach to equilibrium was shown to be

$$\frac{m_t}{m_\infty} = 1 - \frac{6}{\pi^2} \sum_{n=1}^{\infty} \frac{1}{n^2} \exp\left(- \frac{n^2 \pi^2 D_c t}{r_c^2} \right) \tag{4.22}$$

When the fractional uptake is greater than 70%, only the first term of the summation is retained. When, on the other hand, the fractional uptake is less than 30%

$$\frac{m_t}{m_m} = 6 \left(\frac{D_c t}{\pi r_c^2} \right)^{1/2} \tag{4.23}$$

is a good approximation.

The intracrystalline diffusion coefficient D_c was considered to be independent of adsorbate concentration in the above analysis of Ruckenstein *et al.* (1971). However, if the initial quantity of adsorbate admitted to the adsorbent is such that the vapour phase concentration does not remain constant, then account should be taken of the variation of the intracrystalline diffusivity with concentration. This dependence of diffusivity on concentration may be derived by equating the Fickian flux to the thermodynamically defined flux, the latter depending on the product of concentration and the gradient of chemical potential. It then follows (Ruthven 1984, Yang 1987) that the diffusion coefficient is related to adsorbed phase concentration by the equation

$$D_c = D_o \, d \ln p / d \ln q \tag{4.24}$$

in which D_o is independent of concentration. If the adsorbate–adsorbent system obeys a Langmuir relation then

$$D_c = D_o/(1 - (q/q_m)) \tag{4.25}$$

The diffusion equation is then written

$$\frac{\partial q}{\partial t} = \frac{D_o}{r^2} \frac{\partial}{\partial r} \left\{ \frac{r^2}{(1 - (q/q_m))} \frac{\partial q}{\partial r} \right\} \tag{4.26}$$

Garg and Ruthven (1972) solved equation (4.26) numerically but relaxed the assumption that only a small amount of adsorbate is admitted to the system. They defined a parameter $\lambda = (q_o - q_{oi})/(q_m - q_{oi})$ while D_o was modified to $D_o/(1 - q_{oi}/q_m)$. q_o and q_{oi} are defined by equations (4.19) and (4.20) respectively, while q_m is the amount adsorbed at equilibrium. In addition these authors also considered how the uptake curve would differ if Volmer's isotherm (see Section 3.3.6) were obeyed rather than the Langmuir isotherm. Figure 4.2 illustrates how m_t/m_∞ varies with the dimensionless quantity $(D_o t/r_c^2)^{1/2}$ for both adsorption and desorption when a Langmuir isotherm is obeyed and D_c follows equation (4.25). The curves demonstrate that the uptake of adsorbate is influenced by the quantity of adsorbate initially introduced (the parameter λ) to the batch adsorbate–adsorbent system. Figure 4.3 shows how the effective diffusivity D_e[1] is dependent on λ. This latter diffusivity should not to be confused with the effective diffusivity D_e described earlier; D_e lies between the extremes of the concentration independent diffusivity D_o and the average diffusivity $\bar{D}$ over the concentration range $0 < q < q_o$.

The theory outlined above is supported by the experimental work of Kondis and Dranoff (1970, 1971) who measured differential uptakes

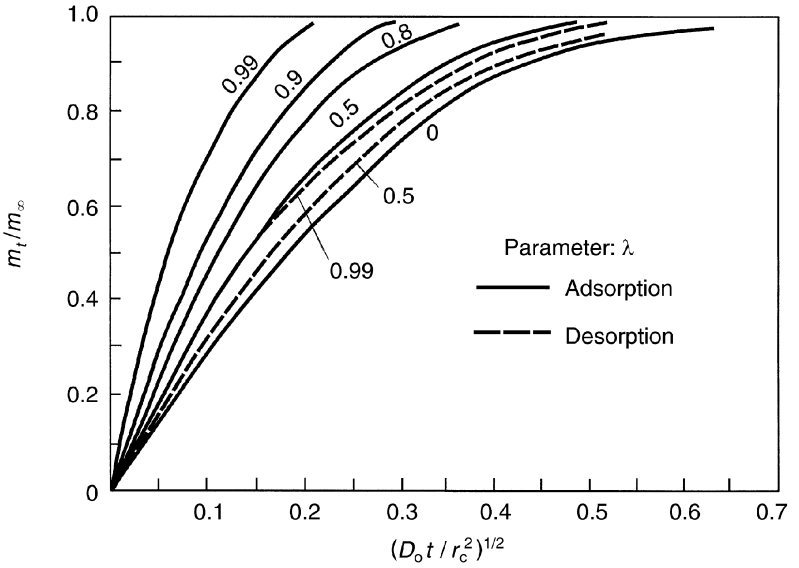

Figure 4.2 *Uptake curves for intercrystalline diffusion (source: Garg and Ruthven 1972).*

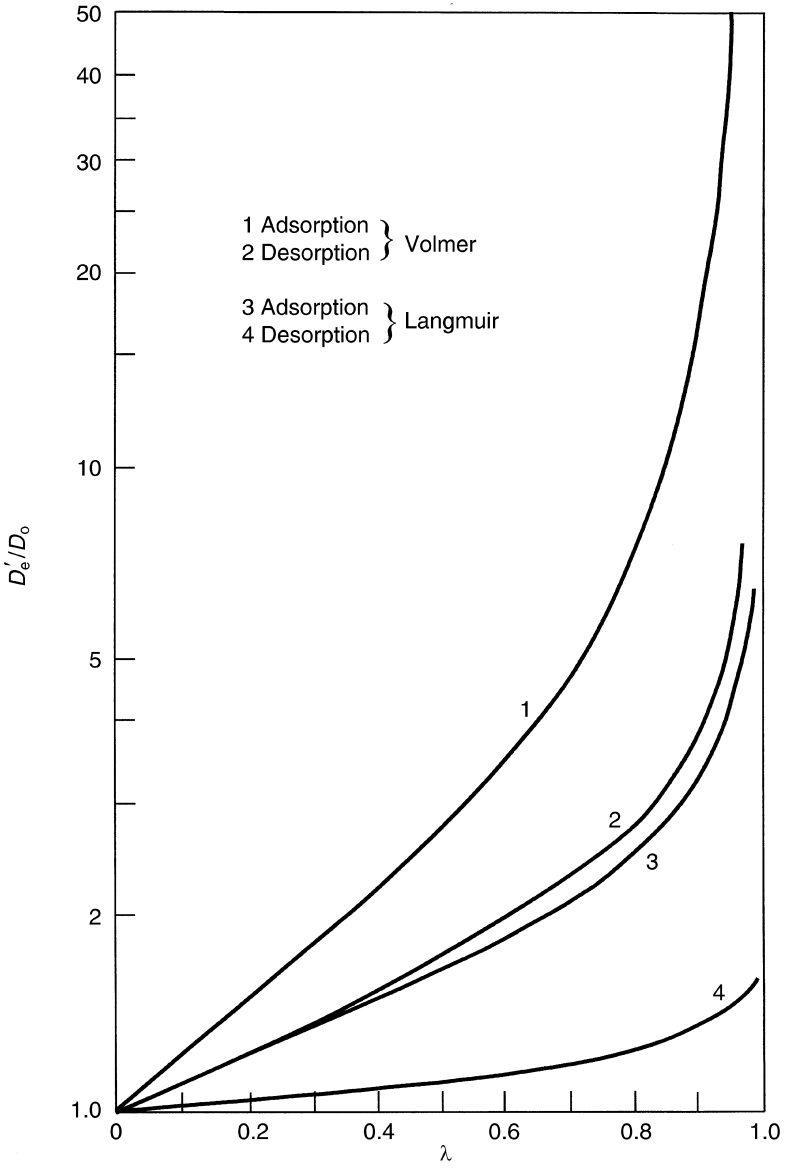

Figure 4.3 D_e'/D_o as a function of λ (source: Garg and Ruthven 1972).

of ethane on a 4A zeolite adsorbent. Garg and Ruthven (1972) compared their calculations based on the solution to equation (4.22) with the

published experimental work and, as Figure 4.4 shows, obtained close agreement for differential amounts of ethane adsorbed and desorbed.

Diffusion in commercial zeolite pellets

Commercial zeolites have to be sufficiently robust to withstand sudden changes in pressure such as occur in pressure swing adsorbers (see Section 5.6). The crystalline zeolite adsorbent is therefore bound together with a material such as clay to form a composite structure which contains macropores and micropores as illustrated by Figure 4.5. The individual zeolite crystallites, which have narrow molecular size windows and channels by means of which adsorbates access the larger cavities within each crystal, are regarded as the microporous material within the composite pellet. Intercrystalline voids then form a network of larger macropores while the clay binder also contains micropores. The relative importance of resistances to interparticle mass transfer, intracrystalline diffusion and intraparticle diffusion may be assessed by an experimental method involving step changes

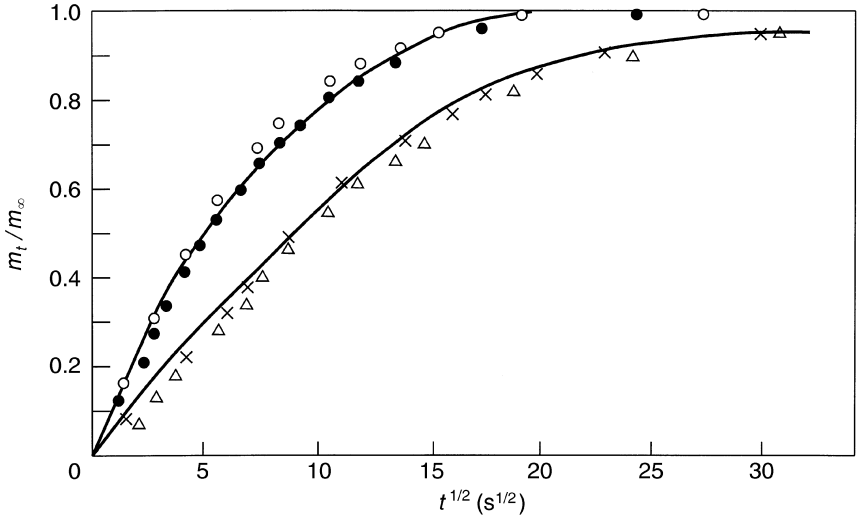

Figure 4.4 *Comparison of experimental and theoretical curves for the uptake of C_2H_6 on a 4A zeolite. The experimental data are those of Kondis and Dranoff (1970); o and • adsorption experiments, × and △ desorption experiments; — theoretical curves corresponding to $D_o/r_c^2 = 2.45 \times 10^{-4}\ s^{-1}$* (source: Garg and Ruthven 1972).

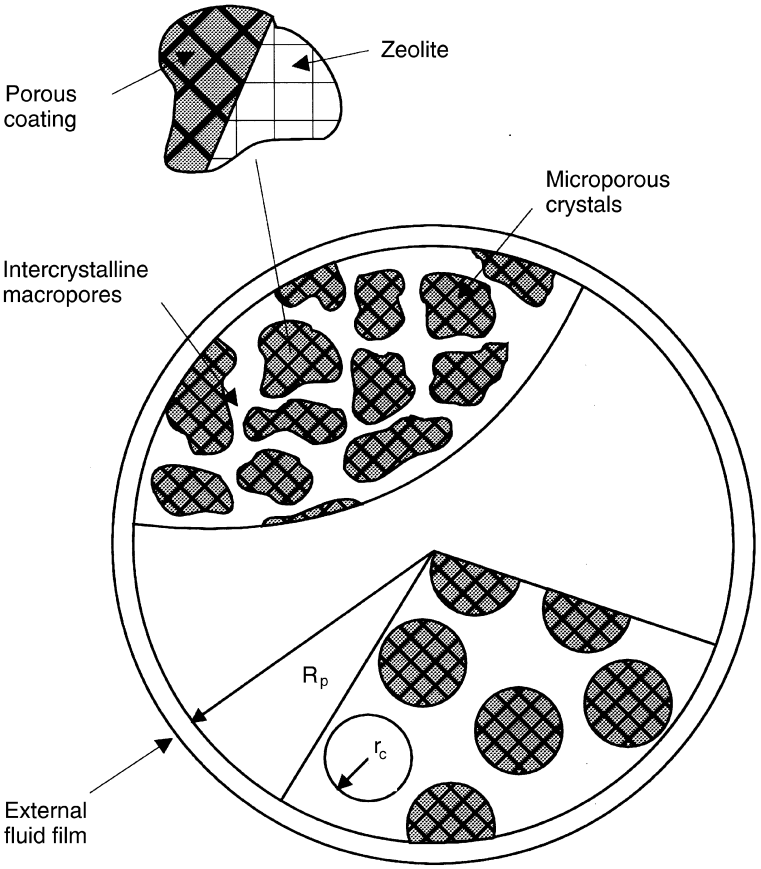

Figure 4.5 *Composite pellet containing macropores, micropores and crystals.*

in concentration of a continuous feed of inert carrier gas and adsorbate to an isothermal column packed with particles of the adsorbent. The method is outlined in Section 4.4.

A model of a composite zeolite pellet must thus be represented by a combination of coupled equations for intracrystalline diffusion and macropore diffusion. The diffusion of adsorbate within crystals was discussed in the previous section and intracrystalline diffusion is given by equation (4.17). Macropore diffusion for a spherical pellet of radius R_p, macropore diffusivity D_p and porosity ε_p is described by

$$\frac{1}{R^2}\frac{\partial}{\partial R}\left(R^2 D_p \frac{\partial c}{\partial R}\right) = \frac{\partial c}{\partial t} + \left(\frac{1-\varepsilon_p}{\varepsilon_p}\right)\frac{\partial \bar{q}}{\partial t} \tag{4.27}$$

where the average adsorbate concentration $\bar{q}$ is expressed by equation (4.21). The coupled equations (4.17) and (4.27) were first solved analytically by Ruckenstein *et al.* (1971) who assumed a step change in concentration at the gas–solid interface of a composite pellet containing micropores and macropores. Ma and Lee (1976) extended the analysis to include the possibility of a progressive change in concentration of the gas external to the pellet as adsorption proceeds. The boundary conditions which then apply to the coupled equations (4.17), (4.21) and (4.27) are, for the centre of the microporous crystalline spheres,

$$r = 0 \qquad \frac{\partial q}{\partial r} = 0 \quad \text{for all } t \geq 0 \qquad \text{(equation (4.18))}$$

and at the periphery of the crystals

$$r = r_c \qquad q = Kc \tag{4.28}$$

assuming a linear isotherm over the concentration range considered and where c is the gas phase concentration in the macropore structure of the whole pellet at a radial position r at a given time t. For diffusion in the macropores the boundary conditions are, at the pellet centre

$$R = 0 \qquad \frac{\partial c}{\partial R} = 0 \quad \text{for all } t \geq 0 \tag{4.29}$$

while at the interface between bulk gas phase and pellet

$$R = R_p \qquad c = c_o \quad \text{for all } t \geq 0 \tag{4.30}$$

Initial conditions apposite to the stated problem are

$$t = 0 \qquad c = 0 = q \quad \text{for all } R \geq 0 \tag{4.31}$$

The analytical solution given by Ruckenstein *et al.* (1971) expresses the dimensionless uptake of adsorbate m_t/m_∞ as a function of time. The solution is complex and involves two parameters defined by $\alpha = (D_c/r_c^2)/(D_p/R_p^2)$ and $\beta = 3\alpha\,(1-\varepsilon_p)\,q_o/\varepsilon_p c_o$. When the resistance to diffusion is controlled by diffusion in the micropores ($\beta \to 0$), the system is described by equations (4.17) to (4.21) inclusive, the uptake of adsorbate being represented by equation (4.22). When, on the other hand, macropore resistance dominates the diffusion process ($\beta \to \infty$), then equations (4.27) to (4.30) inclusive apply and the condition (4.18) is redundant because the concentration throughout the crystal is uniform. The solution is then identical to equation (4.22) with r_p and D_p replacing r_c and D_c, respectively.

For intermediate values of β the uptake curves are different and cannot be represented by such a simple solution. Lee (1978) demonstrated how the uptake curves depend on the value of the parameter β. Figure 4.6 shows the gradual transition in shape adopted by the uptake curves as the rate of adsorption changes from micropore to macropore diffusion control corresponding to β varying between 0 and 10. It is also apparent that the curves are sensitive to variation in the fluid phase concentration external to the adsorbent as represented by the dimensionless parameter Λ, which is a measure of the extent by which the fluid concentration has diminished to the equilibrium concentration (when further adsorption has ceased) compared with the initial fluid concentration. In a batch system such a change could occur if there is only a small amount of adsorbate present and then the boundary condition given by equation (4.30) would need to be replaced by a time-dependent function. If, however, there is a large excess of adsorbate Λ is approximately zero and the boundary condition (4.30) applies.

4.2.3 Heat transfer during adsorption

Because heat is released during the process of adsorption, it follows that the adsorbate–adsorbent system is not strictly isothermal. Departures from isothermality depend on the relative rates of inter- and intraparticle mass

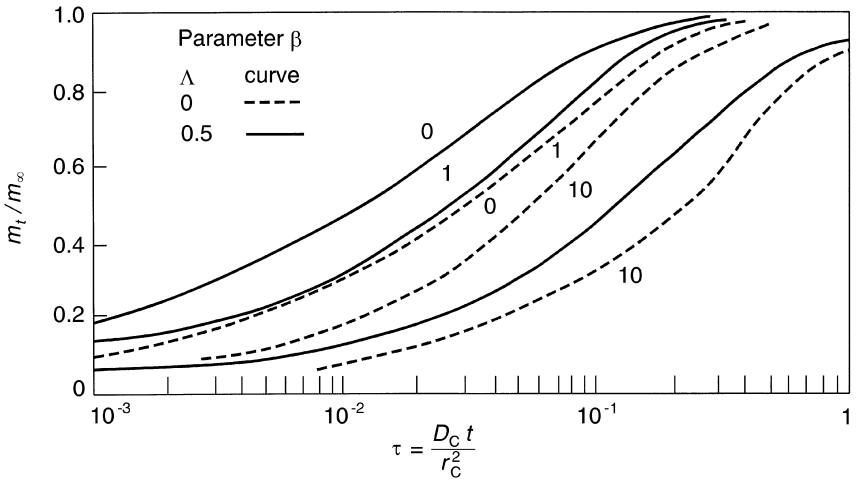

Figure 4.6 *Transition from micropore to macropore diffusion control; figures on curves represent the parameter β. Discontinuous curves are for $\Lambda = 0$ and continuous curves are for $\Lambda = 1$ (see text) (source: Lee 1978).*

and heat transfer. In the steady state the mass flux across the film between bulk adsorbate and particle surface is equal to the diffusive flux at the interface between particle and bulk phase and hence

$$k(c_g - c) = D_e(\partial c/\partial R) \text{ at } R = R_p \tag{4.32}$$

Similarly, heat transferred across the film from the particle periphery to the bulk fluid will be equal to the heat flux in the steady state so

$$h(T - T_g) = k_e(\partial T/\partial R) \text{ at } R = R_p \tag{4.33}$$

where k_e is the effective thermal conductivity of the adsorbent (analogous to the effective diffusivity).

Casting both of the above equations into dimensionless form by writing $c/c_g = y$, $T/T_g = \theta$ and $R/R_p = z$ the equations become, respectively,

$$(\partial y/\partial z)/(1 - y) = kR_p/D_e = Bi_m \quad \text{at } z = 1 \tag{4.34}$$

and

$$(\partial \theta/\partial z)/(\theta - 1) = hR_p/k_e = Bi_h \quad \text{at } z = 1 \tag{4.35}$$

We see that the ratio of rates of interparticle mass transfer to intraparticle mass transfer is given by the mass Biot number Bi_m $(= kR_p/D_e)$. The ratio of rates of interparticle heat transfer to intraparticle heat transfer is similarly given by the Biot number for heat transfer Bi_h $(= hR_p/k_e)$. When either one of the Biot numbers is large, the major resistance to the appropriate transport process is within the pellet rather than external to the pellet. Froment and Bischoff (1979) indicate that, for the majority of cases, the major resistance to mass transfer is within the porous pellet whereas the major resistance to heat transfer is in the gaseous boundary layer (the gas film) between particle and bulk fluid. For heterogeneously catalysed reactions this is generally the situation (Kehoe and Butt 1972, Carberry 1975) although exceptions are known. For physical adsorption processes, however, mass transfer resistance is invariably within the adsorbent pellet. Heat transfer resistance is generally external to the adsorbent pellet but Brunovska *et al.* (1978) have shown that the relative rates of inter- and intraphase particle transport depend on the adsorbate–adsorbent pair. In some circumstances, particularly, for example, when the adsorbate is chemisorbed, resistance to heat transfer within the particle should not be eschewed.

For heuristic purposes we consider a zeolite crystal and assume that heat transfer resistance is wholly within the gas film surrounding the crystal and that intracrystalline diffusion is the rate-controlling mass transfer process. The set of equations which have to be solved to yield an expression for the

uptake of adsorbate by an adsorbent particle when only a small step change in adsorbate concentration is introduced to the particle periphery includes unsteady state balances for both mass and heat transfer. The transient mass balance is

$$\frac{1}{r^2}\frac{\partial}{\partial r}\left(r^2 D_c \frac{\partial q}{\partial r}\right) = \frac{\partial q}{\partial t} \qquad \text{(equation (4.17))}$$

with the average adsorbed phase concentration given by

$$\bar{q} = \frac{3}{r_c^3}\int_0^{r_c} qr^2\,\mathrm{d}r \qquad \text{(equation 4.21))}$$

The unsteady state heat transfer equation is

$$(-\Delta H)\frac{\mathrm{d}\bar{q}}{\mathrm{d}t} = c_s\frac{\mathrm{d}T}{\mathrm{d}t} + ha\,(T - T_g) \qquad (4.36)$$

in which c_s represents the heat capacity of the solid porous adsorbent particle. Note that equation (4.36) is an ordinary differential equation (as opposed to a partial differential equation) because the temperature within the particle depends only on the average adsorbed phase concentration in the particle, the temperature being uniform throughout the particle because all the heat transfer resistance is external to the particle. At the surface of the crystal a linear equilibrium relationship is assumed to exist

$$\frac{q - q_o}{q_\infty - q_o} = 1 + \left(\frac{\partial q^*}{\partial T}\right)_p\left(\frac{T - T_o}{q_\infty - q_o}\right) \quad \text{at } r = r_c \qquad (4.37)$$

where q_o and T_o are the initial values of the adsorbed phase concentration and the temperature, respectively, and q_∞ is the final adsorbed phase concentration after adsorption has ceased. The term $(\partial q^*/\partial T)_p$ is the gradient of the equilibrium isobar for the essentially constant partial pressure at which the small step change in concentration occurs. Boundary conditions apposite to this problem as it has been posed are

$$\partial q/\partial r = 0 \quad \text{at } r = 0 \quad \text{for all } t \geq 0 \qquad \text{(equation (4.18))}$$

and

$$q = 0 \quad \text{at } t = 0 \quad \text{for all } r \geq 0 \qquad (4.38)$$

The solution to the above set of equations, commencing with the restated equation (4.18) through to equation (4.38), is given in a paper by Ruthven *et al.* (1980). The principal features of the uptake curves are illustrated by Figure 4.7. Two parameters γ $(= har_c^2/c_sD_c)$ and δ $(= \Delta H\,(\partial q^*/\partial T)/c_s)$ are required to describe the behaviour of the solution. The symbol c_s

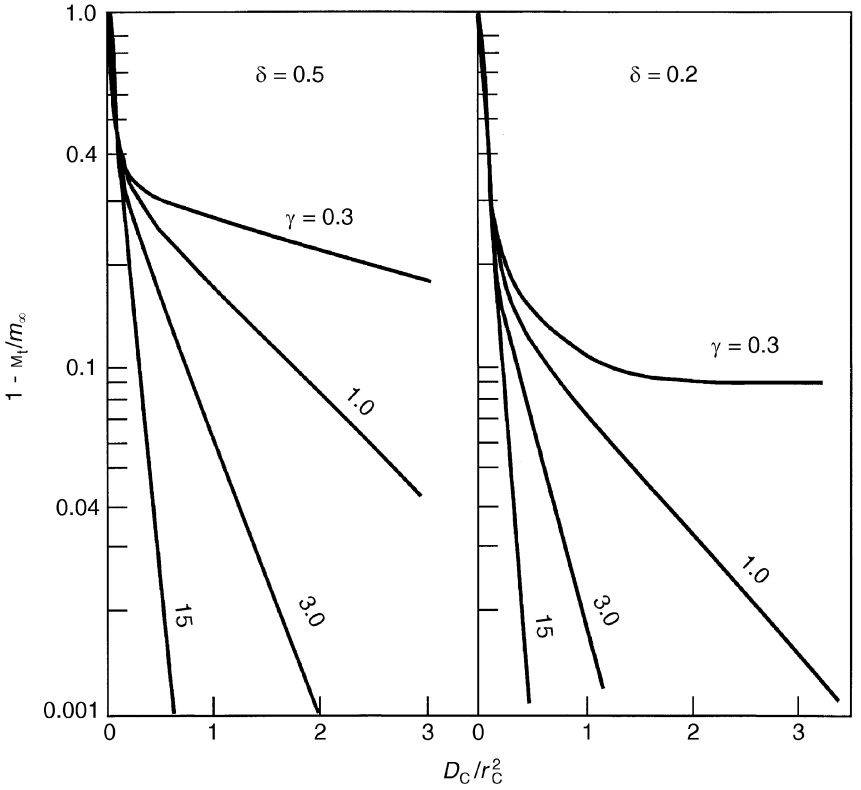

Figure 4.7 *Effect of heat transfer resistance on uptake of adsorbates. The figures on the curves represent the parameter γ. The left-hand diagram is for δ = 0.5 and the right-hand diagram is for δ = 0.2 (see text) (source: Ruthven et al.* 1980).

represents the heat capacity of the solid adsorbent. When γ is sufficiently small, the rate of uptake is controlled by heat transfer, but when $\gamma \to \infty$ the system behaves isothermally (large heat transfer coefficient) and conforms to the equation (4.22) corresponding to adsorption by crystals at isothermal conditions. For small values of γ when heat transfer is the controlling factor the solution for the uptake curve yields

$$\frac{m_t}{m_\infty} = 1 - \left(\frac{\delta}{1+\delta}\right)\exp\left\{-\frac{hat}{c_s(1+\delta)}\right\} \tag{4.39}$$

Equation (4.39) may also be obtained from a heat balance on the crystal

assuming that equilibrium between adsorbate and adsorbent is maintained (Ruthven *et al.* 1980).

Figure 4.8 shows some experimental uptake curves for the adsorption of CO_2 in a 5A zeolite which agree very well with equation (4.39) expressing rates of adsorption limited by heat transfer.

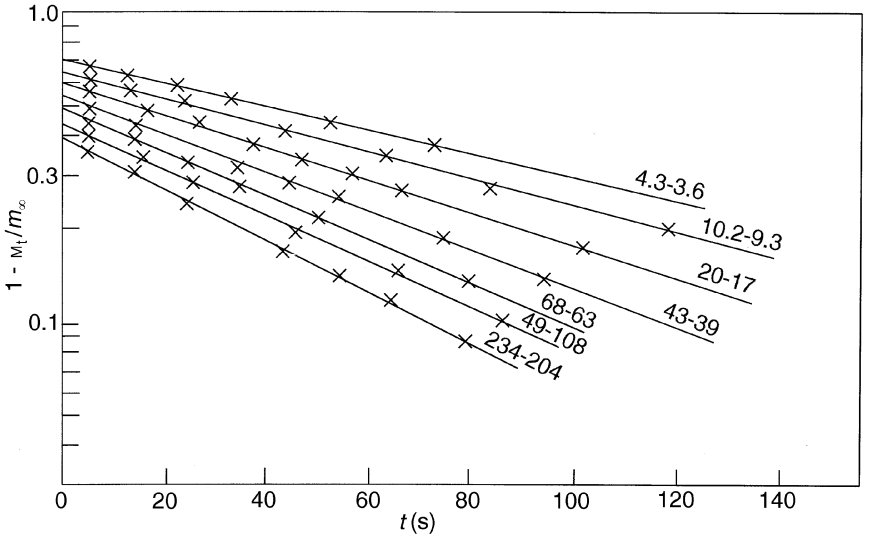

Figure 4.8 *Experimental uptake curves for CO_2 on 5A zeolite demonstrating the limiting behaviour of heat transfer control. Adsorption temperature 273 K. Figures on curves represent various adsorbate pressures which relate to differing effective heat capacities. Curve 1, 4.3 – 3.6 torr; curve 2, 20 – 17 torr; curve 3, 68 – 63 torr; curve 4, 234 – 204 torr.*

4.3 EXPERIMENTAL MEASUREMENT OF DIFFUSION COEFFICIENTS CONCOMITANT WITH ADSORPTION

It should be apparent from what has been discussed in the whole of Section 4.2 that adsorption rates depend explicitly on values of the diffusion coefficient of the adsorbing fluid. A number of experimental techniques have been developed for the measurement of diffusion coefficients, some of which are outlined in the following Sections 4.3.1 to 4.3.4.

4.3.1 The Wicke–Kallenbach cell

The effective diffusivity of a porous adsorbent may be determined as the adsorption process proceeds by passing the gas for which the diffusion coefficient is being measured, diluted and carried by an inert gas, such as helium, across one face of the adsorbent pellet and the inert gas alone across the obverse face of the pellet. The fabricated adsorbent pellet is compressed into a cylindrical shape and sealed within a cell known as a Wicke–Kallenbach cell (shown in Figure 4.9) after the first publication of the method originated by Wicke and Kallenbach (1941). The measurement procedure has since been modified by Henry *et al.* (1961) and Suzuki and Smith (1972). The method adopted by Suzuki and Smith is to allow a pulse of the adsorbate under investigation to be injected into an inert gas stream

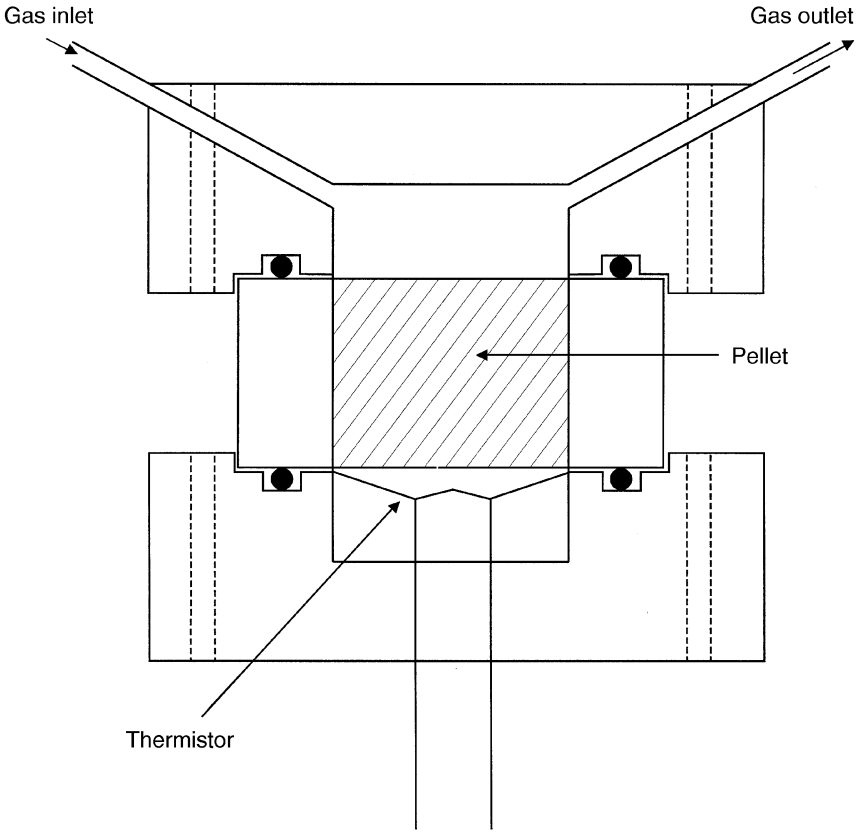

Figure 4.9 *Wicke–Kallenbach diffusion cell.*

(such as helium) across one face of the adsorbent material fabricated into a cylindrical shape and sealed within the cell. A steady stream of pure inert gas is allowed to pass through the detector volume at the obverse face of the pellet where a thermistor detects the response signal arising from the gas diffusing through the pellet from the original input pulse. Gaskets ensure that no gas passes through to the detector volume except by diffusion through the pellet. An unsteady state material balance for the adsorbate in the direction z yields

$$\varepsilon_p \frac{\partial c}{\partial t} + \rho_p \frac{\partial q}{\partial t} = D_e \frac{\partial^2 c}{\partial z^2} \tag{4.40}$$

where ε_p and ρ_p are the porosity and density of the adsorbent pellet, respectively. The net rate of adsorption may be represented by the difference in rates of adsorption and desorption

$$\frac{\partial q}{\partial t} = k_a (c - q/K) \tag{4.41}$$

where k_a is the adsorption rate constant and K the adsorption equilibrium constant. At the face of the pellet there is a pulse input of adsorbate which is represented by

$$z = 0 \qquad c = \mathrm{m}\,\delta\,(\mathrm{t}) \tag{4.42}$$

where m is the magnitude of the concentration pulse and δ (t) is the Dirac delta function. Within the detector perfect mixing is assumed, so if the cross-sectional area of pellet is S and its volume is V the diffusive flux at the obverse face is

$$z = L, \quad D_e (\partial c/\partial z)_{z=L} = -(V/S)(\partial c_L/\partial t) \tag{4.43}$$

The initial condition, when the pulse is admitted to the pellet face, is

$$t = 0 \qquad c = 0 \quad \text{for all } z \geq 0 \tag{4.44}$$

It is unnecessary to solve the above set of equations in the form c (t) because the first absolute moment of the experimentally measured response curve (see Figure 4.10) can be related, by means of Laplace transformation, to the parameters D_e, ε_p, K and V/SL. If a number of adsorbent pellets of differing length are each subjected to the same magnitude of concentration impulse then a plot of the first absolute moment (corrected for dead volume and the finite time of injection) against V/SL yields a straight line of slope $1/D_e$ and intercept $-\varepsilon_p/2$, the latter quantity also being determined independently by pyknometry. For details of the technique of moments analysis the reader should consult a text such as Wen and Fan (1975). Figure 4.10 illustrates the type of input concentration pulse often used for this method and the corresponding output

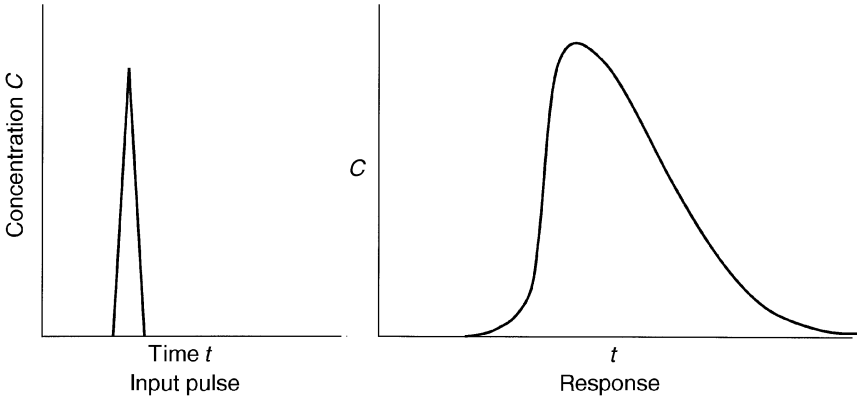

Figure 4.10 *Input pulse and response.*

response to be expected. A typical plot of calculated moments of the response as a function of pellet dimensions is shown in Figure 4.11.

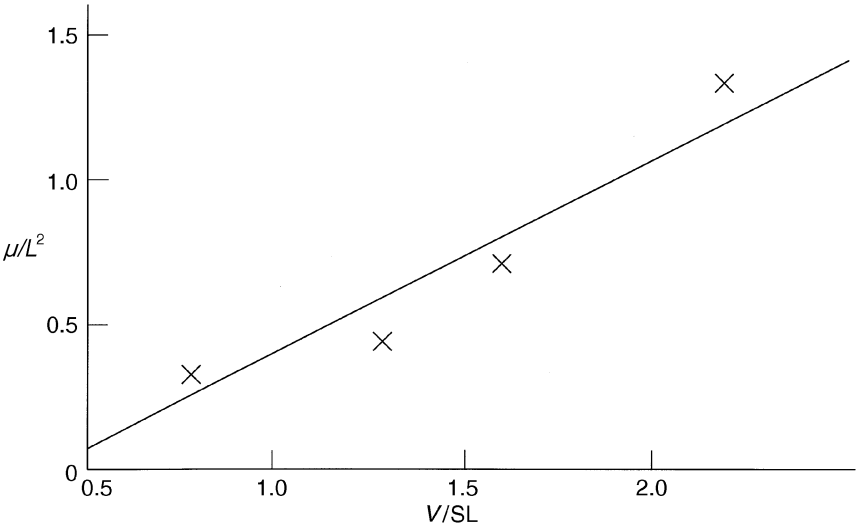

Figure 4.11 *Moments of response as a function of pellet dimensions: μ/L^2 plotted against V/SL for the adsorption of butane on silica at 293 K and the simultaneous diffusion of butane through the compressed pellet (source: England and Thomas 1976).*

4.3.2 Gravimetric measurements

As gas or vapour is adsorbed by an adsorbent so its weight gradually increases until the adsorbent is saturated. Thus if an adsorbate is admitted to an adsorbent and the increase in weight of the adsorbent is measured as a function of elapsed time, the uptake curve can be used to measure the diffusion coefficient by matching the curve obtained with the theoretical uptake curve described by equation (4.22). Provided the experimental conditions are such that isothermal conditions are maintained and the total quantity of gas adsorbed up to the time when the adsorbent is saturated in comparison with the amount of adsorbate remaining in the gas phase is small (essentially constant adsorbate concentration), then equation (4.22) may be used to estimate the effective diffusion coefficient for the adsorbate –adsorbent pair. The gravimetric balance described by Gunn *et al.* (1974) for the adsorption of water vapour by porous polyurethane materials is a suitable description of the construction and operation of the apparatus and also the method of curve fitting used to extract the diffusion coefficient from the experimental uptake curve. The form of the curve in the example cited differs from equation (4.22) because of the hollow cylindrical shape of the sample used which results in radial as well as longitudinal diffusion coefficients being a property of the system. Commercially available gravimetric balances are also available which are suitable for experiments of this type. When interpreting results from gravimetric measurements involving crystalline adsorbents, the portion of the uptake curve which is most suitable for matching with equation (4.22) is when $0.2 < m_t/m_\infty < 0.5$. This is because the initial uptake is sensitive to interparticle transport resistance while portions of the uptake curve at values of $m_t/m_\infty < 0.5$ may be affected by heat transfer resistances.

4.3.3 Nuclear magnetic resonance measurements

Application of nuclear magnetic resonance (NMR) to the study of diffusion of liquids in adsorbents has evolved through the use of the pulsed field gradient (PFG) method originally developed by Stejskal and Tanner (1965 and 1968) who measured self-diffusion coefficients in liquids. In this technique a sample of the material to be investigated is placed in a pulsed magnetic gradient field. Nuclear spins of the sample are then excited by means of a radio frequency pulse. Reversing the magnetic gradient field pulse following a known interval of time produces an attenuation of the signal which is a direct measurement of the mean square distance travelled by the diffusing species in the time interval between the gradient pulses. The diffusion of n-hexane in zeolite crystals has been successfully studied using

this technique (Karger and Pfeifer 1976). The reader is referred to a review article by Gladden (1994) for an overview of the PFG technique.

4.3.4 Isotopic labelling

Sargent and Whitford (1971) measured the self-diffusivity of carbon dioxide in a 5A zeolite by exposing radioactive $C^{13}O_2$ adsorbate at constant total concentration to the adsorbent and measuring the radioactivity as a function of time. This method provides an accurate means of following the $C^{13}O_2$ concentration and thence deducing the self-diffusion coefficient by matching the uptake curve with equation (4.22). Quig and Rees (1976) used a non-radioactive isotopic labelling method when studying the self-diffusion of hydrocarbons in a 5A zeolite, but followed the progress of the uptake with a mass spectrometer.

4.4 MASS TRANSFER RESISTANCES IN SERIES

Provided chemical reaction does not occur simultaneously with the diffusion processes in an adsorbent particle, analysis of the response to a pulse input of an adsorbate to a column packed with an adsorbent provides a convenient experimental method of deducing the separate contributions of inter- and intraphase mass transfer and diffusion to the overall resistance to adsorption. This is because each one of the resistances to mass transfer is in series and thus linearly additive.

Various researchers, including Thomas (1944), Lapidus and Amundson (1952), Levenspiel and Bischoff (1963) and Rosen (1954) have produced analytical solutions to the coupled differential equations describing flow of adsorbate through a bed of adsorbent in which mass transfer and diffusion processes occur. Their solutions differ in detail but numerical representation of the breakthrough curves (see Chapters 5 and 6) of adsorbate from the adsorbent bed produces very similar results. Glueckauf and Coates (1947) and Glueckauf (1955) introduced a linear driving force expression for the rate of adsorption

$$\partial q/\partial t = k_a (q_\infty - q) = k_a K (c - c_\infty) \tag{4.44}$$

where q_∞ and c_∞ are the equilibrium concentrations of adsorbate at the solid and in the gaseous phases respectively, K is the Henry's law (Section 3.3.2) equilibrium constant and k_a the adsorption rate constant. With this assumption of a linear rate expression it was shown that the various analytical solutions could be made numerically equivalent, so reducing computation considerably. By adopting the linear driving force assumption,

a moments analysis of adsorbate breakthrough curves from a column containing a zeolite adsorbent yields an expression which can be used to determine the separate mass transfer and diffusion resistances. Denoting the first moment of the response to an input signal by μ and the second moment by σ^2, the ratio $\sigma^2/2\mu^2$ yields results for a general model formulated by Haynes and Sarma (1973) which may be compared with the same ratio of moments obtained for the simplified model employing a linear driving force for the adsorption rate. When experiments are confined to a low Reynolds number region of flow (u being the superficial fluid velocity through the bed of voidage e) the result for the general model is

$$\frac{\sigma^2}{2\mu^2}\frac{L}{u} = \frac{D_L}{u^2} + \left(\frac{e}{1-e}\right)\left(\frac{R_p{}^2}{3D_m} + \frac{R_p{}^2}{15e_pD_p} + \frac{r_c{}^2}{15KD_c}\right)\left(1 + \frac{e}{K(1-e)}\right)^{-2} \tag{4.45}$$

where K is the Henry's law constant.

For the linear rate model of Glueckauf and Coates the corresponding result is

$$\frac{\sigma^2}{2\mu^2}\frac{L}{u} = \frac{D_L}{u^2} + \left(\frac{e}{1-e)}\right)\frac{1}{k_aK}\left(1 + \frac{e}{(1-\mathrm{e})\,K}\right)^{-2} \tag{4.46}$$

where k_a is the rate coefficient corresponding to the linear driving force model (equation 4.45).

Both models become equivalent if

$$\frac{1}{k_aK} = \frac{R_p{}^2}{3D_m} + \frac{R_p{}^2}{15e_pD_p} + \frac{r_c{}^2}{15KD_c} \tag{4.47}$$

The individual axial dispersion term D_L, the molecular diffusion coefficient D_m and the intraparticle and intracrystalline diffusivities may thus be extracted from equation (4.45) from a plot of $(\sigma^2/2\mu^2)\,(L/u)$ against $1/u^2$ for a range of particle sizes. Figure 4.12 shows such an experimental plot for three different adsorbates, N_2, CF_4 and i–C_4H_{10} passed at low velocity through a bed of 4A zeolite (Kumar *et al.* 1982). The slope of the lines yields the numerical value of the dispersion coefficient D_L while the intercepts provide the determination of k_aK. Repeating the experiments with different size particles enables the evaluation of the molecular diffusion coefficient D_m and the intraparticle diffusivity D_p. To estimate $D_c/r_c{}^2$ an adsorbate such as CF_4 or i–C_4H_{10} – molecules too large to penetrate into the crystalline zeolite cavities – is employed. The lines for N_2 are temperature sensitive and this reflects dominant intracrystalline diffusion resistance. Subtraction of the intercepts (determined at the same temperature) for N_2 and CF_4 then provides an estimate of the intracrystalline diffusivity. Crystallites of different sizes would yield similar information.

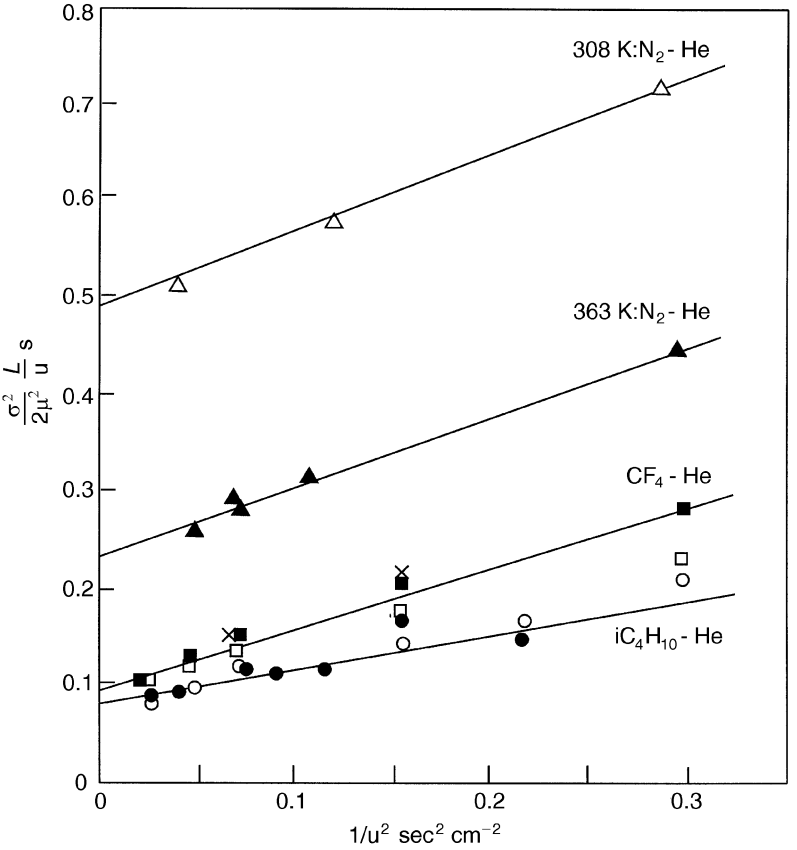

Figure 4.12 *Extraction of axial dispersion and molecular diffusion coefficients and intraparticle diffusivities. Plot of* $(\sigma^2/2\mu^2)$ *L/u against* l/u^2 *for* N_2, CF_4 *and i* C_4H_{10} *in a 4A zeolite (source: Kumar et al.* 1982).

REFERENCES

Barrett, E. P., Joyner, L. G. and Halenda, P. P. (1951) *J. Am. Chem. Soc.,* **73**, 373

Brunovska, A., Hlavacek, V., Ilavsky, J. and Valtyai, J. (1978) *Chem. Eng. Sci.,* **33**, 1385

Carberry, J. J. (1975) *Ind. Eng. Chem. Fund.,* **14**(2), 129

Chapman, S. and Cowling, T. G. (1951) *Mathematical Theory of Non-Uniform Gases*, p. 55, McGraw-Hill

Chilton, T. H. and Colburn, A. P. (1934) *Ind. Eng. Chem.*, **26**, 1183

Crittenden, B. D., Guan, J., Ng, W. N. and Thomas, W. J. (1995) *Chem. Eng. Sci.,* **50**, 1417

Currie, J. A. (1960) *Brit. J. Appl. Phys*., **11**, 318

England, R. and Thomas, W. J. (1976) *Trans. I Chem. Eng.*, **54**, 115

Froment, G. F. and Bischoff, K. B. (1979) *Chemical Reactor Analysis and Design*, pp. 200–214, Wiley & Sons

Garg, D. R. and Ruthven, D. M. (1972) *Chem. Eng. Sci.,* **27**, 417

Gilliland, E. R., Baddour, R. E., Perkinson, G. F. and Sladek, K. J. (1974) *Ind. Eng. Chem. Fund.,* **13**, 95

Gladden, L. F. (1994) *Chem. Eng. Sci.,* **49**, 3339

Glueckauf, E. (1955) *Trans. Faraday Soc.,* **51**, 1540

Glueckauf, E. and Coates, J. E. (1947) *J. Chem. Soc.,* 1315

Gunn, D. J., Moores, D. R., Thomas, W. J. and Wardle, A. P. (1974) *Chem. Eng. Sci.,* **29**, 549

Haynes, H. W. and Sarma, P. N. (1973) *AIChE J.,* **19**, 1043

Henry, J. P., Chennakesavan, B. and Smith, J. M. (1961) *AIChE J.,* **7**, 10

Johnson, M. F. L. and Stewart, W. E., (1965) *J. Catalysis,* **4**, 248

Karger, J. and Pfeifer, H. (1976) *Z. Chemie,* **16**, 85

Kehoe, J. P. G. and Butt, J. B. (1972) *AIChE J.,* **18**, 347

Kondis, E. F. and Dranoff, J. S. (1971) *Ind. Eng. Chem. Proc. Design and Dev.,* **10**, 108

Kondis, E. F. and Dranoff, J. S. (1970) *Adv. Chem.,* **102**, 171

Kumar, R., Duncan, R. C. and Ruthven, D. M. (1982) *Can. J. Chem. Eng.,* **60**, 493

Lapidus, L. and Amundson, N. R. (1952) *J. Phys. Chem.,* **56**, 984

Lee, L.-K. (1978) *AIChE J.,* **24**, 531

Lemcoff, N. O., Pereira Duarte, S. I. and Martinez, O. M. (1990) *Rev. Chem. Eng.,* **6**, 222

Leva, M. (1949) *Chem. Eng.,* **56**, 115

Levenspiel, O. and Bischoff, K. B. (1963) *Adv. Chem. Eng.,* **4**, 95

Ma, Y. A. and Lee, T. Y. (1976) *AIChE J.,* **22**, 147

McAdams, W. H. (1954) *Heat Transmission*, 3rd edn, McGraw-Hill

Pollard, W. G. and Present, R. D. *Phys. Rev.*, **73**, 762

Present, R. D. (1958) *Kinetic Theory of Gases*, McGraw-Hill

Quig, A. and Rees, L. V. C. (1976) *J. Chem. Soc. Faraday Trans.,* **72**, 771

Ranz, W. E. and Marshall, W. E. (1952) *Chem. Eng. Prog.,* **48**, 173

Rosen, J. B. (1954) *Ind. Eng. Chem.,* **46**, 1590

Ruckenstein, E., Vaidyanathan, A. S. and Youngquist, G. R. (1971) *Chem. Eng. Sci.,* **26**, 1306

Ruthven, D. M. (1984) *Principles of Adsorption and Adsorption Processes*, p. 125, Wiley

Ruthven, D. M., Lee, L.-K. and Yucel, H. (1980) *AIChE J.,* **26**, 16

Sargent, R. W. and Whitford, C. J. (1971) *Adv. Chem.,* **102**, 155

Satterfield, C. N. (1970) *Mass Transfer in Heterogeneous Catalysis*, MIT Press

Schneider, P. and Smith, J. M. (1968) *AIChE J.,* **14**, 762

Sladek, K. J., Gilliland, E. R. and Baddour, R. F. (1974) *Ind. Eng. Chem. Fund.,* **13**, 100

Stejskal, E. O. and Tanner, J. E. (1965, 1968) *J. Chem. Phys.,* **42**, 288 and **49**, 1768

Suzuki, M. and Smith, J. M. (1972) *AIChE J.,* **18**, 326

Thomas, H. C (1944) *J. Am. Chem. Soc.,* **66**, 1664

Wakao, N. and Funazkri, T. (1978) *Chem. Eng. Sci.,* **33**, 1375

Wakao, N. and Smith, J. M. (1962) *Chem. Eng. Sci.,* **17**, 825

Wen, C. Y. and Fan, L. T. (1975) *Models for Flow Systems and Chemical Reactors*, Chem. Proc. Eng. Series, **3**, eds L. F. Albright, R. N. Maddox and J. J. McKetta., Marcel Dekker

Wicke, E. and Kallenbach, R. (1941) *Kolloid-Z,* **17**, 135

Yang, R. T. (1987) *Gas Separation by Adsorption Processes*, p. 120, Butterworths

Yang, R. T. and Liu, R. T. (1982) *Ind. Eng. Chem. Fund.,* **21**, 262

5

Processes and cycles

Adsorbent particles have a finite capacity for fluid phase molecules and therefore extended contact with a feedstock will ultimately lead to the creation of a thermodynamic equilibrium between the solid and fluid phases. At this equilibrium condition the rates of adsorption and desorption are equal and the net loading on the solid cannot increase further. It now becomes necessary either to regenerate the adsorbent or to dispose of it. For those applications in which it is economically favourable to regenerate the adsorbent it is necessary to devise processes in which the regeneration method can be incorporated.

5.1 FIXED AND MOVING BED PROCESSES

Vessels and columns which hold the adsorbent in a fixed position appear initially to provide distinct advantages over their counterparts in which the adsorbent is allowed to move. First, such equipment is simple and relatively inexpensive to fabricate. Secondly, minimal attrition of adsorbent occurs when it remains fixed in position, although it should be noted that attrition in fixed bed processes which are subject to frequent changes of pressure and flow direction still remains a practical industrial problem. However, despite their simplicity, fixed beds have many disadvantages:

(1) As fluid is passed through a fixed bed of adsorbent the transfer of adsorbate molecules from the feed to the solid initially occurs at the bed

entrance. Once the adsorbent in this region becomes saturated with the adsorbate molecules, the zone in which the mass transfer occurs moves progressively through the bed towards the exit, as shown schematically in Figure 5.1. When breakthrough of the adsorbate begins to occur it is necessary to take the bed off-line so that the adsorbent can be regenerated. At any instant in time in the adsorption step it is clear from Figure 5.1 that the adsorbent particles upstream and downstream of the mass transfer zone (MTZ) do not participate in the mass transfer processes. Upstream of the

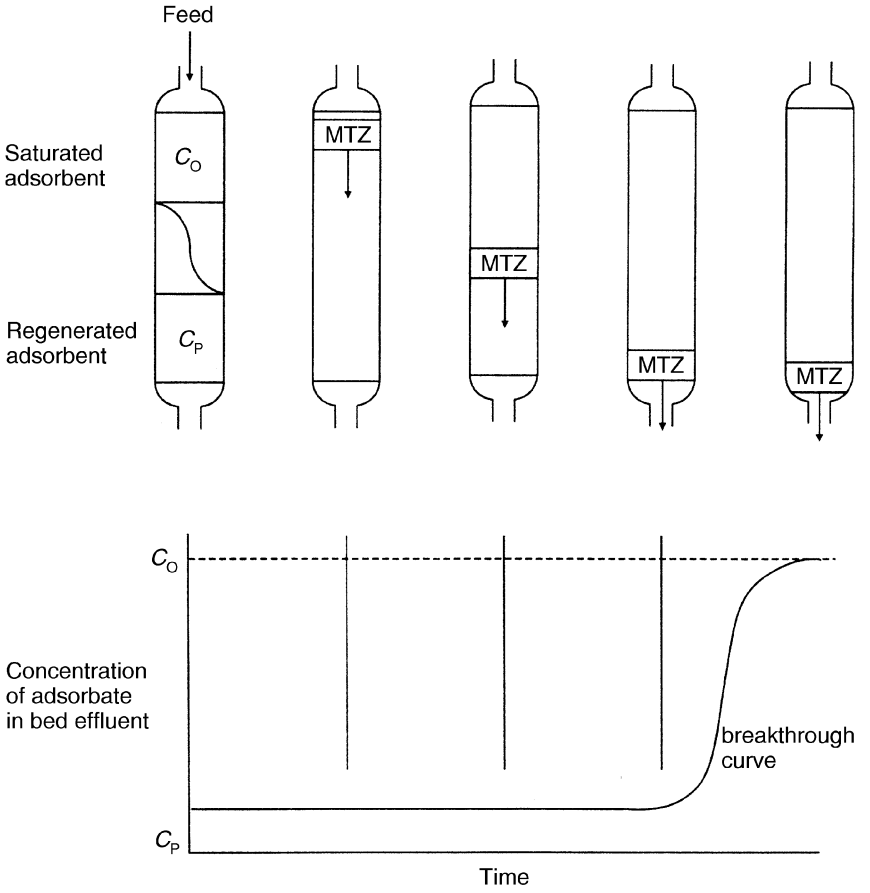

Figure 5.1 *Sketch showing the concentration profile, mass transfer and breakthrough curve in packed bed adsorption (redrawn from Crittenden 1992, p. 4.19).*

MTZ, the adsorbent will be in equilibrium with the feed and unable to adsorb further adsorbate molecules. Downstream of the MTZ, the adsorbent will not have been in contact with any adsorbate molecules and therefore, despite having the capability of doing so, will also be unable to adsorb adsorbate molecules. Thus, if the time selected for progress of the MTZ through the bed is long the bed will be large and it will contain a large inventory of expensive adsorbent. In addition the pressure drop will be proportionately large.

(2) Any time up to breakthrough it is practicable to take the adsorbent bed off-line. Therefore, in order to have a continuous stream of product it is necessary to have more than one bed of adsorbent in the overall adsorption equipment. The regeneration time for the second bed must not be longer than the time to reach breakthrough of the adsorbate during adsorption in the first bed. In practice more than two beds are often used which introduces the need for complex pipe and valve arrangements together with a control system.

(3) Adsorption is always an exothermic process (see Section 3.1) and desorption can therefore be effected by raising the temperature of the adsorbent. In thermal regeneration, or thermal swing, processes it is difficult to heat and cool large beds of highly porous adsorbent materials quickly because the heat transfer processes are not especially good. Poor heat transfer leads to long heating and cooling times which thereby creates the need for large beds. A further disadvantage of poor heat transfer can manifest itself in a rise in the temperature of the bed in or near to the MTZ due to the exothermic nature of the adsorption process. Since the loading of an adsorbate is reduced by increasing the temperature of the adsorbent, the performance of the bed will become inferior and the product purity may become poorer if the bed cannot be kept cool near the exit end.

(4) Despite the apparent simplicity of fixed beds they are difficult to design accurately because the progress of the MTZ introduces time into the design equations. To solve the problem rigorously it is necessary, in most practical applications, to solve sets of partial differential equations which describe the mass and heat transfer phenomena. Several short-cut design techniques exist but they can vary considerably in their accuracy. The uncertainties which arise, and the simplifications which are often required, inevitably introduce conservatism into the bed sizing calculations. In turn, this leads to equipment sizes and adsorbent inventories being larger than the minimum requirements.

The main advantage of moving bed processes is that the adsorbent can be regenerated as soon as its role in the adsorption step has been completed. Thus, in theory at least, the inventory of adsorbent can be kept to a

minimum. Additionally, heat transfer in moving bed and fluidized bed systems is better than in fixed beds. Thus if the technical challenges of designing adsorbents which are sufficiently rugged for moving bed and fluidized bed processes can be overcome then not only will less inventory of adsorbent be required but also the processes will be easier to design. In contrast, the equipment required for a moving bed process will inevitably be more complex and hence more expensive than fixed beds. In addition equipment will need to be provided to cope with attrition of the adsorbent which will inevitably occur. In order to gain the best advantages of both the fixed bed and the moving bed it is technically and economically feasible to operate a single fixed bed in such a way that a continuous steady state process can be simulated.

5.2 BATCH PROCESSES

Batch processes are important examples in which the adsorbent moves relative to the walls of the containment vessel. The simplest process involves mixing a batch of adsorbent with a batch of fluid, most commonly a liquid, as shown in Figure 5.2. After a predetermined time the adsorbent can be

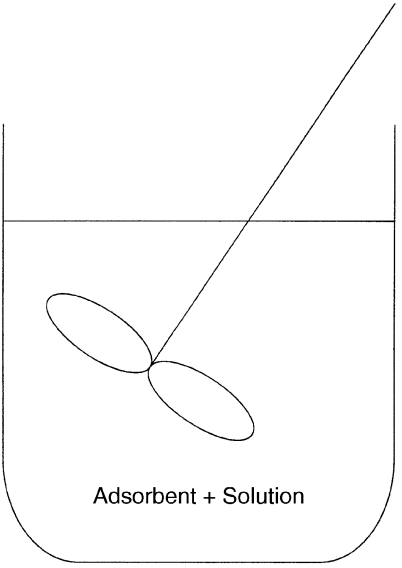

Figure 5.2 *Basic equipment for the contacting of a liquid with a single batch adsorbent.*

separated from the fluid by sedimentation, filtration, etc. either for disposal or for reuse. Powdered activated carbon (PAC) is often used in this way to remove tastes and odours from waters. If sufficient time is allowed for equilibrium to be reached then the loading of the adsorbate on the adsorbent will be related to the final concentration of the adsorbate in the solution via the thermodynamic isotherm which applies at the final temperature in the process.

Powdered or granular adsorbents are usually added to the equipment in slurry form in such a way as to allow adequate dispersion and mixing. The adsorbent can be removed as a settled sludge. When large quantities of adsorbent are required consideration should be given to using a multiple batch or cross-flow system. For example, one way of reducing the total amount of adsorbent required is to carry out the batch processing in two steps, as shown in Figure 5.3. The feed is first contacted with a fresh batch of adsorbent. After separation of the fluid from the adsorbent the fluid is contacted with a further fresh batch of adsorbent. Each subsequent batch of adsorbent removes less and less impurity as the concentration of the impurity in the fluid decreases. The overall mass balance equations which describe batch adsorption processes are given in Chapter 6. Equations which describe the dynamics of batch adsorption are provided in Chapter 4.

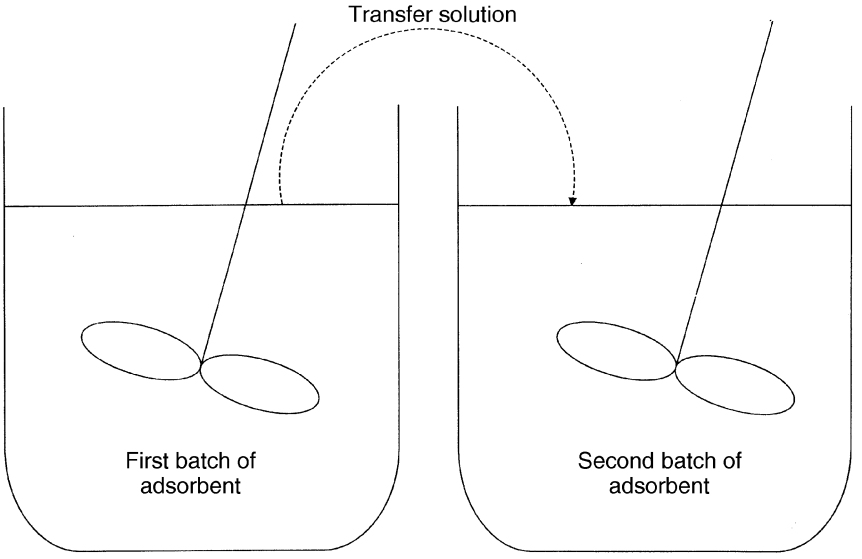

Figure 5.3 *Basic equipment for the contacting of a liquid with two batches of adsorbent.*

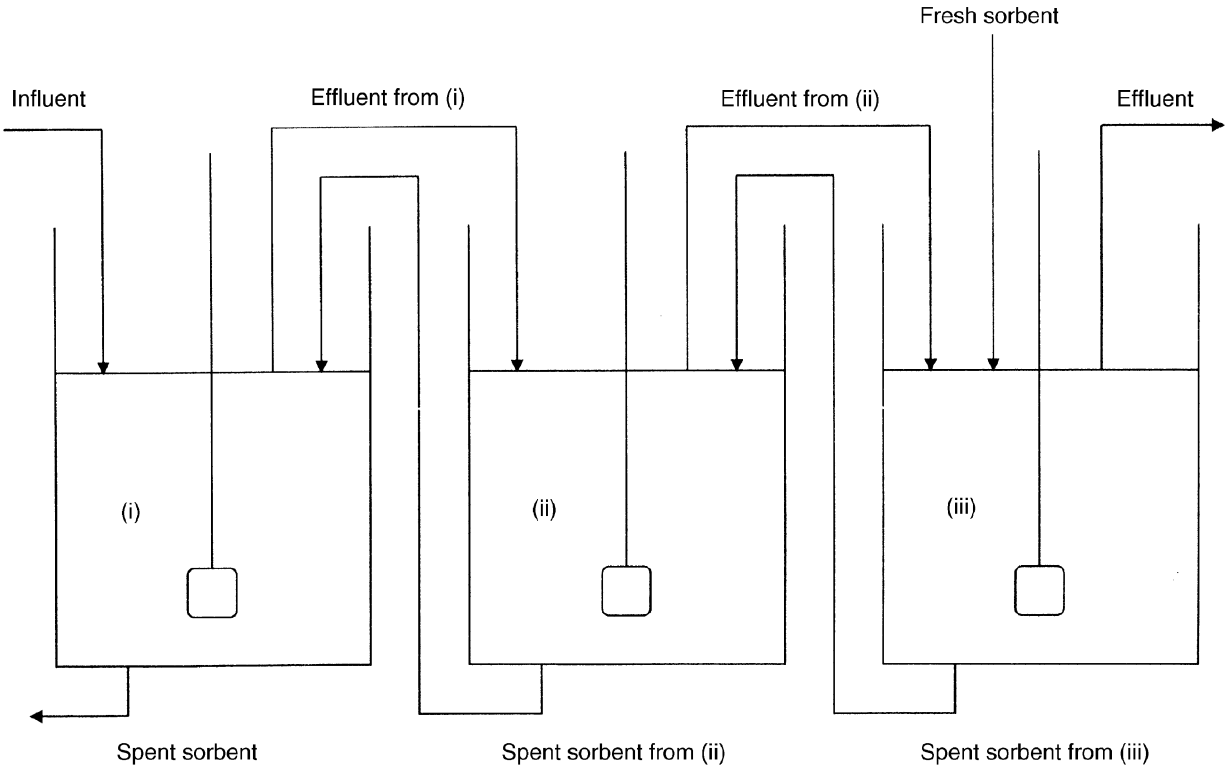

Figure 5.4 *Three-stage countercurrent contacting.*

A more efficient way of carrying out a multistage purification or separation is to adopt a countercurrent configuration of fluid and adsorbent flows as shown, for example, for a three-stage continuous process in Figure 5.4. Here, the feed is contacted initially with a quantity of adsorbent which has passed through two other stages. As with the cross-current method, the quantity of adsorbent required for a given separation can be reduced by increasing the number of stages. Clearly an economic evaluation is required to find the optimum number of stages but it should be noted that there is a minimum amount of adsorbent in a countercurrent operation which will cause the number of stages required to increase to infinity (Ruthven and Ching 1989). This phenomenon is similar to the minimum solvent-to-feed ratio which occurs in solvent extraction (Crittenden 1991) and to the minimum reflux ratio which occurs in distillation.

5.3 FIXED BED PROCESSES

Separation in a fixed bed of adsorbent is, in virtually all practical cases, an unsteady state rate controlled process. This means that conditions at any particular point within the fixed bed vary with time. Adsorption therefore occurs only in a particular region of the bed, known as the mass transfer zone, which moves through the bed with time.

5.3.1 The mass transfer zone (MTZ)

Progress of the mass transfer zone (MTZ) through a fixed bed for a single adsorbate in a diluent is shown schematically in Figures 5.1 and 5.5. In practice, it is difficult to follow the progress of the MTZ inside a column packed with adsorbent because it is difficult to make meaningful measurements of parameters other than temperature. By following the progress of the exotherm which accompanies the adsorption process it is possible to gain an indication of the position of the MTZ. Methods have now been devised for applications in which the temperature rise is small because the adsorbing species are dilute (Lockett *et al.* 1992). It is, of course, much easier to measure the concentration of an adsorbate as it leaves the fixed bed but this clearly cannot be done routinely in an industrial process since breakthrough of the species which is meant to be retained within the bed will have occured. A detector could be placed within the adsorbent bed but there is then the risk that uncertainties about the shape of the MTZ and the possibility of channeling could lead to breakthrough earlier than anticipated. In spite of such difficulties, much information valuable to the design

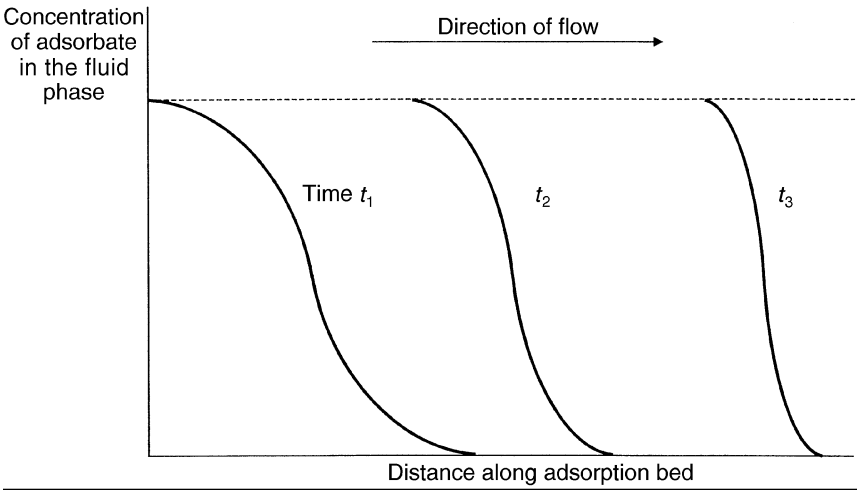

Figure 5.5 *Development and progression of a mass transfer wave along a fixed adsorption bed.*

process can be gleaned from the time to breakthrough and from the shape of the breakthrough curve.

Figure 5.6 (a) shows the breakthrough curve for a single adsorbate from a fixed bed of adsorbent. Breakthrough is deemed to commence at a time t_b when the concentration of the adsorbate at the end of the bed increases beyond a certain level, c_e. This may be the level of detection for the adsorbate or it may be the maximum allowable concentration for admission to downstream process units such as catalytic reactors. As breakthrough continues the concentration of the adsorbate in the effluent increases gradually up to the feed value c_o. When this has occurred no more adsorption can take place in the adsorption bed. The concentration of the adsorbate on the adsorbent will then be related to the concentration of the adsorbate in the feed by the thermodynamic equilibrium.

In practical operations the adsorption step must be terminated at some time earlier than t_b. It can be seen from Figure 5.6 (b) that part of the adsorbent bed (from $z = 0$ to $z = L_e$) will have become in equilibrium with the feed entering the bed (at concentration c_o) and the remaining part of the bed (from $z = L_e$ to $z = L$) will contain the mass transfer zone. Across the mass transfer zone the adsorbate concentration in the fluid decreases strictly from c_o to zero if the adsorbent is initially completely free from the adsorbate.

Fig. 5.6a

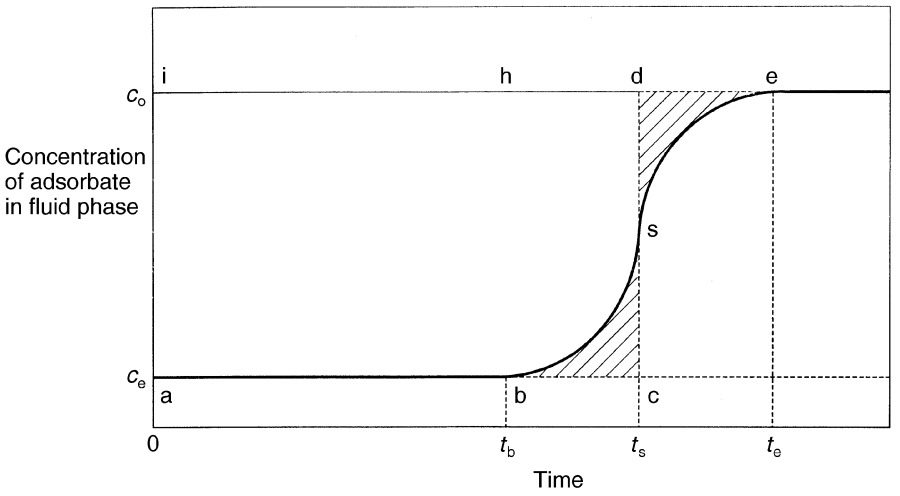

Fig. 5.6b

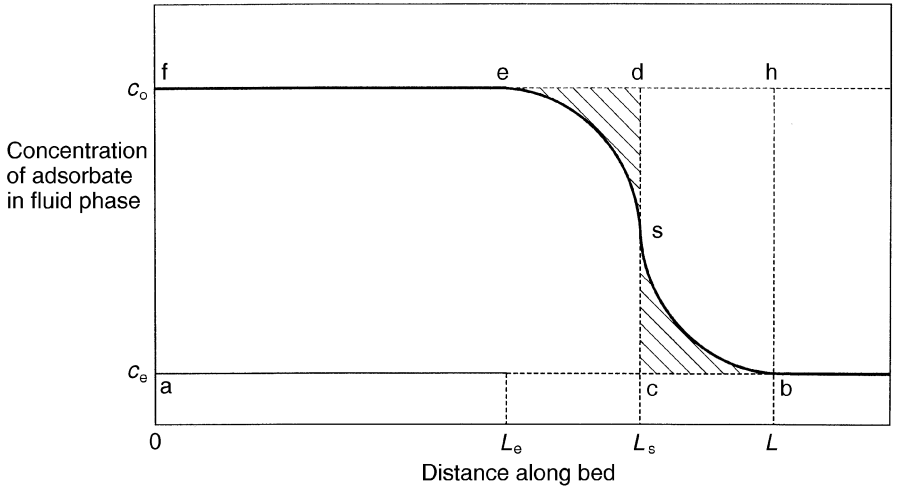

Figure 5.6 *Packed bed dynamics: (a) breakthrough curve (single transition) and (b) mass transfer zone inside the bed (redrawn from Keller et al. 1987, p. 672).*

5.3.2 Adsorbent support and flow distribution

Adsorbent particles can be supported in one of two ways in an adsorption vessel. The first comprises a series of grids with each successively higher layer having a finer mesh. The second comprises a graded system of inert particles which may range from ceramic balls down in size to gravel. For those applications where the adsorbent may have to be removed from the bottom outlet there may be no support system but the flow distributors may, as a result, be complex.

At the top of a bed a layer of inert support balls may be used as ballast in order to prevent movement and hence attrition of the adsorbent. The ballast needs to be denser and significantly larger than the adsorbent particles and a retention screen is normally placed on top in order to prevent the ballast from migrating downwards through the bed. The retention screen cannot be fixed to the column wall because it must be capable of taking up bed settlement in cyclic processes. For gas phase applications in which frequent changes of bed pressure and flow direction occur it is generally necessary to use a pre-load on the top of the adsorbent bed. This pre-load, which might take the form of a spring or compressed fibre pad, is used to prevent movement and automatically allows for settlement.

Intermediate bed supports might be required when the adsorbent is susceptible to damage by crushing. Intermediate bed supports might also be used in compound adsorbent systems in which it may be necessary periodically to change individual adsorbent materials.

Poor fluid flow distribution can be avoided using a variety of techniques. First, sufficient plenum spaces should be allowed above and below the fixed bed. Secondly, baffle plates should be fitted when symmetrically placed inlet and outlet nozzles are used. The baffle plates, which may be solid, slotted or perforated, should be sufficiently large to ensure that the incoming fluid is redirected, its momentum is broken and it cannot impinge directly on the adsorbent particles. If balls and/or gravel are used to further aid distribution, then screens should be used to surround the baffles. Thirdly, it may be necessary to use nozzle headers in which flow can enter the bed from several nozzles along a distribution system. The holes along such a distribution system may not necessarily be of uniform size.

5.3.3 Flow direction

Fixed bed adsorbers commonly are vertical and cylindrical vessels. While horizontal vessels are occasionally used, vertical orientation is preferred to avoid the creation of flow maldistribution when settling of a bed or movement of particles within it occurs. Flow can be arranged vertically

through a cylindrical vessel which is lying horizontally. In some applications, notably cyclic processes which have many changes of pressure and flow direction, a pre-load is placed on the top of the adsorbent bed to keep the adsorbent particles restrained. If flow is required to be horizontal through a bed lying horizontally then it is likely that flow redistributors will be needed inside the bed to ensure that flow cannot preferentially take place along the top of the vessel once settlement has occured.

The flow direction for adsorption in a vertical fixed bed is determined not only by the potential for lifting or fluidizing the bed but also by whether the feed is a gas or a liquid. For gas and vapour phase applications velocities which cause crushing of an adsorbent tend to be much higher than those required to lift a bed and therefore it is convenient to arrange to have the highest flowrate in the downwards direction through a vertical bed.

For liquid phase applications the buoyancy forces need to be considered as well. The flow velocity in the upwards direction should normally be sufficiently low to prevent bed lifting. However, in some applications it is desirable to allow some bed expansion to occur and so limit the pressure drop. As the minimum velocity to cause lifting is exceeded, the pressure drop increases only slightly with further increases in velocity. Too much expansion, however, can cause the bed to become well mixed. If this were to occur within a fixed bed then it would resemble the batch process and create the risk of reduced purity in the product. Other problems caused by high velocities include abrasion, attrition and erosion. When desirable, expansion is accordingly limited normally to about 10%.

If the liquid contains suspended solids it may be preferable for flow to be in a downwards direction. In water treatment applications the adsorbent bed when so used can act as a particulate trap as well as a means of removing tastes, odours and pollutants. As filtration proceeds the pressure drop increases and backwashing is therefore required periodically. Water treatment beds can be either of the gravity or the pressure type. Gravity beds are similar to concrete sand filters but incorporate provisions for the addition and removal of adsorbent, usually granular activated carbon (GAC), and for about 50% expansion during backwashing. The minimum depth of GAC is around 1 m and the hydraulic loading is in the range 0.09–0.27 $m^3/min/m^2$ of bed cross-sectional area. A pressure filter, which takes fluid in downflow, comprises a lined steel pressure vessel, an adsorbent support system, drainage, influent and effluent distribution, surface wash and backwash conveyance systems. The pressure vessel has a higher hydraulic loading than a gravity vessel, typically in the range 0.09–0.45 $m^3/min/m^2$ but is limited in size to a maximum diameter of 4 m and length 20 m. If the feed is free from particulate material then flow in water treatment applications can be upwards. Smaller adsorbent particles

can be used to obtain higher adsorption rates but care must be taken to prevent expansion. Without particulate material being present there is no need for backwashing. Thus the MTZ remains undisturbed and a greater adsorption efficiency can be maintained.

The expanded bed adsorber with flow in the upwards direction is also popular in the water industry. Expansion of about 10% separates individual adsorbent particles and allows suspended solids to pass straight through. The hydraulic loading is typically around 0.27 $m^3/min/m^2$ but its exact value depends on the size of the particles.

5.3.4 Drainage and filling in liquid phase adsorption

For the design of a bed used in a liquid phase application which is to be regenerated using a hot gas it is important to consider the arrangements for draining after the adsorption step and filling with liquid again after the regeneration step. Clearly, drainage must be downwards and if the adsorption step is also downwards then the collected fluid can be added to the product since it will have left from the cleanest part of the adsorption bed. Conversely, if the adsorption step has the flow in the upwards direction, then the drained fluid must be collected and returned to the feed, or otherwise disposed of. Gravitational flow, sometimes assisted by a 1–2 bar pressure gradient, is used for drainage. The time of this step could be significant, perhaps 30 minutes, and even after this period a significant hold-up of liquid on the adsorbent, perhaps up to 40 $cm^3/100$ g of adsorbent, might remain in the micro- and macropores of the adsorbent and in the bridges between adjacent adsorbent particles. In processes in which regeneration is effected by an increase in temperature this remaining liquid will consume additional energy when it is vaporized from the bed.

It is preferable in a liquid phase application to refill an adsorbent bed in the upwards direction because it is easier to sweep out pockets of gas or vapour and so prevent maldistribution in the proceeding adsorption step. Consideration must be given to the time required to ensure that the gas and vapour pockets have been removed completely otherwise there is a risk that they will contaminate the product in the adsorption step and cause excessive bed lifting if flow is upwards during the adsorption step.

For those processes in which a second liquid is used to displace the first in the regeneration step the problem of 'fingering' should be avoided. This phenomenon arises due to density and viscosity differences at the liquid –liquid interfaces and can cause columns of one fluid to pass through the other even in well packed beds. Hydrodynamic instability can be created when a denser fluid is located above a less dense fluid. Also, if a less viscous fluid is displacing a more viscous one then any bulge in the interface will tend

to grow because the resistance to flow is less and the less viscous fluid will continue to intrude. For those situations in which the less dense fluid is the upper fluid, or the more viscous fluid is the displacing fluid, then flow instabilities are likely to become corrected.

5.3.5 Number of beds

The factors which determine the number and arrangement of fixed beds include total feed flowrate, allowable pressure drop, other energy demands, the length of the mass transfer zone, the method of adsorbent regeneration and the capital investment. In order to achieve a steady flow of product most applications include at least two beds such that one is in the adsorption mode while the other is in the regeneration mode (if regeneration of the adsorbent is being carried out *in situ*). For liquid phase applications more than one bed in the adsorption mode can be operated in parallel, in series or in combination. A single bed would be used in the adsorption step with a relatively low total flowrate and a short MTZ length (which would produce a sharp breakthrough curve). Multiple beds in parallel would be used with a relatively high total flowrate and a short MTZ length while multiple beds in series would be used if the MTZ were long. Hence, for high flowrates and large MTZ lengths the choice is likely to be multiple beds in series and parallel. Similar principles apply for gas phase separations. For processes in which regeneration is effected by a reduction in pressure, multiple bed systems are used to gain other processing advantages such as a reduction in overall energy demand by equalizing the pressure between beds of high and low pressure.

5.3.6 Fixed bed pulsed processes (chromatographic processes)

Strictly, a chromatographic process requires the adsorbent to be contained within a fixed packed bed and the mixture which is to be separated is introduced as a pulse into a flowing stream of a carrier fluid. Separation of the components in the feed then occurs as the pulse of feed passes through the column if the repetitive steps of adsorption and desorption are different in nature (equilibrium and/or rate) for each adsorbate.

5.4 MOVING BED PROCESSES

Two general possibilities exist to have the adsorbent in motion. In the first the adsorbent particles move relative to the walls of the containing vessel and in the second the particles remain in a fixed position relative to the walls

of the vessel. The simple mixed tank shown in Figure 5.2 is an example of the former.

5.4.1 Solids in plug flow

The ideal countercurrent steady state configuration can be achieved conceptually by allowing the adsorbent particles to fall in plug flow through the rising stream of gas or liquid which is to be separated or purified. This process arrangement would lead to a minimum adsorbent inventory and would allow for good heat transfer performance. While conceptually simple, there are several practical problems to be overcome. First, it is necessary to have an adsorbent which is sufficiently rugged to withstand attrition. Secondly it is necessary to devise a flow system to transport the adsorbent back to the top of the adsorption column. Thirdly, it is necessary to incorporate an adsorbent regeneration section somewhere in the process scheme. This might be at the bottom of the adsorption column or in the transportation section. In either case it is necessary to regenerate the adsorbent to such an extent that the overall process can operate at steady state.

Such moving bed processes were proposed in the 1930s and around 1950 the erstwhile Hypersorption process shown schematically in Figure 5.7 was commercialized for separating various light hydrocarbons on activated carbon. An example application was the recovery of ethene and propene from cracked gas consisting otherwise of hydrogen, methane, ethane, propane and butane. The adsorption column, which was about 1.5 m diameter and 25 m tall, allowed the adsorbent to be transported downwards in the rising gas flow. A heated stripping section was located at the bottom and a cooler was located at the top. Between these two heat exchangers were located four trays with the feed being introduced through a distribution tray near the middle of the column. The lean overhead product gas was disengaged through a tray which was located immediately below the cooling section. The adsorbates were removed in two streams according to their volatilities. The ethene was released on a disengaging tray which was located immediately below the feed point. The propene which was more strongly adsorbed was released with the carrier stream on a disengaging tray near the bottom of the column. Heavier products could also be removed below the feed point.

Typical processing conditions for a Hypersorption unit were 0.6 m^3/s of feed gas at 5 bar with a maximum carbon recirculation rate of 15 000 kg/h. The stripping and cooling section temperatures were 265 and 210°C, respectively. The literature contains very little performance data on the process but the principal problems of inadequate carbon regeneration and of

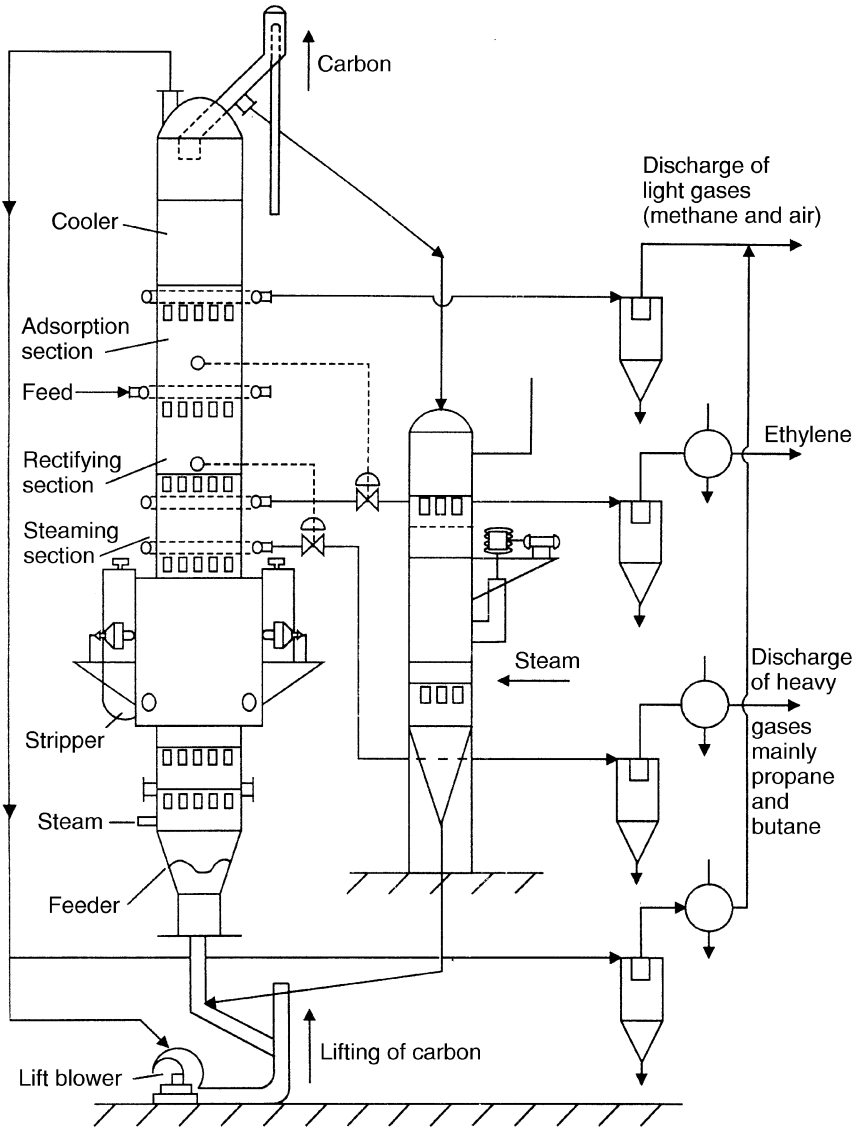

Figure 5.7 *Simplified schematic of a Hypersorption column (adapted and redrawn from Berg 1946).*

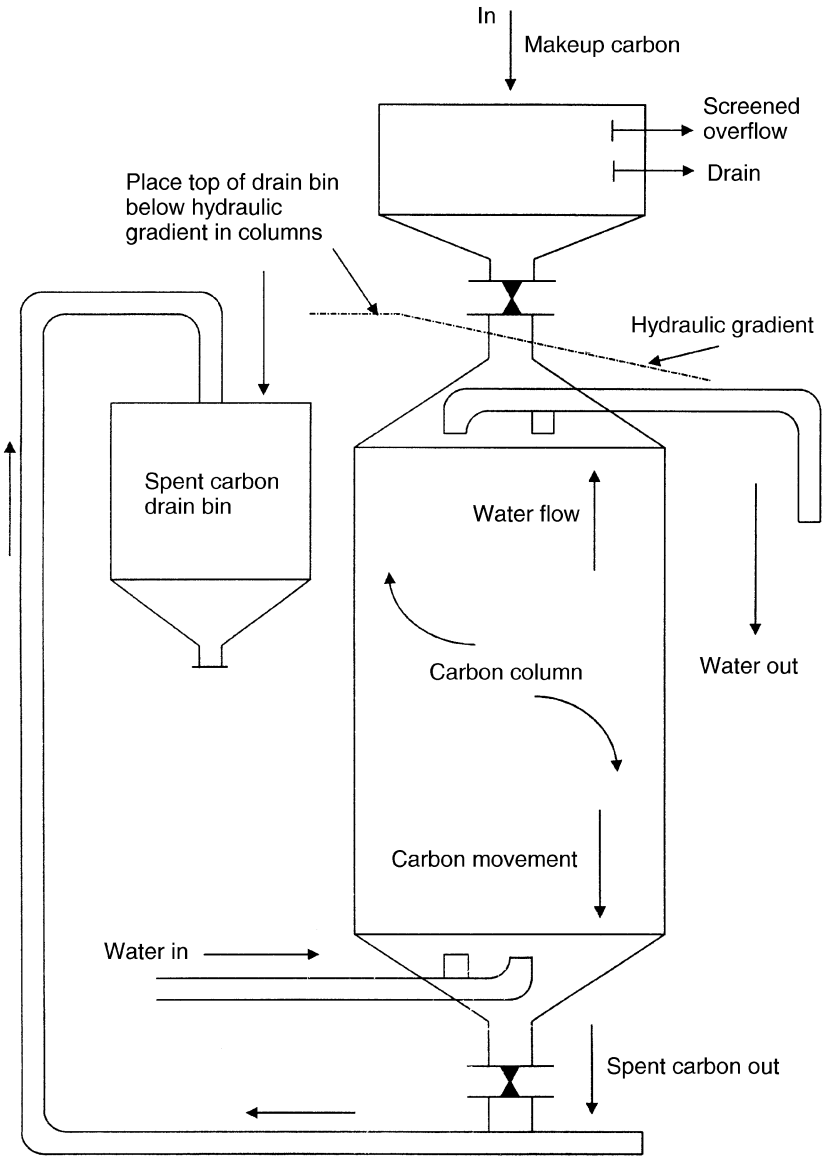

Figure 5.8 *Schematic of a pulsed flow adsorber (adapted and redrawn from Faust and Aly, 1987).*

carbon loss through attrition and elutriation seem to have caused all the plants to have been closed down.

5.4.2 Pulsed flow

As shown schematically in Figure 5.8 the feed enters the pulsed flow adsorber at the bottom and flows upwards. The adsorber is designed such that the effluent carries some adsorbent out from the top of the bed and this loss is made up at the bottom with freshly regenerated adsorbent. In this way the mass transfer zone can be retained inside the column. In practice the removal and addition of adsorbent is not generally carried out continuously. Instead it is more common for the column to be operated on a semi-continuous basis in which a predetermined amount of adsorbent is removed and added periodically. The column can therefore be likened to a series of fixed beds stacked on top of each other with the top one being removed and a new one being added at the bottom. The adsorbent flow should be as close as possible to plug flow. The column is normally full with adsorbent so that no expansion can occur which would cause mixing, lengthening of the mass transfer zone and hence reduced efficiency.

5.4.3 Fluidized bed

The literature contains many references to the use of fluidized bed adsorption processes. Applications have included the removal of organic compounds from air and vent streams (Avery and Tracey 1968, Rowson 1963) and the drying of air with silica gel (Ermenc 1961, Cox 1958). Fluidized beds are attractive because, when fully fluidized, the pressure drop is independent of flowrate and heat and mass transfer processes external to the adsorbent particles are very good. The main problems lie, as with many moving bed processes, with the mechanical strength of the adsorbent particles.

The Purasiv HR fluidized bed/moving bed process shown schematically in Figure 5.9 became technically feasible following the development of a hard microspherical activated carbon known as bead activated carbon (BAC). The principal application has been the removal of small amounts of solvent vapour, typically 100–10 000 ppm, from air and vent streams with flowrates in the range 2–50 m^3/s (Anon 1977). Feed gas is passed upwards through trays which are similar to those used in distillation and on which the BAC is fluidized. The BAC passes down through the column via downcomers, again in a manner similar to that in distillation. The BAC is passed ultimately into a heated moving bed regeneration zone in which the adsorbed species are desorbed for recovery. An air lift is used to transport the adsorbent to the top tray in the adsorption section. The process has been adapted for use with polymeric adsorbents, again for the removal of volatile organic compounds from air streams.

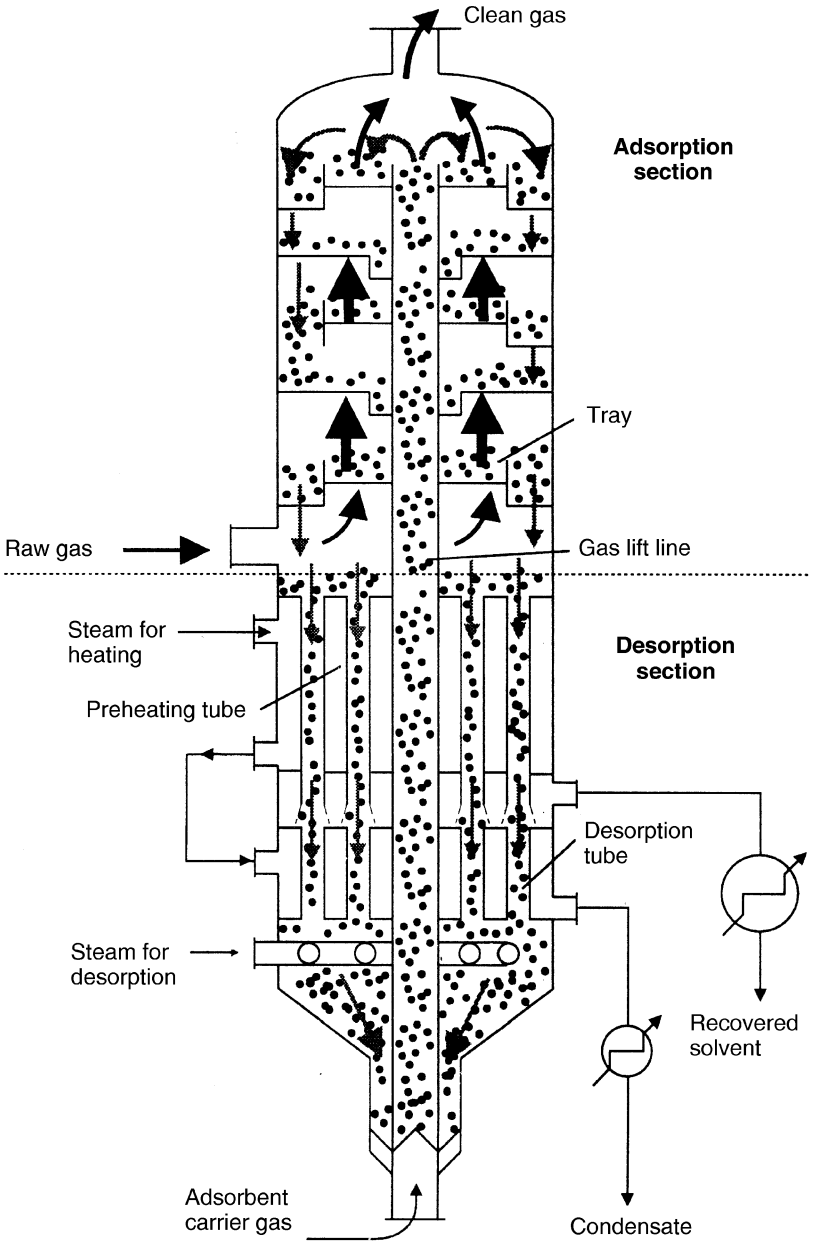

Figure 5.9 *Schematic of a Purasiv HR fluidized bed adsorber (adapted from Keller et al.* 1987, p. 665).

5.4.4 Rotary beds

Two processes have been devised to combine the advantage of the fixed bed in which attrition losses are small and the moving bed in which the adsorbent is more effectively utilized. Both processes have the adsorbent in a fixed position relative to the wall of the containment vessel. In order for the process to operate on a continuous and steady state basis therefore, it is necessary both to move the position of the fixed bed relative to the feed and product lines and to incorporate a desorption or regeneration section.

Two types of rotary bed adsorber exist. Both are used for removing and/or recovering solvents from air streams. Figure 5.10 shows the rotary bed adsorber which comprises a rotating drum containing the adsorbent in several sections. It is used generally for solvent recovery from air streams. The air enters the drum circumference to pass inwards through the adsorbent. Cleaned air then leaves via a duct which is connected along the drum's rotational axis. One or more of the adsorbent sections is regenerated by passing steam in the reverse direction from the central axis to the circumference whence it leaves and passes to condensers. After the regeneration step the adsorbent is not cooled because the proportion of the adsorbent annulus which is cooling at any one time is relatively small and the effect of a warm sector on the overall efficiency is relatively small.

The adsorbent wheel shown schematically in Figure 5.11 is used particularly for the removal of volatile organic compounds (VOCs) from vent streams. Whether the removed VOCs can be recovered depends upon the magnitude of the increase in concentration from the adsorption step to the desorption step. Solvent-laden air passes via a duct through one side of the wheel which rotates slowly. On the desorption side a lower flowrate of heated air is used to desorb the VOCs. The two gas ducts do not have to be of the same size but it is obvious that the time for desorption must be less than or equal to the time for adsorption.

5.5 FIXED BEDS USED TO SIMULATE MOVING BEDS

Two basic approaches can be adopted for using fixed beds to simulate the operation of moving beds. In the first, multiple fixed beds are used in cascade, as shown in Figure 5.12 (and described later in Section 7.7.1) to gain most of the benefit of a continuous steady state countercurrent process. The concept is similar to that used in the pulsed bed. At each switch in the cascade a fully regenerated bed is added to the outlet end of a sequence of beds in series when breakthrough is about to occur. At the same time the

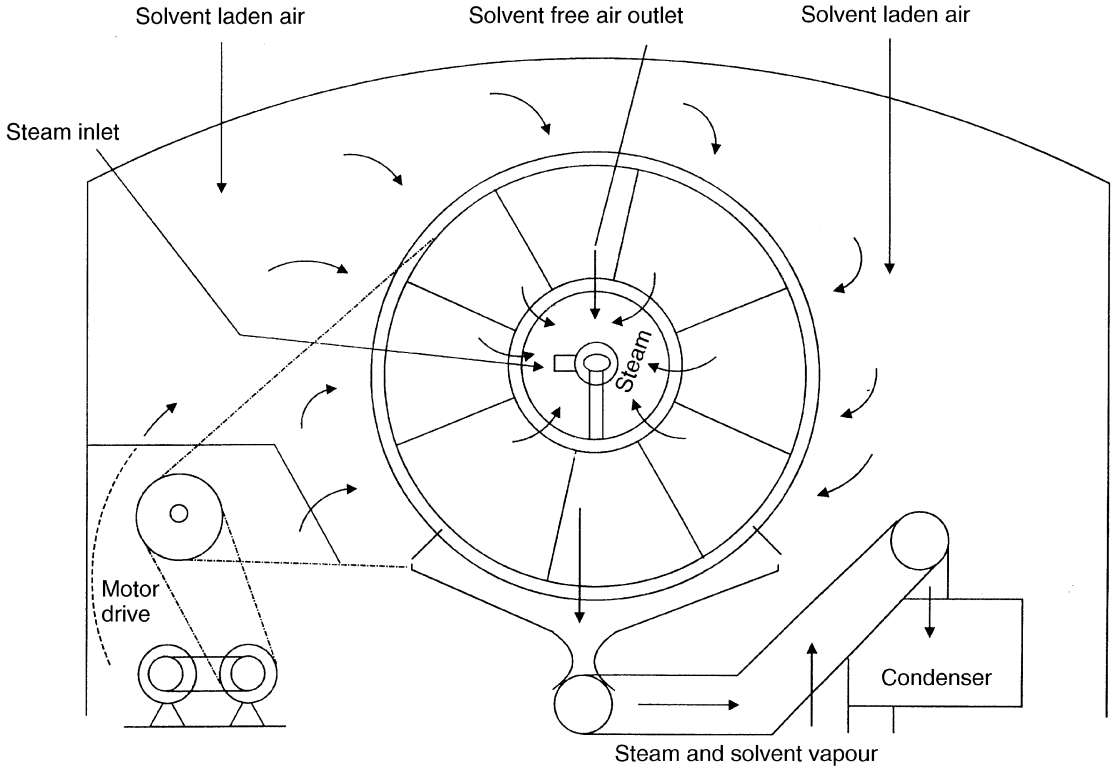

Figure 5.10 *Schematic of a rotary bed adsorber (adapted from Coulson et al.* 1991, p. 793).

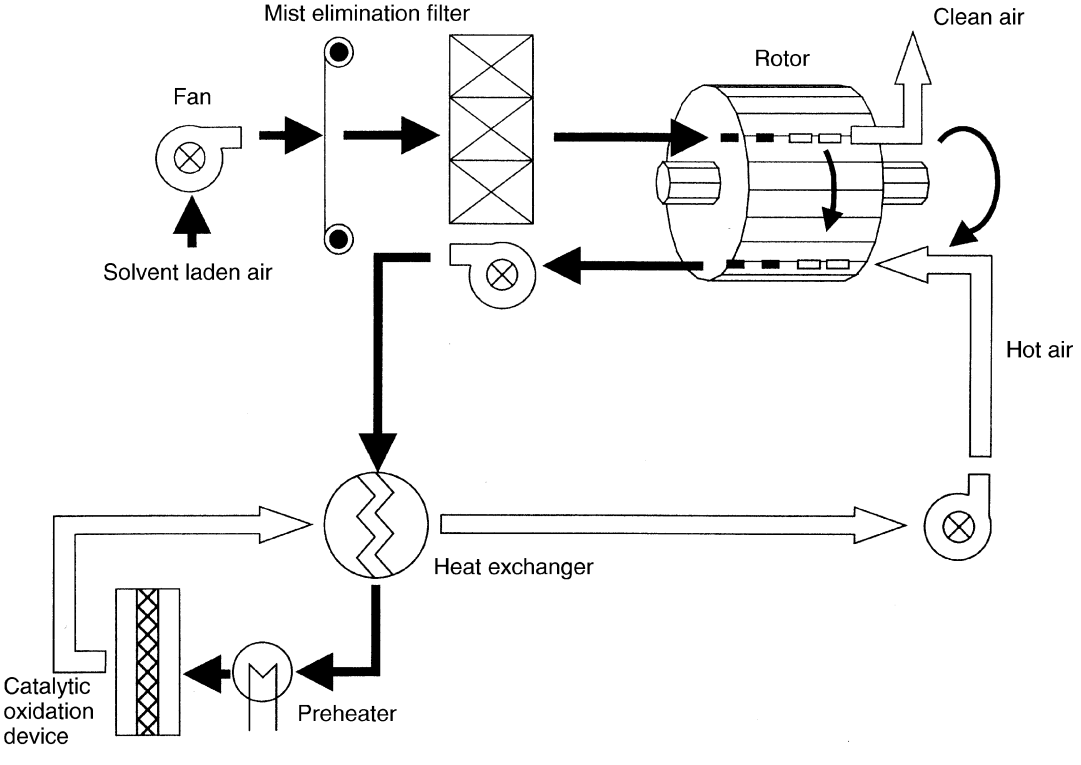

Figure 5.11 *Schematic of the solvent wheel used to remove solvents from air streams.*

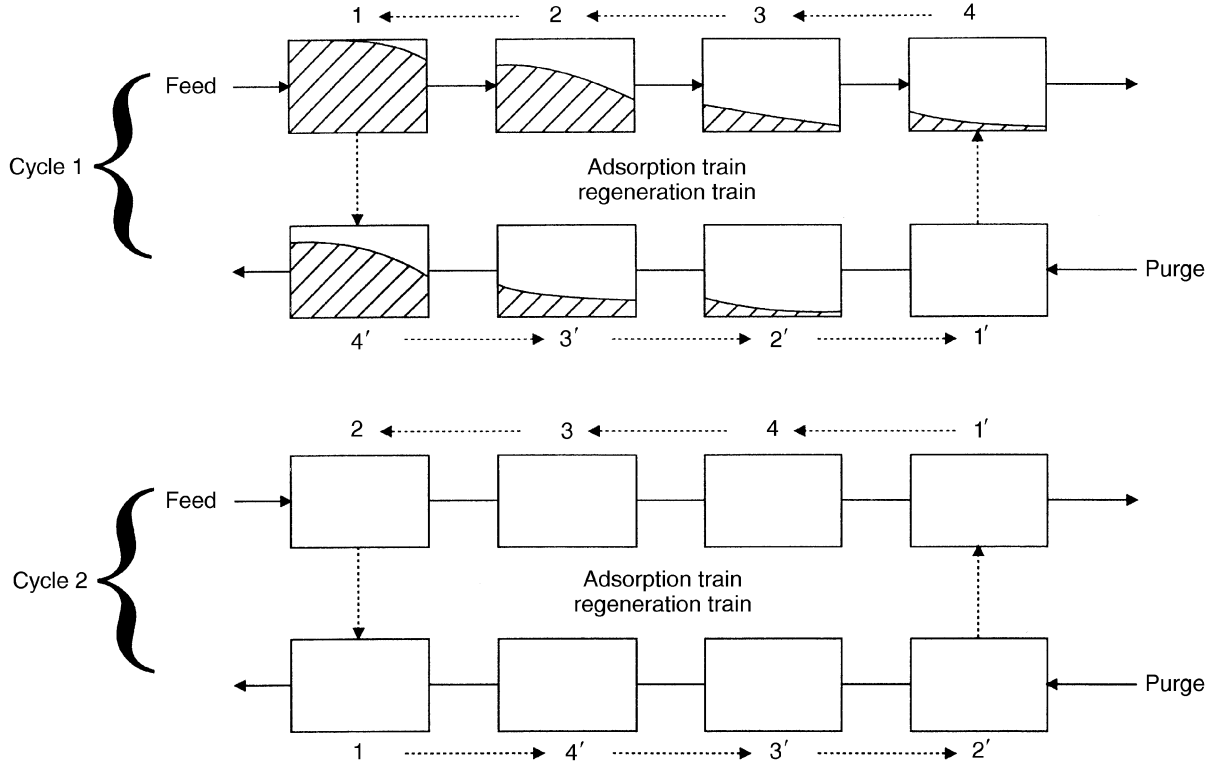

Figure 5.12 *Schematic diagram showing the sequence of column switching in a simulated moving bed countercurrent adsorption system; the shading indicates the concentration profiles just prior to switching (redrawn from Ruthven and Ching 1989).*

Table 5.1 Countercurrent adsorption fractionation processes

Process	*Separation*	*Adsorbent*	*Contacting system*	*Regeneration*	*References*
Hypersorption	C_2H_4 from refinery gas	activated carbon	Dense moving bed	Steam stripping	Berg (1946, 1951) Kehde *et al.* (1984)
Arosorb	Separation of aromatics and saturates from cracked naphtha	silica gel	SMB (eight-column)	Displacement (pentane desorbent)	Eagle and Rudy (1950)
Aromax	*p*-xylene from C_8 aromatics	X or Y zeolite	Three-section SMB cascade	Heavy aromatic desorbent	Otani (1973)
Adsep (1WT)	Fructose from fructose-glucose	Ca^{2+} resin	Eight-column, four-section SMB	Water desorbent	Illinois Water Treatment Mitsubishi Chemical
Molex	Linear/branched paraffins	5A zeolite	Sorbex	Light naphtha desorbent	Broughton (1968) Broughton and Carson (1969)
Olex	Olefins from saturated Isomers	CaX or SrX?	Sorbex	Heavy naphtha	Broughton and Berg (1969)
Parex	*p*-xylene from C_8 aromatics	Sr-BaY K-BaX	Sorbex	*p*-diethyl benzene toluene	Broughton *et al.* (1970)
Ebex	Ethylbenzene from C_8 aromatics	NaY	Sorbex	Toluene	de Rosset *et al.* (1978)
Sarex	Fructose from fructose-glucose	CaY	Sorbex	Water	Neuzil and Jensen (1978) Bieser and de Rosset (1977)
SCCR4	Fructose from fructose-glucose	Ca^{2+} resin	Three-section SMB	Water	Barker and Ching (1980)
SCCR5	Clinical dextran	Ca^{2+} resin	Three-section SMB	Water	Alsop *et al.* (1984)

Adapted from Ruthven and Ching (1989)

fully loaded bed at the feed end of the process is taken off-line and switched to the outlet end of a parallel regeneration train. In this way the adsorbent effectively moves countercurrent to the flow of fluids in both the adsorption and regeneration steps. The perfect analogue with the truly continuous countercurrent process exists when there is a very large number of beds but the process advantages are gained only at the expense of a large number of small beds with a complex system of pipes, valves and a control system. Most of the advantages of this flow arrangement can be gained, however, with relatively few beds in each train (Ruthven and Ching 1989). Some examples of commercial processes are shown in Table 5.1.

In the second approach a single bed is used and the feed and product line positions are changed periodically by means of valve arrangements. The Sorbex simulated moving bed, shown schematically in Figure 5.13 (and described more fully in Section 7.7.5), uses a relatively high boiling point displacement fluid to regenerate the adsorbent. The feed, product and displacement fluid lines are moved as a function of time by a complex rotary valve. A pump is used to circulate the displacement fluid continuously from the bottom to the top of the bed. The displacement fluid is separated from the extract and raffinate products by distillation in separate units. Several commercial applications of the Sorbex process exist as shown in Table 5.1.

5.6 DESORPTION AND REGENERATION OF ADSORBENTS

In certain applications it may be economic to discard the adsorbent after use in which case it may be necessary to describe it as a waste. Clearly the nature and concentration of the adsorbates will dictate the disposal route to be followed. Disposal would be favoured when the adsorbent is of low cost, is very difficult to regenerate (perhaps because adsorbates are held by chemical forces) and the non-adsorbed products of the adsorptive separation are of very high value. In the majority of process applications, disposal of the adsorbent as a waste is not an economic option and therefore regeneration is carried out either *in situ* or external to the adsorption vessel to a extent sufficient that the adsorbent can be reused. Practical methods of desorption and regeneration include one, or more usually a combination, of the following:

(1) increase in temperature;
(2) reduction in partial pressure;
(3) reduction in concentration;
(4) purging with an inert fluid;
(5) displacement with a more strongly adsorbing species;
(6) change of chemical condition such as pH.

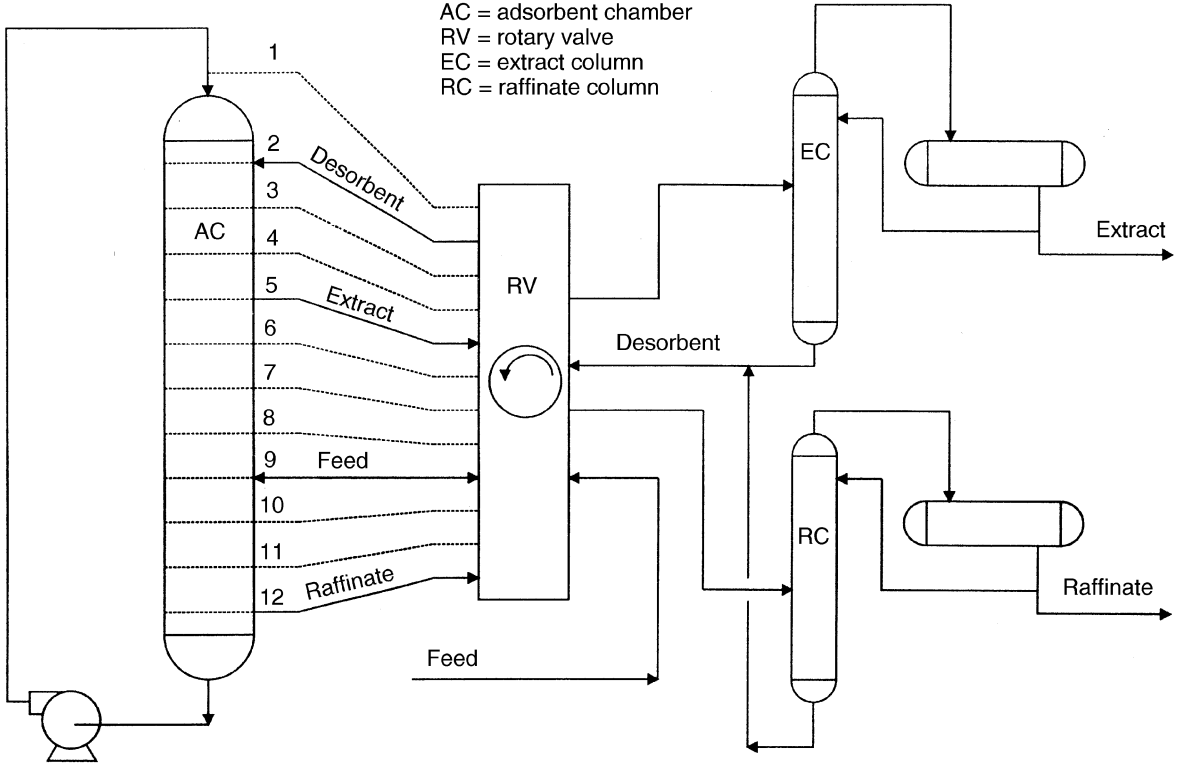

Figure 5.13 *Schematic diagram of the Sorbex process (redrawn from Broughton et al.* 1970).

*Table 5.2 Methods of regeneration, with process examples**

Method	*Advantages*	*Disadvantages*	*Process*	Examples of use *Adsorbent*	*Selectivity*
Thermal swing	Good for strongly adsorbed species. Desorbate recovered at high concentrations. For gases and liquids	Thermal ageing of sorbent. Heat loss leads to thermal inefficiency. Long cycle times mean inefficient use of sorbent. High latent heat for liquids	Drying of gases. Drying of solvents	3A, 4A, 13X 4A	Equilibrium Equilibrium
Pressure swing	Good for weakly adsorbed species required in high purity	Very low P may be required	Drying of gases. Hydrogen recovery Air separation	3A, 4A, 13X Mol sieve Carb mol sieve	Equilibrium Equilibrium Kinetic
		Mechanical energy more expensive than heat	Air separation	Zeolite	Equilibrium
Vacuum (special case of pressure swing)	Rapid cycling gives efficient use of sorbent	Desorbate recovered at low purity	Separation of linear paraffins	5A mol sieve	Shape selective sieving
Displacement	Good for strongly held species. Avoids risk of cracking reactions during regeneration. Avoids thermal ageing of sorbent	Product separation and recovery needed (choice of desorbent fluid is crucial)	Separation of linear from branched and cyclic paraffins	5A mol sieve	Shape selective sieving
Purge gas stripping	Essentially at constant T and P	Only for weakly sorbed species, purge flow is high. Not normally used when desorbate needs to be recovered	Relatively uncommon without thermal swing since purging alone is only suitable for weakly adsorbed species		
Steam stripping (combination of thermal swing and displacement)	As for thermal swing and displacement above		Waste water purification. Solvent recovery	Activated carbon	Equilibrium

* Adapted from Ruthven 1984, p. 339 and Crittenden 1992, p. 4.15.

As a variable for changing thermodynamic potential, a change in temperature is much more effective than a change in pressure. However, the final choice of regeneration method(s) depends upon technical and economic considerations. The most common methods are changes in temperature (thermal swing adsorption) and changes in pressure (pressure swing adsorption). The general advantages and disadvantages of each method together with some process examples are shown in Table 5.2.

5.7 REDUCTION IN PARTIAL PRESSURE

Figure 5.14(a) shows schematically the effect of partial pressure on equilibrium loading for a Type I isotherm with a temperature, say T_1. Reducing the partial pressure from p_1 to p_2 causes the equilibrium loading to be reduced from q_1 to q_2. There are two ways in which the partial pressure can be lowered. First, the total pressure in the system can be reduced. Secondly, an inert gas can be used to lower the partial pressure while maintaining the total system pressure. In the majority of pressure swing separations a combination of the two methods is employed. Use of a purge fluid alone is unusual. Changes of pressure can be effected very much more quickly than changes of temperature and thus cycle times of pressure swing adsorption (PSA) processes are typically of the order of minutes, and for rapid cycle systems of the order of seconds. The faster the cycle time the lower is the size of the equipment and the inventory of adsorbent. Thus PSA processes are attractive for bulk gas separations and purifications for those situations in which the adsorptive forces are relatively weak. Some PSA processes are based on kinetic effects rather than on equilibrium effects in which case it can be important not to allow sufficient time for the gases in the bed to reach thermodynamic equilibrium with the adsorbent.

PSA processes are often operated at low adsorbent loadings because selectivity between gaseous components is often greatest in the Henry's Law region. An example of this is the separation of air components on 5A zeolite. It is desirable to operate PSA processes close to ambient temperature to take advantage of the fact that for a given partial pressure the loading is increased as the temperature is decreased. It is not usually worth attempting to reduce the temperature to below ambient.

The basic PSA process uses two beds which operate 180° out of phase with each other in four steps as shown schematically in Figure 5.15. The steps are (i) pressurization with feed, although the product could be used instead, (ii) production at elevated pressure, (iii) countercurrent depressurization, although this could be cocurrent, and (iv) purge with a fraction of the

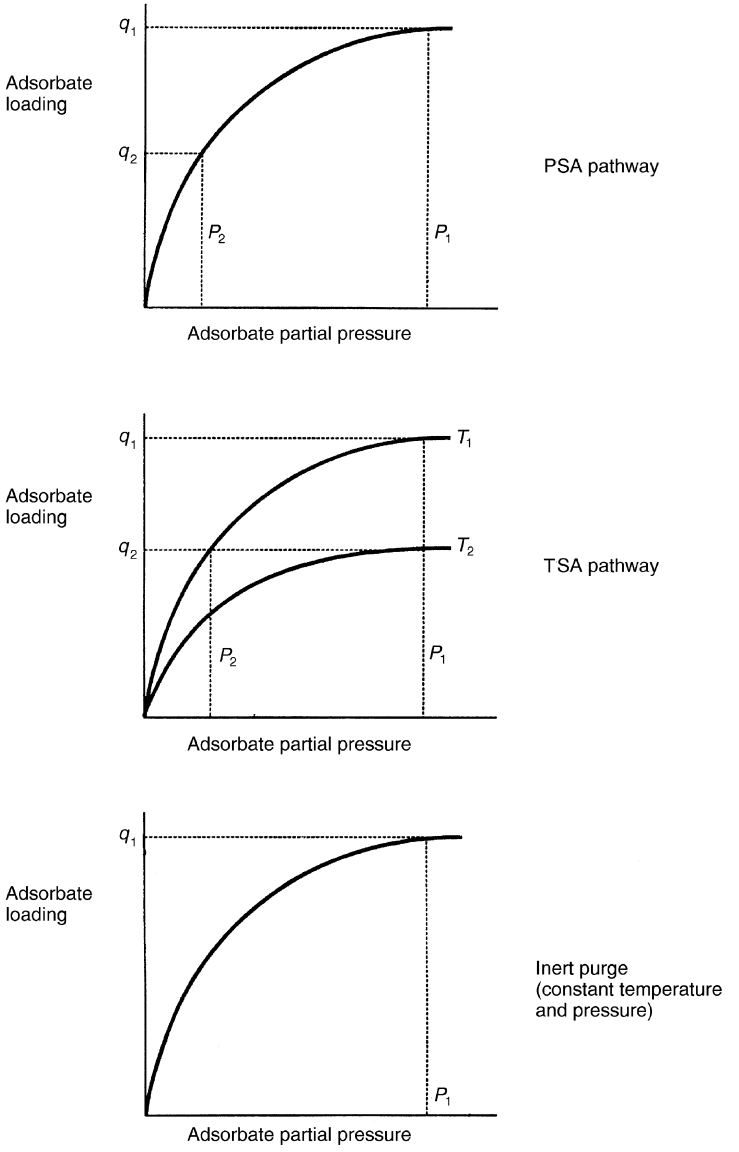

Figure 5.14 *The effect of process variables on the adsorption equilibrium for a Type I isotherm: (a) the effect of adsorbate partial pressure, (b) the effect of temperature and (c) the effect of an inert purge (redrawn from Keller et al. 1987, pp. 655–657).*

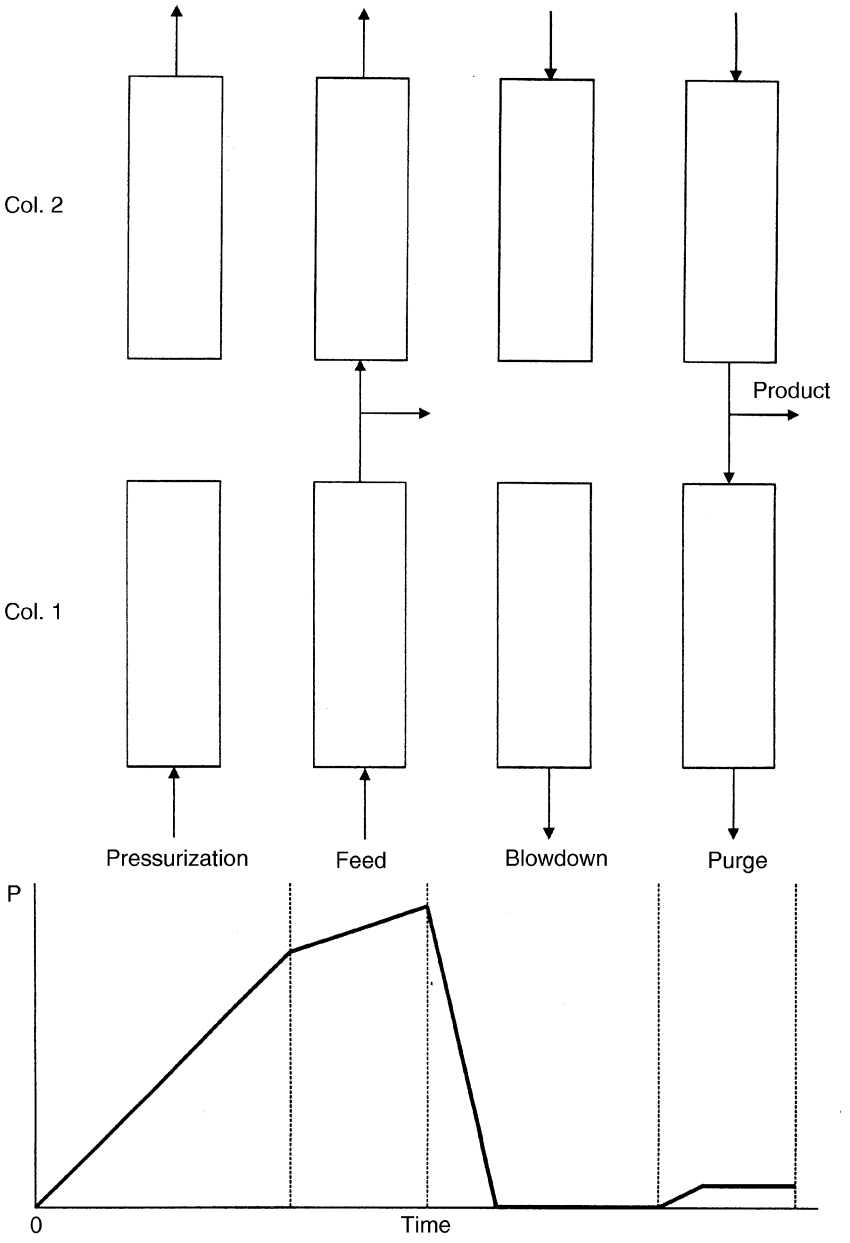

Figure 5.15 *Sequence of steps in the basic PSA cycle (adapted from Ruthven 1984, p. 362).*

product. The production step may occur at a pressure greater than atmospheric with the desorption pressure being atmospheric. This practice is normal for the production of oxygen from air using a 5A zeolite. Alternatively, the production step could be carried out at atmospheric pressure and the desorption step under vacuum. This is normal practice for kinetically based separations such as the production of nitrogen from air using a carbon molecular sieve. Vacuum regeneration is used in this case to remove most of the oxygen which has been adsorbed in order to avoid slow uptake of nitrogen which would saturate the adsorbent and reduce its effectiveness for taking up oxygen during the subsequent adsorption step. Figure 5.16 shows the simplest practical hardware layout for a PSA process shown in schematic form in Figure 5.15. The example is the production of nitrogen using a pressure swing between atmospheric pressure and a vacuum.

The purge step is very important for efficient operation because the use of a purified component flowing in the reverse direction causes the strongly adsorbed species to be pushed back towards the bed inlet for the subsequent adsorption step. The more strongly adsorbed components therefore are unlikely to contaminate the product on the next adsorption step. The volume of the purge gas, measured at the low pressure, should normally not be less than 1–2 times the volume of the feed measured at the high pressure. The product purity increases as the fraction of the product used for the purge is increased but after a certain value this gain becomes marginal. Because the increase in volume from high to low pressure becomes greater the higher the ratio of high to low pressure in the process, it can be seen that the actual fraction of the product stream required for the purge could be quite small if the pressure ratio were high. The disadvantage of a high pressure ratio, however, is the increased energy demand. Clearly the design of a PSA gas separation process requires engineering compromises to be made.

Much effort has been devoted to reducing the overall energy demands of PSA separation processes. One of the simplest techniques for multibed processes is to use pressure equalization between beds, i.e. to release the pressure of a bed which is at the end of its production step to a bed which has come to the end of its desorption step. In this way some of the energy associated with compression can be conserved within the process. Further details on the development of PSA cycles and their applications are provided in Sections 7.2 and 7.3.

It is possible to operate PSA with a single packed bed. The rapid pressure swing adsorption process (RPSA) can be considered to be a hybrid between the four step cycle of a more conventional PSA process and parametric pumping in which pressure is the thermodynamic parameter which causes

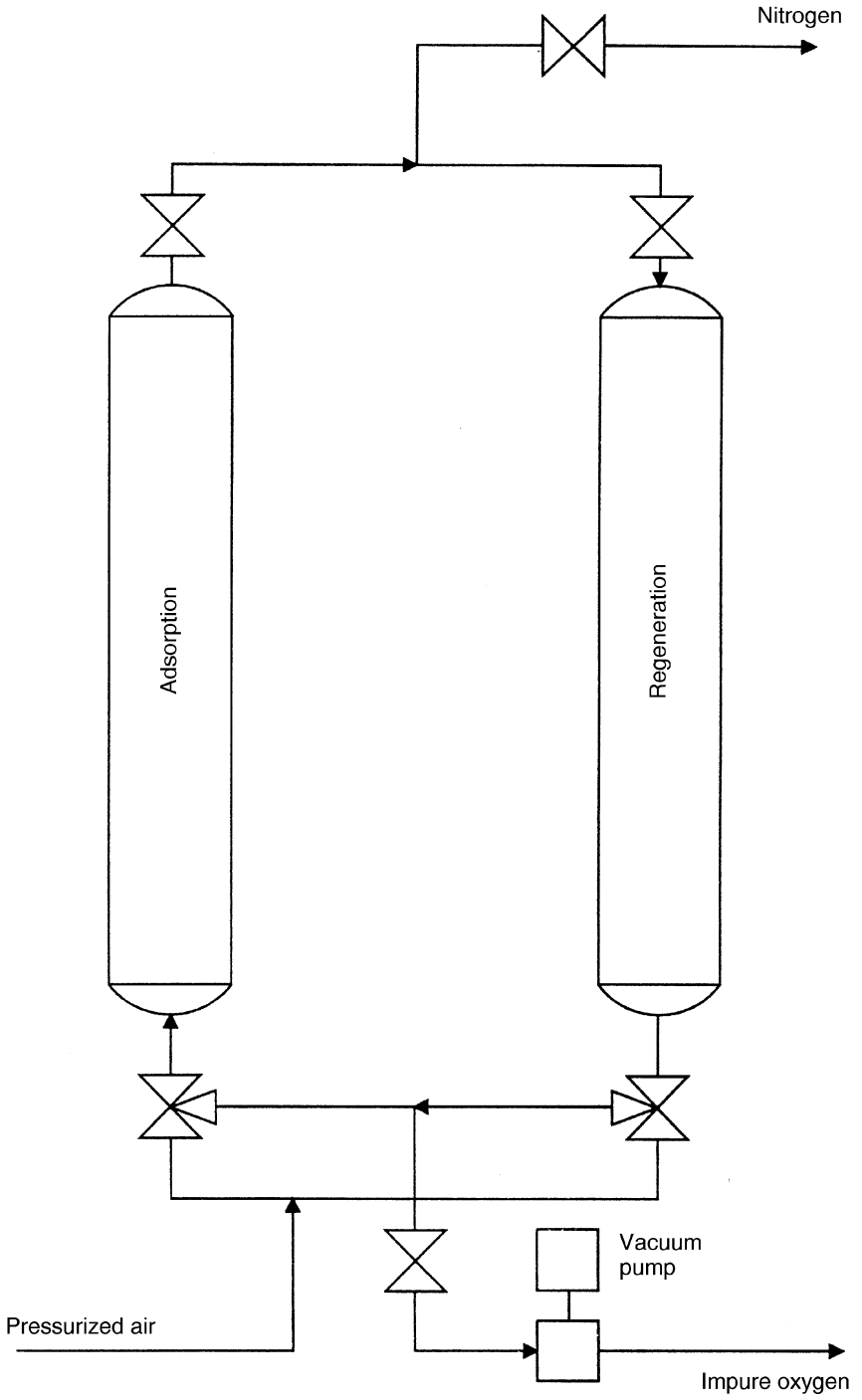
Nitrogen
Adsorption
Regeneration
Vacuum
pump
Pressurized air
Impure oxygen

the separation. The flowsheet of a single bed RPSA process is shown in Figure 5.17. There are two steps of equal duration, namely (i) feed/pressurization and (ii) exhaust/depressurization. Figure 5.17 shows that the feed and exhaust take place at the same end of the bed and that the product is withdrawn from the opposite end. The cycle time is short, typically less than 20 seconds, and small particles are used to create both a high pressure gradient across the bed and a short diffusional path for the adsorbate. The principal disadvantage of the single bed RPSA process is that while relatively high product purities can be obtained the product recovery (defined as the amount of component recovered in the product per amount of the component entering in the feed) can be low. A low product recovery in any PSA process is undesirable because, for a given production rate, the flowrate of feed, which must be compressed, will be high and consequently the power requirements will be high. Descriptions of recent developments in RPSA are provided in Chapter 7.

In practice the pressure changes with time are more complex than those shown in Figure 5.15. Pressure does not vary linearly with time during either the pressurization or depressurization steps (Crittenden *et al*. 1994; 1995). Instead, as pressurization occurs there will be a pressure distribution along the length of the bed and at each point the pressure will tend to increase exponentially up to the final value. Exponentially shaped pressure–time curves will occur also for the depressurization step. To make matters even more complicated adsorption can occur as pressurization proceeds and desorption can occur as depressurization proceeds. This is a particularly important consideration for RPSA processes.

The pressurization step creates a region near the closed end of the bed where enrichment in the least adsorbable component occurs. This region is displaced in the production step at more or less constant pressure by the inflow of feed gas at the other end of the bed. Depressurization and subsequent purging are normally carried out in the reverse direction. In most commercial PSA applications the adsorbent is selected so that the most desired product is the least adsorbed species. The gas which is discharged during the depressurization and purge steps is normally, but not necessarily, a waste stream.

Figure 5.16 *Two-bed vacuum swing adsorption process for the production of nitrogen with a carbon molecular sieve (redrawn from Knoblauch 1978).*

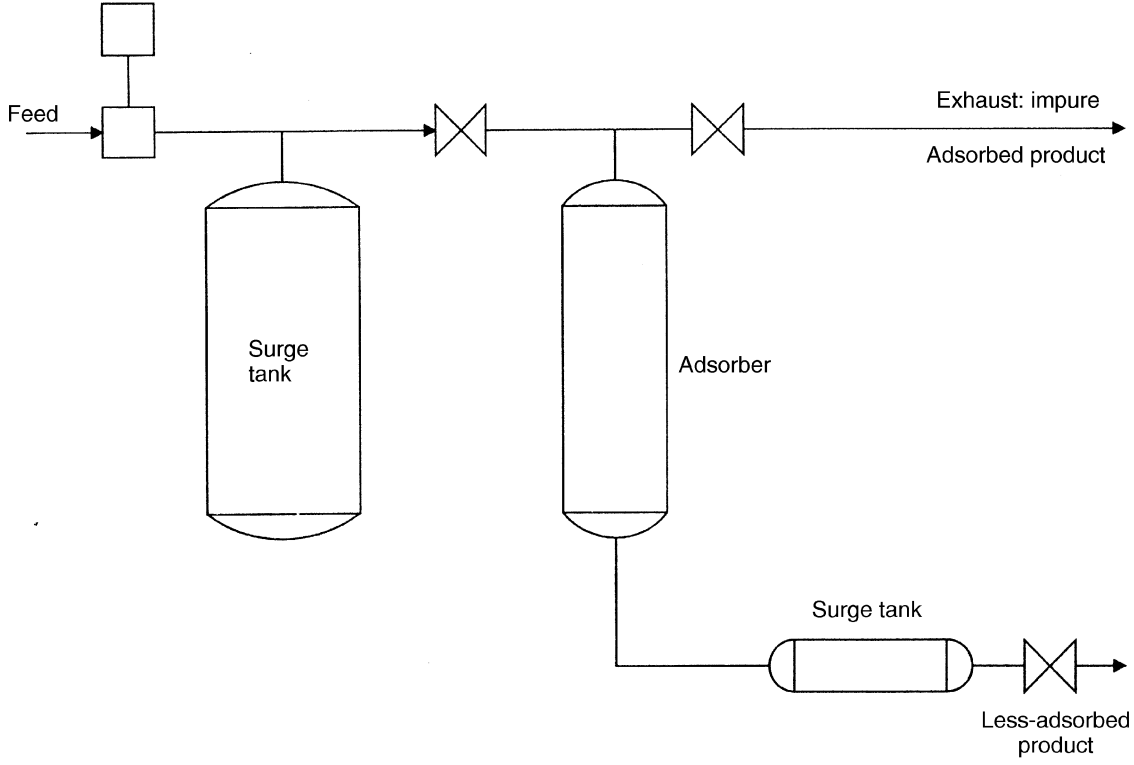

Figure 5.17 *Single-bed rapid pressure swing adsorption (redrawn from Keller et al.* 1987, p. 661).

5.8 INCREASE IN TEMPERATURE

Figure 5.14(b) shows schematically the effect of temperature on the adsorption equilibrium of a single adsorbate. The type I isotherm is used for illustrative purposes. For any given partial pressure of the adsorbate in the gas phase (or concentration in the liquid phase) an increase in temperature leads to a decrease in the quantity adsorbed. Hence, increasing the temperature from T_1 to T_2 will decrease the equilibrium loading from q_1 to q_2 assuming that the partial pressure in the gas phase remains constant. The dependency of the loading on absolute temperature is generally well described by the van't Hoff equation. Because the most strongly adsorbed species have the greatest heats of adsorption a relatively large decrease in loading can be achieved by a relatively modest increase in temperature. Adsorption isotherms tend to become unfavourable for adsorption at increased temperature and hence they become more favourable to desorption. It is therefore generally possible to desorb any species provided that the temperature is high enough. However, it is important to ensure that the regeneration temperature does not exceed that required to degrade the adsorbent or cause it to behave catalytically with the chemicals involved in the process.

A change in temperature alone is not used in commercial processes because there is no mechanism for removing the adsorbate from the adsorption equipment once desorption from the internal pores has occurred. Passage of a hot purge gas, or steam, through the equipment to sweep out the desorbed species is almost always used in conjunction with the increase in temperature. This is the case for both gas and liquid phase adsorption processes. For liquid phase separations the liquid is drained from the adsorption equipment prior to the passage of hot gas.

Figure 5.18 shows one of the simplest practical thermal swing adsorption cycles based on two beds. The feedstock containing the adsorbate at a partial pressure p_1 is passed through the first bed at temperature T_1. The partial pressure of the adsorbate in the bed effluent may be zero or very low. When breakthrough is about to occur this bed is taken off-line and the feed is switched to the second bed. Simultaneously the first bed is regenerated by raising its temperature to T_2 and purging with a hot gas normally in a flow direction opposite to that used for the adsorption step. This is to ensure that the outlet end of each bed when used on the next adsorption step (for which the greatest product purity is required) has the lowest loading of adsorbate at the end of the regeneration step. The bed which has been regenerated must now be cooled to temperature T_1 and this can be done by using either cold inert gas or the feedstock. This flow is normally in the direction for adsorption.

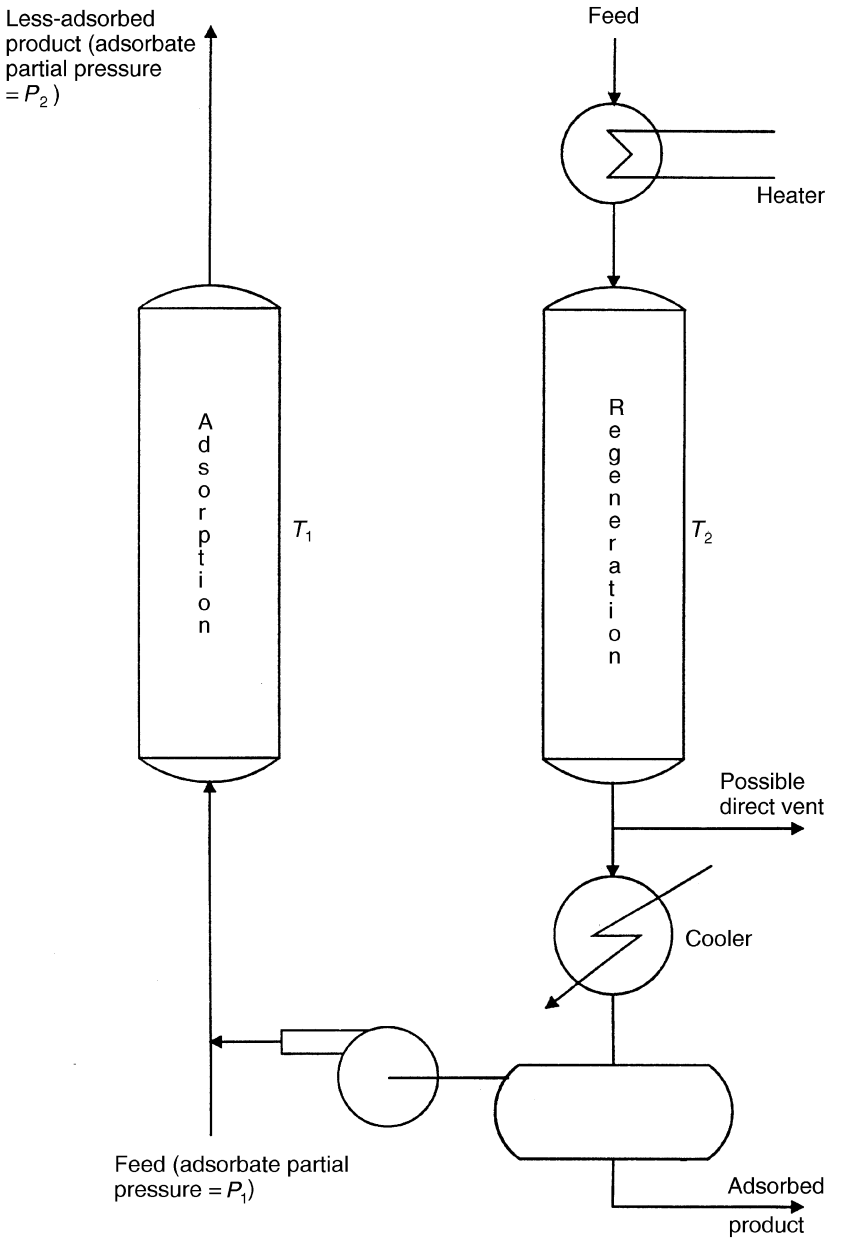

Figure 5.18 *Basic thermal swing adsorption process (redrawn from Keller et al.* 1987, p. 655).

A special bed cooling step is not always required. For example, if the thermal wave caused by the heat of adsorption runs ahead of the mass transfer zone on the adsorption step then the temperature in the MTZ will be more or less equal to the feed temperature and may be unaffected by the temperature used during desorption or regeneration.

The basic TSA cycle clearly consists of four steps, namely (i) adsorption onto a regenerated solid at T_1, (ii) a temperature increase to T_2 by means of hot feed, hot purge gas, steam, etc, (iii) desorption with feed or purge fluid at T_2 and (iv) cooling to T_1 with cold feed or inert purge. Desorption with hot feed is practicable only if high purity is not required on the subsequent adsorption step. The loading on the adsorbent in the adsorption step is improved by operating the bed at the lowest temperature which avoids condensation. In practice, ambient temperature is often used. The desorption temperature and the purge flowrate are related. That is, the same extent of desorption could be achieved either with a low purge flowrate and a high temperature, or with a high purge flowrate and a low temperature.

The heating and desorption steps must provide sufficient energy to perform a number of functions. First, the adsorbent, its associated adsorbate and the containment vessel must be raised to the desorption temperature. Secondly, the heat of desorption must be provided. Thirdly, the adsorbent and vessel temperature must be raised to the final regeneration temperature if this needs to be higher than that used for desorption. Energy will also be required if there are heat losses and if vaporization of undrained liquid is necessary. TSA cycles can therefore consume large amounts of energy per unit quantity of adsorbate.

Because beds of adsorbent cannot normally be heated and cooled quickly, the cycle time of a typical TSA process may range from several hours for a bulk separation to several days for a purification. Long cycle times inevitably mean large bed lengths with consequential high adsorbent inventories. Thus the effective use of the adsorbent is poor if the mass transfer zone length is short. The times for the adsorption and desorption/regeneration steps must be equal in a TSA process and the cycle time may be controlled by events in the desorption part of the cycle. The purge step becomes the limiting step for situations in which the purge does not have sufficient capacity to remove the adsorbate as quickly as it can provide the energy for desorption. Purge-limited desorption/regeneration occurs if the regeneration pressure is relatively high, the regeneration temperature is relatively low and the adsorbates are strongly adsorbed. For such situations direct heating with the purge gas should be employed. If the desorption/regeneration process is thermally controlled then it is better to employ indirect heating such as electrical elements or heating coils. The use of heating coils offers a further advantage in that they can be used to provide indirect cooling as well.

Common examples of thermal swing adsorption include solvent recovery with activated carbons, and drying of gases or liquids with type A zeolites. Drying of organic vapours using type A zeolites can overcome the difficulty in distillation of reaching high purities in chemical systems which contain vapour–liquid azeotropes. All these processes can be carried out without the need to remove the adsorbent from its vessel. In contrast, granular activated carbon (GAC) which is used to adsorb high molecular weight, low volatility or strongly adsorbed species, must usually be removed from the adsorption vessel for regeneration in special furnaces. In this case the GAC needs to be heated to over 800°C. Multiple hearth, rotary kiln, fluised bed and electric belt furnaces are available (Liu and Wagner 1985). The multiple hearth furnace is shown in Figure 2.8. Further developments and examples of TSA are provided in Sections 7.4 and 7.5.

A practical problem in thermal swing processes is the reduction in the capacity or life of the adsorbent when it is subjected to repeated thermal cycling. Another problem is the formation of coke in applications in which reactive hydrocarbons are exposed to elevated temperatures during the desorption/regeneration step.

5.9 DISPLACEMENT FLUID

Adsorbates can be removed from the adsorbent surface by replacing them with a more preferentially adsorbed species. This displacement fluid, which can be a gas, vapour or liquid, should adsorb about as strongly as the species which are to be desorbed. If the displacement fluid is adsorbed too strongly then there may be subsequent difficulties in removing it from the adsorbent. The mechanism for desorption of the original adsorbate involves two aspects. First, the partial pressure of the original adsorbate in the gas phase surrounding the adsorbent is reduced (or the concentration is reduced in the case of a liquid displacement fluid). Secondly, there is competitive adsorption of the displacement fluid. The displacement fluid is present on the adsorbent at the next adsorption step and thus it will contaminate the product. A practical process therefore requires that the displacement fluid must be recoverable from the products of the adsorptive separation by a process such as simple distillation. This is the basis of the Sorbex type process shown in Figure 5.13.

One advantage of the displacement fluid method of regeneration is that the net heat generated or consumed in the adsorbent will be close to zero because the heat of adsorption of the displacement fluid is likely to be close to that of the original adsorbate. Thus the temperature of the adsorbent should remain more or less constant throughout the cycle. In turn this leads

to the ability to have relatively high loading differences between the adsorption and desorption steps with relatively short cycle times. Examples of displacement purge cycles are provided in Section 7.6.

REFERENCES

Alsop, R. M., Barker, P. E. and Vlachogiannis, G. J. (1984), *Chemical Engineer*, No. 399, 24–27

Anon (1977), *Chem. Eng.,* **84**, August 39–40

Avery, D. A. and Tracey, D. H. (1968) *IChemE Symp. Series* (*Fluidisation*), **30**, 28–33

Barker, P. E. and Ching, C. B. (1980) *Eur. Fed. Chem. Eng. Kemtek,* 5, Copenhagen

Berg, C. (1946) *Trans. AIChE,* **42**, 665–680

Berg, C. (1951) *Chem. Eng. Prog.,* **47**, 585–591

Bieser, H. J. and de Rosset, A. J. (1977) Continuous counter-current separation of saccharides with inorganic adsorbents, *28th Starch Covention*, Detmold, Germany

Broughton, D. B. (1968) *Chem. Eng. Prog.,* **64**(8), 60–65

Broughton, D. B. and Berg, R. C. (1969) *Hydrocarb. Process.,* **48**(6), 115–120

Broughton, D. B. and Carson, D. B. (1969) *Petrol Refiner*, **38**(4), 130–134

Broughton, D. B., Neuzil, R. W., Pharis, J. M. and Brearley, C. S. (1970) *Chem. Eng. Prog.,* **66**(9), 70–75

Coulson, J. M. and Richardson, J. F. with Backhurst, J. R. and Harker, J. H. (1991) *Chemical Engineering*, vol. 2, 4th edn, Pergamon, Oxford

Cox, M. (1958) *Trans. IChemE*, **36**, 29–42

Crittenden, B. D. (1991) *Chem. Eng. Educ.*, **25**, 106–110

Crittenden, B. D. (1992) Selective adsorption – a maturing but poorly understood technology, in *Current Best Practice in Separations Technology*, The R&D Clearing House, London

Crittenden, B. D., Guan, J., Ng, W. N. and Thomas, W. J. (1994) *Chem. Eng. Sci.,* **49**, 2657–2669

Crittenden, B. D., Guan, J., Ng, W. N. and Thomas, W. J. (1995) *Chem. Eng. Sci.,* **50**, 1417–1428

de Rosset, A. J., Neuzil, R. W. and Korous, D. J. (1978) *Ind. Eng. Chem. Process. Design Dev.,* **15**, 261–266

Eagle, S. and Rudy, C. E. (1950) *Ind. Eng. Chem.,* **42**, 1294–1299

Ermenc, E. D. (1961) *Chem. Eng.,* **May 29**, 87–94

Faust, S. D. and Aly, O. M. (1987) *Adsorption Processes for Water Treatment*, Butterworths, Boston

Kehde, A., Fairfield, K. G., Frank, J. C. and Zahnstecher, L. W. (1984) *Chem. Eng. Prog.,* **44**, 575–578

Keller II, G. E., Anderson, R. A. and Yon, C. H. (1987) Adsorption, in *Handbook of Separation Process Technology*, edited by R. W. Rousseau, Wiley Interscience, New York

Knoblauch, K. (1978) *Chem. Eng.* **85**(25), 87–89

Liu, P. K. T. and Wagner, N. J. (1985) *Environmental Progress*, **4**(2), 136–140

Lockett, A. D., Yang, M. and Hubble, J. (1992) In situ monitoring of adsorption column performance. *Proc. 4th Int. Conf. on Analytical Methods, Systems and Strategies in Biotechnology*, pp. 95–106

Neuzil, R. W. and Jensen, R. A. (1978) Development of the Sarex process for separation of saccharides. Paper presented at *22nd AIChE meeting*, Philadelphia

Otani, S. (1973) *Chem. Eng.,* **80**(21), 106– 107

Rowson, H. M. (1963) *Brit. Chem. Eng.,* **8**, 180–184

Ruthven, D. M. (1984) *Principles of Adsorption and Adsorption Processes*, Wiley Interscience, New York

Ruthven, D. M. and Ching, C. B. (1989) *Chem. Eng. Sci.,* **44**, 1011–1038

6

Design procedures

Fixed beds are mechanically simpler than moving beds but operate in an unsteady, and usually cyclic, manner. As a consequence, extensive computation may be required to predict rigorously the amount of adsorbent which is required in a fixed bed for a given duty. The variation of parameters with time needs to be taken into account in formulating the design model. Moving beds, on the other hand, may pose greater challenges in the mechanical design rather than in the process design, since the latter would not normally include the dimension of time. To illustrate this simplicity, the process design of an ideal fluidized bed adsorber in which the solids are assumed to be uniformly mixed would be similar to the design of a stirred tank reactor. Also, the design of an adsorber with the solids in plug flow would be similar to that for other types of countercurrent contactors. In general, the principles of design pertaining to the adsorption steps described in this chapter are applicable equally to the desorption steps.

6.1 DATA REQUIREMENTS

Data in five categories are required for the process and equipment design phases of any adsorption process.

(1) *Adsorbate–adsorbent thermodynamic equilibrium relationships (as described in Chapter 3), including appropriate interaction data for multicomponent systems*; it is necessary initially to identify an adsorbent which is

capable of effecting the required separation. Then it is necessary to consider the effect that the other adsorbates in a multicomponent feedstock may have on the equilibrium of each component, and the method by which the adsorbent is to be regenerated if it is not going to be discarded after the adsorption step.

(2) *Adsorbate–adsorbent kinetic relationships (as described in Chapter 4), again including appropriate interaction data for multicomponent systems*; separations are rarely controlled by equilibrium considerations alone and therefore it is necessary to determine whether or not the selected adsorbent has the requisite kinetic properties. The rate of adsorption will determine the size of the equipment for those separations which do not have extremely fast kinetics, i.e. those which cannot be described as being equilibrium controlled.

(3) *Heat of adsorption as a function of the operating conditions including the composition*; whether the process can be considered to be isothermal or not depends on the magnitude of the heat of adsorption per mol and the concentration(s) of the adsorbate(s) in the feedstock. The design process using rigorous methods is simplified considerably if the heat released on adsorption is low. Even so, energy balance calculations may still be required if desorption, or regeneration of the adsorbent is to be carried out at elevated temperature.

(4) *Hydrodynamic data*; such data are required to determine pressure gradients and to evaluate the importance of dispersion in the design process.

(5) *Physical property data*; basic information required over the ranges of temperature, pressure and composition to be encountered in the process includes the density, viscosity, thermal conductivity, specific heat and molecular diffusivities of fluids together with the specific heat of the adsorbent and the bulk voidage and bulk density of the adsorbent bed. Many more properties of the system may need to be obtained if rigorous approaches to the design problem are adopted.

6.2 STAGEWISE CONTACTING

The design principles of stagewise contacting may be illustrated by use of a simple pollution control example shown schematically in Figure 6.1. Consider a volume V m^3 of water which contains an impurity at a very dilute concentration of c_o kg/m^3 which is to be reduced to a concentration of c_f kg/m^3 by adsorption onto M kg of granular activated carbon (GAC).

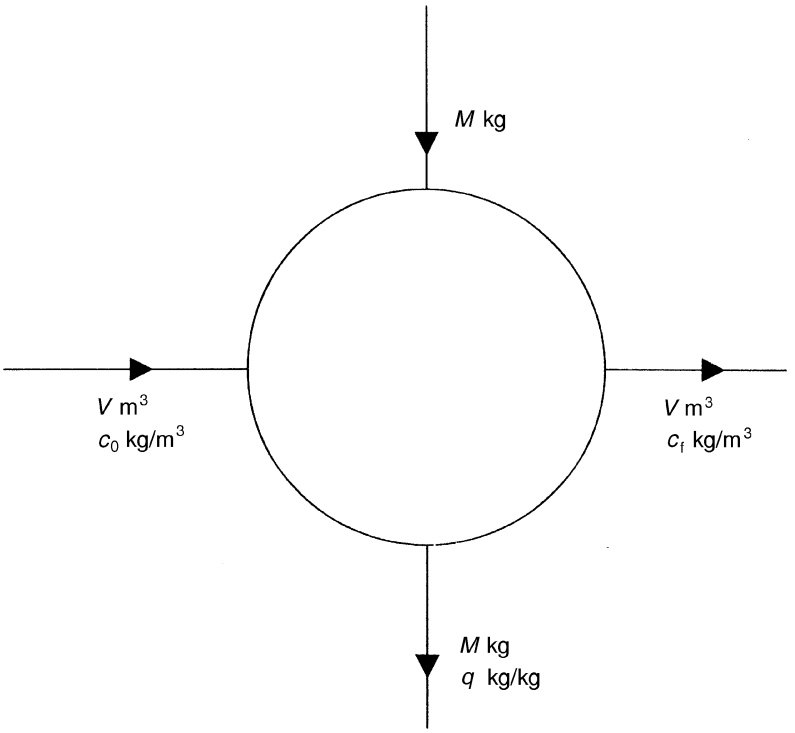

Figure 6.1 *Single-stage contacting of a batch of fluid with a batch of adsorbent.*

The adsorbent is initially free from the impurity. The isotherm is linear (that is, it follows Henry's law as described in Section 3.3.2) and is given by:

$$q = Kc \tag{6.1}$$

where q is the loading of the impurity on the GAC (kg impurity/kg GAC) in equilibrium with the impurity concentration in the water, c (kg/m^3), and K is the equilibrium constant (m^3/kg).

It is assumed that water is not adsorbed and since the impurity concentration is always low, the volume of solution does not change. The mass balance on the impurity is therefore as follows:

$$V(c_0 - c_f) = Mq \tag{6.2}$$

If the adsorbent were not initially free from the impurity but had been

regenerated to a residual loading of q_0 then it would be necessary to replace the right-hand side of equation (6.2) by $M\ (q–q_0)$. After contacting, the equilibrium is given by:

$$q = Kc_f \tag{6.3}$$

Simultaneous solution of equations (6.2) and (6.3) gives the mass of adsorbent required to effect the purification:

$$M = \frac{V}{K}\left(\frac{c_0}{c_f} - 1\right) \tag{6.4}$$

This equation shows that the mass of adsorbent required can be reduced if an adsorbent with a higher equilibrium constant can be found. Equation (6.2) can be rearranged to give a linear relationship between q and c_f:

$$q = \frac{V}{M}(c_0 - c_f) \tag{6.5}$$

If the adsorbent were not initially free from the impurity at the start of the adsorption process then the linear relationship would be:

$$q = \frac{V}{M}(c_0 - c_f) + q_0 \tag{6.6}$$

The simultaneous solution to equations (6.3) and either (6.5) or (6.6) can be found graphically, as shown in Figure 6.2 (a) and (b), respectively. Whether or not an analytical solution can be found in the case of a non-linear isotherm depends on the shape of the isotherm. If an analytical solution is not possible then the solution may be found graphically as shown in Figure 6.2 (c).

Powdered or granular adsorbents are usually added to a process in slurry form in such a way as to allow adequate dispersion and mixing. The adsorbent can be removed as a settled sludge. When large quantities of adsorbent are required consideration should be given to using a multiple batch or cross-flow system. For example, one way of reducing the amount of adsorbent required is to carry out the batch processing in two steps, as shown in Figure 6.3. Here the total amount of adsorbent is split arbitrarily into two parts M_1 and M_2. The feed is first contacted with a fresh batch of adsorbent and the impurity concentration is reduced to c_1. After separation of the fluid from the adsorbent in the first stage the fluid is contacted with a further fresh batch of adsorbent. In multibatch systems each subsequent batch of adsorbent removes less and less impurity as the impurity concentration decreases.

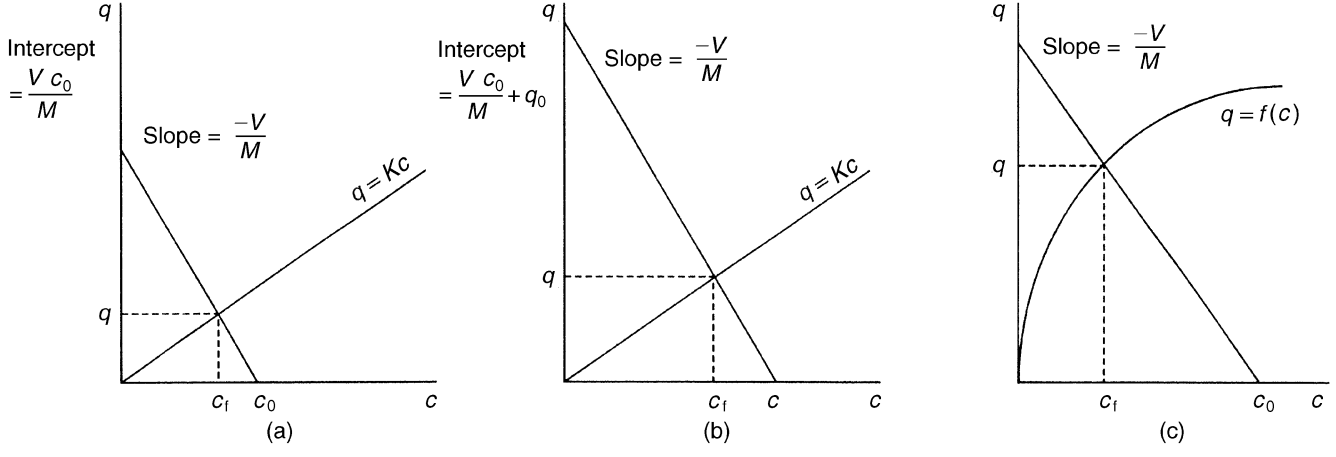

Figure 6.2 *Graphical solution to the single-stage contacting example: (a) Henry's law isotherm with an adsorbent intitially free from the adsorbate; (b) Henry's law isotherm with an adsorbent initially having an adsorbate loading of q_0; and (c) general Type I isotherm with an adsorbent initially free from the adsorbate.*

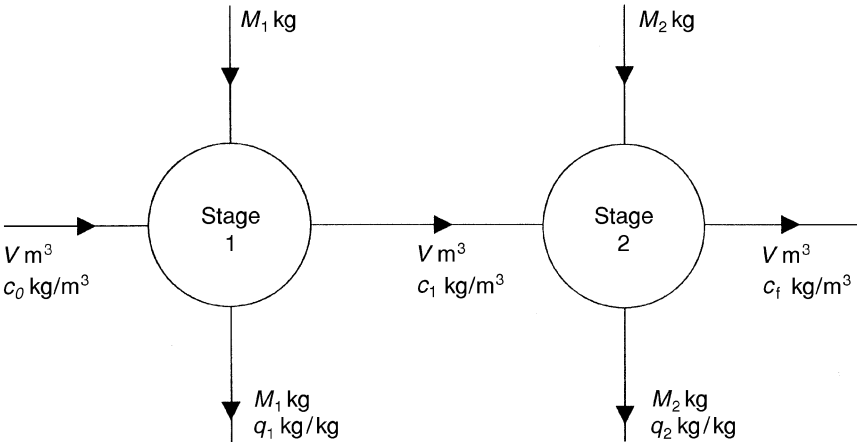

Figure 6.3 *Stagewise contacting of a batch of fluid with three batches of adsorbent.*

Simultaneous solution of the impurity mass balance with the equilibrium relationship for the first batch vessel yields M_1:

$$M_1 = \frac{V}{K}\left(\frac{c_0}{c_1} - 1\right) \tag{6.7}$$

The loading q_1 is in equilibrium with the intermediate concentration c_1. Simultaneous solution of the impurity mass balance with the equilibrium relationship for the second batch vessel yields M_2:

$$M_2 = \frac{V}{K}\left(\frac{c_1}{c_f} - 1\right) \tag{6.8}$$

For the total mass of adsorbent to be a minimum, the differential of (M_1 + M_2) with respect to the intermediate concentration c_1 needs to be zero. Hence, it can be shown that:

$$c_1 = (c_0.c_f)^{0.5} \tag{6.9}$$

Substitution of c_1 from equation (6.9) into equations (6.7) and (6.8) shows that the minimum amount of adsorbent for this purification is given when:

$$M_1 = M_2 = \left[\frac{V}{K}\left(\frac{c_0}{c_f}\right)^{0.5} - 1\right] \tag{6.10}$$

For a multistage process involving N stages the general result for a linear (Henry's law) isotherm is:

$$\Sigma\,(M_1 + M_2 \ldots + M_N) = \frac{NV}{K}\left\{\left(\frac{c_0}{c_f}\right)^{1/N} - 1\right\} \tag{6.11}$$

Comparing equation (6.11), when N=2, with equation (6.4) shows that by splitting the adsorbent into two equal amounts the total amount of adsorbent required for the given purification is reduced from that required when all the adsorbent is used in one stage:

$$\frac{M_1 + M_2}{M} = \frac{2\left\{\left(\frac{c_0}{c_f}\right)^{0.5} - 1\right\}}{\left(\frac{c_0}{c_f}\right) - 1} = \frac{2}{\left(\frac{c_0}{c_f}\right)^{0.5} + 1} \tag{6.12}$$

Since c_0 is greater than c_f then from equation (6.12):

$$\frac{(M_1 + M_2)}{M} < 1 \tag{6.13}$$

Clearly the reduction in the amount of adsorbent is achieved at the expense of more processing stages. Conversely, a better purification could be achieved with a given amount of adsorbent M if it were divided equally among a number of stages. The optimum number of stages needs to be obtained from an economic evaluation.

The above analysis can be extended to cases involving non-linear isotherms, although in such cases it would not necessarily be optimal to split the adsorbent equally between stages. The graphical solution to a three-stage example is shown in Figure 6.4. A three-stage countercurrent stagewise contactor is depicted in Figure 6.5. In this case the adsorbent would need to be transported from stage to stage in the opposite flow direction to the fluid being treated.

The above stagewise analyses provide only the steady state overall mass balances. The design of batch processing equipment requires solution of the dynamic equations (introduced in Chapter 4) which describe the rate of uptake of the adsorbate by the adsorbent. Important matters to consider include the shape of the isotherm, whether V may be considered to be finite or infinite, and the nature of the adsorbent and the intraparticle rate processes (Tien 1994).

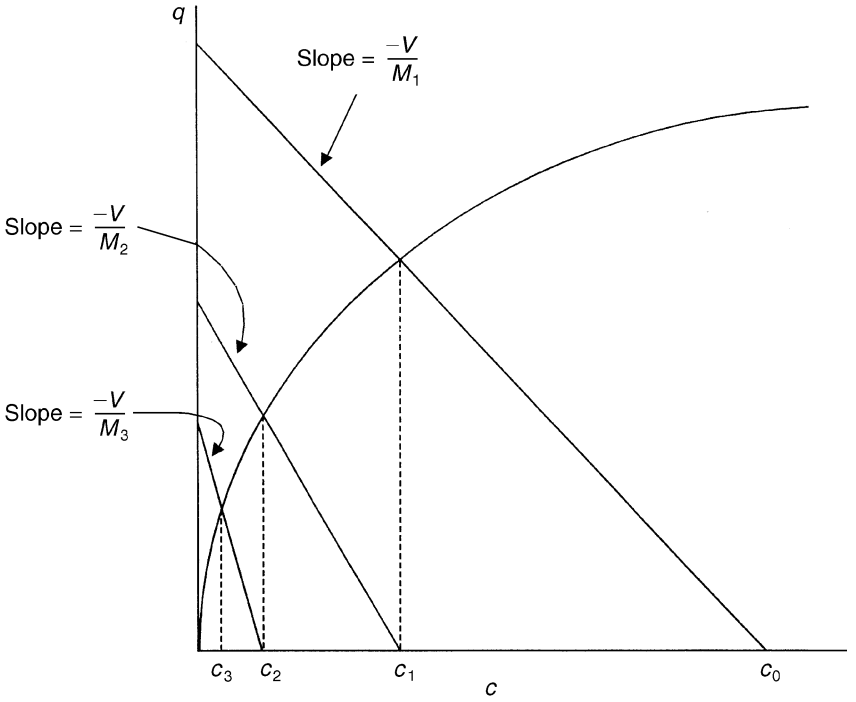

Figure 6.4 *Graphical solution to stagewise contacting of fluid with three batches of adsorbent.*

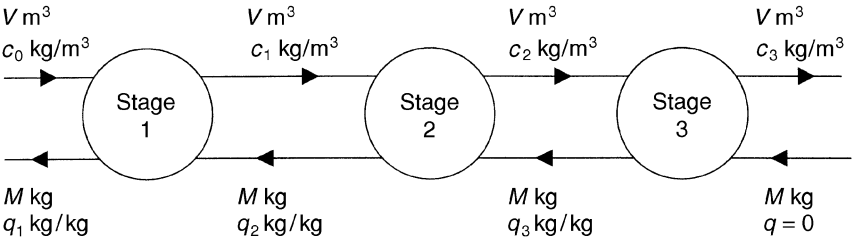

Figure 6.5 *Three-stage countercurrent stagewise contacting.*

6.3 DIFFERENTIAL CONTINUOUS CONTACTING

If the multiple stages described above were to be merged into a continuously moving bed such as that for solids in plug flow, then a stagewise calculation procedure could be used to provide the number of equivalent theoretical stages (or plates) required for the given separation. Given that the height equivalent to a theoretical plate, HETP, is available for the adsorbate–adsorbent combination, then the required height of the column would be given by:

$$L = (\textit{number of equilibrium stages}) \times HETP \tag{6.14}$$

Unlike in distillation and absorption, very little is known about HETP values in adsorption. As a consequence, it may be preferable to use the transfer unit concept for continuous flow adsorbers like the solids in plug flow unit. A differential mass balance on the sorbate across an incremental length of bed, dz, as shown in Figure 6.6, yields:

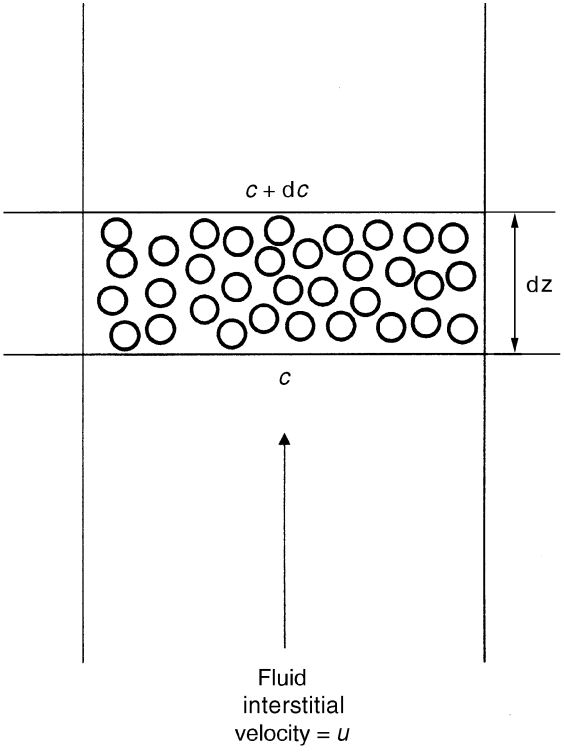

Figure 6.6 *Incremental length of adsorbent bed for the differential contacting model.*

$$ueA\,\mathrm{d}c = -k_{\mathrm{f}}A\,(1-e)\,a_{\mathrm{p}}\,(c-c_{\mathrm{i}})\mathrm{d}z \tag{6.15}$$

where A is the cross sectional area of the column
a_{p} is the external surface area of the adsorbent particle per unit volume of particle
u is the fluid superficial velocity
c is the adsorbate concentration in the fluid bulk
c_{i} is the adsorbate concentration at the fluid–adsorbent interface
e is the bed voidage.

In this example it is assumed that the mass transfer process is fluid film controlled, and that the fluid film mass transfer coefficient is k_{f}. Equation (6.15) cannot be readily integrated since the interfacial concentration c_{i} is not known. The rate of mass transfer is therefore expressed in terms of an overall driving force (c–c^*) in which c^* is the adsorbate concentration in equilibrium with the mean sorbed phase concentration. The length of the adsorbent bed L is then given by equation (6.16),

$$L = \frac{ue}{(1-e)k_0 a_{\mathrm{p}}} \int_{c_{\mathrm{B}}}^{c_{\mathrm{E}}} \frac{\mathrm{d}c}{c-c^*} \tag{6.16}$$

or

$$L = NTU \times HTU \tag{6.17}$$

where k_0 is the overall mass transfer coefficient
c_{E} and c_{B} are the fluid phase adsorbate concentrations into and out of the moving bed
NTU is the number of transfer units
HTU is the height of a transfer unit.

An analytical solution to the continuous equivalent countercurrent representation of a simulated moving bed process is provided in Section 7.7.4.

6.4 FIXED BEDS

Two extreme approaches can be taken for the design of fixed beds. One involves rigorous solution of the conservation, transport and thermodynamic equations and the other makes use of short-cut techniques which are based on laboratory-scale, pilot-scale or industrial-scale data. In the former approach, a certain amount of experimental work may be required where data is lacking in the literature.

In order to optimize a design it is desirable to carry out predictive mathematical modelling of the heat, mass and momentum transfer processes occurring in both the adsorption and the desorption stages in a process. This helps to avoid the need to carry out expensive and time-consuming experiments. Research on fixed bed adsorption is very active and so a large number of models exist, each of which can be complex, require extensive computation and need verification. The accuracy of the predictions will be related to the accuracy and availability of fundamental data as well as to the number and importance of the assumptions and approximations which need to be made in order to obtain the solution. For the simplest cases, or for those cases in which many simplifying assumptions and approximations are made, the solutions can be analytical. For most practical situations it is likely that the solutions will need to be obtained by numerical analysis.

The concentration profile of a single adsorbate as it breaks through from a fixed bed of length L is shown schematically in Figure 5.6 (a). For a single component such a breakthrough curve can be obtained relatively easily from laboratory-scale, pilot-scale or industrial-scale experiments by placing an analytical sensor at the bed exit. For example, a katharometer would suffice for a hydrocarbon. For multicomponent adsorption it would be necessary to take samples from the bed effluent at different times for subsequent analysis of composition. Breakthrough is deemed to have occurred at some time t_b when the concentration of the adsorbate leaving the bed increases to an arbitrarily defined value, c_e, which is often the minimum detectable or maximum allowable concentration of the component to be removed in the bed effluent. Figure 5.6 (b) shows the concentration profile of the adsorbate in the fluid phase inside the bed at time t_b. At the point of initial breakthrough, the mass transfer zone (MTZ) will have passed through the bed from its entrance to its exit at L_e. The fluid within the bed from the entrance up to L_e will be at the same concentration as that of the feed, namely c_o. The adsorbent loading in this region of the bed will be in equilibrium with the feed concentration. The MTZ will exist from L_e to the end of the bed L.

It is clearly possible to design a fixed adsorption bed by adding together the lengths which correspond first to the equilibrium portion (0 to L_e) and second to the MTZ (L_e to L). The former length can be obtained from a simple mass balance and requires that the equilibrium isotherm relationship is known (see Chapter 3). In contrast, rigorous and/or short-cut techniques must be used to obtain the MTZ length and to determine its rate of progress through the packed bed.

6.5 RIGOROUS METHODS

Many events occur in the MTZ during adsorption which render the analysis complex. First, one or more adsorbates transfer from the fluid bulk by convection or diffusion across the fluid film which is external to the solid surface. Secondly, these adsorbates penetrate the particle by Maxwell, Knudsen and surface diffusion mechanisms (see Chapter 4), and adsorb onto the internal surface where the heat of adsorption is released. Heat may then be transferred to the adsorbent, to the flowing process fluid, and, via the vessel wall, to the surrounding environment. Heat and mass transfer may occur in the MTZ by bulk and diffusive flows in both the radial and axial directions. An additional complexity is that the flow through a packed bed may not be uniform across its entire cross-sectional area. This may be because of channelling of fluid at the wall or because of temperature gradients created when the heat of adsorption is released.

An additional complication arises in cyclic fixed bed processes. A number of cycles will be required from start-up of the equipment up to the point at which each successive cycle is identical, this situation being that which is desired for normal operation. The fundamental governing equations do not change during this start-up phase. However, the boundary conditions vary with the cycle number and are dependent on the previous cycle. This start-up phase is normally of short duration compared with the period of steady operation, and thus is perhaps of more academic than practical interest. Analyses of start-up events can be found in Ruthven (1984), Yang (1987), Ruthven *et al*. (1994) and Tien (1994).

Situations which particularly complicate the design process include non-ideal gas behaviour (with high pressures), multicomponent separations (requiring the relevant thermodynamic and kinetic information), high heats of adsorption (e.g. with water on zeolites) which cause significant variations in temperature, axial and radial dispersions of mass and heat, and high concentrations of adsorbates in the feedstock (e.g. separation of air into oxygen and nitrogen).

6.5.1 Thermal effects

For the sake of simplicity many fixed bed designs incorporate the isothermal assumption which is normally valid when the adsorbable component concentration is low, or the heat of adsorption is low, or the thermal wave and the mass transfer zone are well separated at the end of the bed. A relatively simple method is available to test whether the last criterion is valid (Ruthven 1984).

The rate at which the heat can be carried out of the mass transfer zone by

the flowing fluid compared with the speed at which the MTZ can travel is critical since it is in the MTZ that the heat is being generated by adsorption. The cross-over ratio R is defined as:

$$\mathrm{R} = \frac{c_\mathrm{f}\,(q_0^* - q_\mathrm{res})}{c_\mathrm{s}\,(c_0 - c^*_\mathrm{res})} \tag{6.18}$$

where c_f is the fluid specific heat
c_s is the solid specific heat
q_0^* is the adsorbate loading in equilibrium with the feed concentration c_0
c^*_res is the fluid concentration in equilibrium with the residual loading on the adsorbent after a regeneration step, q_res.

When $R = 1$ the thermal wave progresses through the bed more or less at the same speed as the mass transfer zone. Hence, virtually all the heat released on adsorption can be expected to be retained in the MTZ and the isothermal assumption should not be made unless either the heat of adsorption is low and/or the concentration of the adsorbable component is low. When R is very much less than unity the thermal wave lags behind the MTZ and hence the heat of adsorption can be retained in the equilibrium portion of the bed (that is, from the entrance up to L_e shown in Figure 5.6 (b)). Retention of the heat of adsorption in this way is beneficial to the subsequent desorption step (Garg and Ausikaitis 1983). When R is very much greater than unity the heat is easily removed from the MTZ and it is safe to invoke the isothermal assumption. Further discussion on the cross-over ratio is given in Section 7.5.3.

Energy balances may need to be retained in the rigorous model if the heat of adsorption is significant and is retained in, or lags behind, the MTZ. Real packed bed adsorption systems are likely to encompass the entire spectrum from near-isothermal to near-adiabatic operation. Since the behaviour of each extreme is quite different it is important to know whether either of the extreme cases can be regarded as a reasonable representation or whether a more general model is required.

6.5.2 Isothermal operation

If it is possible to assume isothermal conditions exist within a packed bed then the energy balance may be omitted from the analysis and only the mass conservation equation is required. Derivation of the bed mass conservation equation is provided in most texts describing the principles of adsorption

(e.g. Coulson *et al.* 1991, Ruthven 1984) and is not repeated again here. If the flow pattern can be represented as axially dispersed plug flow then the differential fluid phase mass balance for a single adsorbate is given by:

$$-D_{\mathrm{L}}\frac{\partial^2 \mathrm{c}}{\partial \mathrm{z}^2} + \frac{\partial\,(\mathrm{uc})}{\partial \mathrm{z}} + \frac{\partial \mathrm{c}}{\partial \mathrm{t}} + \rho_p\left(\frac{1-e}{e}\right)\frac{\partial q}{\partial t} = 0 \tag{6.19}$$

The equation is written in terms of concentration and therefore is suitable for a liquid feedstock. By use of an appropriate equation of state, equation 6.19 is readily adapted for a gas feed. The loading on the adsorbent q is expressed in units of mass/mass. The first term represents axial dispersion within the bed; the axial dispersion coefficient is D_{L}. The second term represents convective flow within the bed; the interstitial velocity is u (and is equal to the superficial velocity divided by the bed voidage). The third term represents the accumulation of adsorbate in the fluid phase while the fourth term represents the rate of adsorption which may be a function of both the fluid phase concentration and the loading on the adsorbent. In general:

$$\frac{\partial q}{\partial t} = f(q, c) \tag{6.20}$$

The dynamic response of the bed is given by the simultaneous solution of equations (6.19) and (6.20), subject to the imposed initial and boundary conditions. If the fluid comprises more than one adsorbate then the conservation equation (6.19) and the rate equation (6.20) must be written for each component. In addition, the continuity equation must be satisfied. For example, for a system which contains two adsorbable components, rather than one adsorbate in a non-adsorbing carrier fluid, equations (6.19) and (6.20), which must be written for both components, are not independent and there is only one MTZ. The continuity equation must be satisfied:

$$(c_1 + c_2) = c \tag{6.21}$$

The situation is quite different for a system which comprises two adsorbates in a non-adsorbing carrier fluid. In this case two distinct mass transfer zones will be formed.

The shape of the MTZ which is generated by a particular design model is determined by a number of factors, the most important of which are the shape of the equilibrium isotherm, the concentration of the adsorbable components, the choice of flow model, and the choice of kinetic model.

The shape of the isotherm has an important role to play in determining whether the MTZ will sharpen, disperse or remain of fixed shape. When the isotherm is linear the MTZ will exhibit dispersive behaviour unless the adsorption is equilibrium controlled. Analytical solutions to the conserva-

tion equation may be obtained for step and impulse inputs of the adsorbate. With isotherms of favourable shape in the region of interest, that is, type I isotherms the MTZ tends to sharpen as it progresses through the bed until the dispersive actions of axial dispersion and intraparticle diffusion cause the MTZ to take on a constant shape, or pattern. Again, analytical solutions for the constant pattern MTZ may be obtained. With isotherms of unfavourable shape in the region of interest, the MTZ broadens as it passes through the bed and analytical solutions are not generally possible.

Changes in bulk fluid velocity across the MTZ are negligible in the case of a system comprising a very dilute adsorbable component in a non-adsorbing carrier fluid. The second term in equation (6.19) can then be simplified by taking the velocity u outside the differential. On the other hand, if the adsorbable components are present at high concentration, such as in the case of air separation, then the fluid velocity across the MTZ will decrease from the trailing to the leading edge and the variation of u with distance must be retained in the model.

The axial dispersion term, the first term in equation (6.19), can be omitted if pure plug flow can be assumed. The conservation equation then reduces to first-order hyperbolic form. If axial dispersion is significant, then the first term in equation (6.19) must be retained, and the flow is known as axially dispersed plug flow. It is generally undesirable to have radially dispersed flow in an adsorption bed, and thus this aspect is generally not incorporated into flow models for adsorption.

Instantaneous equilibrium can be assumed to occur at all points in an adsorption bed only if all resistances to mass transfer, including those outside and inside the adsorbent particles, are negligible. The equilibrium assumption can rarely be invoked, and therefore it is necessary to incorporate a specific rate expression for the fourth term of equation (6.19). The simplest rate expression contains only one mass transfer resistance, while the most complex may contain three.

Possibilities for a single resistance include a linear rate expression with a lumped parameter mass transfer coefficient based either on the external fluid film or on a hypothetical 'solid' film, depending on which film is controlling the rate of uptake of adsorbate. A quadratic driving force expression, again with a lumped parameter mass transfer coefficient, may be used instead. Alternatively, intraparticle diffusion, if the dominant form of mass transfer, may be described by the general diffusion equation (Fick's second law) with its appropriate boundary conditions, as described in Chapter 4.

Example models with two resistances include external fluid film resistance plus intraparticle diffusion or two internal diffusional resistances such as macropore and micropore. A complex three-resistance model might include the external film resistance plus two intraparticle resistances. Such a

complex model should be sufficiently general to provide a good description in most systems.

Isothermal, equilibrium controlled systems

The simplest packed bed design arises with a single dilute adsorbate in a carrier fluid when it can be assumed that the process is isothermal, that there is plug flow, and that there are no mass transfer resistances. In such a situation, instantaneous equilibrium exists at all points in the system. Without the axial dispersion term and taking the velocity outside the partial differential term for the convective flow, equation (6.19) is simplified to:

$$u\frac{\partial c}{\partial z}+\frac{\partial c}{\partial t}+\rho_{\mathrm{p}}\left(\frac{1-e}{e}\right)\frac{\partial q}{\partial t}=0 \tag{6.22}$$

The full derivation of this equation is provided elsewhere (Ruthven 1984, Coulson *et al*. 1991). In general terms the equilibrium isotherm may be described as follows:

$$q^{*}=f(c) \tag{6.23}$$

As shown by Coulson *et al*. (1991) the velocity with which a point of given fluid concentration propagates through the bed is given as follows:

$$\left(\frac{\partial z}{\partial t}\right)_{c}=\frac{u}{1+\rho_{\mathrm{p}}\left(\dfrac{1-e}{e}\right)\dfrac{dq^{*}}{dc}} \tag{6.24}$$

For a given point on the isotherm the speed of that point in the MTZ is seen to be constant and to be dependent on the bulk fluid velocity, the bed voidage and the slope of the isotherm at the concentration in question. With an unfavourable isotherm the gradient dq*/dc increases as the fluid concentration c increases. Hence, using equation (6.24) it can be seen that a point of high concentration in the MTZ will move at a slower rate than a point of low concentration. Thus the MTZ will broaden out as it progresses through the bed. On the other hand, for a favourable isotherm (such as a Type I isotherm described in Section 3.2), a point of high concentration, i.e. one near the trailing edge of the MTZ, will travel faster through the column and catch up with points of lower concentration at the leading edge of the MTZ. In theory it would seem from equation (6.24) that points of high concentration could overtake points of low concentration in the MTZ. In practice however, the effects of axial dispersion (omitted from equation

(6.22)) and a finite mass transfer rate will prevent the formation of the limiting condition which is a compressive shock transition (step change) that travels through the bed with a velocity determined by a mass balance over the MTZ:

$$\frac{\mathrm{d}z}{\mathrm{d}t} = \frac{u}{1 + \rho_{\mathrm{p}} \left(\frac{1-e}{e}\right) \frac{\Delta q^*}{\Delta c}} \tag{6.25}$$

A perfect shock front can only be attained if there are no dispersive effects, i.e. if there is no axial dispersion, and if there are no mass transfer resistances to the adsorption process. Such a situation is most unlikely, since even if the mass transfer resistances were extremely low, the axial dispersion effects would become significant as the step change or shock were approached and the shape of the MTZ would tend to become fixed.

There can be no change of shape in the MTZ if the isotherm is linear (equation (6.26)) because in this case all the terms on the right-hand side of equation (6.24) would be independent of the fluid phase concentration c.

$$q^* = Kc \tag{6.26}$$

The time taken for a point of given fluid concentration to move through the bed can be obtained from equation (6.24). Consider the case of a linear isotherm and an initially clean bed. Assume that breakthrough occurs when the fluid phase concentration is just about to increase beyond zero. By setting $\mathrm{d}q^*/\mathrm{d}c = K$ in equation (6.24), the time to breakthrough for a given bed length can be obtained or, vice versa, a bed length for a given time to breakthrough can be obtained:

$$t = \frac{L}{u}\left[1 + \rho_p \left(\frac{1-e}{e}\right) K\right] \tag{6.27}$$

In the case of a Langmuir isotherm (see Section 3.3.1):

$$q^* = \frac{bq_m c}{1 + bc} \tag{6.28}$$

the slope of the isotherm is as follows:

$$\frac{\mathrm{d}q^*}{\mathrm{d}c} = \frac{bq_{\mathrm{m}}}{(1 + bc)^2} \tag{6.29}$$

Thus, the time for the leading edge of the MTZ to pass through a bed of length L is given by:

$$t = \frac{L}{u}\left[1 + \rho_p\left(\frac{1-e}{e}\right) bq_m\right] \tag{6.30}$$

For most adsorption systems of industrial significance, the isotherm is favourable towards adsorption over the range of concentration of interest. Whilst this might be good for the adsorption step, the isotherm is of course unfavourable for the desorption step. Therefore in desorption the MTZ is usually expected to be dispersive, thereby leading to a continuously spreading concentration profile. Ruthven (1984) provides further information for isotherms which have more complicated shapes, including those which have a point of inflection.

This simple analysis for an isothermal and equilibrium controlled process can be extended to concentrated systems in which u must remain within the differential of the second term in equation (6.19). The analysis can also be extended to systems which include more than a single adsorbable component. Consider the case of a feed stream which contains only two adsorbable components, i.e. a system which does not include a non-adsorbing carrier fluid. In this case both components can be expected to be concentrated in the fluid and hence the variation in fluid velocity over the MTZ must be taken into account. Two differential fluid phase mass balance equations must be written, one for each component. Equation (6.31) is shown for component 1. The axial dispersion term is retained to create a general equation.

$$-D_L\frac{\partial^2 c_1}{\partial z^2} + u\frac{\partial c_1}{\partial z} + c_1\frac{\partial u}{\partial z} + \frac{\partial c_1}{\partial t} + \rho_p\left(\frac{1-e}{e}\right)\frac{\partial q_1}{dt} = 0 \tag{6.31}$$

A similar equation can be written for component 2. In addition the continuity equation (6.21) must be written and so the two conservation equations are not independent. If it can be assumed that the total concentration in the fluid phase c remains constant, which is likely to be true for gaseous systems in which the pressure drop is small, and approximately true for liquid mixtures when the components have similar molar volumes, then the mass conservation equations can be combined. If it is possible to neglect axial dispersion, then the propagation velocity of points of given concentration in the MTZ is given by:

$$\left(\frac{\partial z}{\partial t}\right)_{c_1} = \frac{u}{1 + \rho_p\left(\frac{1-e}{e}\right)\left[(1-y_1)\frac{dq^*_1}{dc_1} + y_1\frac{dq^*_2}{dc_2}\right]} \tag{6.32}$$

where y_1 is the mole fraction of component 1 in the fluid phase. The propagation velocity of points of given concentration in the MTZ therefore depend on the equilibria of both components. Setting $y_1 = 0$ in equation (6.32) yields equation (6.24) for a trace component. If y_1 is finite then even when the carrier fluid is non-adsorbing, i.e. $\mathrm{d}q^*_2/\mathrm{d}c_2 = 0$, the propagation velocity varies with composition according to equation (6.33).

$$\left(\frac{dz}{dt}\right)_{c_1} = \frac{u}{1 + \rho_p\left(\frac{1-e}{e}\right)(1-y_1)\frac{\mathrm{d}q^*_1}{\mathrm{d}c_1}} \tag{6.33}$$

Isothermal, rate controlled systems

In most practical adsorption systems finite resistances to mass transfer of adsorbing molecules must be expected. Even for processes which are commonly assumed to be equilibrium controlled, such as the production of oxygen-enriched air using a zeolite, mass transfer resistances are likely to have an impact on performance, and hence must be included in its design, especially when cycle times are very short (Sircar and Hanley 1995). Some analytical solutions to the general mass conservation equation (6.19) are available but in order to be able to use them a number of simplifying assumptions and approximations must be valid. Typical of these are assumptions of a linear isotherm, a rectangular isotherm (irreversible equilibrium), a non-linear (Langmuir) isotherm with a *pseudo* second-order reaction kinetic rate law, and plug flow.

Consider a dilute system containing a single adsorbable component. The fluid phase mass balance is given by equation (6.19), in which the adsorbate loading over the whole adsorbent pellet is given by

$$q = \left(\frac{3}{R_p^3}\right)\int_0^{R_p} R^2 q \, \mathrm{d}R \tag{6.34}$$

For an adsorbent bed which is initially free from the adsorbate (that is, it has been perfectly regenerated), and for a step change in adsorbate concentration at the bed entrance at time zero, the initial and boundary conditions are given by

$$q\,(R,0,z) = c(0,z) = 0 \text{ for } t < 0 \tag{6.35}$$

$$c\,(t,0) = c_0 \text{ for } t > 0 \tag{6.36}$$

Equations (6.19) and (6.34)–(6.36) must be solved simultaneously with an appropriate rate expression which must be consistent with the equilibrium isotherm which describes the adsorption. Table 6.1 summarizes the sources

Table 6.1 *Summary of available analytical solutions for breakthrough curves in linear rate, isothermal, trace component systems*

Rate expression	*Plug flow model*	*Dispersed plug flow model*
Linearized rate	Anzelius (1926) Walter (1945) Furnas (1930) Nusselt (1930) Klinkenberg (1954)	Lapidus and Amundson (1952) Levenspiel and Bischoff (1963)
Intraparticle diffusion control (no external mass transfer resistance)	Rosen (1952, 1954) Cartón *et al.* (1987)	Rasmuson and Neretnieks (1980)
Intraparticle diffusion with external mass transfer resistance	Rosen (1952, 1954) Masamune and Smith (1965)	Rasmuson and Neretnieks (1980
Macropore–micropore diffusion with external film resistance	Kawazoe and Takeuchi (1974) Cen and Yang (1986)	Rasmuson (1982)

of solutions to the breakthrough curve for various combinations of flow model and linear rate expression. The analytical solutions to many of these models are cumbersome and of limited practical value. With the advent and widespread availability of high speed digital computers it is probably more appropriate to adopt numerical approaches to design. Some analytical solutions have also been obtained for special cases in which the isotherm may be described as being rectangular or irreversible. The sources of solutions for such isotherms when it is safe to make the assumption of plug flow are provided in Table 6.2.

Thomas (1944) has provided a general analytical solution for a non-linear Langmuir system with a *pseudo* second-order reaction kinetic law. The results, which are given in graphical form by Hiester and Vermeulen (1952), provide a means of assessing the importance of a mass transfer resistance in any system for which the rate constant and equilibrium parameters are

Table 6.2 *Summary of available analytical solutions for breakthrough curves in isothermal, trace component systems with plug flow and a rectangular isotherm*

Rate expression	*Plug flow model*
Quasi-chemical	Bohart and Adams (1920)
Linear rate-solid film	Cooper (1965)
Linear rate-fluid film	Cooper (1965)
Solid diffusion	Cooper (1965)
Pore diffusion	Cooper and Liberman (1970)
Film + pore diffusion	Weber and Chakravorti (1974)
Fluid film + solid diffusion	Yoshida *et al.* (1984)

known. The rate expression is somewhat unrealistic in this model, but the differences between breakthrough curves calculated from the model and from a more realistic diffusion equation are relatively small.

Beyond these relatively simple systems and for all other non-linear isotherms, it is necessary to obtain solutions for the breakthrough curves by applying numerical approximation techniques to the model equations. Standard finite difference or collocation methods are commonly used. Table 6.3 provides a brief source list to solutions for plug flow and axially dispersed models with Langmuir, Freundlich or more general isotherms.

6.5.3 Non-isothermal and multicomponent systems

So far it has been assumed that operation has been isothermal and that, for the most part, the system has comprised a single adsorbate present at low concentration in an inert carrier gas or solvent. In such systems there will be only a single transition or mass transfer zone. For many systems of practical significance however, the situation will in reality be much more complex because the adsorption column is more likely to be operated adiabatically and there will often be more than one adsorbable component in the feedstock. The concentration profile will show more than one mass transfer zone in such cases.

A simplification arises if the concentrations of all adsorbable species in a non-adsorbing carrier gas or solvent are very low. In this case the equilibria remain within the Henry's law region, i.e. equation (6.26) applies, and thereby each component's equilibrium can safely be considered to be unaffected by the presence of the other components. Extension of the analyses provided above for single components then becomes relatively

Table 6.3 *Summary of available numerical solutions for breakthrough curves in isothermal systems with plug flow or axially dispersed flow and Freundlich, Langmuir or other non-linear isotherms*

Rate Expression	*Equilibrium model*	*Flow model*	*Source*
Fluid film	General	Plug	Chi and Wasan (1970)
Combined resistances	General	Plug	Acrivos (1956)
Fluid film		Plug	Zwiebel *et al.* (1972)
Solid film	Langmuir	Plug	Garg and Ruthven (1973)
External + solid films	Freundlich	Plug	Tien and Thodos (1959)
Solid diffusion	Langmuir	Plug	Antonson and Dranoff (1969)
Solid diffusion	Langmuir	Plug	Garg and Ruthven (1973, 1974a)
Solid diffusion	Freundlich	Plug	Kyte (1973)
Pore diffusion	Langmuir	Plug	Carter and Husain (1972)
Pore diffusion external + micropore	Langmuir 4th order polynomial	Plug axially dispersed	Garg and Ruthven (1974b) Lee and Weber (1969)
External + micropore	Freundlich (multicomponent)	Plug	Moon and Lee (1986)
External + micropore	Empirical (binary)	Axially dispersed	Liapis and Rippin (1978)
Micropore	Empirical (multicomponent)	Axially dispersed	Balzli *et al.* (1978)

trivial. In such cases it would be possible to assume isothermal operation since the concentrations of all the adsorbing components would be low. In contrast, systems comprising high adsorbate concentrations would inevitably result in each individual isotherm being affected by the presence of the other components, as well as by the temperature. Indeed, if the concentrations and heats of adsorption are significant, then the temperature rises inside a packed bed may become large and it is then necessary to couple

the differential heat and mass balance equations for the individual components. The analysis becomes even more complex when the rate of adsorption of any individual species is affected by the presence of the others. This could arise, for example, when individual diffusion coefficients are found to be functions of composition. Clearly the complexity and hence the degree of difficulty in obtaining solutions for the MTZ and breakthrough curve increase rapidly as the number of components increases. Very few analytical solutions are available and therefore considerable research effort has been directed at the simultaneous numerical solution of the set of coupled heat and mass balance equations, the set of rate expressions, and the set of equilibrium expressions, all being subject to a set of initial and boundary conditions.

Consider the case when the flow pattern can be assumed to be axially dispersed plug flow. By not making the assumption that the system is dilute, the differential fluid phase material balance for each component is given by:

$$-D_{\mathrm{L}}\frac{\partial^2 c_{\mathrm{i}}}{\partial z^2} + \frac{\partial(uc_{\mathrm{i}})}{\partial z} + \frac{\partial c_{\mathrm{i}}}{\partial t} + \rho_{\mathrm{p}}\left(\frac{1-e}{e}\right)\frac{\partial \bar{q}_{\mathrm{i}}}{\partial t} = 0 \tag{6.37}$$

The particle phase mass balance which provides the adsorption rate equation for each component may be written in generalized form as follows:

$$\frac{\partial q_i}{\partial t} = f(q_i, q_j \ldots .. c_i, c_j \ldots) \tag{6.38}$$

Rather than being a simple algebraic expression, the function f is more likely to represent a set of diffusion equations with their associated boundary conditions. The continuity equation must also be satisfied, and so in the general case the mass balance equations may not all be independent. When the process cannot be considered to be isothermal, then energy balances for both the element of packed bed (equation (6.39)) and the adsorbent particle (equation (6.40)) are also required:

$$-\mathrm{k_L}\frac{\partial^2 T_{\mathrm{f}}}{\partial z^2} + c_{\mathrm{f}}\frac{\partial(uT_{\mathrm{f}})}{\partial z} + \left(\frac{1-e}{e}\right)c_{\mathrm{s}}\frac{\partial T_{\mathrm{s}}}{\partial t} + c_{\mathrm{f}}\frac{\partial T_{\mathrm{f}}}{\partial t} \tag{6.39}$$

$$= \left(\frac{1-e}{e}\right)\sum_i(-\Delta H_i)\frac{\partial \bar{q}_i}{\partial t} - \frac{4h_i}{ed}(T_f - T_w)$$

$$c_{\mathrm{s}}\frac{\partial T_{\mathrm{s}}}{\partial t} - \frac{3h}{R_{\mathrm{p}}}(T_{\mathrm{f}} - T_{\mathrm{s}}) = \sum_i(-\Delta H_i)\frac{\partial \bar{q}_i}{\partial t} \tag{6.40}$$

The response to a change in inlet conditions will generate a set of (n–1) mass transfer zones which propagate through the column when there are n

components, including inerts, and the process is isothermal. A non-isothermal system will include an additional mass transfer zone which propagates with the velocity of the temperature front because the adsorption equilibria are temperature dependent. A non-isothermal system of n components therefore could be considered to be equivalent to an isothermal system with $(n+1)$ components.

As the number of components increases the solutions to the set of design equations, with their appropriate boundary conditions, become increasingly difficult and therefore it is usually necessary to make approximations. The mathematical models which are thereby obtained differ in their generality and in their applicability according to the extent and severity of the approximations which have been made. As an example of the number and type of assumptions and approximations which might need to be invoked for a non-isothermal process, let us consider the relatively simple model of Cooney (1974). In this case it is assumed that

(1) there is only one adsorbable component, and therefore there is only one material balance equation;
(2) axial dispersion is negligible and hence the first term of equation (6.19) is omitted;
(3) the adsorbate is dilute and hence u can be taken outside the differential of the second term in equation (6.19); in association with this simplification it is also assumed that the effect of temperature on u is ignored;
(4) the equilibrium is described by the Langmuir isotherm for which the van't Hoff equation is applicable;
(5) the local rate of adsorption is described by a linear driving force expression in which the mass transfer coefficient is assumed to be independent of temperature;
(6) axial conduction of heat is negligible and thus k_L in equation (6.39) is set equal to zero;
(7) the bed is initially free of the adsorbate and is at a uniform temperature T_0 throughout; and
(8) there is a step change at time zero to a feed of fixed concentration at the inlet, and the feed is at T_0.

The fluid phase mass balance, fluid phase heat balance, adsorption rate, heat transfer rate, isotherm and van't Hoff equations which describe the process are as follows:

$$\frac{\partial c}{\partial t} + u\frac{\partial c}{\partial z} + \rho_p\left(\frac{1-e}{e}\right)\frac{\partial \bar{q}}{\partial t} = 0 \tag{6.41}$$

$$\frac{\partial T_f}{\partial t} + u\frac{\partial T_f}{\partial z} + \frac{c_s}{c_f}\left(\frac{1-e}{e}\right)\frac{\partial T_s}{\partial t} + \frac{\Delta H}{c_f}\frac{\partial \bar{q}}{\partial t}\left(\frac{1-e}{e}\right) = 0 \tag{6.42}$$

$$\frac{\partial \bar{q}}{\partial t} = k(q^* - \bar{q}) \tag{6.43}$$

$$\frac{\partial T_s}{\partial t} = ha\,(T_f - T_s) - \frac{\Delta H}{c_s}\frac{\partial \bar{q}}{\partial t} \tag{6.44}$$

$$q^* = \frac{bcq_m}{(1+bc)} \tag{6.45}$$

$$b = b_0 \exp\left(\frac{-\Delta H}{R_g T}\right) \tag{6.46}$$

Because of the number of assumptions made, this model is perhaps one of the simplest non-isothermal examples which has been solved by finite difference numerical approximations. There are many examples in the research literature of models which contain fewer simplifications. One example is described by Sowerby and Crittenden (1991). In this example a significant proportion of the feed is adsorbed, i.e. u is not constant, the equilibrium is more complex, the rate equation contains two film resistances, the film coefficients are temperature dependent and heat loss from the column is allowed for. Further guidance on the subject of multicomponent, non-isothermal adsorption can be obtained by reference to Ruthven (1984), Yang (1987) and Tien (1994).

6.5.4 Cyclic fixed bed process design

The *a priori* design of cyclic PSA and TSA processes is not absolutely reliable because fundamental mathematical models of all the component steps are not yet sufficiently developed and tested. Much of the necessary input data is probably still of questionable accuracy. Mathematical models are therefore of most use in predicting the location of optimum operating conditions but are less accurate in predicting exact product compositions. Consequently the modelling of both PSA and TSA is a fertile ground for fundamental research, as manifested by the growth in the number of publications on the subject (Sircar 1991). Sophisticated numerical analysis techniques which require substantial computing resources are often used to solve the model equations. Most are tested only on small-scale laboratory apparatus and hence few models could be applied to industrial-scale plant

with any degree of confidence without resorting to further testing on pilot or full-scale plant.

Cyclic PSA and TSA processes are both time-dependent dynamic processes, and thus for design purposes the *pseudo*-steady-state is required in which all the product concentrations and bed profiles of pressure, temperature, velocity and composition are reproduced exactly from cycle to cycle. Any rigorous design model should be capable of being used from the initial start-up conditions until the individual steps and their boundary conditions converge and the cyclic *pseudo*-steady-state is obtained. The problem is more difficult for PSA processes than for TSA processes, and becomes more complex as the cycle time is reduced.

General models comprise a system of non-linear partial differential equations which are highly coupled and very stiff. There is an equally complex set of initial and boundary conditions and a large number of physical constants and other parameters, some of which may only be known approximately. In order to be able to predict the composition, pressure, flowrate and temperature of the fluid emerging from the ends of the bed during each step in a cyclic process it is necessary to predict the composition, pressure, flowrate and temperature profiles within the beds. There are six groups of equations which need to be considered in order to complete a rigorous design:

(1) For each component, a mass balance equation can be written using an infinitesimal element of the bed as a control volume; this is equation (6.37). The terms in this equation account for convection and axial dispersion (if applicable) into and out of the control volume, together with the rate of adsorption and the accumulation in the fluid phase.
(2) The fluid phase heat balance equation on the small element of the bed includes the sensible heat changes due to gas convection, thermal conduction, heat transfer within the solid, heat transfer within the column wall and accumulation within the element; this is equation (6.39).
(3) The heat balance on the particles includes the heat released on adsorption (or taken up in desorption, depending on the step in the cycle), conduction to the surface of the adsorbent, and heat transfer to the adjacent particles as well as to the bulk fluid phase; this is equation (6.40).
(4) Empirical relationships are generally used to relate the rate of change of pressure with position and time to the local gas velocity in PSA processes, or to determine the pressure drops in TSA processes. The Ergun equation or Darcy's law are often used to

calculate pressure drops in which case the variation of fluid physical properties with composition and temperature should be included when using these equations which represent an approximate momentum balance. For rapid PSA processes attention needs to be paid to the fact that the pressurization step is unlikely to be completely divorced from adsorption. Equally, desorption is likely to occur simultaneously with depressurization. The interest in improving the efficiency of PSA processes by reducing the cycle time has led to strong research activity in the dynamics of the pressure changing steps (Crittenden *et al*. 1994 and 1995).

(5) Mass transfer through the external fluid film, and macropore, micropore and surface diffusion may all need to be accounted for within the particles in order to represent the mechanisms by which components arrive at and leave adsorption sites. In many cases identification of the rate controlling mechanism(s) allows for simplification of the model. To complicate matters, however, the external film coefficient and the intraparticle diffusivities may each depend on composition, temperature and pressure. In addition the external film coefficient is dependent on the local fluid velocity which may change with position and time in the adsorption bed.

(6) The adsorption isotherms relate the local fluid phase composition within the particles to the amount adsorbed on the surface. The amount of any one species that is adsorbed depends on the local temperature and on the partial pressure or concentration of that component, and because of co-adsorption effects, on the partial pressures or concentrations of all the other components.

No general analytical solution exists and the computational effort precludes numerical solution of the full set of equations. Simplifying assumptions therefore are usually made. The principal differences between models lie in the ways in which the mass and heat transfer processes are handled.

If the process can be assumed to be isothermal then there are several significant gains to be made in reducing the complexity of the design equations. This is perhaps the most important simplification. First, the heat balance equations (6.39) and (6.40) can be omitted. Second, the dependencies of physical properties, fluid velocities, adsorption equilibria and other parameters on temperature are no longer required and can be omitted. Guidance on when it is likely to be safe to assume isothermal operation has been provided earlier in this chapter.

The second most important simplification is the assumption of instantaneous local equilibrium, i.e. there are no mass transfer resistances and the adsorbates are uniformly distributed throughout the particles. The benefits

of being able to invoke this assumption together with the isothermal assumption are evident from earlier considerations in this chapter. Strictly, the equilibrium assumption cannot be invoked for any adsorption process since mass transfer resistances will inevitably be present in the system. However, the assumption is often invoked for PSA air separation to produce oxygen by adsorption on zeolites. This is because the separation in this case is determined by the preferential equilibrium in favour of one of the components (nitrogen). In contrast, the assumption must not be invoked for the production of nitrogen using carbon molecular sieve since the separation in this case depends on the differences in rates of diffusion of nitrogen and oxygen. Nor should the assumption be invoked for rapid pressure swing adsorption processes (Sircar and Hanley 1995). The assumption of equilibrium control has limited applicability for gas phase separations and it is doubtful whether it can be used safely for the design of any liquid phase separation.

Axial dispersion was often ignored in early modelling of PSA separations not only because the material balance equations, e.g. equation (6.37), could be simplified substantially, but also because the diffusional fluxes were generally, but not always, small compared with the convective fluxes. This, however, may not be the case for vapour phase TSA separations and for liquid phase separations.

Despite the wide choice of mass transfer models which are available, the simplest and most popular adsorption rate expression is the linear driving force model because it represents actual processes reasonably well and reduces the computational effort required. An example of how this and various other simplifications and empirical correlations can be incorporated into the design and analysis of pressure swing adsorption processes is provided by White and Barkley (1989). The example used is the drying of air. Examples of how simplifying assumptions can aid the modelling of PSA air separation processes is provided by Knaebel and Hill (1985) and by Kayser and Knaebel (1989). Further information on cycle models can be found in Ruthven (1984), Yang (1987), Ruthven (1990) and Ruthven *et al.* (1994).

6.6 CONSTANT PATTERN BEHAVIOUR

It is fortunate that for many fixed bed adsorption processes of commercial interest the shape of the mass transfer zone remains unaltered as it progresses through the majority of the bed because this leads to substantial simplifications in design. For a favourable isotherm, particularly one of Type I, the mass transfer wave spreads from a shock front as it progresses through the initial region of the bed. As explained earlier in this chapter the

shape of the isotherm causes the MTZ to take on an asymptotic or constant pattern form at some distance from the bed inlet. The MTZ then becomes stable and does not change its shape. Cooney and Lightfoot (1965) provide a mathematical proof of the constant pattern MTZ and Coulson *et al.* (1991) provide a simplified analysis. For many practical systems the distance required to develop a constant pattern MTZ is small, but it does depend on the degree of non-linearity of the isotherm and on the kinetics. The constant pattern condition may be described as follows:

$$\frac{c}{c_0} = \frac{\bar{q}}{q_0} \tag{6.47}$$

For a single component under constant pattern conditions an expression for the asymptotic form of breakthrough curve can be obtained by integrating the appropriate rate expression, subject to the constant pattern condition. Consider the case of plug flow and constant velocity, a linear rate of adsorption based on solid phase conditions (equation (6.48)), a Langmuir isotherm, a simple substitution (equation (6.49)) and the constant pattern condition (equation (6.47)):

$$\frac{\partial \bar{q}}{\partial t} = k(q^* - q) \tag{6.48}$$

$$\beta = 1 - \frac{q_0}{q_s} \tag{6.49}$$

The solution is given by equations (6.50) to (6.52):

$$k(t_2 - t_1) = \frac{1}{1-\beta} \ln \left[\frac{\Phi_2(1-\Phi_1)}{\Phi_1(1-\Phi_2)}\right] + \ln \left(\frac{\Phi_1}{\Phi_2}\right) \tag{6.50}$$

$$\Phi_1 = \frac{c_1}{c_0} \tag{6.51}$$

$$\Phi_2 = \frac{c_2}{c_0} \tag{6.52}$$

Table 6.4 provides a summary of solutions for single-component constant pattern behaviour with a Langmuir isotherm and plug flow. Several kinetic models are listed but it is important to note that for highly non-linear systems the use of an incorrect kinetic model can lead to large errors in the prediction of dynamic capacity.

Table 6.4 Summary of constant pattern solutions for the breakthrough curve with a Langmuir isotherm

Kinetic model	*Form of solution*	*Source*
Linear, fluid film	Algebraic	Michaels (1952)
Linear, solid film	Algebraic	Hall *et al.* (1966)
Solid diffusion, with constant D	Numerical tabulation	Hall *et al.* (1966)
Solid diffusion, variable D	Graphical solution	Garg and Ruthven (1973)
Pore diffusion	Numerical tabulation	Hall *et al.* (1966)
Pore diffusion	Graphical solution	Garg and Ruthven (1973)

If axial dispersion is considered to be important reference should be made to Acrivos (1960) and Garg and Ruthven (1975). Acrivos (1960) also provides an analytical expression for constant pattern behaviour with a rectangular (irreversible) isotherm. Garg *et al.* (1975) and Ruthven (1984) provide information and solutions for the constant pattern situation under non-isothermal conditions.

6.7 SHORT-CUT AND SCOPING METHODS

Empirical or short-cut methods are still used extensively for the design of fixed beds. This is not only due to their simplicity and reliability but also because of the formidable nature of the more rigorous alternatives. With thermal swing processes, for which cycle times are generally long, it can be argued that a reasonably accurate design can be made using short-cut methods since much of the bed behind the MTZ will contain adsorbent which is in equilibrium with the feedstock. Even so, special care should still be exercised when determining the applicability of short-cut methods for a particular design problem. Methods include the length or weight of unused bed (LUB or WUB), the mass transfer zone length (MTZL), the empty bed contact time (EBCT), the bed depth service time (BDST), the transfer unit approach (NTU and HTU) and the capacity at breakpoint.

6.7.1 Length of unused bed (LUB)

The LUB design method requires that constant pattern behaviour occurs. It provides the basis for a very simple design method which allows the design and scale-up from small-scale laboratory experiments particularly for dilute single-component systems in which there is a favourable isotherm. A dilute system implies that the process will be isothermal. Care must be taken if the process is not isothermal because it is possible for the temperature effects to cause a favourable isotherm to take on effectively an unfavourable shape.

Reference is made to Figures 5.6 (a) and 5.6 (b) in the following analysis of the LUB concept. The length of the MTZ increases as the mass transfer resistance increases in adsorption. However, for situations in which mass transfer rates are very high, the process approaches equilibrium control and the mass transfer front esb tends to become a straight line, or shock, dsc, and is known as the stoichiometric front. The used adsorbent capacity is represented by the area fesbaf (Figure 5.6(b)) while the unused adsorbent capacity is represented by the area ehbse. The area fesbaf is equal to the area fdcaf since the latter area up to the stoichiometric front also represents used capacity.

Up to the stoichiometric point, s, the length (or weight) of equivalent equilibrium section, LES (or WES) is represented by the area fesbaf. The rest of the bed from the stoichiometric point, s, to the breakthrough point, b, is equivalent to the length (or weight) of unused bed, LUB (or WUB), because it is equivalent to a bed at the residual loading in the stoichiometric interpretation. Thus the design of an adsorption bed can be obtained by adding LES and LUB together. LUB is defined as follows:

$$LUB = \left(1 - \frac{t_b}{t_s}\right) L \tag{6.53}$$

A single dynamic adsorption experiment which generates the entire breakthrough curve shown in Figure 5.6(a) is sufficient to enable the breakthrough time, t_b, and the stoichiometric time, t_s to be determined. The LUB depends only on the adsorbate–adsorbent combination, the temperature and the fluid velocity. With constant pattern behaviour it is independent of column length. The LUB can therefore be measured at the design velocity in a small-scale laboratory column packed with the selected adsorbent. The design of the full-scale adsorption column can be obtained by simply adding the LUB to the length of bed needed to achieve the required stoichiometric capacity (LES).

The LUB (WUB) method should not be used for adsorbate–adsorbent

combinations in which the isotherm is unfavourable and special consideration may need to be given if the isotherm is linear. For the case of a favourable isotherm, the validity of the method is very much dependent on the conditions used in the small-scale laboratory column being similar to those in the full-scale unit. Factors which must be taken into account include the diameter of columns and axial dispersion. Large diameter columns tend to operate adiabatically and thus it is important that the laboratory column is well insulated. If the heat loss from a small-scale laboratory column is significant, then the apparent LUB will be erroneously low and will lead to underdesign of the full-scale column. Differences in the extent of axial dispersion in small-scale laboratory and full-size columns may also cause discrepancies. The small-scale laboratory column should therefore be designed to simulate as closely as possible the axial dispersion conditions of the larger unit (see Sections 6.8.4 and 6.9).

6.7.2 Mass transfer zone length (MTZL)

The length of the bed, $L - L_e$, shown in Figure 5.6 (b) is known as the mass transfer zone length or MTZL. The adsorption literature contains some data for the correlation of MTZL with flowrate or velocity. However, care should be exercised when using this data because the experimental conditions may be far removed from those for the intended design. It is far preferable to obtain the MTZL from small-scale laboratory experiments on the adsorbate–adsorbent system under consideration and with temperatures and velocities which are representative of those to be used in the full-size unit. A practical disadvantage of the MTZL method is that if a bed length is obtained by adding together the equilibrium zone length and the MTZ length, then more adsorbent will be installed than is necessary because some adsorption actually occurs in the mass transfer zone.

6.7.3 Empty bed contact time (EBCT)

The empty bed contact time (EBCT) method is primarily used by the water industry for the design of large-scale adsorbers from pilot-scale data. There is no reason why the method should not be applied, however, to other industrial situations, in particular to liquid phase separations.

As shown in Figure 6.7 a number of pilot-scale columns in series are used to obtain breakthrough curves with flow at the desired velocity. Three or more columns are usually used to represent different bed depths and different contact times. The column diameters may range from 2.5 to 15 cm in water treatment applications. As shown in Figure 6.8 a horizontal line that

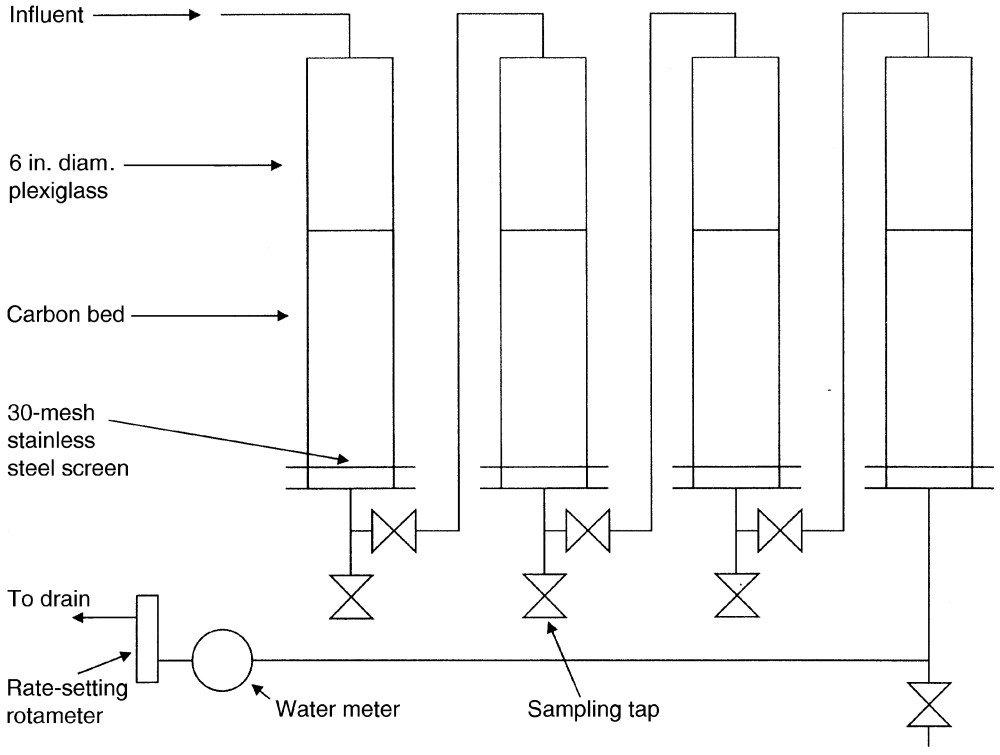

Figure 6.7 *Downflow pilot plant columns used in water treatment applications (adapted from Faust and Aly 1987).*

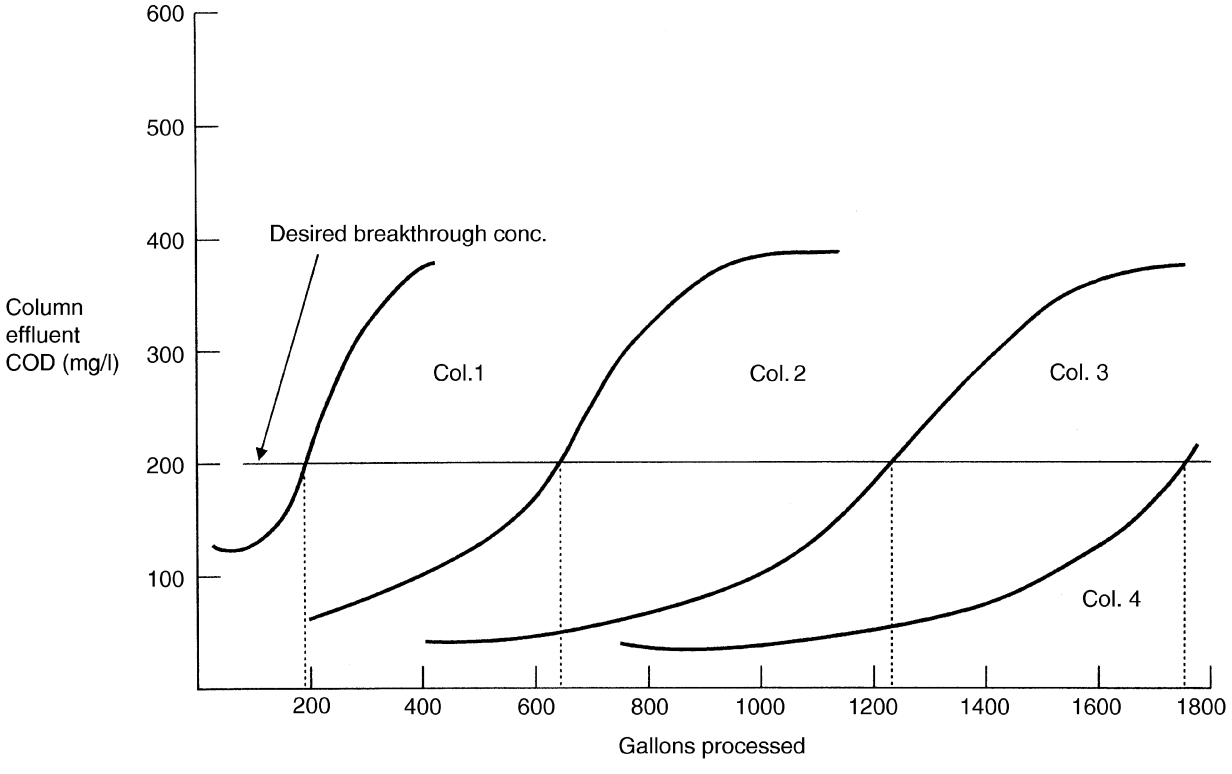

Figure 6.8 *Breakthrough curves from pilot plant columns in series used in water treatment applications (adapted from Faust and Aly 1987).*

intersects the breakthrough curves at the desired breakthrough concentration is then drawn to determine the breakthrough volume for each column. The empty bed contact time (EBCT) is defined as follows:

$$EBCT = \frac{bed\ volume}{flowrate} \tag{6.54}$$

The usage rate of adsorbent (usually activated carbon in the water industry) is then plotted in Figure 6.9 against *EBCT* to show that after an initial rapid decrease in usage rate with increasing *EBCT*, the curve flattens and no significant reduction in usage rate is gained with increasing contact time. The process design therefore requires an economic optimization of the benefits of increasing *EBCT* with the slight gain from reduced adsorbent usage. The size of the full-scale adsorbent bed can be determined once an *EBCT* has been selected for the design flowrate. Faust and Aly (1987) provide further information on the EBCT method.

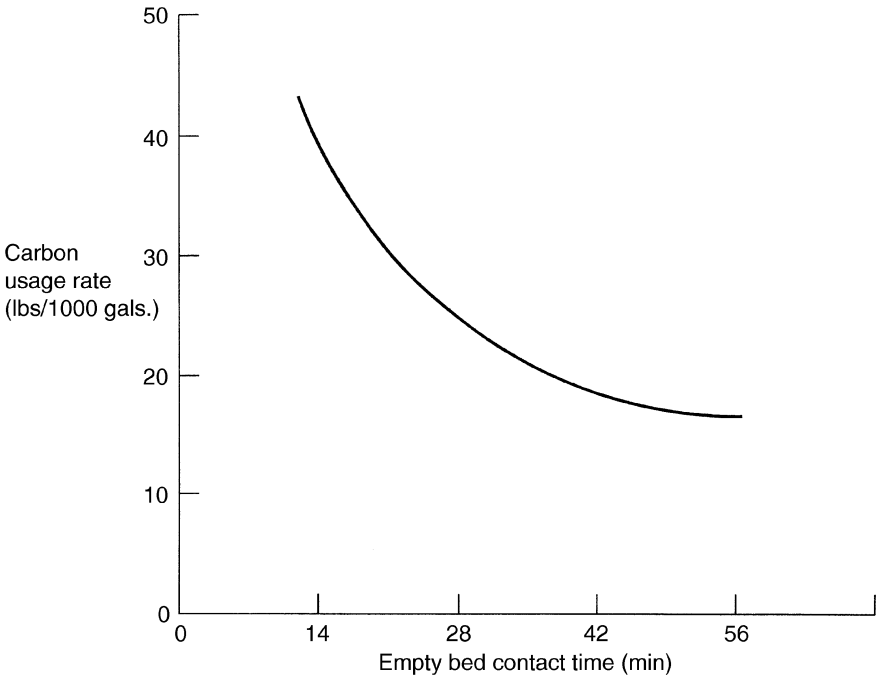

Figure 6.9 *Adsorbent usage rate versus residence time (adapted from Faust and Aly 1987).*

6.7.4 Bed depth service time (BDST)

As for the empty bed contact time method, the BDST method is also used extensively by the water industry and can be applied to other industrial situations. The assumption is that the adsorption rate is proportional to both the residual adsorbent capacity and the remaining adsorbate concentration. The relationship between the service time, t, the linear velocity, u, the depth of adsorbent bed, L, the rate constant, k, the adsorptive capacity, N_0 (mass per unit volume), the influent concentration, c_0, and the concentration at breakthrough, c_b is given by the following equation in which dimensionally consistent units must be used:

$$t = \frac{N_0}{c_0 u}\left[L - \frac{u}{kN_0}\ln\left(\frac{c_0}{c_b} - 1\right)\right] \tag{6.55}$$

The critical bed depth is the theoretical depth of adsorbent that is just sufficient to prevent the effluent concentration from exceeding c_b at zero time and clearly is equal to the mass transfer zone length MTZL described above. The critical bed depth may be calculated by substituting $t = 0$ into equation (6.55):

$$MTZL = \frac{u}{kN_0}\ln\left(\frac{c_0}{c_b} - 1\right) \tag{6.56}$$

As shown in Figure 6.10, the adsorptive capacity of the system, N_0, and the rate constant, k, can be obtained from the slope and intercept, respectively, of a plot of t against L, which, according to equation (6.55), should be a straight line. The raw data for the BDST plot are obtained from a small-scale or pilot-scale experiment using at least three columns in series, in the manner shown in Figure 6.7. The total bed depth and flow velocity should approximate to those values which are anticipated for the full-scale unit. From the breakthrough curves, the breakthrough points, t_b, expressed as service time, are plotted against bed depth in the form of Figure 6.10. Service times at different bed depths can be obtained either from the graph or from equation (6.55). The selection of an acceptable service time with its corresponding bed depth may be based on judgement, on experience or following a full economic evaluation which yields the lowest annual cost taking both capital investment and operating costs into account.

Faust and Aly (1987) describe how the BDST model can be used to calculate design information for flowrates other than that used to derive the original BDST plot. The slope, a, of the original plot is defined as follows:

$$\text{slope} = a = \frac{N_0}{c_0 u} \tag{6.57}$$

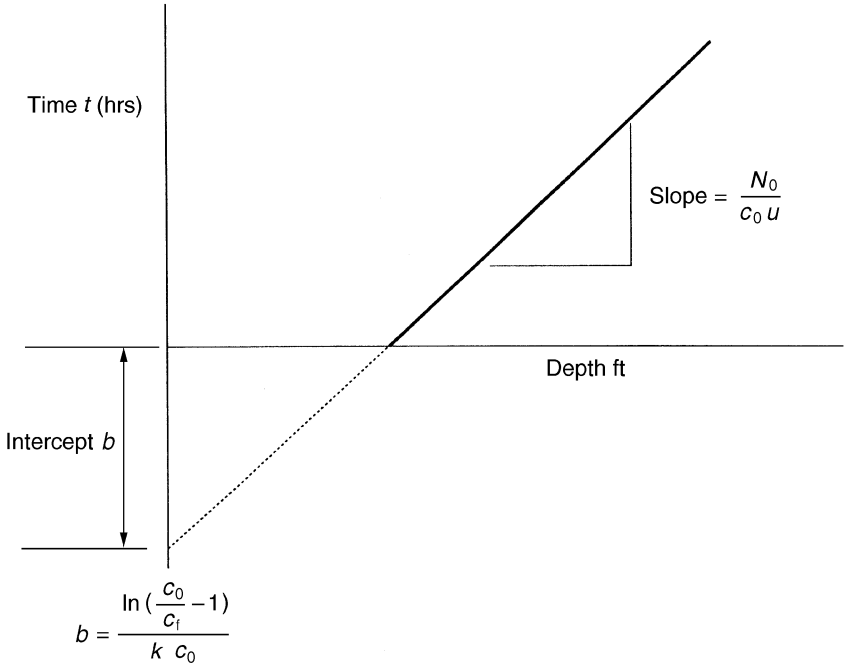

Figure 6.10 *Bed depth service time graph (adapted from Faust and Aly 1987).*

The slope can be modified from the original value a to the new value a' to take account of a change in velocity from u to u' as follows:

$$\text{new slope} = a' = \frac{au}{u'} \tag{6.58}$$

Equation (6.58) is valid for the new flow velocity because velocity has little or no effect on the intercept of the BDST plot which is given by b, as follows:

$$\text{intercept } b = \frac{1}{c_0 \mathrm{k}} \ln\left(\frac{c_0}{c_\mathrm{b}} - 1\right) \tag{6.59}$$

The assumption is made here that the kinetics of adsorption are not influenced to any appreciable extent by conditions external to the adsorbent, that is the rate of adsorption is controlled solely by processes which occur inside the adsorbent particles. If this assumption is valid then data from small-scale experiments can be reliably scaled up to other flow rates without running pilot tests in larger columns.

Faust and Aly (1987) also describe how the BDST model can be modified to account for changes in feed concentration from c_0 to c_1 such that the original and new effluent concentrations are c_b and c_f, respectively:

$$\text{new slope } a' = a\frac{c_0}{c_1} \tag{6.60}$$

$$\text{new intercept } b' = b\left(\frac{c_0}{c_1}\right) \cdot \frac{\ln\left[\dfrac{c_1}{c_f} - 1\right]}{\ln\left[\dfrac{c_0}{c_b} - 1\right]} \tag{6.61}$$

Of course it may be desirable that c_b and c_f should be equal. This method for estimating the effect of changing feed concentration appears to work well when single-component impurities are removed from water on carbon. However, further validation is required before the method can be applied to multicomponent and non-dilute systems.

The BDST equation describes how the mass transfer zone progresses through a single fixed bed of adsorbent. The equation can be adapted to include series of fixed beds and moving bed systems in which either a bed is removed or fresh adsorbent is added, respectively, when breakthrough from one bed occurs. These methods of operation are popular in the water industry. Clearly, the most reliable method of determining the speed of the MTZ is to conduct an experimental test. However, a good estimate of the speed by which the MTZ moves through an adsorbent bed can be made by applying the BDST equation with an assumed average concentration of adsorbable species in the feed and the appropriate factors shown in Table 6.5 (Faust and Aly 1987). The factors in this table were developed by assuming that the moving bed is pulsed, or a column is removed, just as the wave front begins to exit from the system. This is the point at which the adsorbent is exhausted, i.e. the adsorbent phase is in equilibrium with the feed concentration.

The factors in Table 6.5 are the fractions of the original impurity concentration that is assumed to be the average fed to freshly added adsorbent. If it can be assumed that the intercept of the BDST equation is not significant in a series or moving bed system, then the slope of a BDST equation describing the movement of a wave front through fresh or regenerated adsorbent can be estimated from equation (6.62) in which f is the factor from Table 6.5.

$$a' = \frac{a}{f} \tag{6.62}$$

Table 6.5 *Factors for modifying the BDST equation**

Factor	*Required removal of adsorbable impurities (%)*					
	50	*60*	*70*	*80*	*90*	*95*
Moving bed factors, pulsing 5% of bed	0.51	0.41	0.31	0.21	0.107	0.054
Series of factors for number of columns						
2	0.70	0.63	0.54	0.44	0.31	0.22
3	0.59	0.50	0.40	0.30	0.18	0.11
4	0.56	0.46	0.37	0.26	0.144	0.080
5	0.55	0.44	0.35	0.24	0.133	0.072

* From Faust and Aly (1987)

The BDST equation has no value if the column feed is not representative of the normal plant system. Thus, as with any other form of small-scale experimentation, it is important that actual feedstocks are used in the tests. For the most accurate results, the MTZ should move through the column at a constant rate and so a constant pattern MTZ, a constant feed concentration and a constant feed flowrate are all required.

6.7.5 Transfer unit approach (NTU and HTU)

The transfer unit concept described in Section 6.3 for differential continuous contacting can be extended to the design of fixed beds which operate with a constant pattern mass transfer zone. A fixed bed of adsorbent must be sufficiently long not only to contain the MTZ but also to allow it a convenient residence time. In the transfer unit method the MTZ is brought to rest hypothetically by giving the adsorbent a velocity equal and opposite to that of the MTZ. It is necessary to use the methods described earlier in this chapter to calculate both the NTU and the HTU in order to estimate the length of the MTZ. For the NTU, the concentrations c_E and c_B refer to those at the end and at the beginning of the MTZ. The overall mass transfer coefficient must be calculated by taking all relevant film coefficients into account in order that the HTU may be calculated. The length of the MTZ is then the product of NTU and HTU. Treybal (1955) describes in more detail how the transfer unit method can be used to plot the shape of the MTZ.

6.7.6 Capacity at breakpoint

The capacity at the breakthrough point is defined as the mass per cent, or

fraction, of adsorbate retained by an initially adsorbate–free bed up to the breakthrough point. It has been found that the parameter does not vary appreciably with operating conditions other than temperature and thus can be used for design.

In the adsorptive drying of gases, several researchers (Miller and Roberts 1958, Bowen and Donald 1963, 1964) have found that the capacity at breakthrough depends linearly on the relative concentration at the inlet, this parameter being defined as the ratio of adsorbate (water) concentration in the feed to the concentration of adsorbate (water) that would saturate the feed at the mean temperature of the bed during operation. The capacity at breakpoint is a useful concept when the overall energy requirements of a cyclic operation are being assessed. Bowen (1971) provides details for estimating the times for adsorption, bed heating and bed cooling of a two-bed system.

6.8 HYDRODYNAMICS

Four major considerations must be made when selecting the size of adsorbent particles, namely the availability of commercial materials, the effect of size on mass transfer and adsorption rate, the effect of size on pressure drop, and the effect of size on axial dispersion.

Pressure drops in fixed beds can be reduced by selecting larger particle sizes. However, large particle sizes can give rise to low mass transfer rates, which in turn would lead to increased bed sizes. Small particles can increase the effect of axial dispersion. A balance therefore needs to be struck between the need to keep operating costs low by keeping the pressure drop low and the need to keep capital investment low by ensuring a high adsorption rate without high axial dispersion. The pressure drop must not be too low, otherwise poor flow distribution in the bed may occur. In some applications it might become necessary to use beds which contain two sizes of adsorbent in order to avoid to some extent the trade-off that must be made between pressure drop and mass transfer rate. The highest pressure drop is likely to occur during the regeneration step, since in this step the fluid is usually at its highest temperature and/or its lowest pressure. For cyclic fixed bed processes therefore it is important that a pressure drop analysis is carried out for each step in the cycle.

6.8.1 Pressure drop

The particle Reynolds number is generally required in the several correlations which are available for estimating pressure drop:

$$Re = \frac{d_p G}{\mu} \tag{6.63}$$

where d_p is the particle diameter, G is the mass flux, and μ is the fluid viscosity.

A dimensionless friction factor, f, is defined by:

$$\frac{\Delta P}{L} = \frac{f G^2}{2 d_p \rho} \tag{6.64}$$

where ΔP is the pressure drop, L is the bed length, and ρ is the fluid density.

Equation (6.65) is used to calculate f for the Ergun (1952) correlation:

$$f = \left[3.5 + 300\left(\frac{1-e}{Re}\right)\right]\left(\frac{1-e}{e^3}\right) \tag{6.65}$$

The particle diameter d_p is defined to be the equivalent diameter of a sphere having the same specific surface area (i.e. particle area/particle volume) as the particle. It is important also to note that the coefficients 3.5 and 300 in equation (6.65) were obtained by Ergun for specific packings. Thus the equation may not be strictly valid for the majority of adsorption columns in which the adsorbent is expected to be in granular or pelleted forms. In order to overcome this limitation, Handley and Heggs (1968) provide further data on the coefficients and on a method which can be adopted for determining the appropriate coefficients for any particular fluid–adsorbent combination.

In the Leva correlation (1949) the friction factor f is derived from another factor f' which is a function only of Re and a shape factor ϕ_s:

$$f = \frac{f' (1-e)^{3-n}}{\Phi_s^{3-n} e^3} \tag{6.66}$$

In the Leva correlation the particle diameter is the equivalent diameter of a sphere having the same volume as the particle. The value of the coefficient n increases from 1 to 2 as flow is changed from the laminar to the turbulent regimes. In order to take into account the effect of flowrate on pressure drop, Chilton and Colburn (1931) provide two correlations for the friction factor, depending on the value of Re:

$$f = \frac{805}{Re} \text{ for } Re < 40 \tag{6.67}$$

$$f = \frac{38}{Re^{0.15}} \text{ for } Re > 40 \tag{6.68}$$

The Darcy equation should be used if the flow through a packed bed is

laminar, i.e. $Re < 10$. The pressure gradient is directly proportional to the superficial velocity u (or mass velocity G):

$$\frac{\Delta P}{L} = \frac{\mu e u}{B} \tag{6.69}$$

where μ is the fluid viscosity, and B is the permeability coefficient, which must be determined experimentally.

Channelling at the wall may become significant if the ratio of the adsorber bed diameter to particle diameter is less than 30. Consider for example the situation in which the void fraction near the walls of a packed bed is 0.5 while the void fraction in the central region is 0.35. The Ergun equation could be used to calculate that the ratio of the velocities in the two regions would be between 2 and 5 for a given pressure drop across the bed. This disparity in velocity will be the greatest when the velocity is relatively low. This is because the pressure gradient at low velocities is controlled by viscous

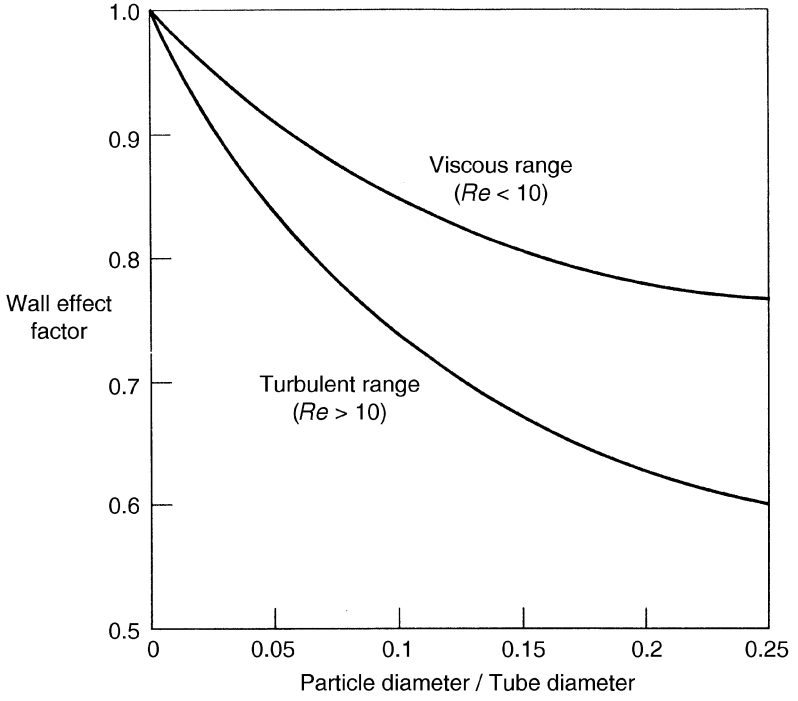

Figure 6.11 *Dependence of wall factor on particle diameter to bed diameter ratio (adapted from Furnas 1929).*

energy losses. In order to promote intermixing of the flow streams in the two velocity regions (wall and centre) it is desirable that the bed length should be at least 100 times the adsorbent particle diameter. The correction factor which may need to be applied to the pressure drop in order to take into account flow maldistributions is shown in Figure 6.11.

In low pressure gas phase applications such as vent stream cleaning and solvent recovery, high pressure drops are liable to occur due to the low density and high velocity of the fluid. To overcome this problem very shallow adsorption beds are sometimes used. Adsorption beds with low aspect ratios, however, may result in flow distribution problems, and therefore some of the pressure drop that is saved must be sacrificed by adding flow distribution systems of manifolds, baffles and screens. Other ways of keeping the pressure drop to a minimum in low pressure gas phase applications include the use of specially shaped adsorbents such as the trilobe and monolithic materials shown in Figure 2.7 in Chapter 2.

Two other factors deserve consideration. First, all the correlations described above for pressure drop were obtained from steady state flow measurements, and therefore may not be applicable to situations in which velocities are rapidly changing with time, e.g. in the pressurization and depressurization steps of PSA processes. Secondly, the changes in superficial velocity along the axis of an adsorption bed which is used for a bulk separation process, such as air separation, may be sufficiently large to require the summation of the pressure gradient across incremental lengths of the bed.

6.8.2 Fluidization

At high flowrates the potential exists for an adsorption bed to expand, lift or fluidize. At the point of expansion, the net weight of the bed is fully supported by the drag forces due to the flow of fluid:

$$\frac{\Delta P}{L} = (1 - e)\,(\rho_s - \rho)g \tag{6.70}$$

where ρ_s is the density of the solid, and e is the voidage at the point of expansion.

Without a retaining device, the bed will start to expand if flow in the upwards direction is sufficiently high. Even if a bed retaining device is fitted the particles will still tend to move and rub against each other and cause attrition to occur. In order to avoid this problem it is normal practice to limit the allowable upwards velocity for packed beds to less than about 80% of the minimum fluidization velocity calculated from equation (6.70).

Large differential pressures can occur at the commencement of both the pressurization and depressurization steps in PSA cycles. Flowrates therefore should be controlled to prevent fluid velocities from exceeding the value which would cause significant attrition to occur. Continual pressure cycling (perhaps of the order of a million times per year for rapid PSA processes), external mechanical vibrations and compressor pulsations can all exacerbate the problem. A practical solution to the attrition problem is to immobilize the adsorbent particles by mixing a suitable adhesive binder throughout the bed and interlocking the particles into a common rigid structure. Immobilization is sometimes used in compact high throughput PSA units for high technology applications. An alternative concept is to manufacture the adsorbent bed as a monolith.

Equation (6.70) can be used for the design of fluidized bed adsorbers. It should be noted, however, that the bed voidage will vary from the point of bed expansion to full fluidization. Once fully fluidized the pressure drop ceases to become a function of the flowrate.

6.8.3 Bed crushing

The possibility of crushing the adsorbent must be considered for those steps in the process in which flow is downwards. The drag forces must be added to the weight of the bed and compared with the crushing strength of the adsorbent.

6.8.4 Axial dispersion

There is a tendency for both axial and radial dispersion of mass to occur when a fluid flows through a packed bed. Since the bed diameter is normally far greater than the particle diameter in an adsorption bed, it is common not to have to consider the effects of radial dispersion. Hence the prevalence of plug and axially dispersed plug flow models in rigorous design methods.

It is desirable to reduce axial dispersion because it can reduce the efficiency of separation. The effects of axial dispersion differ for gas and liquid phase systems, and special considerations may be needed for porous particles when flowrates are low. Axial dispersion is caused by the twin effects of molecular diffusion and turbulent mixing which arises from the splitting and recombination of flows around particles. To a first approximation, these effects are generally considered additive (Ruthven 1984):

$$D_L = \gamma_1 D_M + \gamma_2 d_p u \tag{6.71}$$

where for non-porous particles γ_1 and γ_2 take values of approximately 0.7

and 0.5, respectively. Equation (6.71) can be written in non-dimensional form as follows:

$$\frac{1}{Pe'} = \frac{D_L}{ud_p} = \frac{\gamma_1 D_M}{ud_p} + \gamma_2 = \frac{\gamma_1 e}{ReSc} + \gamma_2 \tag{6.72}$$

The coefficient γ_1 is dependent on bed voidage as follows:

$$\gamma_1 = 0.45 + 0.55e \tag{6.73}$$

The coefficient γ_2 is dependent upon flow characteristics as follows:

$$\gamma_2 = \frac{1}{Pe'_\infty \left(1 + \frac{\beta\gamma_1 D_m}{ud_p}\right)} \tag{6.74}$$

At high Reynolds numbers the asymptotic value of the Peclet number takes the value of 2 for relatively large particles, i.e. $d_p > 0.3$ cm. For smaller particles, i.e. $d_p < 0.3$ cm, experimental data show much smaller limiting Peclet numbers, given approximately as follows:

$$Pe'_\infty = 1.68 d_p \tag{6.75}$$

This behaviour is believed to be due to the tendency of small particles to form clusters which act effectively as single particles. Thus the advantage of reducing pore diffusional resistances by using small particles could well be offset to some extent by an increase in axial dispersion.

The variations of Peclet number with Reynolds number for gas and liquid phase systems are compared in Figure 6.12. At high *Re*, the asymptotic value of $Pe' = 2$ is reached for liquids, but at lower values of *Re*, the axial dispersion is greater than that for gases. The increased dispersion with liquids is believed to be due to the effect of greater liquid hold-up in the laminar boundary layer surrounding particles, together with small random fluctuations in the flow (Ruthven 1984).

If adsorption is fast and strong then the concentration profile through a particle may become asymmetric. This can lead to a significant additional contribution to axial dispersion for gases at low *Re*. The effect is likely to be most significant when most of the adsorption occurs at the outside of the particle, as would occur in the initial stages of uptake in a mass transfer zone. Equation (6.76) has been suggested for a rectangular isotherm as an alternative to equation (6.72). In this case γ_1 is typically 50, compared with the value of 0.7 for non-porous particles:

$$\frac{1}{Pe'} = \frac{20}{ReSc} + \frac{1}{2} \tag{6.76}$$

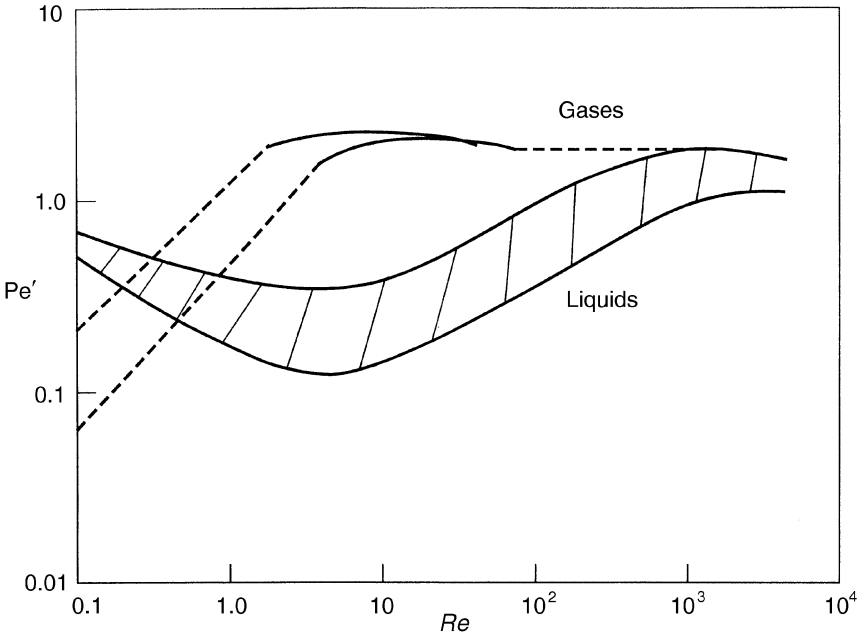

Figure 6.12 *Variation of Peclet number with Reynolds number for axial dispersion in both liquid and gas phase systems (adapted from Levenspiel 1972, p. 282).*

Consequently axial dispersion for porous particles may be important with strongly adsorbed species under laminar flow conditions, even though it may be insignificant for non-porous particles.

6.9 SCALE-UP AND PILOT-PLANT STUDIES

Several factors need to be taken into account when designing small-scale experiments in order to obtain data for the design of full-size plant. Clearly, it is necessary in the small-scale study to use the same fluid and adsorbent as will be used in the full-scale plant. Special attention needs to be paid to the choice of the length, diameter and flowrate in the small-scale experiments since all can affect the hydrodynamics and the the dispersion characteristics. The length of a bed is related to the cycle time and the product purity and so a small-scale column should be long enough to retain several mass transfer zone lengths. If a full-size design is to be based on analysis of the breakthrough curve, it is also important to know that a constant pattern

MTZ has been achieved in the small-scale column. A constant pattern MTZ can only be achieved if the equilibrium isotherm is favourable to adsorption. The bed length for the full-size plant can then be obtained by adding to the length of bed which contains the equilibrium section that part which must contain the region in which mass transfer is occurring, that is the MTZL.

If the isotherm is unfavourable to adsorption then the full-scale bed length should be set equal to the small-scale bed length which gives the required performance. For multicomponent and/or non-adiabatic systems, more than one mass transfer zone will occur for either favourable, unfavourable or mixed isotherms. Again in such cases it would be prudent to ensure that the bed lengths for both small-scale and full-scale plants were the same.

Hydrodynamic and dispersion effects should be taken into account from the outset. The aim should always be to ensure that the adsorption bed is well packed and that there is no flow maldistribution. While a high pressure drop in a gas phase application might lead to a better bed loading near the bed entrance it could possibly lead to condensation. Problems with axial dispersion may be avoidable if empirical guidelines, available from reaction engineering experience, are taken into account. Carberry (1976) suggests that for isothermal operations the column length to diameter ratio should be more than 20 and flow should be turbulent, i.e. $Re > 10$. The axial Peclet number has been shown to be important only when the ratio of column diameter to particle diameter is less than 12, and when the column length to particle diameter is less than 50 (Gunn and Malik 1968, Carberry 1976). Carberry suggests that in order to maintain plug flow for non-isothermal operations the column length to particle diameter ratio should be more than 150.

LeVan and Vermeulen (1984) report that to avoid channelling, the ratio of bed diameter to particle diameter should be greater than 20. On the other hand, Carberry (1976) suggests that in order to avoid radial temperature gradients, the ratio of bed diameter to particle diameter should be less than 5 or 6. Clearly it might be necessary to make a compromise in the design of adsorption beds in which heat needs to be added or removed via the walls.

Scale-up could be achieved simply by retaining the same suitable superficial velocity in the small-scale and full-size plants and increasing the cross-sectional area for flow by increasing the number of beds which operate in parallel and/or by increasing the diameter of a single bed. The first option requires the highest capital investment but the advantage gained is that the full-size facility should operate identically to the small-scale unit. The second option leads to simpler and cheaper plant but it is necessary to ensure that good flow distribution, and redistribution if necessary, is provided.

Care needs to be taken if data is taken from small-scale equipment which is of a different configuration or design, or differs in any other important

respect, from the full-size design. Kinetic data which is obtained from batch stirred experiments can only be used in rigorous design models and cannot be used in any of the short-cut design techniques for packed beds, for example.

Kinetic data which is obtained from dynamic mini-column experiments must be treated carefully. The mini-column, or rapid adsorption, experiment is based on the principle of high pressure liquid chromatography (Rosene and Manes 1976) and was designed particularly for the water industry in order to provide rapid evaluation of dynamic adsorbent performance to complement data from isotherm experiments. The apparatus typically comprises a high pressure liquid pump and a small diameter stainless steel column which contains pulverized adsorbent. The effluent concentration is monitored for breakthrough and the adsorptive capacity calculated from the known mass of adsorbent in the column and the volume of liquid passed. Flows are typically in the range 2 to 3 cm^3/min with a fine carbon (200 × 325 mesh range) packed to a depth of about 20 to 25 mm (Bilello and Beaudet 1983). Direct scale-up of mini-column breakthrough profiles to full-scale systems is not easy because of the substantial differences in sizes, flow distribution and wall effects. The technique should not be used for the *ab initio* design of large-scale plant. Rather it should be used as a screening technique for different types of adsorbent or for the effects of preferential adsorption and desorption in water purification applications.

6.10 ADSORPTION PROCESS DESIGN AND SIMULATION

The design of any adsorption process should be based on sound fundamental principles, backed up by laboratory- and pilot-scale experimentation and modelling. A process simulator which incorporates an adsorption module can be a useful tool to aid optimization of a design. However, a process simulator is only as good as the adsorption model and associated data it incorporates. One of the more comprehensive computer packages is ADSIM™ (available from AspenTech) which is capable of simulating and designing adsorption processes for the commercial separation and purification of gases and liquids. ADSIM™ is a dynamic simulator based on the equation-solving software known as SPEEDUP™, and comprises three components. The Preprocessor is used to generate adsorption bed models and flowsheets. Here the choice of many different model attributes may be made, including for example the choice of isothermal, adiabatic or non-isothermal heat effects, the choice of mass transfer kinetic model, the choice of equilibrium model, etc. A wide range of both single component and multicomponent adsorption isotherm models are included. The Library

consists of ancillary adsorption process models. The Cycle Manager is used to specify the cyclic operation. Example industrial processes include thermal swing adsorption, pressure swing adsorption, vacuum swing adsorption, isobaric fixed bed adsorption, chromatography and ion exchange. Processes can consist of single or multiple bed systems.

REFERENCES

Acrivos, A. (1956) *Ind. Eng. Chem.*, **48**, 703–710

Acrivos, A. (1960) *Chem. Eng. Sci.*, **13**, 1–6

Antonson, C. R. and Dranoff, J. S. (1969) *AIChE Symp. Series*, **65** (96), pp. 20 and 27

Anzelius, A. (1926) *Angew Math. Mech.*, **6**, 291

Balzli, M. W., Liapis, A. I. and Rippin, D. W. T. (1978) *Trans. IChemE*, **56**, 145–156

Bilello, L. J. and Beaudet, B. A. (1983) Evaluation of activated carbon by the dynamic minicolumn adsorption technique, in *Treatment of Water by Granular Activated Carbon*, edited by M. J. McGuire and I. H. Suffet, Advances in Chemistry Series, No 292, American Chemical Society, Washington, pp. 213–246

Bohart, G. and Adams, E. (1920) *J. Am. Chem. Soc.*, **42**, 523–544

Bowen, J. H. (1971) Sorption processes, in *Chemical Engineering*, Vol 3, edited by J. F. Richardson and D. G. Peacock, Pergamon, Oxford, pp. 475–577

Bowen, J. H. and Donald, M. B. (1963) *Chem. Eng. Sci.*, **18**, 599–611

Bowen, J. H. and Donald, M. B. (1964) *Trans. IChemE*, **42**, T259–T265

Carberry, J. (1976) *Chemical and Catalytic Reaction Engineering*, McGraw Hill, New York, pp. 156–171

Carter, J. W. and Husain, H. (1972) *Trans. IChemE*, **50**, 69–75

Cartón, A., González, G., Iñiguez de la Torre, A. and Cabezas, J. L. (1987) *J. Chem. Tech. & Biotechnol.*, **39**, 125–132

Cen, P. L. and Yang, R. T. (1986) *AIChE J.*, **32**, 1635–1641

Chi, C. W. and Wasan, D. T. (1970) *AIChE J.*, **16**, 23–31

Chilton, T. H. and Colburn, A. P. (1931) *Trans. AIChE*, **26**, 178

Cooney, D. O. (1974) *Ing. Eng. Chem. Proc. Design Dev.*, **13**, (4), 368–373

Cooney, D. O. and Lightfoot, N. (1965) *Ind. Eng. Chem. Fund.*, **4**, 233–236

Cooper, R. S. (1965) *Ind. Eng. Chem. Fund*., **4**, 308–313

Cooper, R. S. and Liberman, D. A. (1970) *Ind. Eng. Chem. Fund*., **9**, 620–623

Coulson, J. M., Richardson, J. F., Backhurst, J. R. and Harker, J. H. (1991) *Chemical Engineering*, Vol. 2, 4th edition, Chapter 17, Pergamon Press, Oxford

Crittenden, B. D., Guan, J., Ng, W. N. and Thomas, W. J. (1994) *Chem. Eng. Sci.*, **49**, 2657–2669

Crittenden, D., Guan, J., Ng, W. N. and Thomas, W. J. (1995) *Chem. Eng. Sci.*, **50**, 1417–1428

Ergun, S. (1952) *Chem. Eng. Prog*., **48**, 89

Faust, S. D. and Aly, O. M. (1987), *Adsorption Processes for Water Treatment*, Butterworths, Boston

Furnas, C. C. (1929) US Bureau of Mines Bulletin No. 307

Furnas, C. C. (1930) *Trans. AIChE,* **24**, 142–193

Garg, D. R. and Ausikaitis, J. P. (1983) *Chem. Eng. Prog*., **79** (4), 60–65

Garg, D. R. and Ruthven, D. M. (1973) *Chem. Eng. Sci*., **28**, 791–798 and 799–805

Garg, D. R. and Ruthven, D. M. (1974a)*Chem. Eng. Sci*., **29**, 571–581

Garg, D. R. and Ruthven, D. M. (1974b) *Chem. Eng. Sci*., **29**, 1961–1967

Garg, D. R. and Ruthven, D. M. (1975) *Chem. Eng. Sci*., **30**, 1192–1194

Garg, D. R., Ruthven, D. M. and Crawford, R. M. (1975) *Chem. Eng. Sci*., **30**, 803–810

Gunn, D. J. and Malik, A. (1968) *Chemical Engineer*, London (219), CE 153

Hall, K. R., Eagleton, L. C., Acrivos, A. and Vermeulen, T. (1966) *Ind. Eng. Chem. Fund*., **5**(2), 212–223

Handley, D. and Heggs, P. J. (1968) *Trans. IChemE*, **46**, 251–264

Hiester, N. K. and Vermeulen, T. (1952) *Chem. Eng. Prog*., **48** (10), 505–516

Kawazoe, K. and Takeuchi, Y. (1974) *J. Chem. Eng. Japan*, **7**, 431–437

Kayser, J. C. and Knaebel, K. S. (1989) *Chem. Eng. Sci*., **44**, 1–8

Klinkenberg, A. (1954) *Ind. Eng. Chem*., **46**, 2285–2289

Knaebel, K. S. and Hill, F. B. (1985) *Chem. Eng. Sci*., **40**, 2351–2360

Kyte, W. S. (1973) *Chem. Eng. Sci*., **28**, 1853–1856

Lapidus, L. and Amundson, N. R. (1952) *J. Phys. Chem*., **56**, 984–988

Lee, R. G. and Weber, T. W. (1969) *Can. J. Chem. Eng*., **47**, 60–65

Leva, M. (1949) *Chem. Eng*., **56**, (5), 115– 117

LeVan, M. D. and Vermeulen, T. (1984) *AIChE Symp. Series*, **233** (80), 34–43

Levenspiel, O. (1972) *Chemical Reaction Engineering*, 2nd edn, Wiley, New York, p. 282

Levenspiel, O. and Bischoff, K. B. (1963) *Adv. Chem. Eng.,* **4**, 95–198

Liapis, A. I. and Rippin, D. W. T. (1978) *Chem. Eng. Sci*., **33**, 593–600

Masamune, S. and Smith, J. M. (1965) *AIChE J*., **11**, 34–40

Michaels, A. S. (1952) *Ind. Eng. Chem*. **44**, 1922–1930

Miller, A. W. and Roberts, C. W. (1958) *Ind. Chemist*, **34**, 141–145

Moon, H. and Lee, W. K. (1986) *Chem. Eng. Sci*., **41**, 1995–2004

Nusselt, W. (1930) *Tech. Mech. Thermodynam*., **1**, 417

Rasmuson, A. (1982) *Chem. Eng. Sci*., **37**, 787– 788

Rasmuson, A. and Neretnieks, I. (1980) *AIChE J*., **26**, 686–688

Rosen, J. B. (1952) *J. Chem. Phys*., **20**, 387–394

Rosen, J. B. (1954) *Ind. Eng. Chem*., **46**, 1590–1594

Rosene, M. R. and Manes, M. (1976) *J. Phys. Chem*., **80** (23), 2586–2589

Ruthven, D. M. (1984) *Principles of Adsorption and Adsorption Processes*, Wiley Interscience, New York

Ruthven, D. M. (1990) Dynamic modelling of pressure swing adsorption separation processes, in *Separation of Gases, 5th BOC Priestley Conference*, Royal Society of Chemistry, pp. 256–272

Ruthven, D. M., Farooq, S. and Knaebel, K. S. (1994) *Pressure Swing Adsorption*, VCH, New York

Sircar, S. (1991) Recent trends in pressure swing adsorption, in *Adsorption Processes for Gas Separation*, edited by F. Meunier and M. D. LeVan, Recents Progres en Genie des Procedes, **5**(17), Groupe Francais de Genie des Procedes, Nancy, pp. 9–14

Sircar, S. and Hanley, B. F. (1995) *Adsorption*, **1**, 313

Sowerby, B. and Crittenden, B. D. (1991) *Trans. IChemE*, **69A**, 3–13

Thomas, H. C. (1944) *J. Am. Chem. Soc*., **66**, 1664–1666

Tien, C. (1994) *Adsorption Calculations and Modelling,* Butterworth-Heinemann, Boston

Tien, C. and Thodos, G. (1959) *AIChE J.*, **5**, 373

Treybal, R. E. (1955) *Mass Transfer Operations*, McGraw-Hill, New York

Walter, J. E. (1945) *J. Chem. Phys.*, **13**, 229–234, 332–336

Weber, T. W. and Chakravorti, R. K. (1974) *AIChE J.*, **20**, 228–238

White, D. H. and Barkley, P. G. (1989) *Chem. Eng. Prog.*, **85**(1), 25–33

Yang, R. T. (1987). *Gas Separation by Adsorption Processes*, Butterworths, Boston

Yoshida, Y., Kataoka, T. and Ruthven, D. M. (1984) *Chem. Eng. Sci.*, **39**, 1489–1497

Zwiebel, I., Gariepy, R. L. and Schnitzer, J. J. (1972) *AIChE J.*, **18**, 1139–1147

7

Selected adsorption processes

7.1 INTRODUCTION

To illustrate some of the features of adsorption processes a number of examples have been selected which vary in their mode of design and operation. Purification of gases is by far the oldest type of process and includes the drying of air and other industrial gases, the sweetening (removal of acidic gases) of natural gas, air purification and removal of solvents from air streams. A second category of adsorption process is the separation of a component gas, or gases, from a mixture of gases. The production of oxygen and nitrogen from air are two well-known separation processes as are the separation of n-paraffins from iso-paraffins and the recovery of hydrogen from industrial gas mixtures. The two most common adsorbents used for gas separation are activated carbon and zeolites of various types (see Chapter 2). The adsorbent properties which enable the separation of gases are the nature of the adsorbate–adsorbent equilibrium and the rates at which gaseous components diffuse into the pore structure of the adsorbent. The sieving property of zeolites is prominent in the separation of n-paraffins from iso-paraffins and in the drying of gaseous streams. The production of nitrogen from air using a molecular sieve carbon depends on the difference in rates of diffusion of nitrogen and oxygen within the adsorbent pore structure.

Most commercial processes for drying and separation of gases utilize two or more packed adsorbent beds. The simplest of such arrangements is two packed beds, one acting as an adsorbent bed while the other (having already been exposed to the gas stream as an adsorbent bed) acts as a regenerator. The role of each bed is then reversed, the adsorber being regenerated while the freshly regenerated bed becomes the adsorber. The cycle is then repeated at predetermined intervals. Although each bed is being operated batchwise, a continuous flow of feed and product is achieved which reaches a steady state following a number of cycles of operation. The length of a cycle depends primarily on whether each adsorbent bed is regenerated by raising its temperature (thermal swing) or lowering its pressure (pressure swing).

The choice between thermal and pressure swing modes of operation is largely dictated by economics although other technical factors are of importance. Because adsorption is an exothermic process and strongly adsorbed species have relatively high heats of adsorption, a small increase in temperature is capable of reducing the bed loading of strongly adsorbed components by large amounts. This means that the desorbate can be recovered at high concentration. Heat losses from beds of adsorbents militate against high efficiency and the large thermal capacity of an adsorbent bed translates into relatively long times for heating and cooling, thus contributing to lengthy cycle times. The most convenient way of raising the temperature of the bed to be regenerated is by purging the bed with a preheated gaseous stream. Availability of low grade steam or waste heat at an adjacent plant location would be one factor favouring the choice of thermal swing operation. On the other hand pressure swing operation would be preferred when a relatively weakly adsorbed component of an adsorbable mixture is required as a high purity product. Furthermore, the adsorbent is used efficiently in pressure swing operations and the cycle times are considerably reduced below those needed for thermal swing operations. The desorbed components of the initial mixture fed to a pressure swing unit are, however, only recovered at relatively low purities. Figure 5.14 illustrates the difference between thermal and pressure swing operations. It should be noted that mechanical energy is expended during pressure swing operations whereas thermal energy, being cheaper than mechanical energy, is utilized during thermal swing operations.

Another method of adsorbent regeneration is known as purge stripping. An inert gas purge removes adsorbate from the bed without change of temperature or pressure. Inert purge stripping is uncommon in practice because it is only applicable to rather weakly adsorbed components. A combination of inert purge and thermal swing operations, however, facilitates desorption of more strongly adsorbed components. If the increase in bed temperature is relatively small when an inert purge is employed,

then the disadvantages of purely thermal swing processes are circumvented. The paths of thermal swing and pressure swing operations are illustrated in Figure 5.14. Inert gas purge stripping is also illustrated in Figure 5.14, but during this operation the temperature and total pressure remain constant.

Regeneration of the adsorbent following adsorption can also be accomplished by displacing the adsorbed component with a purge gas or a liquid which is as strongly adsorbed as the adsorbable component of the feed. The displacement fluid is subsequently separated from the extract by distillation. Separation of linear paraffins of intermediate molecular mass from branched chain and cyclic isomers is an example of a displacement purge cycle, ammonia being the strongly adsorbed purge in the Ensorb process of Exxon Corporation (see Section 7.6).

All of the processes alluded to above are fixed bed cyclic batch processes providing a continuous flow of raffinate (the least strongly adsorbed component) and extract (the more strongly adsorbed component). An alternative method of separation of components by adsorption is to employ continuous countercurrent systems (see Section 7.7) in which either the adsorbent is circulated through the flowing feed stream or, by appropriate manipulation of the flowing fluids, to simulate adsorbent circulation. An example of the former methodology is the Hypersorption Process of Union Oil Co. while an example of the latter method of operating is the Sorbex Process of UOP (see Section 7.7.5).

7.2 PRESSURE SWING ADSORPTION (PSA) PROCESSES

7.2.1 The two-bed Skarstrom cycle

The simplest two-bed continuous pressure swing adsorption (PSA) process was invented by Skarstrom (1960). Each bed acts alternately and sequentially as an adsorber and a regenerator to complete one cycle of events. The plant layout and pipework connections between the two columns is illustrated in Figure 7.1 and the cycle is described by Figure 5.15 which shows how each column is utilized during a single cycle. To illustrate the operation, we suppose that each bed in Figure 7.1 contains a molecular sieve zeolite adsorbent whose capacity for adsorbing nitrogen from air is greater than its capacity for adsorbing the oxygen component of air. For the first step column 1 is pressurized to several atmospheres with air while isolated from column 2. During the second step of the cycle columns 1 and 2 are connected and oxygen (which is the least strongly adsorbed component of air) together with some nitrogen remaining unadsorbed issues from both columns;

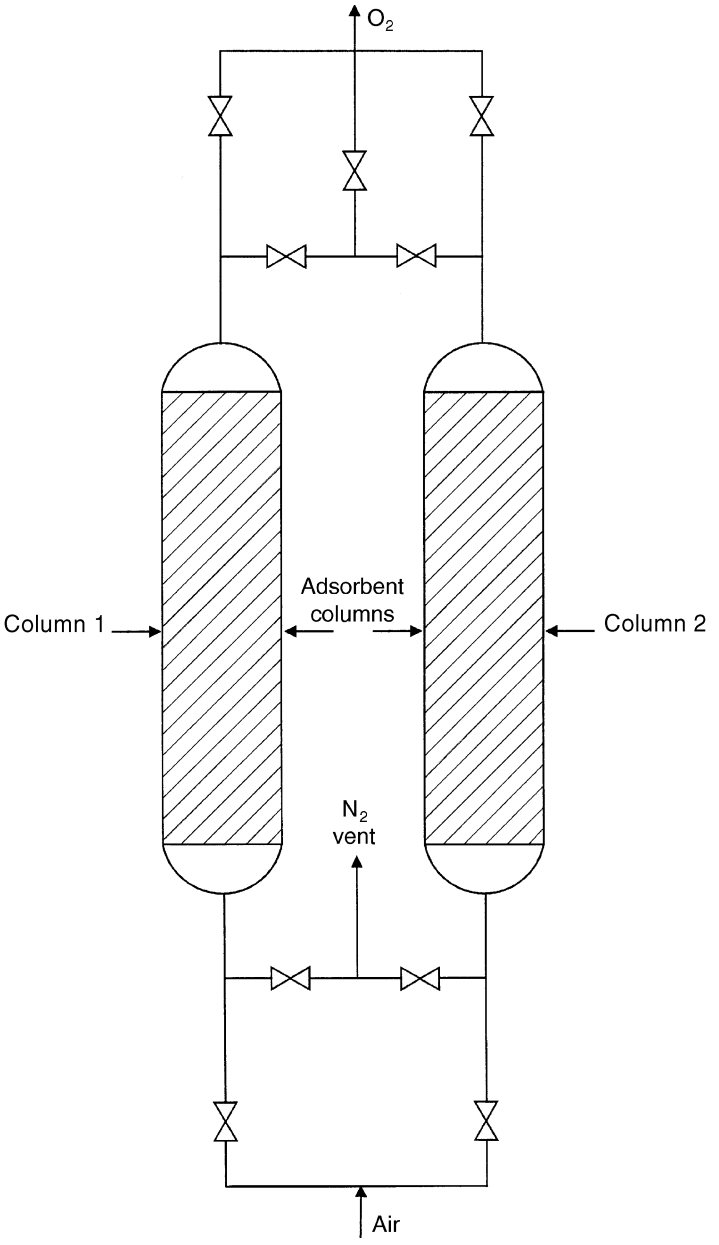

***Figure** 7.1 Basic plant layout of two-bed PSA process for air separation.*

meanwhile the majority of the nitrogen is adsorbed and retained in column 1. The third step occurs when the columns are again isolated and column 1 is depressurized to atmospheric pressure (commonly known as blowdown) causing nitrogen to be desorbed and flow from the bed (countercurrent to the direction of feed in the second step). The last step is for the beds to be reconnected and some oxygen (produced from the second step in the cycle) is passed through both columns countercurrent to the direction of the air feed. This latter step of the cycle ensures that any adsorbed nitrogen in the bed is flushed towards the column entrance thus allowing the major portion of the bed to be free of adsorbed nitrogen and ready for the whole cycle to be repeated. Column 2 goes through a similar cycle of events to column 1 during a cycle. This process for air separation was developed by Skarstrom (1960 and 1975) and is used for small-scale separation units. The original patent was assigned to Exxon Research and Engineering in 1958.

A patent for air separation was also granted to L'Air Liquide in 1964. The cycle was developed by Guerin de Montgareuil and Domine (1964) and is known as the Guerin–Domine cycle. Three steps are involved for each of the two beds. The first step is the pressurization of bed 1 while bed 2 is evacuated. The second step is the downward blowdown of 1 through the previously evacuated bed 2 from which oxygen is collected. The third step is the evacuation of bed 1. The roles played by beds 1 and 2 become reversed for the following cycle. Nitrogen is released from each of the beds 1 and 2 during evacuation. Compared with the basic Skarstrom cycle, the Guerin–Domine cycle gives an improved performance because N_2 is removed efficiently by evacuation thus leaving a clean bed for the elution of O_2. The introduction of an evacuation step nevertheless increases the expenditure of mechanical energy.

7.2.2 Improvements to the basic PSA cycle

Although the Guerin–Domine cycle proved to be more effective for the separation of air than the Skarstrom cycle, the former cycle was not economic. The main improvements over the basic two-bed cycle which have occurred in the last three decades are the introduction to the cycle of cocurrent depressurization and pressure equalization. Extension of the number of beds in series and the sequence of operational steps in the cycle have led to major process improvements.

Cocurrent depressurization

Incorporation of a cocurrent depressurization step immediately following the pressurization and feed steps into the basic Skarstrom cycle increases the

concentration of the most strongly adsorbed component in the bed. This is achieved by removing the gas contained in the adsorbent voids which, following the initial two steps, will have entrapped gas at the same composition as the feed. The pressurization and feed steps, during which adsorption occurs, are shortened in duration so that the cocurrent depressurization step can be initiated before breakthrough of components from the bed. The bed is subsequently desorbed by blowdown and purge steps in the cycle. The net benefit of cocurrent depressurization is increased purity of the most strongly adsorbed component in the product which, in consequence, enhances the recovery of the least strongly adsorbed component.

7.2.3 Pressure equalization

To help conserve expenditure of mechanical energy during a PSA cycle it was suggested by Marsh *et al.* (1964) that two columns could be interconnected at a particular stage of the cycle so that the pressure energy contained by the gas in a bed at high pressure could be shared with a bed which has been subject to blowdown (and thus at a lower pressure) and which, as a result, becomes partially pressurized in readiness for repressurization. Pressure equalization steps enable gas separations to be realized economically on a large scale. It is now common to include pressure equalization in a cycle when four or more beds in series comprise a PSA unit (Berlin 1966, Wagner 1969). Benefits of pressure equalization include increased product recovery and steadier continuous flow of the most strongly adsorbed component from the unit.

7.3 COMMERCIAL PSA PROCESSES

A brief description of the more common PSA processes for drying, purification and separation of gaseous components clarifies how cocurrent depressurization and pressure equalization steps are incorporated into the basic PSA cycle. A variety of different sequences of operation of adsorber beds exists and the manner in which these steps are introduced depends on particular circumstances such as plant utilities, throughput required and cost of equipment and operation.

7.3.1 Drying of air (Skarstrom 1975)

The drying of air and other gaseous streams may be accomplished by thermal swing processes. Pressure swing adsorption operation can, however, achieve even lower dewpoints than thermal swing operation and has

been adopted for many drying plants especially when the air or gas pressure supply is available at a moderately high pressure. In a typical two-bed adsorption unit, each bed is subjected to pressurization and adsorption steps followed by countercurrent blowdown and purge. Cycle times vary from 1 to 10 minutes – very much shorter than the corresponding thermal swing process (compare with Section 7.4.1). Short cycle times help to conserve the heat of adsorption and experimental evidence for this indicates that temperatures in each bed vary by less than 10°C (Chihara and Suzuki 1983). To obtain a high purity product with a low dewpoint the purge to feed flow ratios should be between 1.1 and 2.0 and the ratio of high pressure (when adsorbing) to low pressure (during regeneration) should be greater than the reciprocal of the mole fraction of the product contained in the feed.

7.3.2 Hydrogen purification (Stewart and Heck 1969, Cassidy and Holmes 1984)

Pressure swing adsorption units are used extensively for the purification of hydrogen streams containing small amounts of low molecular weight hydrocarbons. For most adsorbents, hydrogen is hardly adsorbed. Thus the consequence is that ultra-high purity hydrogen may be recovered using almost any adsorbent. Losses from blowdown and purge, although relatively large, do not militate against a PSA process as recoveries of hydrogen over 85% are possible and the feed gases wasted during blowdown and purge steps are of little economic value.

Figure 7.2 is a sketch of a typical four-bed commercial hydrogen purification unit together with the pipe layout and bed interconnections and valves while Figure 7.3 indicates the sequence of steps for each of the four-beds. In bed 1 while adsorption (i.e. when feed flows through the bed at high pressure) is occurring, countercurrent depressurization takes place in bed 2 followed by a purge step and pressure equalization with bed 3. The operations, all of which are occurring simultaneously, are designed (a) to force any adsorbed hydrocarbons to the entrance (bottom) of bed 2 leaving the majority of the adsorbent free of adsorbate in readiness for repressurization with feed and (b) to reduce the consumption of mechanical energy. Pressure is then equalized between beds 1 and 2. Following these two latter steps, bed 1 is depressurized cocurrently and its pressure then equalized with bed 3. Meanwhile, bed 2 is being repressurized countercurrently. Countercurrent depressurization and purge then occur in bed 1 followed by pressure equalization with bed 4 as adsorption occurs in bed 2. Subsequently pressure in bed 1 is equalized with bed 2 followed by the repressurization of bed 1. As bed 1 is repressurized, bed 2 is depressurized and then its pressure shared with bed 4. Purge and pressurization in each bed is achieved by means of the

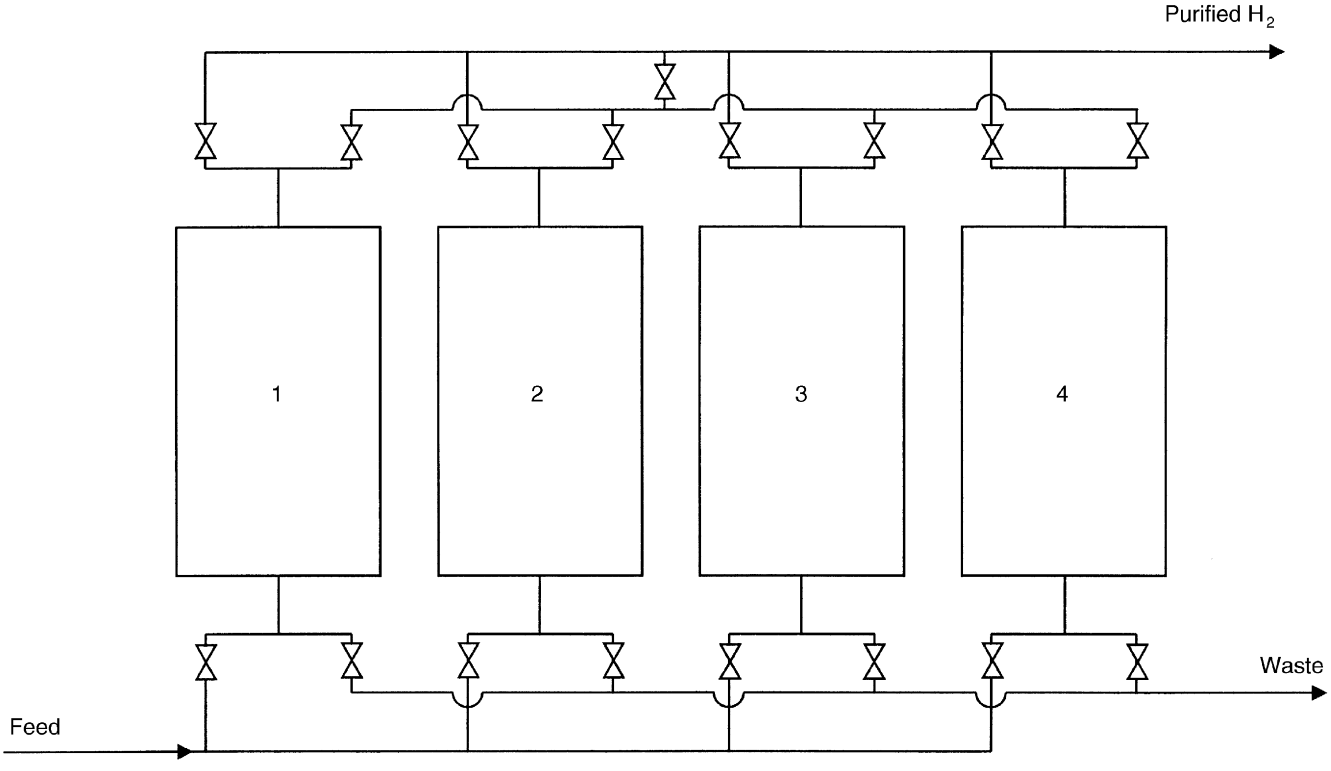

***Figure** 7.2 Bed arrangement for H_2 recovery in a four-bed PSA system (source: Yang, 1987).*

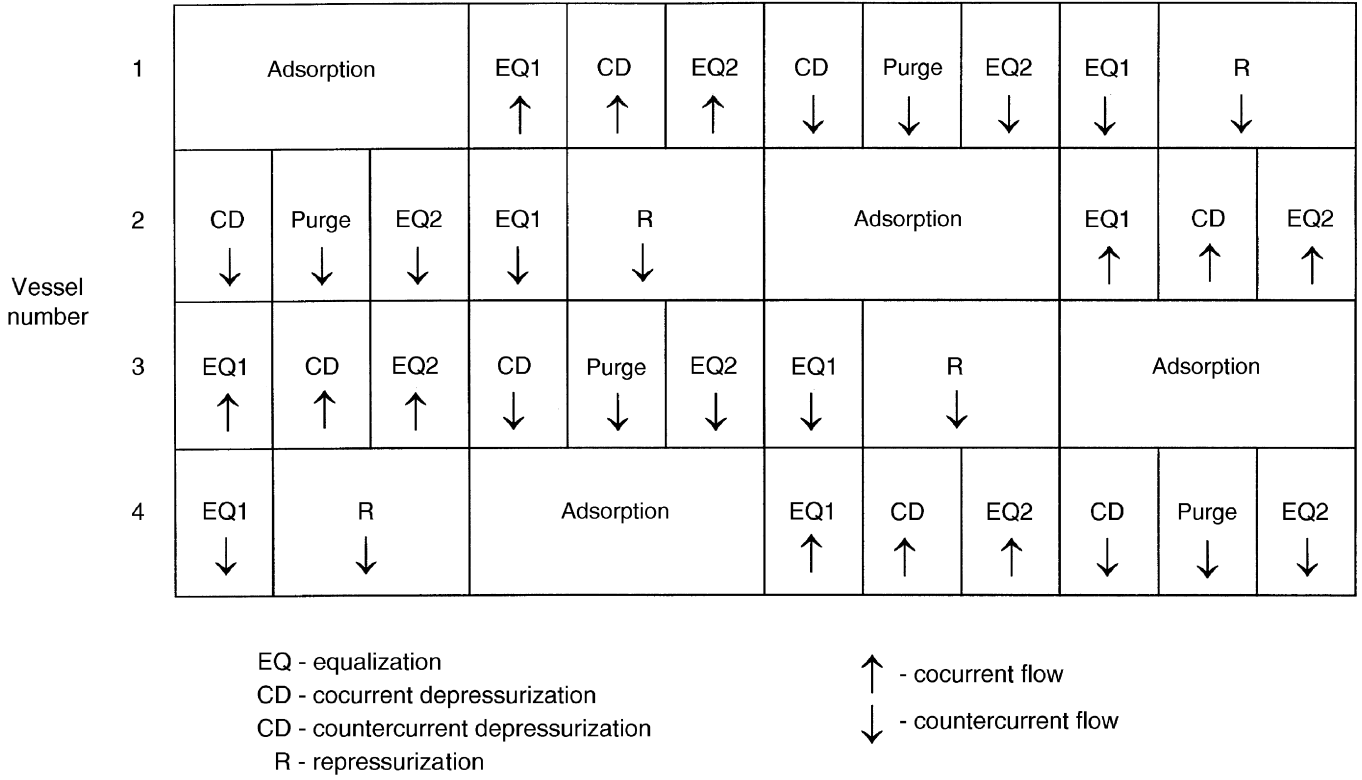

Figure 7.3 Sequence of events during H_2 recovery process from a four-bed unit (source: Cassidy 1980, p. 247).

effluent from the other beds. Union Carbide has employed the four bed PSA process for plants producing 0.4×10^6 m^3 (measured at STP) of H_2 per day. For producing even greater quantities (*ca.* 1.4×10^6 m^3 per day) of ultra-pure hydrogen, as many as nine beds in series are used. For the latter large-scale process the same steps – repressurization, adsorption, cocurrent depressurization, countercurrent blowdown and purge – as for the four-bed process are employed but the sequence and number of pressure equalization steps differ.

7.3.3 Separation of low molecular weight paraffins

Low molecular weight straight chain paraffins less than the molecular weight of the homologue cetane (C_{10} H_{22}) may be recovered at high purity from naphtha feedstocks by the Iso-Siv process introduced by Union Carbide in 1961 (Symoniak 1980, Cassidy and Holmes 1984). Typical feeds are C_5–C_9 hydrocarbons containing as much as 50% n-paraffins. A two-bed process is employed using a 5A zeolite which adsorbs the straight chain hydrocarbons but excludes branched chain isomers. The sequence of steps for the two-bed process is illustrated in Figure 7.4. Following the passage of feed at high pressure through bed 1 when adsorption of n-paraffins occurs, bed 1 is depressurized cocurrently when the product n-paraffins are desorbed and collected. Gases remaining in the voids of the bed are removed by evacuation prior to bed 1 being repressurized. Meanwhile bed 2 goes through the same sequence of steps, the adsorption step in bed 2 occurring simultaneously with cocurrent depressurization, vacuum desorption and repressurization of bed 1.

Separation of hydrocarbons of higher molecular weight than C_{10} H_{12} is accomplished by a different adsorption–separation technique not involving either a change of pressure or temperature. The C_{10}–C_{18} n-paraffins are strongly adsorbed on a 5A zeolite even at high temperatures. Neither pressure swing nor thermal swing operations are therefore efficient in desorbing the adsorbate. Displacement desorption is employed instead, which involves the displacement of the adsorbate by means of a second adsorbate gas purge (Chi and Cummings 1978). This technique will be described in Section 7.6.

7.3.4 Air separation into O_2 and N_2 employing two different processes

First we describe the separation of O_2 from air using a 5A zeolite adsorbent in a PSA process. As indicated in Section 7.2.1, a two-bed process described by Figures 7.1 and 5.15 is used to separate O_2 from air. On a 5A zeolite bed

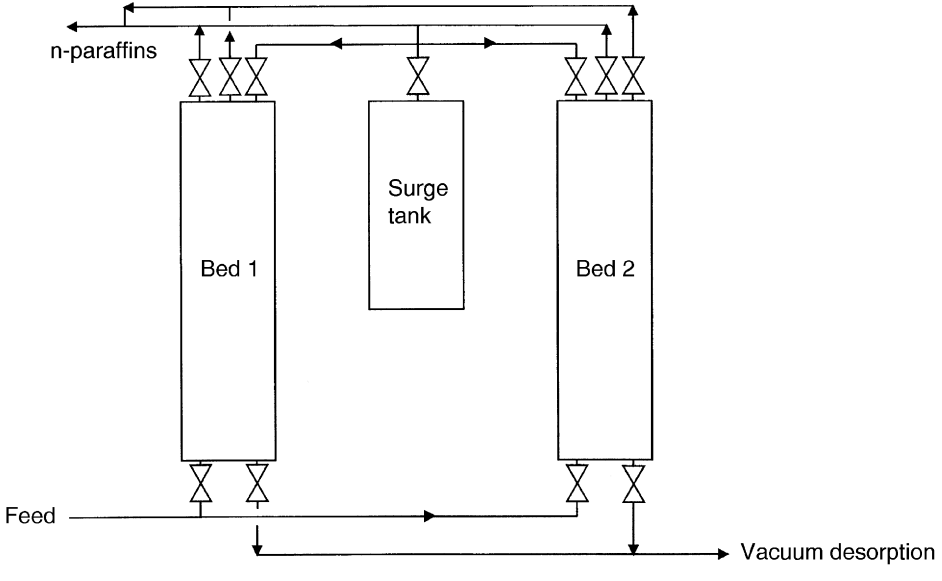

Figure 7.4 n-paraffin separation plant and sequence of events (source: Cassidy 1984).

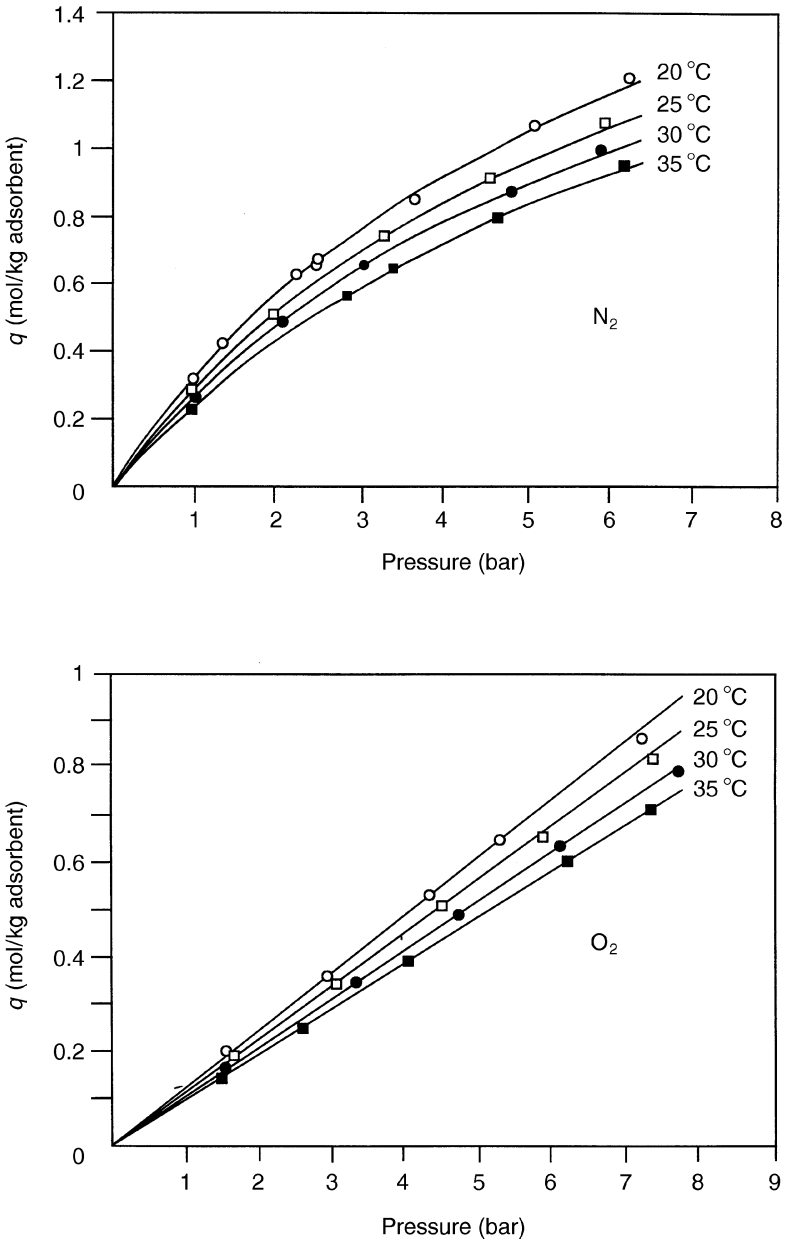

Figure 7.5 *N_2 and O_2 isotherms on a 5A zeolite.*

nitrogen is adsorbed to a much greater extent than oxygen and this is clearly shown in Figure 7.5. Hence, during the basic two-bed Skarstrom cycle for producing oxygen of up to 95% purity on a small scale (e.g. for medical use) oxygen is recovered during the second step of the process when the two beds are connected together following pressurization of the first column with air. Nitrogen is retained in the bed while oxygen (being the least strongly adsorbed component) passes through bed 1 and is collected concomitantly as it flows through bed 2, thus purging the latter bed by countercurrent flow (known as back purging). The oxygen recovery is, however, less than 25% and would be quite uneconomic for the large-scale production of oxygen. Units producing large throughputs of oxygen utilize six steps comprising adsorption, pressure equalization, desorption, back purging, a pressure equalization step and repressurization; this arrangement gives better oxygen recovery. These more complex processes have been reviewed by Davis (1972). A process involving vacuum desorption of nitrogen (and other contaminants such as carbon dioxide and water vapour) has proved to be of commercial value (Sircar and Zondlo 1977). Such a system is capable of producing oxygen of 93% purity (balance N_2 and Ar) at throughputs of 100 tonnes per day. Such plants are now in wide use. Vacuum swing adsorption has two major advantages compared with a pressure swing adsorption operation of similar capacity. First the adsorbent capacity is higher under vacuum operation than pressure swing operation, thus allowing more nitrogen to be adsorbed during the adsorption step, and secondly, there is a smaller demand on energy use with savings of up to 30%. Energy savings accrue because the feed does not require as much compression – just sufficient to overcome the pressure drop of the adsorbent beds. Only three basic steps are necessary for the vacuum adsorption process described and which is illustrated for a three-bed system in Figure 7.6. The steps are adsorption, desorption and repressurization. During the adsorption step air is fed to one of the adsorbent beds by a low pressure blower. Water vapour, carbon dioxide and nitrogen are selectively adsorbed in the bed thus allowing high purity oxygen to pass through the bed to be delivered as product. Oxygen purity declines slightly during the complete cycle of events. The time interval for the adsorption step is thus set to give a specific average oxygen purity. Nitrogen, water vapour and carbon dioxide contaminants are removed during the desorption interval by applying vacuum to the adsorbent bed. The remaining step in the whole cycle is repressurization of the bed which occurs by using atmospheric air together with a fraction of the product oxygen stream. Cycle times for the process are of the order of two minutes.

The production of nitrogen, as opposed to oxygen, is achieved using a molecular sieve carbon which preferentially adsorbs oxygen. Figure 2.5

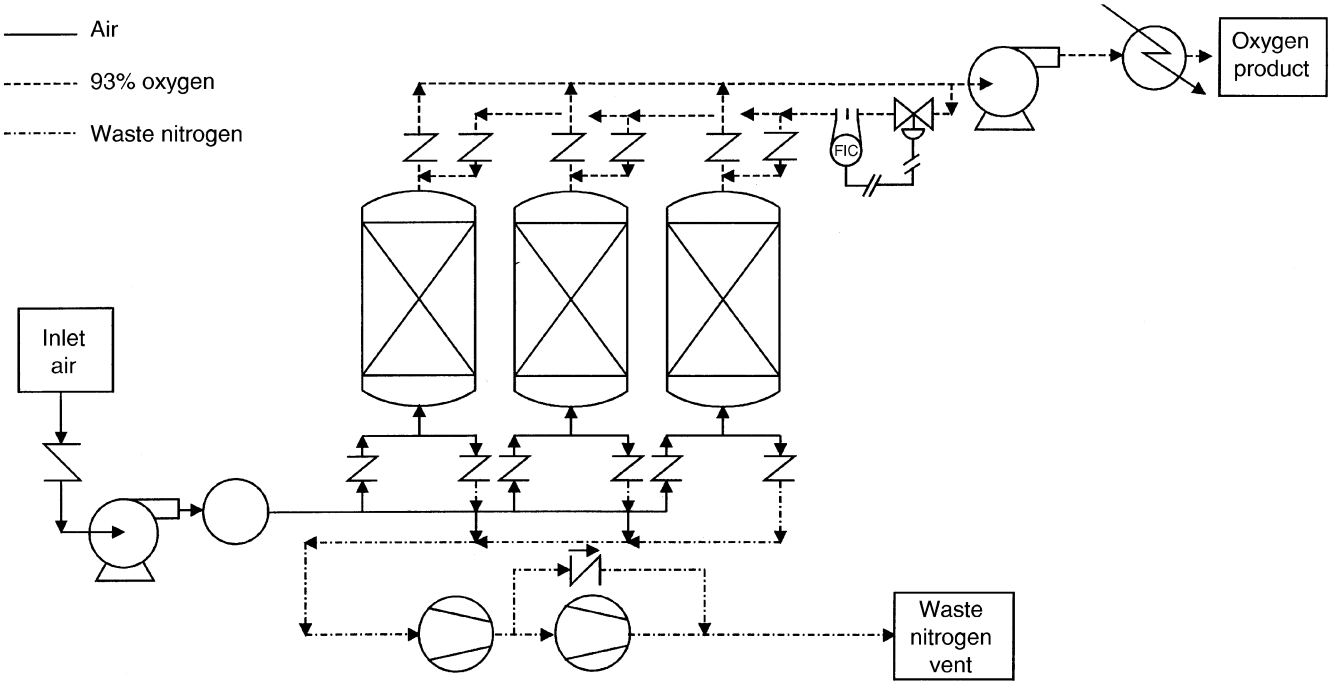

Figure 7.6 Three-bed vacuum swing adsorption process for O_2 production (by kind permission of Air Products plc).

illustrates the much faster rate of uptake of O_2 by a molecular sieve carbon than nitrogen. The rate of adsorption of O_2 is faster than that of N_2 by a factor of approximately 2.5×10^2 and is due to the large diffusion coefficient of O_2 into particles of molecular sieve carbon in comparison with N_2. During the adsorption step of a PSA process, therefore, oxygen is preferentially retained in the adsorbent bed and nitrogen passes through and may be collected. The Bergbau–Forschung process is a simple process for producing N_2 from air and involves a two-step cycle (Knoblauch 1978). During the first step of about one minute interval, adsorption of oxygen occurs at about 3 to 5 bar pressure. The second step is countercurrent evacuation at approximately 0.1 bar pressure and is also of about one minute duration. It is reported that at an adsorbing pressure of 5 bar, the flow of product N_2 at 98% purity is approximately 40 m^3h^{-1}. The balance of gas in the N_2 product is argon. Nitrogen recovery from air by this process is about 50%. The desorption product obtained in the countercurrent evacuation step contains about 35% O_2 (the balance being N_2, CO_2 and water vapour). If an intermediate purge step is introduced into the cycle, the purity of the desorbed oxygen product can be considerably enhanced and utilized for other process operations.

7.4 THERMAL SWING ADSORPTION (TSA) PROCESSES

7.4.1 Two-bed systems

Four operating steps comprise the basic two-bed thermal swing process (see Figure 5.18). Separation of components occurs during the first (adsorption) step of the thermal swing cycle, the most strongly adsorbed component being retained in the adsorbent bed while the least strongly adsorbed component passes through the bed. Thus the feed mixture containing an adsorbate at a partial pressure p_1 is passed through the adsorbent bed, operating at a temperature T_1, where the adsorbate is wholly or partially removed from the feed stream. The loading of adsorbate on the adsorbent at this first stage is q_1 (see Figure 5.14b). When regeneration of bed 1 is required its temperature is raised to T_2 by passing hot feed, hot inert purge or steam through the bed. Raising the temperature of bed 1 to T_2 constitutes the second stage of the thermal swing process during which the adsorbate loading diminishes to q_2. The third stage of the process cycle is that of bed regeneration when bed 1 is heated to an elevated temperature with either hot feed or a hot purge gas. The final process stage is when bed 1 is cooled to the original temperature T_1 (step 4).

During the period when bed 1 is adsorbing, bed 2 is being desorbed which includes the times required for heating and cooling. The two-bed thermal swing process requires that the time taken for desorbing gases from the first bed matches the time allowed for adsorption in the second bed, otherwise flow of the product gas would be discontinuous. Similarly, the time allocated for adsorption in bed 2 must equal the time required for desorption in bed 1. Total cycle times for thermal swing processes are of the order of hours (rather than minutes as for pressure swing adsorption cycles) because of the thermal inertia of the packed beds.

In a two-bed thermal swing process the limitation imposed by equal times for adsorption and desorption engenders inflexibility of operation and reduces the effective loading capacity of the beds. If the more strongly adsorbed component of the mixture to be separated has an equilibrium isotherm convex to the axis representing quantity adsorbed (favourable type of isotherm), the desorption part of the cycle becomes the limiting factor of the overall cycle time. For a favourable type of adsorption isotherm the concentration wave travelling through the bed tends toward a constant pattern, but during desorption the wave becomes dispersed thus broadening the mass transfer zone (see Chapter 6). If, therefore, both flow rate and temperature were maintained at the same values for both adsorption and desorption, a longer period would be required for desorption than adsorption. The requirement for equal adsorption and desorption times in a two-bed temperature swing cycle, therefore, means that only a fraction of the adsorbate present in the feed can be removed during the desorption step of the cycle. Bed capacity is consequently not fully utilized.

Because of the long cycle times required for thermal swing separations this mode of operation is used almost exclusively for the removal of low concentrations of adsorbable gases from feed streams. Furthermore, substantial amounts of energy can be used in supplying sensible heat and the heat of desorption unless the concentration of the component to be removed is small. As mentioned in Section 7.1, a combination of inert gas purge stripping and thermal swing operations may be used for the desorption of strongly adsorbed components.

7.4.2 Three-bed systems

When the length of the mass transfer zone (MTZ) is long relative to the length of the bed in which adsorbate is in equilibrium with adsorbent the extent of bed utilization is small (see Chapter 6). An improvement in total bed capacity usage, however, may be achieved by the use of three adsorbent beds. The operating sequence in such cases is illustrated in

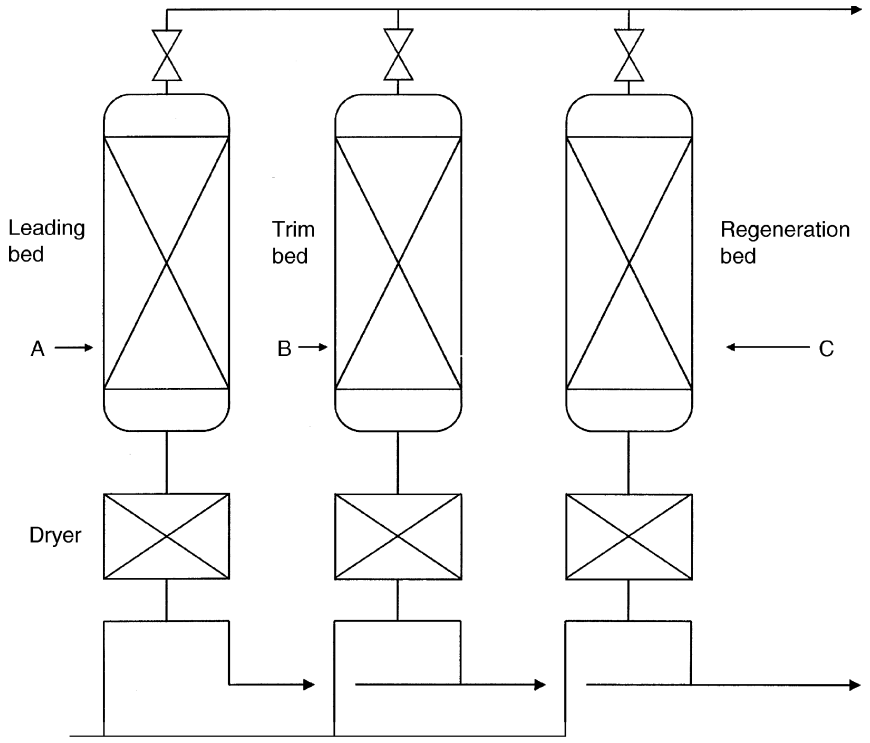

***Figure** 7.7 Improvement of bed capacity using three beds.*

Figure 7.7. Feed first enters bed A (called the lead bed), in which adsorption occurs, and subsequently passes through bed B which has had the least time on stream since regeneration. The adsorbate is allowed to break through bed A prior to passage through bed B (termed the trim bed) without allowing breakthrough from bed B. By this means bed A can be fully utilized before it is taken off stream for regeneration. Bed B then becomes the lead bed and the third bed, bed C, becomes the trim bed. Initially, therefore, bed A is the leading adsorber, bed B the trim adsorber while bed C is being regenerated. Each bed then reverts to an alternative role.

7.5 COMMERCIAL TSA PROCESSES

Commercial applications of thermal swing processes are more commonly for the purification of gases and liquids than for the bulk separation of gases.

Examples of the former are the drying of air or natural gas, the removal of solvent vapours from air streams, the sweetening of natural gas, the removal of diethylbenzene from aromatics and the purification of liquid organic compounds. An example of the bulk separation of components by thermal swing adsorption is the extraction of water from ethanol.

7.5.1 Drying of gases

Removal of low concentrations of water vapour from gases or air is important for the protection of compressors and also for the care of electronic equipment. Dewpoints between −30°C and −50°C may be achieved. Figure 5.18 illustrates a typical two-bed thermal swing process for the drying of gases. Thus the gas to be dried flows initially through an adsorption bed where moisture is removed by a porous material suitable for drying. During the time one bed is adsorbing moisture the other bed is being regenerated at a higher temperature as described in Section 7.4. The operation is reversed once regeneration is complete, the second bed now acting as the adsorber while the first bed is being regenerated.

The choice of adsorbent for the beds depends on the particular drying application. If only a moderate humidity is required for the process air or gas, silica gel is to be preferred as the adsorbent as it has a high capacity and is easily regenerated. If, on the other hand, low dewpoints are required then a molecular sieve is superior.

7.5.2 Gas sweetening

Natural gas process streams sometimes contain components such as hydrogen sulphide, mercaptan, carbon dioxide and water vapour. To remove these undesirable constituents of natural gas (known as sweetening in the petrochemical industries) a three-bed system can be employed. A large-pore zeolite is used as adsorbent, the strength of adsorption of the components to be removed being $H_2O > H_2S > CO_2$. Because three adsorbates are present in the feed the breakthrough of each component in an adsorption bed would display a composite pattern as shown in Figure 7.8. The most weakly adsorbed component, CO_2, breaks through first but as both H_2S and H_2O are more strongly adsorbed, some of the CO_2 is displaced from the adsorbent to give a higher gas phase concentration than was originally present in the feed. As H_2S then begins to break through, some CO_2 is re-adsorbed and its gas phase concentration reverts to that of the feed indicating that the bed is saturated with respect to CO_2. Similarly the more strongly adsorbed water vapour displaces some H_2S from the surface until

finally H_2O begins to break through the bed when the H_2S gas phase concentration returns to its feed concentration. These effects, caused by displacement of a relatively weakly adsorbed component by a more strongly adsorbed component are sometimes referred to as roll-up effects. The composite curve in Figure 7.8 thus contains three constant pattern mass transfer zones (see Chapter 6) separated by two plateau zones. The adsorber can be designed by utilizing the length of unused bed (LUB) concept (see Chapter 6). When, as is more usual, the requirement is to remove H_2S and H_2O only, the adsorber is operated until the H_2S starts to break through the bed. Both the width of the H_2S mass transfer zone and the length of bed saturated with H_2O should be found when estimating the length of unused bed. An empirical correlation for the LUB has been published by Chi and Lee (1973).

Three beds are used for the sweetening of a sour gas stream as depicted in Figure 7.9. One bed is adsorbing while one of the other beds is being cooled (following regeneration) and one regenerated. Formation of undesirable quantities of COS (by interaction of H_2S and CO_2 on the adsorbent surface) can be minimized by using Ca^{2+}-exchanged zeolite adsorbents rather than the usual Na^+-exchanged form. Neither should the clay adsorbent binder contain traces of iron which would catalyse the interaction.

7.5.3 Removal of water from volatile organic compounds

Depending on the nature of the process, the organic compound containing water may be in the form of a vapour or liquid stream. If in the form of an uncondensed vapour issuing, for example, from a distillation column, water removal may be accomplished by using two adsorption columns, each column employed alternately as an adsorber and a regenerator. Furthermore, by judicious choice of operating conditions considerable quantities of the heat of adsorption may be retained within the adsorbent bed to facilitate regeneration. When the mixture of volatile organic and water is in liquid form, a two-column arrangement may still be used but the advantages of retaining heat within the adsorption bed are lost. The two examples described are for the removal of water from an alcohol–water mixture with a composition near to that of the azeotrope. The first example deals with removal of water from a vapour stream and the second example concerns a liquid stream.

The adsorbent normally used in both the vapour and the liquid processes is a zeolite molecular sieve. The particular zeolite used for extracting water from an ethanol–water liquid or vapour stream is the 3A variety in which sodium has been replaced by potassium by ion exchange. As the molecular

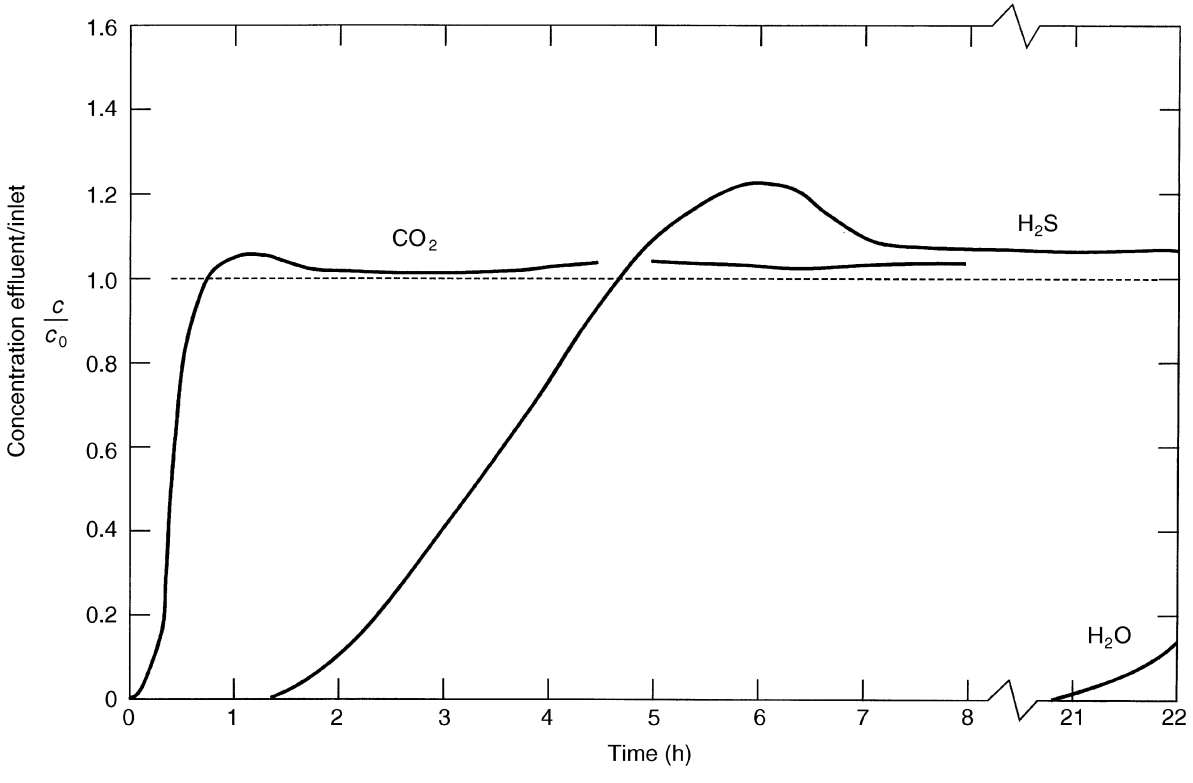

Figure 7.8 *Composite breakthrough for three adsorbable components (H_2O, H_2S and CO_2) on a zeolite (source: Chi and Lee 1973).*

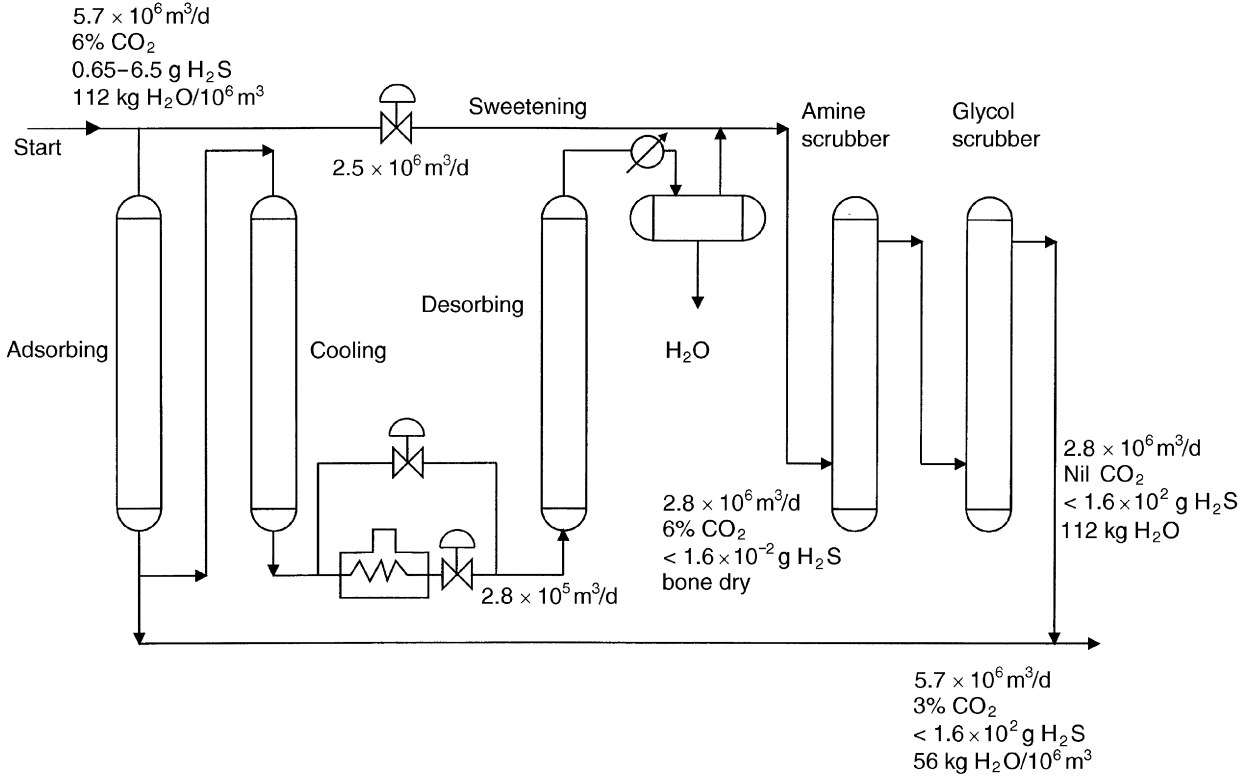

Figure 7.9 *Sweetening of sour gas stream by a thermal swing process (source: Chi and Cummings 1978).*

size of water is 0.28 nm the sieve can adsorb water molecules but exclude the larger ethanol (0.44 nm) molecules.

Drying of vaporized ethanol–water mixtures

The drying of gases and vapours usually implies the removal of low concentrations of water and is accomplished as briefly described in Section 7.5.1. Because of inefficiencies caused by the release of large quantities of heat, such a process is not suitable for the removal of large quantities of water from gaseous streams such as would be present in a vaporized azeotropic mixture of ethanol and water emerging from a distillation column and which has a composition of 10.6 mole % H_2O at 1 bar pressure. Union Carbide, however, operate an adsorptive heat recovery (AHR) drying system (Garg and Ausikaitis 1983, Garg and Yon 1986) which enables much of the heat released on adsorption to be retained by the adsorbent bed thus enabling the stored heat to be utilized for the regeneration step of the cycle.

The principle upon which the design of an AHR system depends is to ensure that the temperature wave front which traverses the adsorption bed travels at a velocity such that it is retained within the mass transfer zone. Both Ruthven (1984) and Yang (1987) have given analytical expressions which describe the conditions for which the concentration and temperature waves travel at identical velocities. Furthermore, Yang (1987) deduced that the condition for coincident temperature and concentration wave fronts is

$$(c_s/c_{pg}) > (q^*/y) \tag{7.1}$$

where c_{pg} is the heat capacity of the adsorbate and other carrier gas, c_s is the heat capacity of the solid adsorbent and (q^*/y) is (at the bed inlet) the ratio of the equilibrium mass of adsorbate adsorbed per unit mass of adsorbent to the mole fraction of adsorbate in the gas phase. This inequality turns out to be similar to the empirical cross-over ratio R (Garg and Ausikaitis 1983) described previously in Chapter 6 (equation 6.18). The parameter R is a measure of the non-isothermality of a system. When $R > 1$ heat is removed from the mass transfer zone with comparative ease and the system remains approximately isothermal. This is because the temperature wave is far ahead of the concentration front so that heat is convected from the bed before the mass transfer zone has traversed the adsorbent bed. When R approaches, or is equal to, unity the temperature wave is located within the mass transfer zone and heat is retained in the bed during the whole time that the concentration front moves through the bed. Finally, when $R < 1$ the temperature wave lags behind the mass transfer zone. Clearly then, if the

bed retains the heat of adsorption while the mass transfer zone travels through the bed, the adsorbent solid could be at a sufficiently high temperature to initiate regeneration of the bed immediately following the adsorption step. The ratio R has also been shown to depend on the initial bed temperature, total pressure and type of adsorbent. By the correct choice of cycle conditions, the heat of adsorption can be stored within or behind the mass transfer zone such that heat is retained in the bed before breakthrough of the adsorbate. However, because of the increase in temperature of the bed the capacity of the adsorbent is lower than that for corresponding isothermal conditions. Nevertheless, efficient heat recovery is possible utilizing the AHR drying method. Garg and Yon (1986) showed that a lower volume and temperature of purge gas and only a fraction of the energy is used for the AHR system than for conventional cycles employed to dry gas streams with a high water content.

Figure 7.10 illustrates the AHR process. Two adsorbent beds are employed, each acting alternately as an adsorber and regenerator. The feed is first superheated sufficiently to prevent formation of liquid within the adsorber and the capillary condensation in the adsorbent pore structure. Flow of feed to the adsorber is continued until the capacity of the bed is nearly exhausted but certainly stopped before either any breakthrough of water or any temperature rise of the effluent. The time required to complete the adsorption step is typically 10 to 60 minutes which is much shorter than in conventional thermal swing processes. Regeneration is achieved within a closed loop utilizing a non-condensable gas such as N_2, CO_2 or natural gas in countercurrent flow. The time required for regeneration is equal to that for adsorption in the two-bed configuration.

Drying liquid streams of alcohol–water mixture

Drying of liquid streams is also accomplished using two packed adsorbent beds, each one acting alternately as a dehydrator or a regenerator. The feed to the dehydrator should be near to the azeotrope composition to obtain the best economic advantage and to avoid physical deterioration of the zeolite adsorbent. The direction of the feed flow is normally upward in adsorption and downward during regeneration. Cooling the adsorbent column with inert gas between the adsorption and desorption stages should be upward if the cooling gas is carrying moisture, but if a dry inert gas is used for cooling, upward or downward flow may be chosen. Liquid stream velocity through the bed should not exceed about 7.5 cm min^{-1} according to the recommendations of the adsorbent manufacturers W.R. Grace and Company.

It is important to consider the process economics carefully before selecting a cycle time. The longest time which is physically and economically

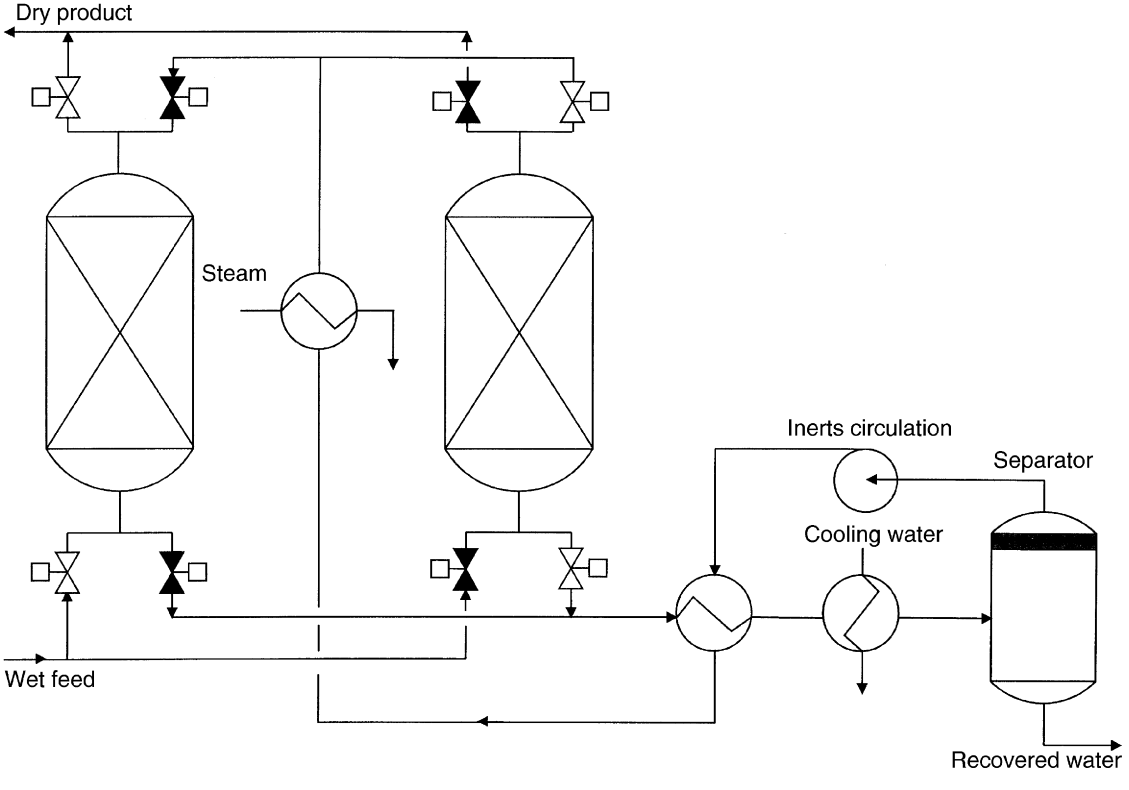

Figure 7.10 Heat recovery system of Union Carbide (source: Garg and Yon 1986).

feasible should be chosen for the adsorption stage. For ethanol dehydration employing a 3A zeolite sieve, W.R. Grace and Company recommend a period not less than 24 hours so that the energy required for heating and cooling the beds of adsorbent and associated vessel and piping is minimized. Hot carbon dioxide or natural gas, depending on the particular process arrangement, may be used for regenerating the bed, the inert gas being passed through a furnace prior to the adsorbent bed. CO_2 from a fermentation unit, or natural gas utilized for firing furnaces, could be employed for regeneration and subsequently used for cooling (after removal of moisture in a typical gas–liquid separator). In this manner a closed loop, containing appropriate heat exchangers, could be usefully employed were CO_2 the inert gas. A semi-closed loop could be used if natural gas were employed, the gas bypassing the furnace during cooling.

7.6 DISPLACEMENT PURGE CYCLES

When regeneration of the adsorbent is not feasible by either a PSA or a TSA process and the relative volatilities of the components militate against distillation, the method of displacement purge regeneration is employed. Neither the pressure nor the temperature of the bed is varied from that during adsorption, regeneration being dependent solely upon the ability of an adsorbable purge to cleanse the bed in readiness for the next adsorption stage. The principle upon which a displacement purge cycle operates (illustrated by means of Figure 7.11) is the reduction of partial pressure of the adsorbate by the displacing purge gas and competitive adsorption of the adsorbate and purge. In Figure 7.11, A is the most strongly adsorbed component of the binary component feed mixture of (A + B) while D is the displacement purge gas. The feed mixture of (A + B) is passed through the bed acting as the adsorber, already loaded with D from the previous cycle (when the column was the regenerator), and a mixture of (B + D) emerges from the top of the column. (B + D) are easily separated by distillation so that the raffinate (B) is collected in a fairly pure state. The displacement purge gas D then enters the second column acting as regenerator and from which emerges a mixture of (A + D) separated without difficulty in a separate distillation column. In effect the original mixture of (A + B), which would have been difficult to separate by PSA or TSA, is separated by the intervention of another strongly adsorbed component D. The ease of separation of A from D and B from D in additional distillation stages is, however, crucial in determining the economics of displacement purge cycle operation.

Commercial processes for the separation of linear paraffins from mixtures

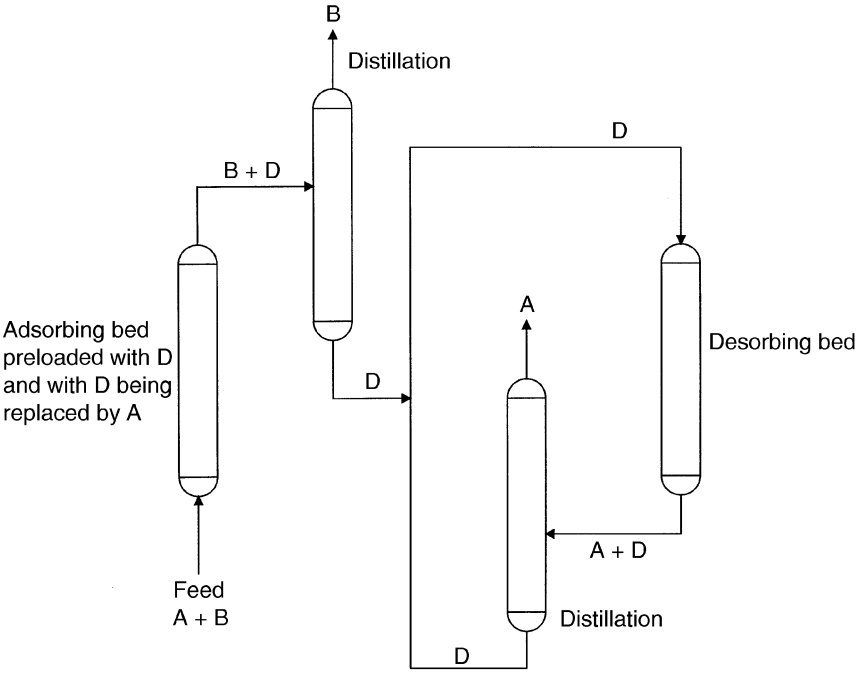

***Figure** 7.11 Principle of a displacement purge cycle operation (source: Keller 1983).*

containing branched chain and cyclic isomers, all with molecular masses typical of hydrocarbons in the C_{10} to C_{18} range, make use of displacement purge gas cycles. The Ensorb process of Exxon, in which ammonia is used as the desorbent, is typical of these displacement purge cycles (Asher *et al.* 1969).

7.7 CONTINUOUS COUNTERCURRENT ADSORPTION SEPARATIONS

Countercurrent operation of an adsorption column in which gaseous or liquid feed is passed continuously through a bed of adsorbent countercurrent to a flow of solid adsorbent is, in principle, more efficient than the previous descriptions of cyclic batch operations because countercurrent flow maximizes the average driving force for mass transfer between fluid and adsorbent. The saturated spent adsorbent emerging from the adsorber

enters a regenerator, in which adsorbent impurities are removed, and is then returned to the adsorber. Figure 7.12 illustrates how such a system would operate. The most strongly adsorbed component of a binary feed consisting of (A + B) is assumed (for the purpose of the illustration) to be A. Pure B emerges as raffinate from the adsorber together with some inert purge P used to remove the adsorbed component A from the adsorbent being circulated through the regenerator. A full review of continuous countercurrent adsorption separation has been given by Ruthven and Ching (1989).

Difficulties of circulating solids through a column in which there is a countercurrent flow of gas or liquid are not easy to overcome. Nevertheless, a number of processes have been developed successfully and a selection of these are described in the following sections.

7.7.1 Removal of a single component from a gaseous or liquid stream

Examples of processes in which a single adsorbable component is removed from a flowing gas or liquid include the drying of air, the removal of

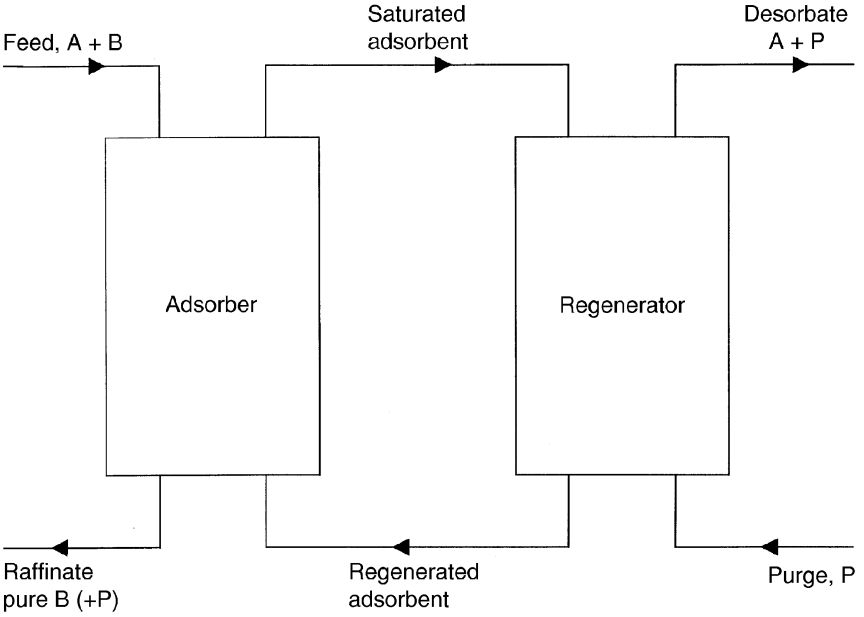

Figure 7.12 *Principle of continuous countercurrent adsorption process.*

vaporized organic solvents from air, the removal of organic compounds from waste water streams, ion exchange processes and sugar decolourization. Although the principle inherent in all of these processes is the adsorption, and hence removal, of an undesirable component from a process fluid which itself is not adsorbed, the mode of operation varies from one process to another. For example, the regeneration of the adsorbent may be by means of heat application or by a purge at a temperature close to that at which the adsorption occurs. In solvent recovery processes, steam stripping is a common procedure for regeneration. The mode of solids conveying also varies from one process to another. The Union Carbide Purasiv process for the recovery of organic solvents from gaseous streams (Keller 1983) is illustrated in Figure 5.9.

The operation of simple countercurrent flow adsorption systems can be represented by a McCabe–Thiele diagram. Figure 7.13 shows the operating lines for adsorption and desorption and a single straight equilibrium line (assuming adsorption and desorption occur at the same temperature). The flow diagram for the process corresponding to the McCabe–Thiele diagram is juxtaposed. The operating lines are defined by mass balances over the adsorption and desorption columns. For adsorption

$$S\,(q - q_{\mathrm{F}}) = F\,(c - c_{\mathrm{F}}) \tag{7.2}$$

and for desorption

$$S\,(q - q_{\mathrm{D}}) = D\,(c - c_{\mathrm{D}}) \tag{7.3}$$

S, F and D represent the flowrates per unit cross section of the adsorbed phase, feed and desorbent, respectively, c_{F} and c_{D} are the concentrations of the single component adsorbate in the feed and desorbing fluid, respectively, and q_{F} and q_{D} are the corresponding adsorbed phase concentrations. The net flow of the adsorbate must be downwards in the adsorption section and upwards in the desorption section in order to achieve removal of the undesired component by the downward flowing adsorbent and regeneration of the contaminated solid by the fluid used for desorption. This implies $F < SK$ and $D > SK$, where K is the adsorptive equilibrium constant. The desorbent flow rate is therefore greater than that of the circulating adsorbent. In order that mass transfer is in the directions required during adsorption and desorption then $c_{\mathrm{E}} < c_{\mathrm{F}}$ and $c_{\mathrm{D}} < c_{\mathrm{R}}$ where subscripts E and R refer to extract and raffinate. Such operations are, in general, uneconomic, and only suitable when there is a plentiful supply of cheap purge fluid.

If regeneration of the adsorbent is achieved at a higher temperature than used for adsorption and without the introduction of an inert purge, the equilibrium line corresponding to desorption will lie below the equilibrium line for adsorption and the requirement that the flow of desorbent be greater

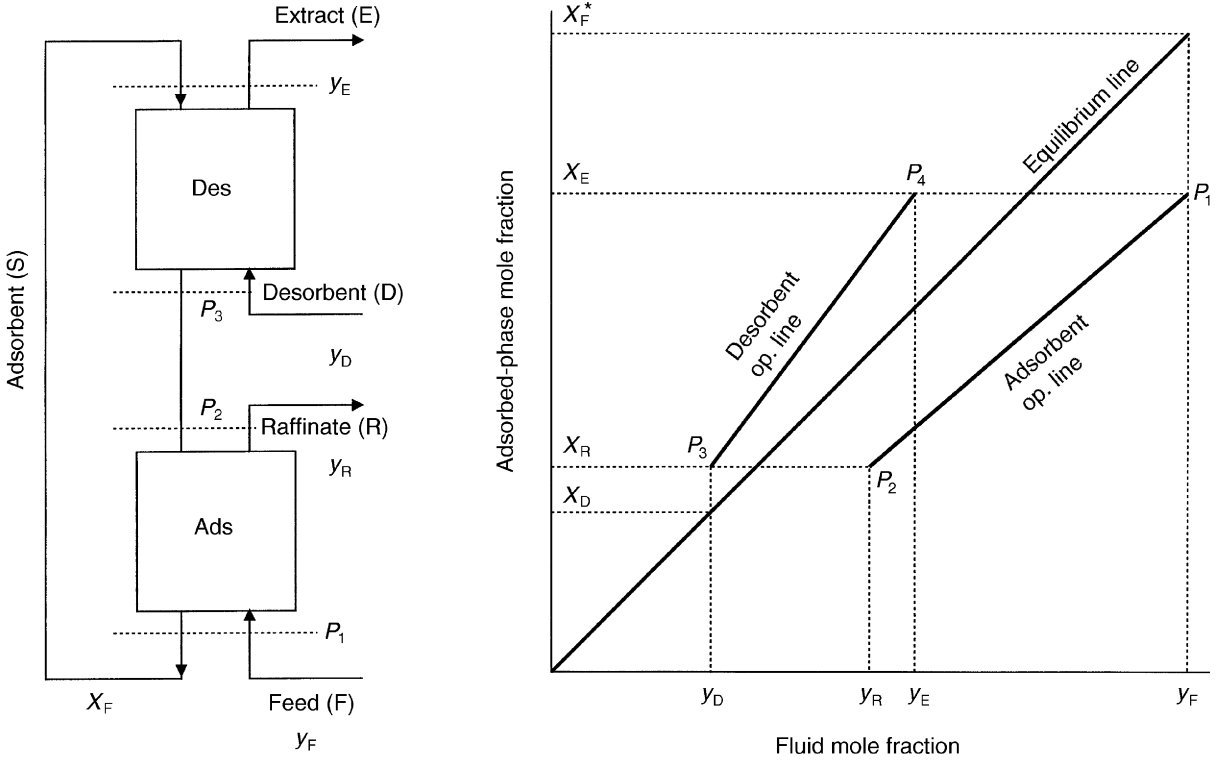

Figure 7.13 *Removal of a single component contaminant from a feed: continuous countercurrent adsorption system and McCabe–Thiele operating diagram (source: Ruthven and Ching 1989).*

than that of the feed is no longer necessary. A fraction of raffinate (the fluid from which the undesired component has been removed) can also be used for regeneration because now $c_F < c_E$. The flow diagram and appropriate McCabe–Thiele diagram for such a system is sketched in Figure 7.14 from which it may be seen that the raffinate has been stripped of the contaminant in the feed. Introducing the feed at the desorption section, however, results in the extract (the fluid containing the undesired component emerging from the desorption section) becoming enriched with the adsorbate.

7.7.2 Adsorptive fractionation

The principles outlined in Section 7.7.1 may be applied to the separation of components from a mixed feed of A (the more strongly adsorbed component) and B (the least strongly adsorbed component). By dividing the column, through which the solid adsorbent flows downward countercurrent to the upward flowing fluid, into a cascade of operating sections and relying on displacement desorption by a third inert fluid D (the desorbent), two products (E the extract and R the raffinate) are generated. The extract will contain a preponderance of A, the more strongly adsorbed component, while the raffinate will consist mainly of B, the least strongly adsorbed component. There is a formal similarity between adsorption fractionation and distillation: introducing a binary component feed F near the middle of the column, a raffinate product enriched in B may be obtained from the uppermost section of the column and an extract product enriched in A from the lower section of the column. The principle of operation may be gleaned from Figure 7.15. Two McCabe –Thiele diagrams are necessary to represent the system, one with the equilibrium line for component A and the other for component B. Flowrates in each of the four sections into which the column is divided are adjusted so that desorption of A and B occurs in the column sections 1 and 2 while adsorption of A and B occurs in sections 3 and 4. The net flow of A should be downwards in sections 1, 2 and 3 and upward in section 4 so that A is moving continuously to the extract port. Similarly the net flow of B should be upwards in sections 2, 3 and 4 and downward in section 1 so that B moves continuously toward the raffinate port. Feed F is introduced between sections 2 and 3 and the desorbent D and solids S circulated in opposite directions, D upwards and S downwards. The operating lines on the McCabe–Thiele diagrams corresponding to each section are shown in Figure 7.15. Note that the operating lines may cross the equilibrium line only at the feed point and effluent (extract and raffinate products) points. The resultant operating lines thus form a hexagon. Slopes of each operating line are determined by relative flowrates.

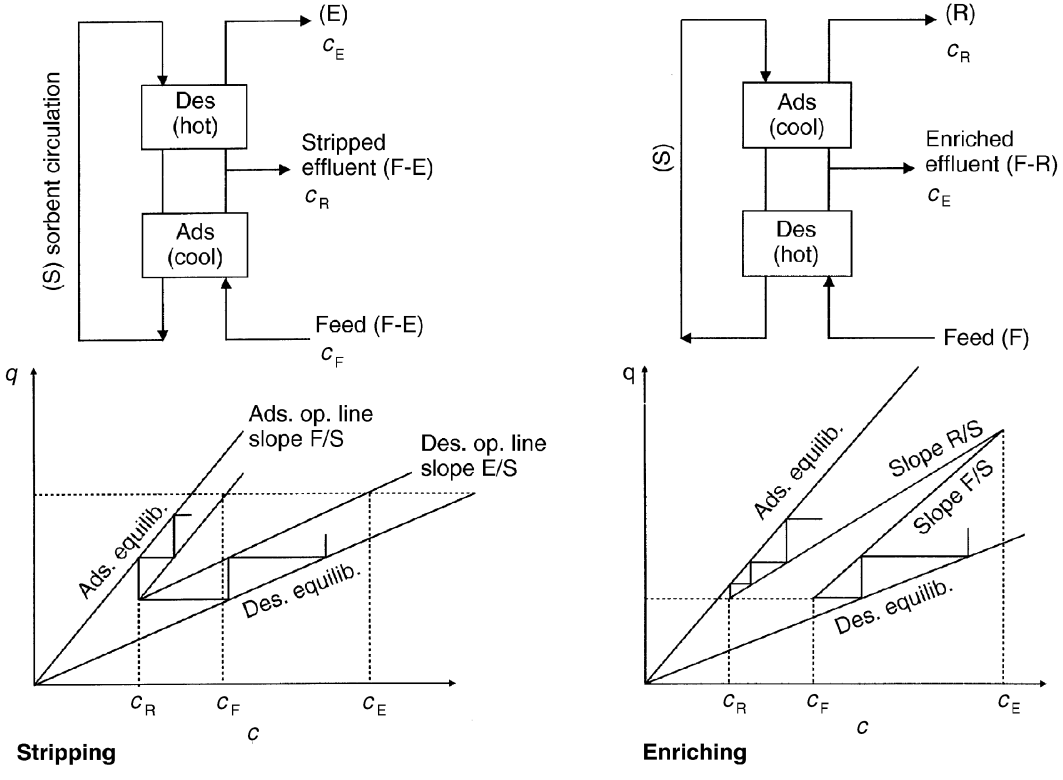

Figure 7.14 *McCabe–Thiele diagrams for stripping and enriching sections of a continuous countercurrent adsorption plant (source: Ruthven and Ching 1989).*

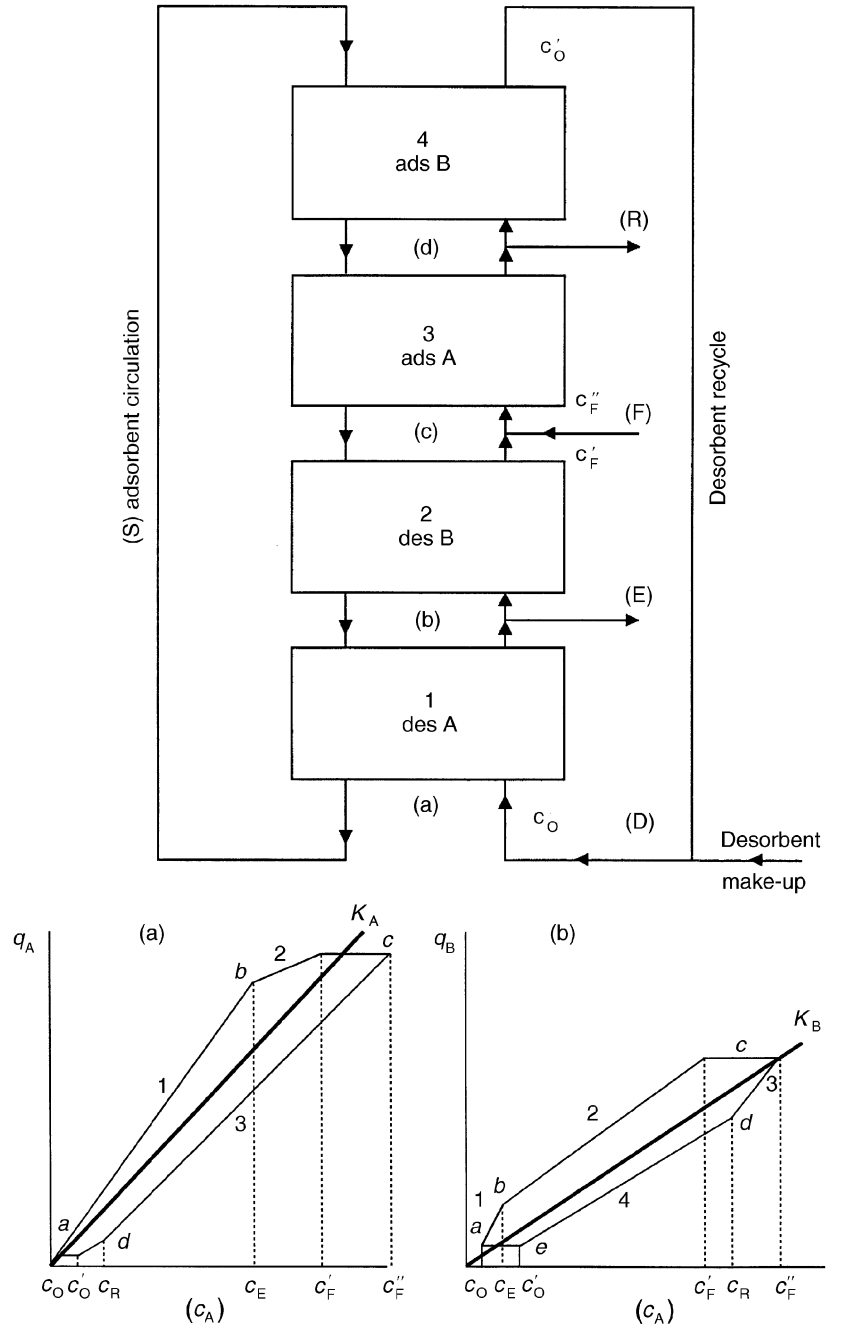

Figure 7.15 *Principle of adsorption fractionation: sketch of flow paths in cascade and corresponding McCabe–Thiele operating diagram for (a) the more strongly adsorbed component and (b) the less strongly adsorbed component (source: Ruthven and Ching 1989).*

Difficulties associated with circulating solids experienced with the discontinued Hypersorption process (Berg 1946) for the recovery of ethylene from a low molecular weight gas have been circumvented by using fluidized beds, one as an adsorbing section and another as a desorbing section. However, losses of efficiency due to the back mixing of solids may severely affect the fractionation when selectivity is constrained by the feed components having similar physical properties. Alternatives including pulsed beds, in which the solid adsorbent is intermittently fluidized, have been reported (Calmon and Gold 1979). Fluid flow is upward for fluidizing and solids transfer and downward when the bed is stationary and contacted with the process fluid. Siegell *et al.* (1986) and Bellows *et al.* (1986) reported the use of magnetically stabilized fluidized beds in which back mixing of solids is substantially reduced.

7.7.3 Simulated moving beds

All of the problems associated with moving solids can be avoided by switching the duty of each of the four sections so that each section assumes the role of its succeeding neighbour downstream (in the direction of fluid flow) by the operation of pneumatic valves (Ruthven and Ching 1989). Each of the four columns is connected in series as shown in the flow diagram of Figure 7.16 but, instead of a countercurrent flow of solids, the solids in each column remain as a stationary bed. Countercurrent operation is then simulated by advancing the desorbent, extract, feed and raffinate ports by one column at specified intervals.

To achieve separation of the components A and B in the feed, certain conditions of flow must be observed. Defining γ_i as the product of the equilibrium constant K_i for component i and the ratio of simulated solid motion S to fluid flow L,

$$\gamma_i = K_i\,(S/L) = K_i \left(\frac{1-e}{e}\right)\left(\frac{u_s}{u}\right) \tag{7.4}$$

where u_s and u are the simulated solids and interstitial fluid velocities, respectively, and e is the bed voidage. The flow conditions which must be observed are, for each bed section,

$$\gamma_A < 1, \gamma_B < 1 \text{ for section 1} \tag{7.5}$$
$$\gamma_A > 1, \gamma_B < 1 \text{ for section 2} \tag{7.6}$$
$$\gamma_A > 1, \gamma_B < 1 \text{ for section 3} \tag{7.7}$$
$$\gamma_A > 1, \gamma_B > 1 \text{ for section 4} \tag{7.8}$$

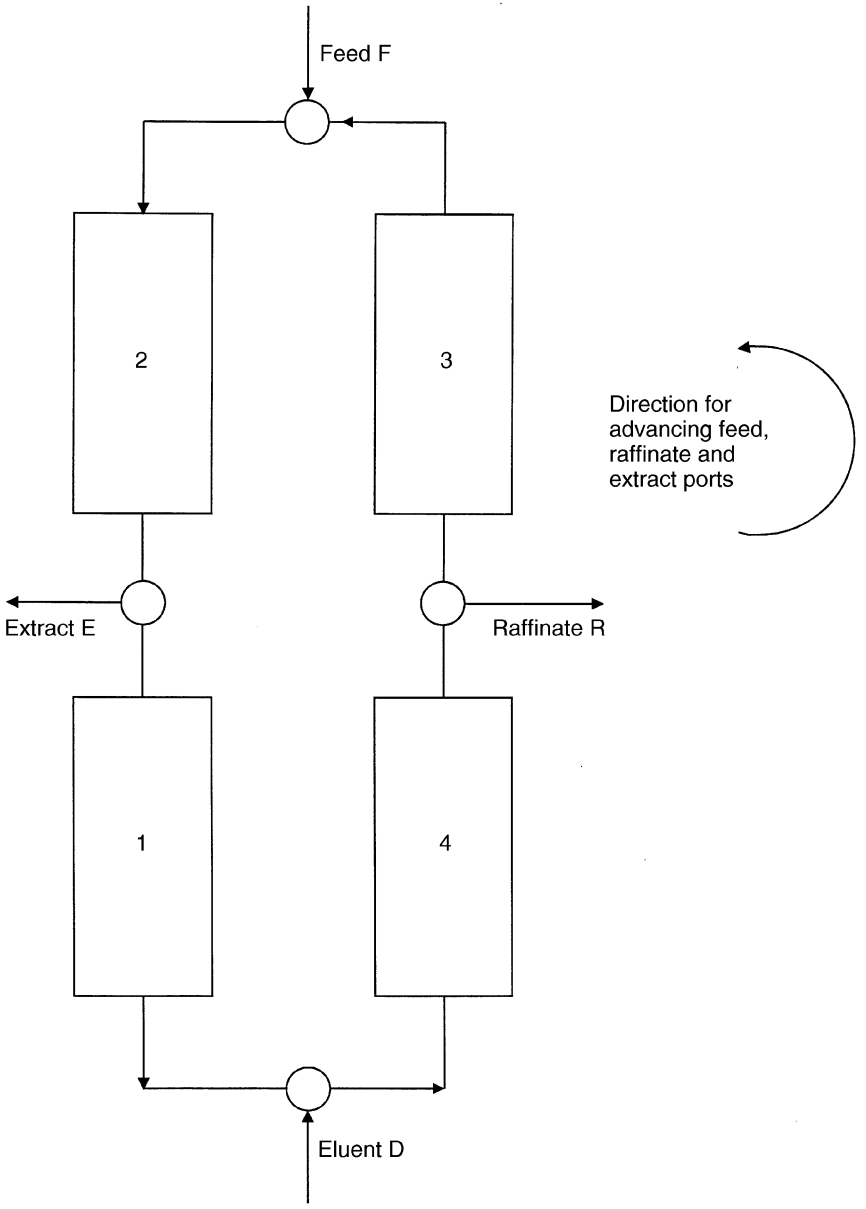

Figure 7.16 *Principle of rotating feed, raffinate and extract points between columns for simulating a moving bed operation.*

If each of the above conditions is met by the same separation factor α (with $\alpha > 1$) the inequalities may be written as mass balances

$$D/S = K_A\,\alpha \text{ in section 1} \tag{7.9}$$
$$(D - E)/S = K_B\,\alpha \text{ in section 2} \tag{7.10}$$
$$\alpha\,(D - E + F)/S = K_A \text{ in section 3} \tag{7.11}$$
$$\alpha\,(D - E + F - R)/S = K_B \text{ in section 4} \tag{7.12}$$

The operating lines in sections 1 and 2 should lie above each of the equilibrium lines while in sections 3 and 4 the operating lines should lie beneath the equilibrium lines. As there are finite changes in flow at the feed inlet and also the raffinate and extract ports, the equilibrium lines will be crossed by operating lines at these positions because there will be sudden changes in the fluid phase composition without any concomitant change in adsorbed phase composition. The McCabe–Thiele diagrams pertaining to components A and B in a simulated moving bed system will be identical to the countercurrent cascade described in Section 7.7.2 and illustrated by Figure 7.15. Most of the separation of components for the extract product E occurs in sections 1 and 3 while the separation of components for the raffinate product R is mainly in sections 2 and 4. Reducing the ratio L/S forces the operating lines closer to the equilibrium lines thus reducing the mass transfer driving force. By analogy with distillation technology this could be interpreted as requiring a larger number of theoretical stages, or, for the simulated moving bed, necessitating that each of the four beds be increased in size. As the conditions for separation of components A and B must be $\gamma_A > 1$ and $\gamma_B < 1$ then the inequality

$$K_A > \frac{D + F}{S} > \frac{D}{S} > K_B \tag{7.13}$$

must hold and there is therefore an optimum choice to be made between the size of each bed and the desorbent flow rate.

7.7.4 Modelling

Modelling both the continuous countercurrent and simulated moving bed processes has been considered by a number of authors. The continuous countercurrent separation process has been addressed by Ching and Ruthven (1984), who assumed axially dispersed flow of fluid and countercurrent plug flow of solids in a column. The fundamental differential equation describing the steady state operation of such a system is, for each component,

$$D_L \frac{d^2c}{dz^2} - u\frac{dc}{dz} + \left(\frac{1-e}{e}\right) u_s \frac{dq}{dz} = 0 \tag{7.14}$$

where e is the bed voidage, c and q are fluid and solid phase concentrations (each on the basis of moles per unit mass) at a point z in the column, u_s and u are the solid and interstitial fluid flow rates and D_L is the axial dispersion coefficient.

Assuming the rate of adsorption dq/dt (equivalent to $-u_s\, dq/dz$) can be represented by a linear driving force $k(q^* - q)$ and that a linear equilibrium relationship $q^* = Kc$ holds, the defining equation becomes

$$D_L \frac{d^2c}{dz^2} - u\frac{dc}{dz} - \left(\frac{1-e}{e}\right) k(Kc - q) = 0 \tag{7.15}$$

A steady state material balance between a plane z in the column and the inlet yields

$$(1-e)\, u_s\, (q - q_0) = eu\, (c - c_0) \tag{7.16}$$

Substitution of this mass balance into the differential equation for the column and application of the usual Dankwerts boundary condition at the column fluid entrance ($z = 0$) and zero change of concentration flux at the column exit ($z = L$) leads to a formal solution for the concentration ratio. When plug flow prevails and mass transfer resistance is small, c_L/c_0 is given by

$$\frac{c_L}{c_0} = \frac{1}{\gamma - 1}\left\{ \; (1 - q_0/K_{C_0})\gamma e^{St(1-\gamma)} + \gamma q_0/Kc_0 - 1 \; \right\} \tag{7.17}$$

where the Stanton number $St = kL/u$ and $\gamma = (1 - e)\, Ku_s/eu$. For a four-column countercurrent adsorptive fractionating system there are four such equations. In conjunction with four mass balances over each of the four beds and two additional mass balances at the feed point and over the fluid recirculating stream, ten equations define the total system enabling ten unknown fluid and adsorbent concentrations to be found. Given values for the Peclet and Stanton numbers (*Pe* and *St*), the two equilibrium constants K_A and K_B, the bed voidage e and the dispersion coefficient D_L, any given adsorptive fractionation of a binary feed may be completely described.

As an alternative to the continuous countercurrent model an equilibrium stage model of the adsorptive fractionation system exists (Ching *et al.* 1985). In effect the concentration ratio c_L/c_0 for each column is represented by the well-known equation (Kremser 1930, Souders and Brown 1932):

$$\frac{c_0 - c_L}{c_0 - c_L/K} = \frac{\gamma^{n+1} - \gamma}{\gamma^{n+1} - 1} \tag{7.18}$$

describing concentration conditions into, c_0, and out of, c_L, a number, n, of equilibrium stages.

Numerical computation of the simulated moving bed system provides a second alternative description to the continuous countercurrent and equilibrium stage models (Barker *et al*. 1983, Ching 1983, Hashimito *et al*. 1983, Carta and Pigford 1986, and Ching *et al*. 1987). Each bed of total volume V is considered to be equivalent to a number, n, of ideal mixing cells in which the fluid and adsorbed phases, volumes V_L and V_s, respectively, are distributed according to

$$V_L = eV/n \text{ and } V_s = (1 - e)\, V/n \tag{7.19}$$

Assuming mass transfer equilibrium in each cell, a differential mass balance for component A across the ith cell gives

$$\frac{dc_i}{dt} = \left(\frac{u}{V_L + KV_s}\right)(c_{i-1} - c_i) \qquad i = 1, 2, \ldots, (n-1), n \tag{7.20}$$

Here u is the constant volumetric flow rate within each of the bed sections but will differ for each of the four sections due to the introduction of feed and withdrawal of products. Similarly, fluid concentration (moles/volume) remains constant within each bed section but will differ between sections 2 and 3 where feed is introduced and between sections 4 and 1 where desorbent make up is added (see Figure 7.16). Both the differences in fluid flow u and concentration c at each stage can easily be represented by simple mass balances over appropriate sections and at the feed and desorbent input points. The unsteady state linear first-order differential equation for n cells within each bed section coupled with the two sets of mass balances can be solved by standard numerical techniques from zero time with defined initial conditions. The calculation is continued by advancing the feed, raffinate, extract and recirculation points at chosen time intervals until a steady state is approached. Figure 7.17 illustrates, for fructose and glucose separation, (Ching *et al*. 1985, Ruthven and Ching 1989) the extent of agreement obtained between the numerical simulation and the countercurrent models.

Isothermal operation is not necessarily suitable for all simulated moving bed systems. The concentration of extract and raffinate streams can never exceed the concentration of feed components for a system with a linear isotherm. Furthermore, when the operating and equilibrium lines are close an excessive number of theoretical plates (to use the parlance of distillation and absorption technology) or height of each bed would be required for separation. Constraints such as these may be circumvented by non- isothermal operation of a simulated moving bed (Ching and Ruthven 1986). By maintaining bed section 1 at an elevated temperature with sections 2, 3 and 4 at a lower temperature,

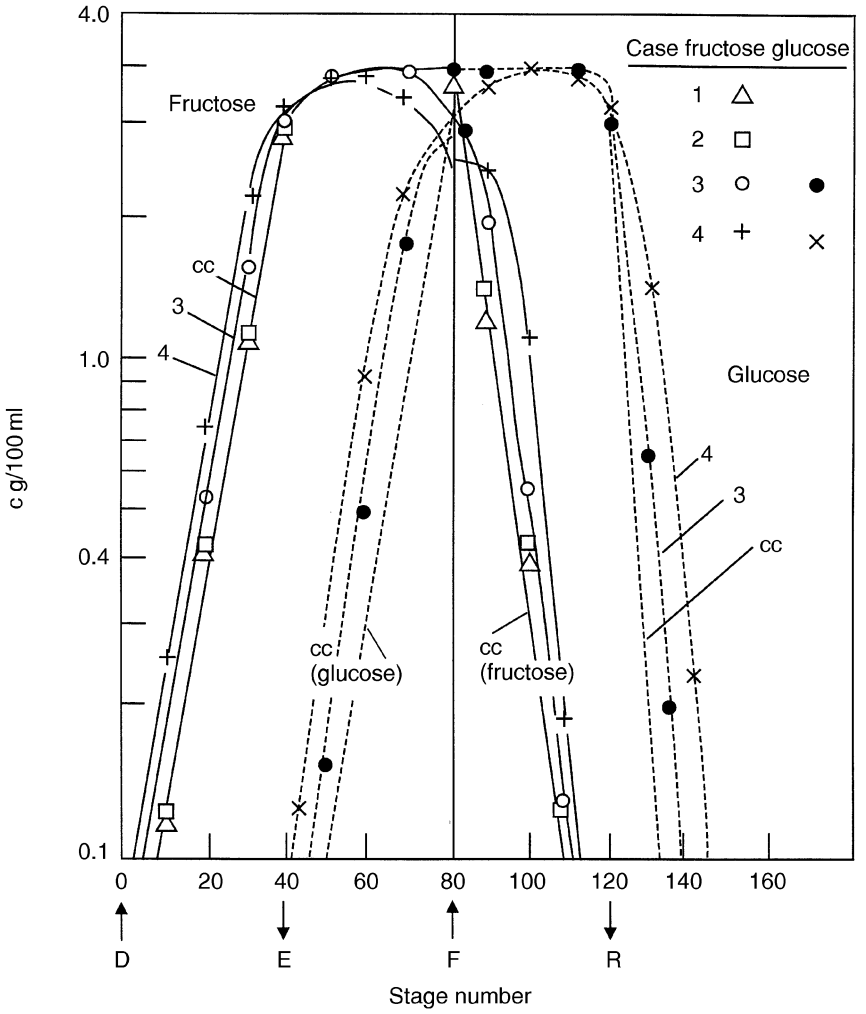

Figure 7.17 *Profiles for fructose–glucose separation calculated from the steady state countercurrent (cc) model compared with results calculated by numerical simulation at the midpoint of the switch interval for eight (case 1), four (case 2), two (case 3) and one (case 4) columns (source: Hidajat et al.* 1986).

the extract product emerges at a higher concentration than would otherwise be achieved. Ching *et al.* (1987) have also investigated systems for which the equilibrium relationship is not linear.

Many industrial countercurrent fractionation processes for the separation of components operate on the principle of either the three and four section cascade or the simulated moving bed. A summary of simulated moving bed and countercurrent fractionation processes is given in Table 5.1. With the exception of the Hypersorption process all are presently operated commercially.

7.7.5 Sorbex processes

A family of similar processes have been developed by UOP for a variety of difficult industrial separations. These have been reviewed by Broughton *et al.* (1970), de Rosset *et al.* (1981) and Broughton and Gembicki (1984). Each of these operates on the same principle as the simulated moving bed system previously described (see Figure 7.16). The generic title of the industrial processes referred to is Sorbex. The configuration of the separation unit is, however, based upon a single packed column rather than three or four interconnected beds. Figure 5.13 shows how the single column is divided up into sections into which fluid may be introduced or from which fluid may be withdrawn by means of specially designed flow distributors. A pump sited external to the column enables circulation of fluid from bottom to top of the packed bed. Only four of twelve connections to the column are utilized at any given time. Flows are switched by means of a rotary valve so that the desorbent, extract, feed and raffinate connections are simultaneously advanced by one bed section in the direction of fluid flow. Because of the switching of connection points between rotary valve and column, flow varies through the circulating pump, which must be capable of handling a steady controlled flow at four different flow rates.

Choice of adsorbent material and desorbent fluid is crucial to the economic viability of any particular Sorbex process. It is important that the extract fluid consisting of the more strongly adsorbed component and desorbent (A + D) and the raffinate product consisting of the least strongly adsorbed component and desorbent (B + D) are capable of being separated by downstream distillation. Ideally the separation factor for A and D, α_{AD}, should be equal to that for B and D, α_{BD}. However, such is rarely the case although when D is adsorbed more strongly than the raffinate product but less strongly than the extract product, specified product purities can normally be achieved.

The Parex process for the separation of isomers of xylene is based on the Sorbex configuration as is the Ebex process for the recovery of ethyl benzene. Both these processes utilize cationic forms of X and Y zeolites with toluene or *p*-diethylbenzene as desorbent in the Parex process and toluene as desorbent for the Ebex process. The Molex process (also based on the

Sorbex configuration) utilizes a 5A zeolite adsorbent and light naphtha as desorbent for the separation of linear and branched chain paraffins. Olefins may be separated from saturated hydrocarbon isomers by the Olex process using CaX zeolite as adsorbent and heavy naphtha as desorbent. Separation of fructose from glucose is achieved in the Sarex process using CaY zeolite as adsorbent and water as desorbent. All of these processes are summarized in Table 5.1.

7.8 CHROMATOGRAPHIC PROCESSES

The principles of chromatographic separation are widely used for gas or liquid analysis. Chromatography has also been applied for the preparation of pharmaceuticals on a scale of about 1 tonne per day. Chromatography requires uniform packing of adsorbent and on a larger processing scale this is difficult. Despite this, however, special packing devices have been designed and a larger-scale chromatographic process is operated commercially by Elf Aquitaine and Société de Récherches Techniques Industrielles (SRTI). The Elf-SRTI process is designed to separate 100 tonnes per year of perfume constituents. A plant to separate 10^5 tonnes per year of normal and iso-paraffins has also been reported (Bernard *et al*. 1981). A flow representation of the Elf-Aquitaine process is shown in Figure 7.18. Heated light naphtha is distributed to a device which is capable of injecting pulses of the naphtha feed into three specially packed chromatographic columns. Injection into each column is arranged in sequence so that a continuous flow can be maintained. Each column, however, is acting in a batchwise manner, the components of the light naphtha separating into its constituents as the pulse of feed traverses the column. The constituent with the least retention time in the column emerges first and is collected in a receiving vessel. Constituent components of the feed with longer retention times then follow and are received in other fraction collectors.

A review of the principles involved in large-scale chromatography has been presented by Conder (1973), LeGoff and Midoux (1981) and Valentin and Midoux (1981). These articles should be consulted for fuller details. Here we discuss, very briefly, what influences the efficiency of component separation in a packed column. Separation of the components of a mixture occurs preferentially according to the relative strengths of adsorption of each component on the solid packing. Equilibration between the flowing gas or vapour (the mobile phase) and the adsorbent (the stationary phase) prevails during the continuous contact between the two phases in the column, thus providing for a much superior efficiency of separation as compared with the other adsorption processes described. Were it not for the

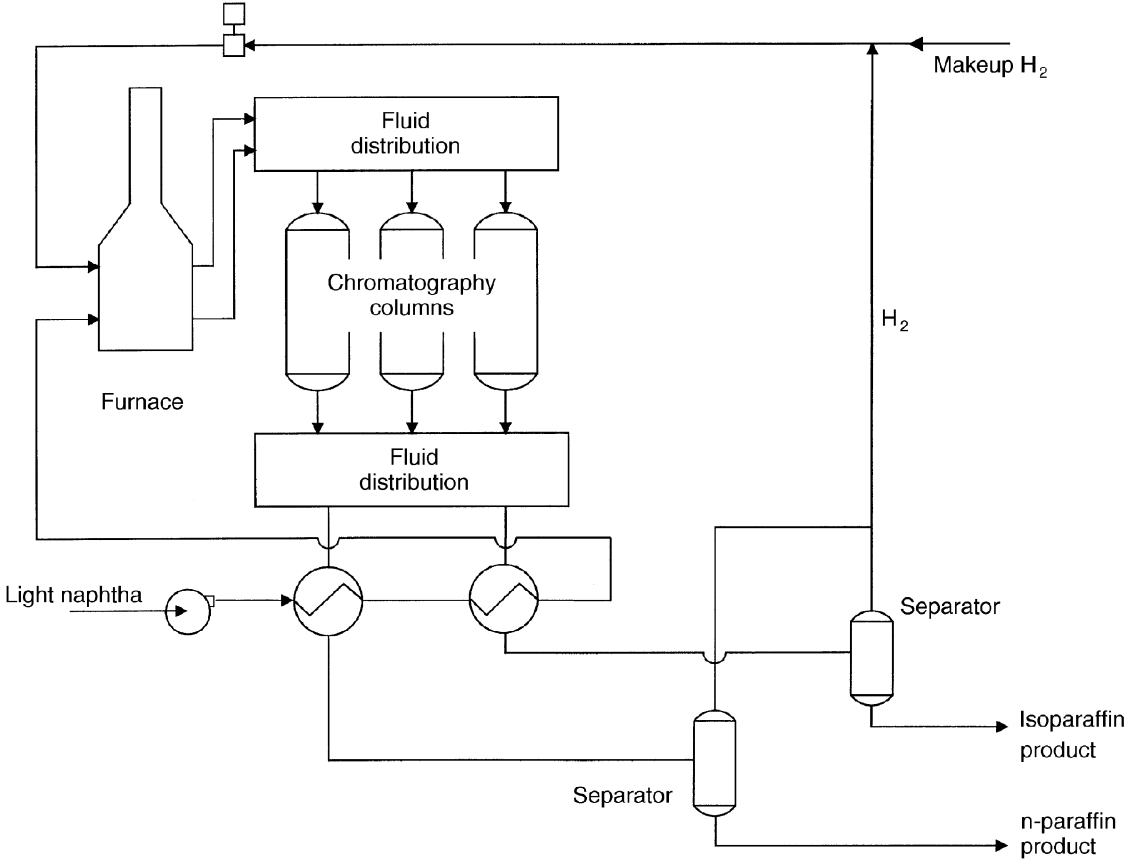

Figure 7.18 *Elf-Aquitaine chromatographic separation of n- and i-paraffins from light naphtha (source: Keller 1983).*

difficulties of packing adsorbent solids homogeneously, large-scale chromatographic processes would be a most helpful method of separating components from gases or liquids when the relative volatilities of the constituents of the mixture are too low for distillation, or the separation factors of components are too small for either pressure or thermal swing adsorption. One large-scale liquid phase chromatographic separation of xylene from ethylbenzene has been designed by the Asahi Company (Seko *et al*. 1979 and 1982).

The concept of the height equivalent of a theoretical plate (HETP), which is common terminology in the subject of chromatography, is useful when referring to column separation efficiencies. Any chromatographic column is considered to consist of a finite number of hypothetical or theoretical plates on each of which equilibrium is established between the fluid and solid phases. The larger the number of theoretical plates in a column of length L the better the separation of the components of a mixture, which depends on the relative strength of adsorption of each component and the rate of mass transfer between the fluid and solid. Mathematical models of the chromatographic column consist of both discretized representations (in which the column is represented as a finite number of mixing cells where mass transfer and equilibrium occur) and continuous flow models with axial dispersion of the fluid and linear mass transfer kinetics as given by Glueckauf and Coates (1947) and alluded to in Section 4.4. Villermaux (1981) has discussed the equivalence between these two alternative model descriptions. The height equivalent of a theoretical plate, *HETP*, may be measured in terms of the output response signal obtained when an input concentration of a component is injected as a pulse into the column. The output response can be characterized by the first moment, μ, about the origin of the output signal and the second central moment or variance σ^2. The first moment gives the location of the centre of gravity or mean of the peak and the second moment measures the dispersion of the data from the mean. The number of theoretical plates required in a column to obtain resolution between component chromatographic peaks is expressed by N $(= \mu^2/\sigma^2)$ and the height equivalent of a theoretical peak is given by HETP $(= L\sigma^2/\mu^2)$. Considering a continuous model of a chromatographic column with bed voidage e, axial dispersion (dispersion coefficient D_L), a rate proportional to the driving force between fluid and solid (rate coefficient k) and a linear adsorption isotherm relating the concentrations in the fluid and adsorbed phases, Villermaux (1981) showed that

$$\text{HETP} = \frac{L\sigma^2}{\mu^2} = \frac{2D_L}{u} + 2u\left(\frac{e}{1-e}\right)\frac{1}{kK}\left[1 + \left(\frac{e}{1-e}\right)\frac{1}{K}\right]^{-2} \tag{7.21}$$

This equation should be compared with equation (4.46). For strong adsorption ($K >> 1$) this becomes

$$\text{HETP} = \frac{2D_L}{u} + 2u\left(\frac{e}{1-e}\right)\frac{1}{kK} \tag{7.22}$$

Two important effects contributing to axial dispersion are molecular diffusion and turbulent mixing. The axial dispersion coefficient may be approximated (Langer *et al*. 1978) by

$$D_L = \gamma_1 D_M + \gamma_2 d_p u \tag{7.23}$$

When inserted into the approximate expression for HETP, the height equivalent of a theoretical plate takes the form of the van Deemter *et al*. (1956) equation

$$\text{HETP} = \frac{A}{u} + B + Cu \tag{7.24}$$

where $A = 2\gamma_1 D_M$, $B = 2\gamma_2 d_p$ and $C = 2e/(1 - e)kK$. An efficient chromatographic process would require HETP to be as small as possible. The optimum fluid velocity giving the minimum HETP is, from the van Deemter equation above, seen to be $u_{opt} = (B/C)^{1/2}$. At values less than u_{opt} peaks become broadened by molecular diffusion while for values greater than u_{opt} broadening of peaks is mainly due to mass transfer resistances.

In plant-scale chromatography the duration of injections must be sufficiently long (10–30 s) to ensure that a desired throughput of products is maintained. The input pulses therefore have a rectangular profile (Figure 7.19). Le Goff and Midoux (1981) showed that the number of theoretical plates necessary for complete resolution is given by

$$\frac{N\,\text{react}}{N\,\text{pulse}} = \left(1 + \frac{\sigma_i}{\sigma_{AB} R_{AB}}\right)^2 \tag{7.25}$$

where N_{pulse} is the number of theoretical plates in the column if a small-scale pulsed column were used, $4\sigma_i$ the duration of the rectangular injection, $\sigma_{AB} = (\sigma_A + \sigma_B)/2$ and $R_{AB} = (t_{RA} - t_{RB})/4\sigma_{AB}$. t_r for each of the components A and B represents the retention time of the component peak measured at a point on the time axis corresponding to its maximum. Both $4\sigma_A$ and t_{RA} refer to the mean retention time and approximate width of a Gaussian elution band for component A as shown in Figure 7.20. N_{pulse} is calculated from the approximate relation $N\ (= \mu^2/\sigma^2) = 16t_R^2/d^2$.

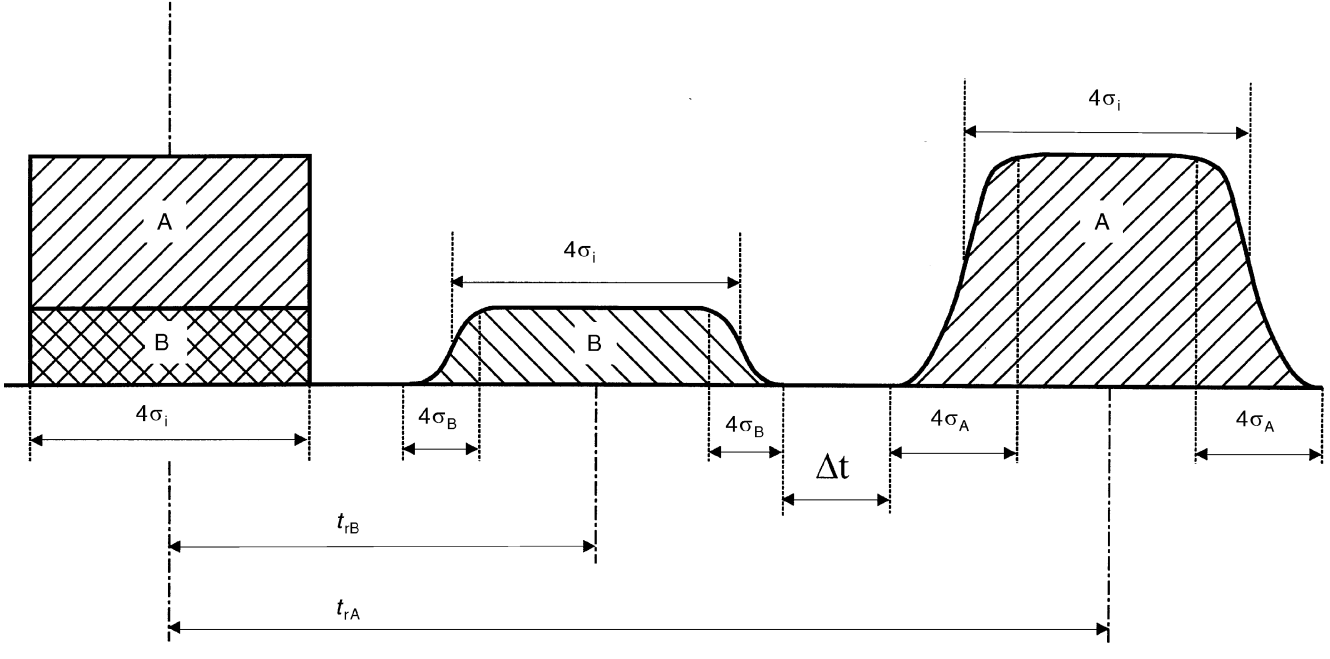

Figure 7.19 *Rectangular pulse injection and corresponding response (source: LeGoff and Midoux 1981, p. 205).*

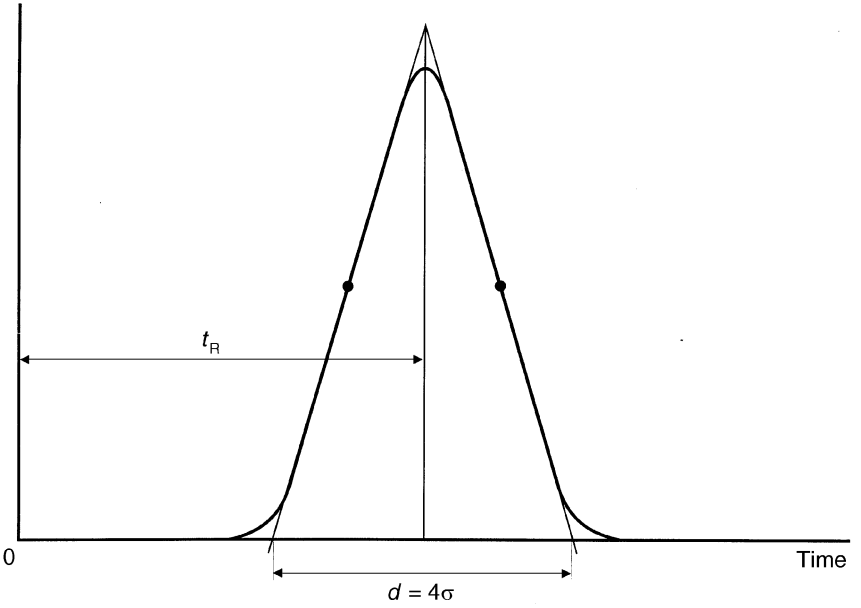

Figure 7.20 *Gaussian elution signal obtained from an instantaneous pulse injection (source: Villeremaux 1981, p. 114).*

7.9 FUTURE DEVELOPMENTS

In view of the rapid growth in new patents for adsorption based processes, it is not surprising that a number of new developments are being examined and assessed prior to possible commercial application.

The first point to be made in this regard is in relation to the relative rapidity of cycle times in pressure swing processes compared with those for thermal swing processes. Further reduction in the cycle time of PSA processes produces greater cycle efficiency with increased rates of production of the desired component. Sircar and Hanley (1995) of Air Products and Chemicals Inc., described a model rapid pressure swing adsorption (RPSA) process in which the rates of adsorption and desorption were expressed in terms of a linear driving force (q.v. Section 4.4) and equal times were allocated to adsorption and desorption. The ratio of the net rate of adsorption, R, to the steady state adsorption capacity, q^*, was shown to be:

$$R/q^* = \frac{1}{2t}\left(\frac{1 - e^{-kt}}{1 + e^{-kt}}\right) \tag{7.26}$$

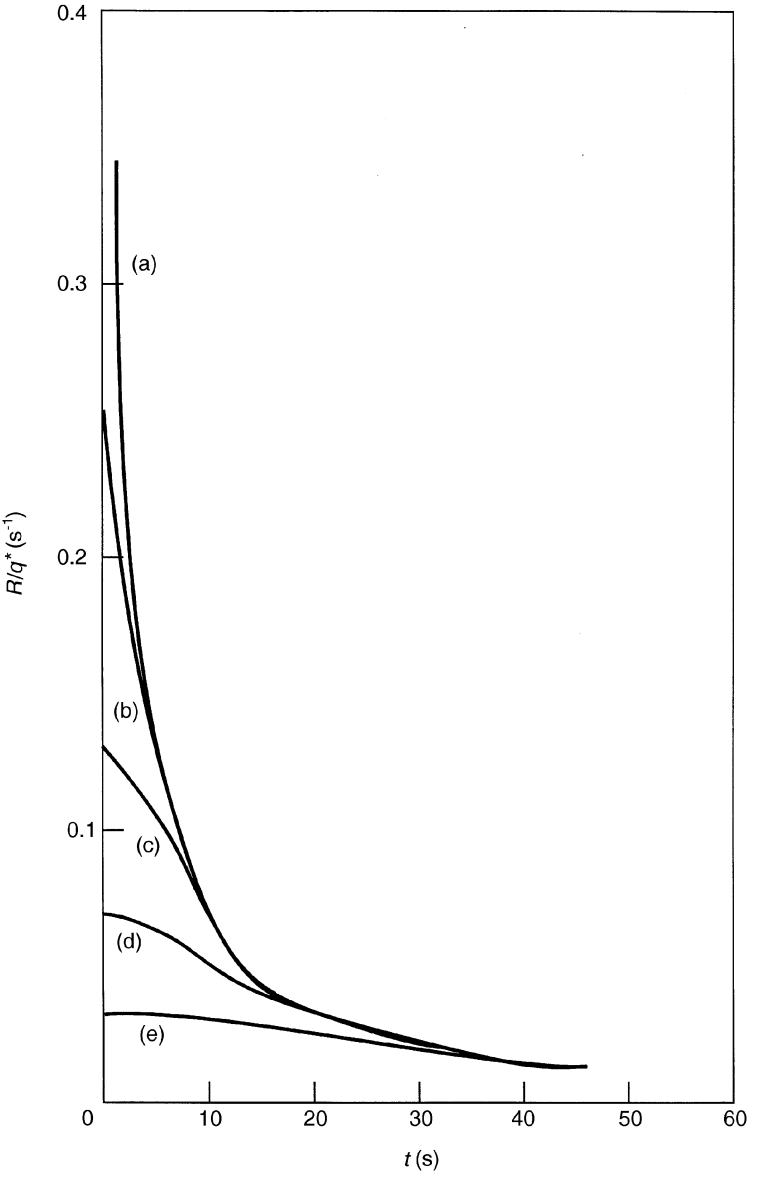

Figure 7.21 *Net rate of adsorption by a single adsorbent during a rapid pressure swing. Curve (a): no mass transfer resistance; curve(b): mass transfer coefficient $k = 1\ s^{-1}$, curve (c): $k = 0.5\ s^{-1}$; curve (d): $k = 0.25\ s^{-1}$; curve (e): $k = 0.1\ s^{-1}$ (source: Sircar and Hanley 1995).*

where t is the time allowed for adsorption in the cycle (equal to desorption) and k is the mass transfer coefficient for adsorption and desorption. Figure 7.21 illustrates how this function behaves with increasing value of t for different values of k. It is apparent that, on the one hand, for an adsorption without mass transfer limitation ($k = \infty$) the net rate of adsorption increases to infinity as t approaches zero. On the other hand, there is a limiting value of $k/4$ as t approaches zero for finite values of k. Furthermore, when t approaches zero the cycle inefficiency, $\eta(= 2tR/q^*)$ also becomes zero. The conclusion to be drawn from this argument is that rapid cycling between the adsorption pressure p_A and the desorption pressure p_D ($<p_A$) leads to a greater net rate of adsorption for a given adsorption capacity and better cycle efficiency. Although a simple model was used to demonstrate this the conclusion is valid for more realistic models of cycles. This has been shown to be true using an experimental rapid pressure swing adsorption apparatus for the separation of N_2 and O_2 from air, sketched in Figure 7.22, consisting of two layers, A and B, of the same zeolite adsorbent separated by a perforated screen. Each layer of adsorbent is subjected to two successive steps:

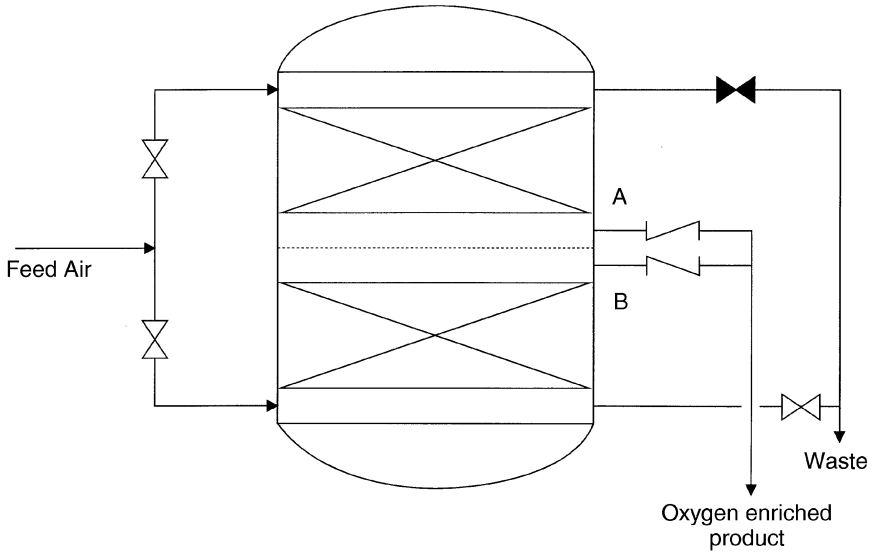

Figure 7.22 *Rapid pressure swing adsorption column containing two separate adsorbent sections for the production of oxygen-enriched air (source: Sircar and Hanley 1995).*

(a) simultaneous pressurization with air when nitrogen is selectively adsorbed by the zeolite adsorbent thus producing a stream enriched in oxygen, part of which is delivered to supply or storage as product, and the remaining portion used as purge gas to the adjacent twin adsorbent layer followed by;
(b) simultaneous countercurrent depressurization and countercurrent purge by the oxygen-enriched gas produced in the other twin adsorbent layer so as to desorb the nitrogen produced in step (a).

The sequence of operations is such that layer A undergoes step (a) for a fixed time between 3 and 10 seconds, while layer B is subjected to step (b) for the same length of time. The roles played by layers A and B are then switched to complete the cycle of total fixed time between 6 and 20 seconds. This allows the continuous supply of a stream of oxygen-enriched product. A sublayer of desiccant can be incorporated before each adsorbent layer to ensure that the feed to each layer is dry prior to effecting separation. Multiple stacks of pairs of adsorbent layers increase the productivity of the adsorber unit. The rate of production of oxygen as a function of oxygen purity obtained from such a unit is shown in Figure 7.23. These production rates are a ten to twenty fold increase over those shown by a conventional PSA process and the oxygen recovery is superior to that in a Skarstrom cycle (usually of a cycle duration of the order of minutes) when the oxygen purity does not exceed 60%. Finally, the plant is simpler having only a single vessel rather than the two or more vessels required in the usual PSA process.

Another novel development, discussed by Sircar (1993a), includes fractional vacuum swing adsorption using a calcium X zeolite for the simultaneous production of *c*. 80–90% pure oxygen and 98% pure nitrogen. Four steps are involved in the cycle:

(a) air at atmospheric pressure is passed through the adsorbent bed which has been presaturated with oxygen-rich air and which is the effluent; the step is continued until N_2 just commences to break through the bed when the effluent is vented until the bed is saturated with air;
(b) the column containing the adsorbent is evacuated to relatively low pressure (approximately 0.5 bar) and the effluent gas wasted;
(c) the bed is then evacuated further and the effluent collected as 98% pure N_2;
(d) the bed is then repressurized to just below atmospheric pressure with a part of the O_2-enriched gas produced during step (a). A new cycle of events is then commenced.

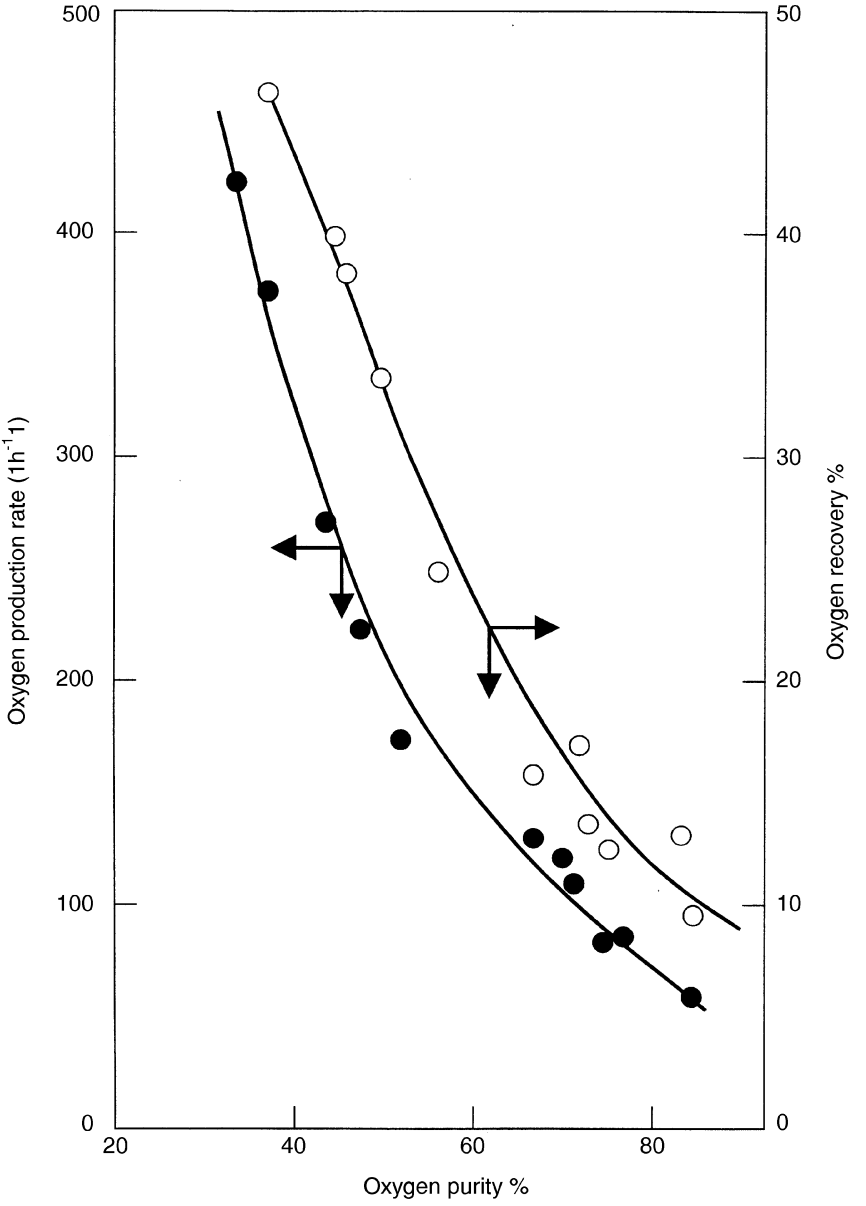

Figure 7.23 *Oxygen production rate and oxygen recovery as a function of product purity for rapid pressure swing adsorption process (source: Sircar and Hanley 1995).*

This fractional vacuum swing process is similar in many respects to the established vacuum swing adsorption process described in Section 7.3.4 but utilizes a CaX zeolite as the adsorbent and uses part of the oxygen-enriched gas produced from the first step of the process.

The phenomenon of surface diffusion, demonstrated by Barrer and Strachan (1955) may be used to advantage for the separation of some hydrogen–hydrocarbon mixtures (Sircar, 1993b). Thus, thin microporous carbon membranes (<5 μm), supported by macroporous sheets of graphite assembled into a plate and frame membrane module, were able to separate H_2 at 63% recovery from a refinery waste gas. The feed was passed at high pressure over the membrane unit which preferentially adsorbed the hydrocarbons and facilitated surface diffusion of these species through the membrane to the low pressure side of the module. Adsorption, accompanied by surface diffusion through a thin microporous membrane, thus offers possible future applications.

One further development in adsorption technology which holds some promise, is a cyclic process applicable to the separation of liquids. The separation method depends on concentration changes and is referred to as concentration swing adsorption (Rao and Sircar 1992). Separation of a binary mixture, such as ethanol–water, occurs by the selective liquid phase adsorption of ethanol (the more strongly adsorbed component) onto the surface of a porous adsorbent. The cycle consists of four steps:

(1) During the first part of the concentration swing adsorption cycle, effluent from the column is pure water. This first step is continued until the whole column is saturated with the ethanol–water feed mixture.
(2) The second cycle step is then started when the column is rinsed with pure ethanol. The section of column ahead of the mass transfer zone is saturated with pure ethanol. The effluent composition during this second step is close to that of the feed mixture and the step is continued until the column is saturated with ethanol.
(3) The third step of the cycle is when desorption of ethanol is achieved by rinsing, in a countercurrent direction, the column with a desorbent liquid which is adsorbed at least as strongly as ethanol and which does not form an azeotrope with water. Step 3 is continued until the column is completely saturated with the desorbent, the effluent ahead of the mass transfer zone being enriched ethanol, part of which is collected as product and the remainder being diverted to provide ethanol rinse for Step 2. If the mass transfer zone for Step 3 is not sharp then the

ethanol-rich product will contain some of the desorbent liquid: when this is the case ethanol and desorbent have to be separated by a subsequent distillation.

(4) During the last and fourth step of the cycle the column is rinsed with water in a countercurrent direction. Initially the effluent is liquid adsorbent which can be recycled to another column in which Step 3 is occurring. Subsequently, the effluent is a mixture of water and desorbent liquid which is separated by distillation so that the desorbent can be recirculated.

Four adsorption columns, with appropriate valves for switching liquid streams between columns, are required to operate this concentration swing cycle so as to obtain a continuous flow of enriched ethanol. The process operates at ambient temperatures and can be designed to produce 98% pure ethanol with a very high recovery of ethanol (as high as 99%) from the feed mixture. It is claimed that the separation of ethanol–water mixtures by concentration swing adsorption has the potential for significant reduction of energy requirements when compared with separation by distillation.

REFERENCES

Asher, W. J., Campbell, W. R., Epperley, W. R. and Robertson, J. L. (1969) *Hydrocarbon Processing*, **48**(1), 134

Ausikaitis, J. P. (1978) in *Encyclopaedia of Chemical Technology*, Vol. 8, p. 126, Wiley

Barker, P. E., England, K. and Vlachogiannis, G. (1983) *Trans. IChemE Res. Dev.,* **61**, 241

Barrer, R. M. and Strachan, E. (1955) *Proc. Roy. Soc.*, **A231**, 52

Bellows, R. J., Pirkle, C. J. and Wu, T. D. (1986) Paper 118e, AIChE Meeting, Miami

Berg, C. (1946) *Trans. IChemE*, **42**, 665

Berlin, N. H. (1966) US Patent 3,280,536, assigned to Exxon Research & Eng.

Bernard, J. R., Gourlia, J. P. and Guttierrez, M. J. (1981) *Chem. Eng.* **88** (May), 92

Broughton, D. B. and Gembicki, S. A. (1984) *AIChE Symp. Series*, **80** (No 233), 62

Broughton, D. B., Neuzil, R. W., Pharis, J. M. and Brearley, C. S. (1970) *Chem. Eng. Prog.*, **66**, (No 9), 70

Calmon, C. and Gold, A. (eds) (1979) *Ion Exchange for Pollution Control*, CRC Press, Florida

Carta, G. and Pigford, R. L. (1986) *Ind. Eng. Chem. Fundamentals*, **25**, 677

Cassidy, R. T. (1980) *ACS Symp. Ser. No 135*, p. 247

Cassidy, R. T. and Holmes, E. S. (1984) *AIChE Symp. Series* **80**, 68

Chi, C. W. and Lee, H. (1973) *AIChE Symp. Series* **69**, 95

Chihara, K. and Suzuki, M. (1983) *J. Chem. Eng. Japan,* **16**, 293

Ching, C. B. (1983) *J. Chem. Eng. Japan,* **16**, 49

Ching, C. B. and Ruthven, D. M. (1984) *Can. J. Chem. Eng.,* **62**, 398

Ching, C. B., Ruthven, D. M. and Hidajat, R. (1985) *Chem. Eng. Sci.,* **40**, 1411

Ching, C. B. and Ruthven, D. M. (1986) *Chem. Eng. Sci.,* **41**, 3063

Ching, C. B., Hidajat, K. Ho, C. and Ruthven, D. M. (1987) *Reactive Polym.,* **6**, 15

Conder, J. R. (1973) *Production scale chromatography*, pp. 137–185 in *New Developments in Gas Chromatography*, edited by J. H. Purnell, Wiley

Davis, J. C. (1972) *Chem. Eng.,* **16**, 18

de Rosset, A. J., Neuzil, R. W. and Broughton, D. B. (1981) Industrial applications of preparative chromatography, in *Percolation Processes: Theory and Applications*, edited by A. E. Rodrigues and D. Tondeur, Sitjhoff and Noordhoff

Garg, D. R. and Ausikaitis, J. P. (1983) CEP, *Chem. Eng. Prog.,* April, 60

Garg, D. R. and Yon, C. M. (1986) CEP, *Chem. Eng. Prog.,* February, 54

Glueckauf, E. and Coates, J. E. (1947) *J. Chem. Soc.,* 1315

Guerin de Montgareuil, P. and Domine, D. (1964) US Patent 3,155,468 assigned to Societe L'Air Liquide

Hashimoto, K., Adachi, S., Noujima, H. and Marayama, A. (1983) *J. Chem. Eng. Japan*, **16**, 400

Hidajat, K., Ching, C. B. and Ruthven, D. M. (1986) *Chem. Eng. Sci.,* **41**, 2953

Keller, G. E. (1983) Gas adsorption processes: state of the art, in *Industrial Gas Separations*, eds T. E. Whyte, C. M. Yon and E. H. Wagener, ACS Symposium Series 223

Knoblauch, K. (1978) *Chem. Eng.*, **85**(25), 87

Kremser, A. (1930) *Nat. Petroleum News,* **22**(21), 42

Langer, G., Roethe, A., Roethe, K.-P. and Gelbin, D. (1978) *Int. J. Heat and Mass Transfer*, **21**, 751

LeGoff, P. and Midoux, N. (1981) in *Percolation Processes*, edited by A. E. Rodrigues and D. Tondeur, Sitjhoff and Noordhoff

Marsh, W. D., Pramuk, F. S., Hoke, R. C. and Skarstrom, C. W. (1964) US Patent 3,142,547, assigned to Exxon Research & Eng.

Rao, M. B. and Sircar, S. (1992) *Separation Sci. Technol.,* **27**, 1875

Ruthven, D. M. (1984) *Principles of Adsorption and Adsorption Processes*, p. 305, Wiley

Ruthven, D. M. and Ching, C. B. (1989) *Chem. Eng. Sci.,* **44**(5), 1011

Salmon, C. and Gold, A., *Ion Exchange for Pollution Control*, CRC Press, Florida, USA, 1979

Seko, M., Miyaki, T. and Inada, K. (1979) *Ind. Eng. Chem. Prod. Res. Dev.,* **18**, 263

Seko, M., Takeuchi, H. and Inada, T. (1982) *Ind. Eng. Chem. Prod. Res. Dev.,* **21**, 656

Siegell, J. H., Dupre, G. D. and Pirkle, C. J. (1986) *Chem. Eng. Progr.,* **82**(11), 57

Sircar, S. (1993a) *Separation Sci. Technol.,* **28**, 2553

Sircar, S. (1993b) *Proceedings of the 4th International Conference on Fundamentals of Adsorption*, Japan, pp. 3–10

Sircar, S. and Hanley, B. F. (1995) *Adsorption,* **1**, 313

Sircar, S. and Zondlo, J. W. (1977) US Patent 4,013,429, assigned to Air Products and Chemicals Inc.

Skarstrom, C. W. (1975) in *Recent Developments in Separation Science*, Vol. 2, edited by N. N. Li, p. 95, CRC Press, Cleveland, OH

Skarstrom, C. W. (1960) US Patent 2,944,627, assigned to Exxon Research & Eng.

Souders, M. and Brown, G. C. (1932) *Ind. Eng. Chem.,* **24**, 519

Stewart, H. A. and Heck, J. L. (1969) *Chem. Eng. Progr.,* **65**(9), 78

Symoniak, M. F. (1980) *Hydrocarbon Processing,* **May**, 1010

Valentin, P. and Midoux, N. (1981) in *Percolation Processes*, edited by A. E. Rodrigues and D. Tondeur, p. 141, Sitjhoff and Noordhoff

van Deemter, J. J., Zuiderweg, F. J. and Klinkenberg, A. (1956) *Chem. Eng. Sci.,* **5**, 271

Villermaux, J. (1981) The chromatographic reactor, in *Percolation Processes*, edited by A. E. Rodrigues and D. Tondeur, p. 539, Sitjhoff and Noordhoff

Wagner, J. L. (1969) US Patent 3,430,418, assigned to Exxon Research & Eng.

Yang, R. T. (1987) *Gas Separation by Adsorption*, p. 163, Butterworths

8

The literature of adsorption

It is not the purpose in this chapter to provide comprehensive reviews of all the literature covering the principles, practices and technology of adsorption. Instead, an overview is provided of selected and principal sources of information which can be used to supplement the information provided in this book. Descriptions of books, and of chapters in handbooks and encyclopedias, are provided in chronological order, and not in any order of importance. The descriptions are not intended to be critical reviews. Rather the intention is to guide the reader towards further information with an emphasis on the process engineering aspects which cover the full range of applications in gas, vapour and liquid separations. Since adsorption is still subject to considerable research worldwide, lists of the more important journals and symposium proceedings which devote attention to the subject are provided at the end of this chapter.

Adsorption (C. L. Mantell, McGraw-Hill, New York, 1945)
This early text in the publisher's Chemical Engineering Series was written in order to correlate the practical, commercial and engineering aspects of adsorption. Adsorption was considered by the author to be a unit operation of chemical engineering. A brief chapter on the theories of adsorption is provided but the remainder of the book addresses practical matters of

interest and relevance to operators and designers of adsorption processes and equipment. Chapters are devoted to fuller's earth and activated clays, aluminium oxide base materials, bone char and related materials, decolourizing and water treatment carbons, metal and medicinal adsorbent chars, gas adsorbent carbons, silica gel, magnesia and hydrous oxides, solvent recovery and adsorption from gases, odour removal, gas masks, gas hydrates, the dehydration of air and gases, ion exchangers and chromatographic adsorption analysis. One chapter deals with the specifications and testing of adsorbents.

Interfacial Phenomena (J. T. Davies and E. K. Rideal, Academic Press, New York, 1961)
In response to a growing literature on the the subject of adsorption of gases onto solids (including physical adsorption, chemisorption and heterogeneous catalysis) this book was written to examine particularly some of the more fundamental properties of various liquid interfaces. Eight well-referenced chapters describe the physics of surfaces, electrostatic phenomena, electrokinetic phenomena, adsorption at liquid interfaces, properties of monolayers, reactions at liquid surfaces, diffusion through interfaces, and disperse systems and adhesion.

Adsorption, Surface Area and Porosity (S. J. Gregg and K. S. W. Sing, Academic Press, London, 1967)
The overall aim of this book was to provide a critical exposition of the use of adsorption data for the evaluation of the surface area and the pore size distribution of finely divided and porous solids. The intended audiences were workers in academic institutions and in industrial laboratories. Considerable space is devoted to the BET method (see Chapter 3 in this book) for determining the specific surface and the use of the Kelvin equation for the calculation of pore size distribution. However, attention is also given to other methods for estimating surface area from adsorption measurements, namely those based on adsorption from solution, on heats of immersion, on chemisorption and on the application of the Gibbs adsorption equation to gaseous adsorption. Each of the eight chapters is extensively referenced.

Mass Transfer Operations, 2nd edition (R. E. Treybal, McGraw-Hill, Tokyo, 1968)
Chapter 11 of this undergraduate textbook devotes 77 pages to adsorption and ion exchange. Single and multicomponent equilibria, for both gaseous and liquid systems are described qualitatively. Stagewise operation, which is

appropriate for liquid phase contacting, and continuous contact processes (such as fluidized and moving beds) are then described at some length to complete the first half of the chapter. The approach adopted for design is identical to that adopted for any steady state countercurrent separation process. The second half of the chapter is devoted to unsteady state fixed bed adsorbers and includes descriptive accounts of the adsorption wave, percolation, elution and chromatography. The design approach is restricted to the transfer unit concept. Problems, worked solutions and references for further reading are provided at the end of the chapter. Part 1 of this textbook (four chapters) provides a useful introduction to molecular diffusion in fluids, mass transfer coefficients, diffusion in solids and interphase mass transfer concepts.

Activated Carbon: Surface Chemistry and Adsorption from Solution (J. S. Mattson and H. B. Mark, Marcel Dekker, New York, 1971)
The authors' aim was to produce a text which critically reviews the available literature on solution adsorption phenomena and offers an interpretation of the surface-related interactions of activated carbons that is consistent for the adsorption of a wide variety of solutes ranging from strong electrolytes to organic non-electrolytes. The seven chapters cover the activation of carbon, surface oxygen functional groups and neutralization of base by acidic surface oxides, spectroscopic methods for molecular structure determinations on surfaces, nature of the electrical double layer, adsorption of electrolytes, and adsorption of weak and non-electrolytes from aqueous solution.

Adsorption on Solids (V. Ponec, Z. Knor and S. Černy, Butterworths, London, 1974)
The English translation of this book by D. Smith and N. G. Adams provides a detailed account of theoretical approaches and experimental techniques of adsorption. The subject matter, essentially comprising physical chemistry, includes defined substances, defined surfaces and their preparation, methods for studying the texture of adsorbents, methods of studying adsorption, the surface structure of solids, theories of adsorption forces, adsorption kinetics and thermodynamics, theories of adsorption equilibria, the mechanisms of physical adsorption and chemisorption, adsorption from flowing gases and liquids, practical applications of adsorption, adsorption from solutions and the relationship between adsorption and catalysis.

Encyclopedia of Chemical Processing and Design, volume 2 (edited by J. J. McKetta, Marcel Dekker, New York, 1977)
T. Vermeulen provides a brief (12 page) introduction to the information

needed for adsorption design, including equilibria, types of breakthrough and rate behaviour. R. A. Anderson then provides further, but still largely descriptive, accounts of adsorption equilibria, mass transfer (particularly the LUB approach), desorption and regeneration, and design considerations which include thermal swing, pressure swing, purge gas stripping and displacement techniques, deactivation and activation. Summary accounts are also provided of practical design matters including choices of adsorbent, flow direction, number of vessels, vessel configuration, vessel internals and cycle time. There is an extensive bibliography.

Carbon Adsorption Handbook (edited by P. N. Cheremisinoff and F. Ellerbusch, Ann Arbor Science, Ann Arbor, 1978)
This book comprises a collection of 27 chapters on gas and liquid phase applications written by various contributors. Each chapter is essentially descriptive in nature and thus the strength of the book lies principally in the guidance of the reader towards practical application and not to the development of theory. Applications which are described include purification of industrial liquids, wastewater treatment, treatment of hazardous industrial wastes, treatment of pesticides and pesticidal wastes, air purification, aerosol and particulate removal, removal of organic and inorganic species from water, cyanide removal from refinery wastewater, removal of phenolic compounds from polluted water, and decolorization. Other chapters deal with the regeneration of carbonaceous adsorbents and include process aspects of regeneration in multiple hearth furnaces and developments in biological and wet air regeneration.

Adsorption (J. Ościk, Ellis Horwood, Chichester, 1982)
The English translation of this book provides a detailed account of adsorption phenomena from a physical chemistry perspective. Adsorption at liquid–gas, solid–gas, solid–liquid and liquid–liquid interfaces is comprehensively described.

Treatment of Water by Granular Activated Carbon (edited by M. J. McGuire and I. H. Suffet, American Chemical Society, Advances in Chemistry Series No 202, Washington, 1983)
Almost all the papers in this book were presented at an ACS symposium on activated carbon in 1981. The editors have presented the 22 papers under four headings, namely theoretical approaches, modelling and competitive adsorption effects, biological/adsorptive interactions and pilot- and large-scale studies.

Computer Methods for Solving Dynamic Separation Problems (C. D. Holland and A. I. Liapis, McGraw-Hill, New York, 1983)
In this book a combination of the principles of separation processes, process modelling, process control and numerical methods is used to describe the dynamic behaviour of separation processes. The text is largely mathematical and analytical in nature. Adsorption processes are commonly operated in a cyclic manner involving complex sequences of individual steps which are dynamic in nature and three chapters in this book specifically address this separation process. Chapter 11 covers the fundamentals of adsorption processes and includes physical adsorption of pure gases and mixtures, mass transfer by convective transport and the roles of pore and surface diffusion in the adsorption process. Chapter 12 addresses the separation of multicomponent mixtures by the use of adsorption columns and includes the Gleuckauf, film resistance and diffusion models and adiabatic operation of a fixed bed adsorption column together with periodic operation. Chapter 14 addresses the thermodynamics of the physical adsorption of pure gases and multicomponent gas mixtures.

Perry's Chemical Engineers' Handbook, 6th edition (edited by R. H. Perry and D. Green, McGraw-Hill, New York, 1984)
In Section 16 of this general chemical engineering handbook, T. Vermeulen, M. D. LeVan, N. K. Hiester and G. Klein provide an overview of adsorption and ion exchange. Subject matter includes sorbent materials and sorbent-process analysis, fluid-sorbent equilibrium, equilibrium-limited transitions, rate-limited constant pattern transitions, linear equilibrium and other rate limited transitions, regeneration, chromatography, multivariant systems, multiple transitions, batch and continuous processes. The authors' comprehensive yet concise approach is essentially analytical in nature and descriptions of processes and equipment are not included.

Principles of Adsorption and Adsorption Processes (D. M. Ruthven, Wiley-Interscience, New York, 1984)
This book, written by an acknowledged expert in the field of adsorption, provides comprehensive coverage of the basic principles of adsorption, including the nature of microporous adsorbents and their characterization, thermodynamics and equilibria, diffusion in porous media, kinetics in batch systems, column dynamics and hydrodynamics. Coverage is extended to multicomponent systems and the various simplifying assumptions which can be made in design are well described. The book was not written to be a design manual and so guidance on invoking simplifying assumptions is

scattered throughout the text. The casual reader may therefore gain the impression that the only way to design an industrial adsorption column is to carry out a full rigorous design. The book also overviews some important commercial processes including those using pressure swing and thermal swing cycles. The engineering aspects are comprehensively underpinned by the scientific fundamentals and so it is appropriate for a broad range of scientists and engineers who have some experience of the subject and as a graduate-level textbook. Each of the 12 chapters contains its own comprehensive list of references.

Adsorption Technology: A Step by Step Approach to Process Evaluation and Application (F. L. Slejko, Marcel Dekker, New York, 1985)
The aim of this book was to provide chemists and engineers with four tools. The first is a working knowledge of basic adsorption theory in order to aid in the design of laboratory and pilot plant experiments and later to help in understanding the meaning of the results. The second is the information necessary for designing and carrying out screening studies of adsorbents. The third is information for designing a conceptual full-scale adsorption plant. The final tool is an appreciation that adsorption technology is not limited to any one kind of adsorbent, but is fundamental to a broad class of materials. The text is largely descriptive with applications concentrated mostly on liquid phase applications.

Large Scale Adsorption and Chromatography, Volumes I and II (P. C. Wankat, CRC Press, Boca Raton, 1986)
The author's aim was to present a unified, up-to-date development of operating methods used for large-scale adsorption and chromatography. Methods were gathered together, classified and compared and the solute movement or local equilibrium theory used as the main underlying theory. Mass transfer and dispersion effects are included with the non-linear mass transfer zone (MTZ) and linear chromatographic models. More complex theories are referenced but not discussed in detail. Volume I contains chapters on the physical picture and simple theories for adsorption and chromatography, packed bed operations and cyclic operations including pressure swing adsorption, parametric pumping and cycling zone adsorption. Volume II contains chapters on large-scale chromatographic separations, moving bed and simulated moving bed countercurrent systems, hybrid chromatographic processes, two-dimensional and centrifugal operating methods.

Handbook of Separation Process Technology (edited by R. W. Rousseau, Wiley-Interscience, New York, 1987)
In Chapter 12 of this handbook (52 pages) George E Keller II *et al.* provide an overview of some of the more practical aspects of the design of adsorption processes. Descriptions of the most common adsorbents (properties, manufacture and applications) are followed by overviews of basic pressure swing, thermal swing and displacement purge cycles together with example process flowsheets. These include gas bulk separations, gas purifications, liquid bulk separations and liquid purifications. Design methods are restricted solely to short-cut techniques such as the length of unused bed concept. Whilst several other texts (notably Ruthven (1984) and Yang (1987)) provide more comprehensive coverage of adsorbents, processes and design techniques, the particular strength of Chapter 12 in this handbook lies in its description of the more practical aspects of design such as bed orientation, flow distribution, adsorbent support, pressure gradients, bed lifting, bed crushing, bed filling, draining and holdup, heating, cooling, etc. The chapter is written from an engineering perspective and is comprehensively referenced.

Adsorption Processes for Water Treatment (S. D. Faust and O. M. Aly, Butterworths, Boston, 1987)
This comprehensive text was written to provide information on carbon and resin based adsorptive processes for potable water treatment. It is aimed at environmental and/or consulting chemists and engineers, water supply and treatment personnel, and regulators. Fundamental aspects covered include the physical and chemical properties of carbonaceous adsorbents, and the basic principles of adsorption phenomena including thermodynamic equilibria and their models, and the kinetics of batch and fixed bed systems. Engineering aspects cover process equipment types including batch systems, fixed beds and fluidized beds. Applications covered include the adsorption of organic and inorganic compounds, operational, pilot plant and case studies, biological activated carbon treatment of drinking water, and adsorption by macroreticular resins. Each of the ten chapters is comprehensively referenced and there is a wealth of practical data, including economic data, which can be used for design purposes.

Gas Separation by Adsorption Processes (R. T. Yang, Butterworths, Boston, 1987)
This book covers all aspects of gas phase adsorption processes ranging from thermodynamics to the modelling and design of cyclic processes, including pressure swing adsorption. The equilibrium adsorption of gas mixtures is

covered in depth. Descriptions are provided on the selection of adsorbents, fundamental theories of adsorption, rate processes and column dynamics. The book is aimed not only at being a starting point for professionals and students interested in gas separation and purification processes but also at serving as a basis for process selection, development and design of new cyclic processes and future research. Each of the eight chapters is referenced.

Ullmann's Encyclopedia of Industrial Chemistry, Vol B3, Unit Operations II (VCH, Weinheim, 1988)

In the 52 pages of Chapter 9 entitled Adsorption, A. Mersmann provides sections on adsorption apparatus, adsorbents, equilibrium, kinetics, regeneration by thermal swing, pressure swing, displacement and extraction methods. He also provides sections describing processes which include purification of gas mixtures, pressure swing processes, separation of nitrogen from oxygen, air purification, removal of radionuclides from exhaust gas, removal of organic compounds from exhaust air, desulphurization, purification of methane, purification of hydrogen and the separation of isomers. A substantial list of references is provided. In the 44 pages of Chapter 10 entitled Process-Scale Chromatography, G. Jagschies provides sections on separation processes which include ion exchange, affinity, hydrophobic, interaction and reversed phase chromatographic techniques as well as gel filtration. Other sections relate to optimization strategies, scale-up and transfer protocols, basic design requirements, plant design, quality assurance and future developments. A substantial list of references is provided.

Handbook of Separation Techniques for Chemical Engineers, 2nd edition (edited by P. A. Schweitzer, McGraw-Hill, New York, 1988)

Four sections in this practical handbook are devoted to adsorption processes. In Section 1.13 R. A. Hutchins provides a general descriptive account of the use of activated carbon systems for the separation of liquids. The design techniques are restricted to short cut methods such as residence time and service time. Analysis of equilibrium data is restricted to the Freundlich isotherm. A brief list of references is provided. In Section 1.15 C.-R. Huang and H. Hollein provide a detailed account of parametric pumping. Subject matter includes thermal swing liquid phase separations, gas phase cyclic separation processes, recuperative-mode parametric pumping, parametric pumping for biochemical separations and electrochemical parametric pumping for desalination. This section is largely descriptive in nature and there is an extensive list of 130 references. In Section 1.16 R. S. Cooley provides a brief (10 page) descriptive overview of high

pressure liquid chromatography. In Section 3.1 of the Handbook, J. L. Kovach provides a large descriptive overview of gas phase adsorption, the subject matter including basic and practical concepts such as equilibria and rates, adsorbent materials, adsorption dynamics, system and equipment design, safety considerations and operational parameters. A list of 39 references is provided.

New Directions in Sorption Technology (edited by G. E. Keller II and R. T. Yang, Butterworths, Boston, 1989)
This book comprises selected papers presented at two symposia as well as some additional material. The objective was to report current developments in sorption technology from which new directions would emerge. The editors have been selective rather than exhaustive and the 13 papers are restricted to four subject areas, namely new sorbents, chromatography, pressure swing adsorption and bioseparations which involve sorption.

Adsorption Equilibrium Data Handbook (D. P. Valenzuela and A. L. Myers, Prentice Hall, Englewood Cliffs, 1989)
This data handbook provides a unique opportunity to locate a substantial amount of adsorption equilibrium data in one source. The book contains a summary of thermodynamic equations for adsorption of gases and liquids and their mixtures and their application to experimental data. The authors' intention was to provide a reference for engineers and scientists interested in the application of adsorption to the separation of gas and liquid mixtures. Since single component isotherms cannot be calculated from first principles, the authors correctly argue that it is necessary to use experimental data. Hence the need for the data book. Once single component data are available it is possible to use models to predict equilibrium data for multicomponent systems. Data sources are fully referenced.

Adsorption Engineering (M. Suzuki, Elsevier, Amsterdam, 1990)
This book comprises 12 chapters covering an introduction, porous adsorbents, adsorption equilibrium, diffusion in porous particles, kinetics of adsorption in a vessel, kinetics of adsorption in a column (chromatographic analysis and breakthrough curves), heat effects, regeneration of spent adsorbent, chromatographic separation, pressure swing adsorption and adsorption for energy transport. The text comprises a blend of mathematical analysis and descriptions of plant and processes. Each chapter is fully referenced.

Preparative and Process Scale Liquid Chromatography (edited by G. Subramanian, Ellis Horwood, New York, 1991)
Liquid phase chromatography provides a means of separating solutes by making use of their different adsorption and desorption characteristics when a solution is percolated through a column packed with a powdered or granular adsorbent. On the large scale the technique is applied routinely and with a high degree of reliability. The aim of this book is to give broad coverage of the state of the art in the subject to those involved in preparative and process scale separations.

Kirk–Othmer Encyclopedia of Chemical Technology, Volume 1, 4th edition (edited by J. I. Krochwitz, John Wiley, New York, 1991)
S. A. Gembicki, A. R. Oroskar and J. A. Johnson provide a 107 page general account of fundamental principles (including forces of adsorption, selectivity, nature of surfaces, capillary condensation and practical adsorbents), adsorption equilibrium, adsorption kinetics, column dynamics and applications.

Chemical Engineering, Volume 2, 4th edition (J. M. Coulson and J. F. Richardson with J. R. Backhurst and J. H. Harker, Pergamon Press, Oxford, 1991)
Chapter 17 (78 pages) of this textbook, which is devoted to particle technology and separation processes, provides a description of the common adsorbents (their structure, properties and applications), adsorption equilibria and adsorption kinetics. The conservation equations which describe isothermal and non-isothermal adsorption in a packed bed are provided and there are basic descriptions of thermal swing, pressure swing, parametric pumping and cycling zone processes, as well as moving bed processes including Hypersorption, rotary beds, Sorbex, fluidized beds and compound beds. The book is designed as an undergraduate text and the chapter on adsorption is appropriate for students in the final years of undergraduate degree courses. There is a comprehensive list of references. Chapters 18 and 19 describe the related subjects of ion exchange and chromatographic separations, respectively.

Unit Operations of Chemical Engineering, 5th edition (W. L. McCabe, J. C. Smith and P. Harriott, McGraw-Hill, New York, 1993)
The twenty seven pages of Chapter 25 in this general chemical engineering undergraduate textbook provide an introduction to the basic principles of adsorption, including a brief descriptive account of equilibria. A description

of breakthrough curves is provided together with how they can be used to design a fixed bed process using the length of unused bed (LUB) concept. The chapter also provides introductory accounts of the conservation of mass in a fixed bed adsorber, and of internal and external mass transfer coefficients, irreversible adsorption and the limiting solution with a linear isotherm. A few problems, worked solutions and references are provided at the end of the chapter. This textbook also contains eight chapters relating to fluid mechanics and seven chapters relating to heat transfer, many details of which are relevant to the design and analysis of adsorption processes.

Carbon Adsorption for Pollution Control (N. P. Cheremisinoff and P. N. Cheremisinoff, Prentice Hall, Englewood Cliffs, 1993)
The authors' intention has been to provide a practical book that can be used by the practitioner as well as being useful as a basic reference for those who wish to study carbon adsorption in the specific field of pollution control. Material which might be too technical or theoretical has been avoided intentionally since the volume is intended to provide a working knowledge and description of adsorption processes involving activated carbon. The book includes a basic coverage of the principles of adsorption processes, and applications which cover the treatment of liquids, gas phase adsorption and air pollution control, and the treatment of hazardous wastes. Remaining chapters cover carbon regeneration, and exposure, controls and safety. A sizeable part of the book is devoted to physical constants and conversion factors. There are no references.

Pressure Swing Adsorption (D. M. Ruthven, D. Farooq and K. S. Knaebel, VCH, New York, 1994)
This book provides a coherent and concise summary of the underlying scientific principles and the technology of pressure swing adsorption. It is aimed at the practising engineer and is indeed most suitable to those who have a working knowledge of the subject, including graduate level students and academics. Two chapters provide in-depth knowledge on equilibrium theory and dynamic numerical solution and one chapter provides an overview of commercial separations which include air drying, air separation, hydrogen recovery, carbon dioxide recovery, methane recovery from landfill gas, hydrocarbon separations, simultaneous production of hydrogen and carbon dioxide from reformer off-gas and the concentration of trace components. One chapter is devoted to extensions of the PSA concept to parametric pumping, thermally coupled PSA, single column rapid PSA and another chapter compares PSA with membrane-based separations. There is substantial mathematical analysis to aid the understanding of principles,

advantages and limitations of various approaches to design and analysis. This is supported by two appendices (one on the method of characteristics, the other on the method of collocation). A third appendix provides a synopsis of the PSA patent literature.

Adsorption Calculations and Modeling (C. Tien, Butterworth-Heinemann, Boston, 1994)
This book is a compendium of models and calculation procedures for the design and analysis of physical adsorption separations. The author's intention was to avoid duplication, as far as possible, with the standard texts by Ruthven (1984), Faust and Aly (1987) and Yang (1987) and so some subjects such as pressure swing adsorption and thermal swing adsorption are not discussed in great detail. Instead, topics such as biological carbon adsorption, adsorption with impregnated adsorbents, and characterization of solutions of unknown composition have been given a more complete coverage. Gas phase and liquid phase separations have been treated as far as possible on a unified basis and are treated with equal emphasis. Thermodynamics, adsorption equilibria and adsorption rate phenomena, including summaries of theories for multicomponent systems, are covered in depth. Subsequent chapters deal with calculations for batch and continuous flow tanks, and for fixed beds. The book is supplied with a computer disk which contains several computer programs so that the reader can carry out simple calculations. Programs are included for equilibrium adsorption calculations (single and multicomponent systems), batch adsorption calculations and fixed bed adsorption calculations.

Separation Technology: The Next Ten Years (edited by J. Garside, Institution of Chemical Engineers, Rugby, 1994)
In his invited contribution to this book, S. Sircar first explains the development of the role of adsorption technology as a key separation technique for the process industries. The principles of pressure and vacuum swing adsorption are described with particular reference to air separation for both oxygen and nitrogen production. The roles of individual steps in each cycle are addressed. Sircar secondly discusses some of the challenges to be faced in the design of new and improved PSA processes. These challenges relate to the complex nature of process cycles, to fundamental understanding of multicomponent gas–solid interactions, to the successful development of simplified specific models, and to the understanding of adsorbent heterogeneity and its effect on multicomponent gas adsorption characteristics before *a priori* designs can be made with acceptable accuracy and confidence.

Journals and Symposia

Many learned and popular journals provide accounts of research and developments in adsorption and closely related subjects. The following list, whilst not comprehensive, will serve to guide the reader of this book to some of the more important journals which publish original research articles. The list includes journals devoted exclusively to adsorption, exclusively to separation processes, and more generally to chemical engineering.

Adsorption: Journal of the International Adsorption Society (Kluwer Academic)
Adsorption Science and Technology (Multi-Science Publishing)
American Institute of Chemical Engineers Journal (American Institute of Chemical Engineers)
Bioseparation – International Journal of Separation Science (Kluwer Academic)
Canadian Journal of Chemical Engineering (Canadian Society for Chemical Engineering)
Carbon (Pergamon)
Chemical Engineering Journal (Elsevier)
Chemical Engineering and Processing (Elsevier)
Chemical Engineering Research and Design (Institution of Chemical Engineers)
Chemical Engineering Science (Pergamon)
Gas Separation and Purification (Elsevier)
Industrial and Engineering Chemistry Research (American Chemical Society)
Journal of Chemical and Engineering Data (American Chemical Society)
Journal of Chemical Technology and Biotechnology (John Wiley)
Separation Science and Technology (Marcel Dekker)
Water Research (Pergamon)
Zeolites (Elsevier USA)

Recent advances in the field of adsorption are reported every few years at the Engineering Foundation Conferences which have been organized by The Engineering Foundation from 1983 when the first one one held in Schloss Elmau, Bavaria in May 1983. The editors of the first volume were A. L. Myers and G. Belfort (Engineering Foundation, New York, 1984). Recent advances in various aspects of adsorptive, chromatographic and ion exchange separation processes are also reported in the American Institute of Chemical Engineers' Symposium Series.

Nomenclature

a	gradient of equation defined by equation (6.57)
a	number of molecules successfully condensing at surface per unit time
a_p	external surface area per unit volume of particle
a_v	external surface area of adsorbent particles per unit bed volume
A	area
A	cross-sectional area of adsorption column
b	constant in Langmuir isotherm
b	intercept of equation defined by equation (6.59)
b	Langmuir constant
b	frequency of molecules leaving surface
b_o	pre-exponential factor in the van't Hoff equation
B	permeability coefficient
Bi_h	$(= hR_p/k_e)$ Biot number for heat transfer
Bi_m	$(= kR_p/D_e)$ Biot number for mass transfer
c	concentration
c_b	concentration at breakthrough
c_B	adsorbate concentration out of a moving bed
c_e	threshold concentration for breakthrough
c_E	adsorbate concentration into a moving bed
c_f	final concentration in stagewise contacting
c_f	specific heat capacity of fluid
c_i	concentration at fluid–solid interface
c_o	concentration of adsorbate in feed
c_p	concentration in exit from packed bed before breakthrough
c_{res}	fluid phase concentration in equilibrium with residual loading
c_s	specific heat capacity of adsorbent particle
c_1	interstage concentration

c^*	fluid phase concentration in equilibrium with mean sorbed phase concentration
d	diameter
d	inside diameter of column
d_p	particle diameter
D	diffusion coefficient
D	flowrate of desorbent per unit cross section of column
D_c	diffusivity in adsorbent crystal
D_k	Knudsen diffusivity
D_L	axial dispersion coefficient
D_m	macropore diffusivity
D_M	molecular diffusivity
$D\mu$	micropore diffusivity
D_o	pre-exponential factor for surface diffusion
D_o	concentration independent diffusivity
D_s	surface diffusivity
e	bed voidage
E	extract flowrate per unit cross section of column
E_a	activation energy
E_L	heat of liquefaction
E_s	activation energy for surface diffusion
f	friction factor
f	factor defined in equation (6.62)
f	fugacity
F	feed rate per unit cross section of column
g	acceleration due to gravity
G	Gibbs free energy
G	mass flux
h_i	heat transfer coefficient between fluid and wall
h	heat transfer coefficient between fluid and particle
H	enthalpy
HETP	height equivalent to a theoretical plate
HTU	height of a transfer unit
I	collision integral
j	mass transfer factor
j_H	heat transfer factor
k	constant in Freundlich equation (3.13)
k	mass transfer coefficient
$\underline{k}$	Boltzmann constant
k	linear rate mass transfer coefficient
k	adsorption rate constant in equation (6.43)
k_a	adsorption rate constant in equation (4.41)

k_d	rate constant for desorption
k_e	effective thermal conductivity
k_f	fluid film mass transfer coefficient
k_L	axial thermal conductivity coefficient
k_o	overall mass transfer coefficient
K	equilibrium constant in Henry's law isotherm
l	length
L	pellet length, column length
L	length or height of packed bed
L_e	length of equilibrium section of packed bed
LUB	length of unused bed
m	mass of molecule
m_o	maximum volumetric capacity for micropore filling
m_t	mass adsorbed at time t
m_∞	mass adsorbed when adsorption completed
M	mass of adsorbent
M	molecular mass
n	dimensionless index in Freundlich equation (3.13)
n	number of moles adsorbed per unit mass of adsorbent
n	number of moles
n	number of components
n	exponent in equation (6.66)
N	number of stages
N	number of theoretical plates in chromatographic column
N_o	adsorptive capacity
NTU	number of transfer units
p	partial pressure
p_a	pressure on adsorption
p_d	pressure on desorption
p_i^o	vapour pressure of i at same spreading pressure and temperature as admixture
p_s	saturated vapour pressure
P	total pressure
Pe′	$(= ud_p/D_L)$ Peclet number
Pr	$(= c_f\mu/\lambda_f)$ Prandtl number
q	quantity adsorbed
q	amount adsorbed per unit weight of adsorbent
$\bar{q}$	average quantity adsorbed per particle volume
q^*	quantity adsorbed at equilibrium
q_m	quantity adsorbed in a monolayer
q_o	initial quantity adsorbed
q_o	quantity adsorbed at particle periphery

q_{oi}	initial quantity adsorbed at particle periphery
q_o	residual amount adsorbed per unit weight of adsorbent
q_o^*	amount adsorbed in equilibrium with feed concentration
q_{res}	residual amount adsorbed per unit weight of adsorbent
q_∞	final quantity adsorbed after infinite time
Q	heat of adsorption
r	distance between molecule and surface
r	radius variable
r_c	radius of crystal
R	radius variable of crystal
R	raffinate flowrate per unit cross section of column
R	rate of adsorption
R	cross–over ratio
R	radius
R_g	universal gas constant
R_h	rate of heat transfer
R_m	rate at which molecules strike unit area of surface
Re	$(= \rho u d_p/\mu)$ Reynolds number
R_p	pellet radius
$\bar{s}$	average number of molecules adsorbed per zeolite cage
S	entropy
S	flowrate of adsorbed phase per unit cross section of column
S	area of pellet cross section
S_g	specific (per unit mass) surface area of adsorbent
Sc	$(= \mu/\rho D)$ Schmidt number
Sh	$(= k d_p/D)$ Sherwood number
St	$(= kL/u)$ Stanton number
t	time
t_b	breakthrough time
t_s	stoichiometric time
T	temperature
T_f	fluid phase temperature
T_o	initial temperature
T_s	solid phase temperature
T_w	wall temperature
u	interstitial velocity
u_s	flow rate of solid
U	potential energy
v	volume adsorbed
v	linear flowrate in BDST equation
V	volume
V	pellet volume

V	volume of equilibrium stage
V_i^o	molar volume of pure component i
V_L	volume of fluid phase in equilibrium stage
V_m	molar volume
V_o	total volumetric capacity of adsorbent to adsorb
V_s	volume of adsorbed phase in equilibrium stage
X_i	equilibrium mol fraction of i in adsorbed phase
X_j	equilibrium mol fraction of j in adsorbed phase
y_1	mol fraction of component 1 in the fluid phase
Y_i	equilibrium mol fraction of i in fluid phase
Y_j	equilibrium mol fraction of j in fluid phase
z	general length along packed bed
z	length variable
z	dimensionless radius of particle
z_m	number of molecules to complete a monolayer
α	effective volume of adsorbate molecule
α	separation factor
α	$(= D_c R_p^2/D_p R_c^2)$ solution parameter for equation (4.27)
β	affinity coefficient
β	parameter defined in equation (6.49)
β	$(= 3\,\alpha\,(1-\varepsilon_p)q_o/\varepsilon_p c_0)$ solution parameter for equation (4.27)
γ	$= h\,a\,r_c^2/c_s D_e)$ parameter in Figure 4.7
γ	$(= (1 - e)\,K u_s/e\,u)$ parameter in equation (7.17)
γ_i	activity coefficient of component i in the adsorbed phase
γ_1, γ_2	coefficients in equations (6.73), (6.74) and (7.23)
δ	$(= \Delta H\,(\partial q^*/\partial T)/c_s)$ parameter in equation (4.39) and Figure 4.7
ΔH	heat (enthalpy) of adsorption
ΔP	pressure drop
ε	adsorption potential
ε_p	particle voidage
η	$(= 2t\,R/q^*)$ cycle efficiency
θ	fraction of surface covered by adsorbate
Θ	ratio of qualtity adsorbed to quantity in monolayer
Θ	dimensionless temperature
κ	constant in Dubinin equation (3.20)
λ	$(= (q_o - q_{oi}) / (q_m - q_{oi})$ parameter for solution of equation (4.26)
λ_f	thermal conductivity of fluid
Λ	dimensionless parameter accounting for variation in fluid phase adsorbate concentration
μ	chemical potential
μ	viscosity
μ	first moment of response

v	effective volume of adsorbate molecule
ρ	fluid density
ρ_p	particle density
ρ_s	solid density
ϕ_i	fugacity coefficient of component i in vapour phase
Φ	volume in adsorption space
Φ	parameter defined in equations (6.51) and (6.52)
Φ_s	shape factor
σ	surface tension
σ^2	second moment of response
$\sigma_{A,B}$	quarter width of chromatographic peak of component A or B
σ_i	quarter width of rectangular injection of adsorbate mixture to chromatographic column

Index